GENETIC EFFECTS IN CONTEXT: CELLULAR AND MOLECULAR QUANTITATIVE TRAIT LOCI IN STIMULATED HUMAN NEURAL PROGENITOR CELLS

Brandon David Le

A dissertation submitted to the faculty of the University of North Carolina at Chapel Hill in partial fulfillment of the requirements for the degree of Doctor of Philosophy in the Department of Genetics in the School of Medicine.

Chapel Hill
2023

Approved by:

Samir Kelada

Michael I Love

Jason L Stein

Hyejung Won

Mark Zylka

ABSTRACT

Brandon David Le: GENETIC EFFECTS IN CONTEXT: CELLULAR AND MOLECULAR QUANTITATIVE TRAIT LOCI IN STIMULATED HUMAN NEURAL PROGENITOR CELLS
(Under the direction of Jason L Stein)

Genome-wide association studies have identified numerous genetic variants, often in non-coding sequences, that tune the expression of complex traits including brain structure, brain function, and clinical responses to psychiatric medications. However, genetic association studies do not directly nominate regulatory elements, genes, or cellular contexts in which genetic variants function to affect the expression of phenotypes. Chromatin accessibility or gene expression associated quantitative trait loci (caQTls or eQTLs, respectively) measured in bulk post-mortem tissue have explained mechanisms for a subset of brain-trait associated loci, yet these studies still do not show detectable gene regulatory function for many brain-trait associated variants. Ostensibly, GWAS variants additively affect gene regulatory mechanisms, and in turn, cellular processes that go on to influence complex traits, but these functions may only occur in particular cellular contexts. Here, I utilized a primary human neural progenitor cell-culture model to characterize the function of genetic variation on molecular and cellular phenotypes following stimulation of the canonical Wnt signaling pathway or exposure to mood stabilizing drugs, identifying novel context-specific mechanisms that may explain GWAS loci and variance in clinical responses to treatment.

Genome-wide effects of Wnt, lithium, and valproic acid stimulation on chromatin accessibility, gene expression, and cellular proliferation were measured, and the genetic diversity across hNPC-lines was used to map QTLs describing common genetic effects on these molecular and cellular phenotypes. Stimulus-specific molecular QTLs colocalized with brain-related GWAS signals, including those for neuropsychiatric disorders and brain structures,

providing novel mechanistic hypotheses explaining associated loci that were undetected at baseline unstimulated conditions or in other QTL studies, underscoring the context-specific nature of functional genetic variation. Genome-wide association to hNPC proliferation following stimulation by Wnt, lithium, or VPA, identified a genome-wide significant association to lithium-sensitive proliferation that colocalized with risk for bipolar disorder, schizophrenia, and intelligence. Functional experiments at this locus led to the identification of GNL3 as a lithium-responsive proliferation gene whose expression is influenced by genetic variation. Ongoing work seeks to better understand the genetic basis for variation in clinical response to lithium or VPA by integrating context-specific genetic effects with pharmacogenomic data.

ACKNOWLEDGEMENTS

The research described herein relied on world-class facilities, faculty, and colleagues within the University of North Carolina at Chapel Hill. Several individuals warrant special mention: Jason L Stein, my thesis advisor, provided an accepting, fertile, and rigorous intellectual environment to conduct my scientific training. Jason's patience, guidance, and drive were vital to the projects described below. The curiosity, energy, and intellect of Justin M Wolter, my original Wnt Bro, was absolutely integral to the experimental portions of this work. Our collaboration became a source of fellowship that I relied upon during challenging times. The talented Jordan M Valone, my second Wnt Bro, worked alongside me countless hours to generate the brunt of the data reported here, tackled important analyses, and managed to make the whole thing fun. The brilliant Nana Matoba, my Wnt Sis, lit the path for me as a bioinformatician. I thank Nana for her knowledge, patience, and good humor, not to mention the important analyses she performed. Other colleagues in the Stein Lab provided vital intellectual and emotional support throughout my graduate studies; they include: Angela Elwell, Oleh Krupa, Michael Lafferty, Dan Liang, Madison Rose Glass, Jessica McAffee, Jessica Mory, Nil Aygün, Ian Curtin, Felix Kyere, and Niya Patel. I thank my thesis committee members for their willingness to apply their expertise to improve this work through spirited discussions and constructive critique. Thesis committee member Michael I Love graciously provided a wealth of expertise regarding statistical methods and analyses to enhance this work, and has been a helpful advocate for the next steps in my science journey. I extend deep gratitude to our fantastic BCB Curriculum Administrator/Student Services Manager, Jonathan Cornett, who

goes above and beyond to champion myself and many other students. Finally, I want to thank my loving parents, Deb and Khoi, and my brother, Nate for their constant support.

CONTRIBUTIONS

Chapter 1.1 “Mapping Causal Pathways from genetics to neuropsychiatric disorders” was written with Jason Stein (Le and Stein 2019).

For results described in data chapter 2, “Wnt activity reveals context-specific genetic effects on gene regulation in neural progenitors”, I supervised hNPC cell-culture and Wnt pathway stimulation performed by Jordan Valone. I prepared ATAC-seq libraries. I isolated RNA with assistance from Jessica Mory. All analyses performed in collaboration with Jordan Valone and Nana Matoba (Matoba et al. 2023).

For results described in data chapter 3, “Cellular Genome-wide Association Study Identifies Common Variation Influencing Lithium-induced neural progenitor proliferation”, I performed hNPC cell-culture and stimulations. Cellular assays were prepared and performed with Justin Wolter. I performed genetic associations, bioinformatic analyses, and designed CRISPR-i/a sgRNA targeting the GNL3 transcriptional start site. Justin Wolter performed CRISPR-i/a experiments (Wolter, Le, et al. 2022).

For results described in data chapter 4, “Genetic effects on gene regulation during response to Lithium and Valproic Acid treatment in primary neural progenitor cells”, and data chapter 5, “Other results”, I supervised hNPC cell-culture and stimuli exposures performed by Jordan Valone. I prepared maternal immune activation stimuli using reagents from Kathleen Metz in the Phanstiel lab. I prepared ATAC-seq libraries. I isolated RNA with assistance from Jessica Mory. All analyses performed in collaboration with Jordan Valone, with guidance from Nana Matoba.

TABLE OF CONTENTS

LIST OF FIGURES

LIST OF ABBREVIATIONS

ATAC-seq	Assay for transposase accessible chromatin sequencing
BD	Bipolar Disorder
caQTL	Chromatin accessibility quantitative trait locus
DAR	Differentially accessible region
DEG	Differentially expressed gene
eQTL	Gene expression quantitative trait locus
FDR	False discovery rate
GWAS	Genome-wide association study
hNPC	Human neural progenitor cell
iPSC	Induced pluripotent stem cell
Li	Lithium
RNA-seq	Ribonucleic acid sequencing
SNP	Single nucleotide polymorphism
TF	Transcription factor
TFBS	Transcription factor binding site
VPA	Valproic acid
WRE	Wnt response element

CHAPTER 1: INTRODUCTION

1.1 Mapping Causal Pathways from genetics to neuropsychiatric disorders

The human genome is composed of approximately three billion base pairs. Between any two humans, the sequence of the genome is different at approximately four million locations (1000 Genomes Project Consortium et al. 2015). Those genetic variations, in aggregate, have a strong impact on inter-individual variability for almost all well measured traits, including brain structure, personality, and risk for neuropsychiatric disorders (Polderman et al. 2015). Most individual variants have an infinitesimally small effect on any of these traits. Based on recent technological advancements reducing the cost of microarray technology and DNA sequencing (Hayden 2014), as well as the collaborative efforts of multiple large consortia (Thompson et al. 2014; Sullivan et al. 2018), genome-wide association studies (GWAS), whole exome sequencing, and whole genome sequencing studies have identified many loci in the genome where genetic variation impacts measurable changes in brain or behavioral traits (Hibar et al. 2017; Adams et al. 2016; Hibar et al. 2015; Purcell et al. 2014; Schizophrenia Working Group of the Psychiatric Genomics Consortium 2014). Neuropsychiatric genetics have reached the point where the wheat (risk alleles) can be separated from the chaff (alleles without a detectable association).

The identification of these genetic loci offers considerable promise because it represents the first knowledge of the causal basis of behaviorally defined neuropsychiatric disorders for which we do not understand pathophysiology (Geschwind and Flint 2015). Because environmental insults like medication or stressful life events do not modify the sequence of the genome at specific loci, and genetic variation is identical in every cell in the body from conception (though small exceptions exist (Lodato et al. 2015)), we make the claim that these loci are causally involved in disorder risk. Risk-associated alleles have a unidirectional, although

not a direct, effect on risk for these disorders. The causal basis of these genetic findings is in stark contrast to years of case-control studies in neuropsychiatry measuring differences across almost every measurable trait(Theo G. M. van Erp et al. 2018; van Rooij et al. 2018; Parikshak et al. 2018; Fromer et al. 2016) that could be either causal or reactive (Harrison 2011).

While exciting, such genetic associations are only a launching pad to reveal biological mechanisms underlying complex disorders. After all, genetic variation itself does not directly cause the altered behavior observed in patients with neuropsychiatric disorders. Instead, genetic variation impacts multiple levels of biology, at certain time points during development, within certain cell-types in the brain, changing development and structure, affecting brain function, and resulting in the behavioral manifestations of the disorder. Thorough characterization of these causal chains is a critical step for developing rational therapeutics. Already, genetics-inspired therapeutic design is underway for many disorders (Visscher et al. 2017; Black and Clark 2016; M. R. Nelson et al. 2015), and beginning for neuropsychiatric disorders (Breen et al. 2016).

Maps of genetic variation impacting multiple levels of biology, termed “quantitative trait loci” or QTLs, allow inference of causal chains leading to risk for neuropsychiatric disorders. The specific phenotypes that are impacted along a causal mechanistic pathway bridging genetic variation to behavioral outcomes are often referred to in psychiatric literature as endophenotypes, and in genetics literature as links in a causal chain, or pathways (Kendler and Neale 8/2010). At the beginning of a causal pathway, genetic risk loci may affect the regulation of gene expression within a given cell type at a given developmental time period. A single nucleotide polymorphism (SNP) may lead to a new transcription factor (TF) binding site and allelic differences in chromatin accessibility, called chromatin accessibility QTLs (caQTLs) (Kumasaka, Knights, and Gaffney 2019). When genetic variation impacts gene expression, sometimes through alterations in chromatin accessibility, these loci are referred to as expression QTLs (eQTLs) (Albert and Kruglyak 2015). Large scale maps of genetic variation impacting

molecular measures, like caQTLs and eQTLs, have been and are continuing to be developed to allow the identification of regulatory elements or genes impacted by genetic variants associated with neuropsychiatric disorders (Schwartzentruber et al. 2018; GTEx Consortium et al. 2017; Ng et al. 2017; Dobbyn et al. 2018) (Figure 1.1). Similarly, maps of loci associated with gross brain structure and function derived from magnetic resonance imaging (MRI) have been used for almost two decades to suggest brain regions or functions within the causal chains leading to a variety of neuropsychiatric disorders (Bigos and Weinberger 2010).

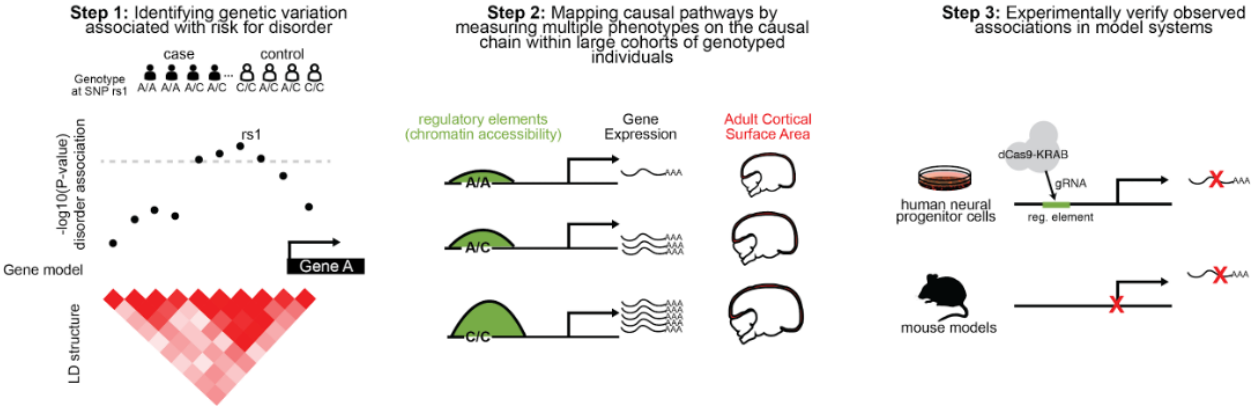

Figure 1.1: From genetic association to mechanism

Studies seeking to define causal pathways between genetic risk and the manifestation of neuropsychiatric disorders may employ a generalized three-step approach. In step 1, high-powered genetic association studies are used to identify variants associated with risk for a disorder. In step 2, genetic association with endophenotypes (chromatin accessibility, gene expression, and brain structure) are used to infer causal pathways leading to risk for a disorder. In step 3, experimental manipulations in human or animal model systems are used to validate mechanistic hypotheses.

The use of gross brain structure and function as links in the mechanistic chain is fueled by two main assumptions - that genetic variation has a stronger impact on brain traits than on

heterogeneous and behaviorally defined disease categories, and that genetic variation associated with brain changes will allow a greater understanding of the mechanism leading to risk for behaviorally defined disorders (Glahn, Thompson, and Blangero 2007). How well are these assumptions met by MRI measures of brain structure and function? How have genetic associations to brain structure and function informed our understanding of the causal chain leading to risk for neuropsychiatric disorders? How can we leverage new imaging methods for a deeper understanding of genetic risk factors for neuropsychiatric disorders?

In this review, we seek to 1) unify the concepts of endophenotypes from psychiatric literature and causal chains/pathways from genetics literature to understand causal mechanistic pathways leading from genetic variation to risk for neuropsychiatric disorders, 2) present detailed molecular pathways impacting risk for disorders discovered from association studies largely outside the realm of neuropsychiatry to inform the study of neuropsychiatric disorders and identify where imaging associations can be leveraged, 3) discuss for which disorders there is evidence that gross brain structure, measured through MRI, lies along a causal genetic pathway, and 4) discuss the application of higher resolution imaging of post-mortem brain tissue to reveal cellular and synaptic phenotypes and refine causal hypotheses derived from genetic associations to MRI measures.

The history and use of endophenotypes in psychiatric literature

Gottesman and Shields adapted the term "endophenotype" to describe internal phenotypes for schizophrenia that were detectable through biochemical tests or microscopy and were ostensibly caused by genetic variation (Irving I. Gottesman and Shields 1972; I. I. Gottesman and Shields 1973). They hoped that studying schizophrenia endophenotypes would side-step the challenging phenotypic heterogeneity found at the clinical level to instead focus on molecular pathways that mediated aspects of the disorder. Brain structure and function as measured through MRI were particularly thought of as excellent endophenotypes (Bigos and

Weinberger 2010). Following this prescient idea, there are currently two predominant uses of endophenotypes in neuropsychiatric literature:

(1) To identify genetic variation associated with the endophenotype, rather than a heterogeneous, clinically defined disorder, because the endophenotype is "closer to the underlying biology", increasing the power of genetic search while still being informative about disorder risk.

(2) To provide mechanistic connections linking genetic variation to behavioral manifestations of neuropsychiatric disorders.

To achieve these goals, there are several assumptions that must be satisfied. First, to achieve higher powered search, genetic variants must have a stronger effect (a higher effect size of the association) on the endophenotype than the disorder. Phenotypes that follow this assumption are often referred to as "closer to the underlying biology" or "closer to genetics" and are detectable within smaller sample sizes (Almasy and Blangero 2001; Meyer-Lindenberg and Weinberger 2006; Kendler and Neale 8/2010; Flint and Munafò 2007). Second, to provide mechanistic insight, genetic variants impacting the endophenotype must lead to risk for the disorder by way of a causal chain (Kendler and Neale 8/2010). Such causation is captured by a mediational model (Kendler and Neale 8/2010), whereby neuropsychiatric disorder risk alleles impact brain structure and function and in turn drive the development of the disorder. In contrast, a liability index model does not provide a mechanistic understanding because a risk allele independently impacts both brain structure and risk for a neuropsychiatric disorder via pleiotropic effects (Kendler and Neale 8/2010) (Figure 1.2). We note that "endophenotype" and "intermediate phenotype" terms are often used without precise definition (Lenzenweger 2013), often failing to differentiate mediational models from liability index models of genetic risk or incorrectly implying that there is only one link on a causal chain between genetic variant and disorder (Kendler and Neale 8/2010; Flint and Munafò 2007; Irving I. Gottesman and Gould 2003). The genetics community instead uses the term "causal pathway" to describe the impact

of genetic variation along multiple phenotypes leading to disease risk. We prefer the specificity of this language and continue to use it here.

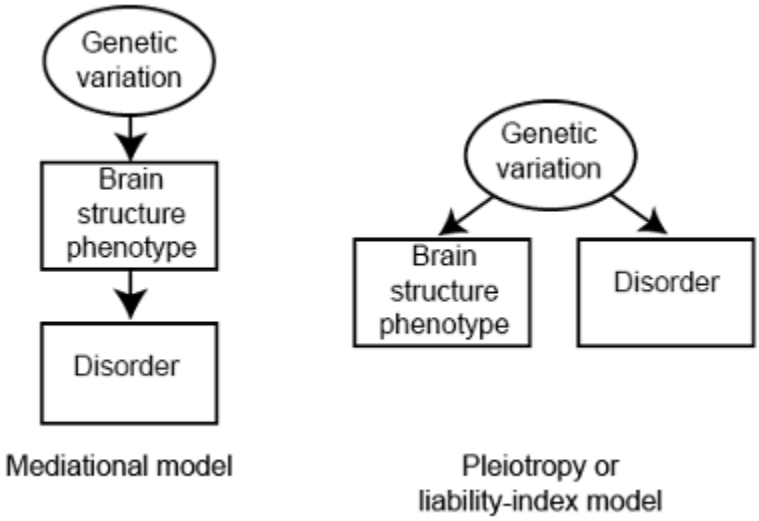

Figure 1.2: Different models that could explain an observed genetic correlation

In the mediational model, genetic variation causes a change in brain structure which then leads to risk for a disorder. If this model is true, experimental manipulation of brain structure will alter risk for the disorder. (Imagine wiggling brain structure and observing that disorder is also wiggling). In the pleiotropy, or liability-index model, genetic variation causes changes in both brain structure and neuropsychiatric disorders, but they are not causally linked. If this model is true, experimental manipulation of a brain structure phenotype does not impact risk for a disorder. (Imagine wiggling brain structure and observing that disorder is staying still). Note that we have simplified this graph to only include one phenotype between genetic variation and a disorder, although we expect that many phenotypes will be found in the true causal pathway.

Despite the behavioral definitions of neuropsychiatric disorders and their phenotypic heterogeneity, genetic search has already identified many risk loci by compiling data from tens

of thousands of individuals (Wray et al. 2018; Pardiñas et al. 2018; Grove et al. 2017). This somewhat obviates the proposed use of endophenotypes as a tool for identifying genetic risk loci for neuropsychiatric illness with higher power (use 1, above). Rather, the most pressing need is to unravel the complex etiology of neuropsychiatric disorders by mapping the underlying mechanisms of risk alleles (use 2 above). Below, we discuss the current evidence about how well gross brain structure satisfies both of these criteria.

How genetic variation has led to identification of causal pathways impacting risk for complex disorders

To illustrate the promise of elucidating causal mechanistic pathways that underlie complex disorders using loci identified from GWASs, we present three examples where considerable causal mechanistic understanding has been achieved in order to motivate similar studies in the context of neuropsychiatric disorders. While two of these examples come from outside the field of psychiatry, their general framework could be readily applied to understand disorders impacting neural tissues. Generally, these studies begin with a common genetic variant of small effect, generally in non-coding and poorly annotated regions of the genome, which is used to identify phenotypes at the molecular, cellular, and systems levels that mediate risk for complex disorders including obesity, type 2 diabetes, and schizophrenia.

A causal pathway by which genetic variation impacts risk for obesity

One of the first large GWASs for body-mass index identified a locus within an intron of the *FTO* gene impacting risk for obesity (Frayling et al. 2007). This locus overlapped a non-coding region so it is unlikely to directly affect protein structure, as is true for most GWAS-identified loci (Hindorff et al. 2009). Instead, given additional functional information describing the activity of the locus in different tissue types (Roadmap Epigenomics Consortium et al. 2015), the locus likely functions as a regulatory element, serving to alter the expression of a proximal gene (Claussnitzer et al. 2015). But what gene(s) does this regulatory element alter? The non-coding variant of interest was mapped to a gene that it regulates using an eQTL approach, where

genotypes in a resource of genetically diverse samples were related to gene expression derived from the tissue of interest. Risk alleles at this locus were associated with increased expression of two genes, *IRX3* and *IRX5*, relatively far (~0.5 and 1.1 Mb, respectively) from the BMI-associated locus in human adipose progenitors (Claussnitzer et al. 2015). Notably, proximity on the genome was insufficient to determine the gene of action, as is often the case (Won et al. 2016). Does the risk allele impact the morphology of adipocytes or fat cells? Again, using a genetically diverse sample derived from multiple individuals with human adipocytes it was found that individuals carrying the risk allele had larger adipocytes than those with the non-risk allele (Claussnitzer et al. 2015). Finally, does modification of *IRX3* or *IRX5* expression lead to changes in metabolism and body weight? Modification of expression levels of these two genes in both human adipose cells and genetically manipulated mice was found to impact metabolism and body weight (Claussnitzer et al. 2015). These findings demonstrate validation of a largely complete causal chain that mapped a non-coding obesity-associated locus to specific biological pathways influencing human obesity.

A causal pathway by which genetic variation impacts risk for type 2 diabetes

In another example, large GWASs have identified many loci associated with risk for type 2 diabetes (Voight et al. 2010). One locus of interest again overlapped a non-coding region near *KLF14* with evidence of regulatory potential in adipose cells(Roadmap Epigenomics Consortium et al. 2015). Which gene(s) might this regulatory element regulate? Again, when genotypes, methylation of the DNA, and gene expression were acquired from a large sample of genetically diverse human tissue samples, the risk allele for type 2 diabetes was associated with increased methylation at the enhancer region and decreased expression of the closest gene, *KLF14*, specifically in adipose tissue (Small et al. 2018). Do carriers of the risk allele exhibit altered morphology of adipocytes? Microscopy of these cells in a genetically diverse sample showed that carriers of risk alleles at this variant have an increased adipocyte volume and area, again demonstrating a morphological consequence to genetic variation. Do carriers of the risk allele

also have increased risk of other phenotypes associated with type 2 diabetes? Through integration with other GWASs, risk alleles at this locus were also found to be associated with increased fasting insulin, decreased high-density lipoprotein cholesterol, and increased triglycerides (Small et al. 2018). Finally, does modulation of the expression of *KLF14* impact risk for type 2 diabetes? Mice harboring a conditional knockout of *Klf14* in adipose tissue recapitulated insulin resistance, decreased high-density lipoprotein cholesterol, and increased triglyceride phenotypes, experimentally validating the observed genetic associations (Small et al. 2018). This again demonstrates a causal chain describing the mechanism for a common variant locus impacting risk for type 2 diabetes.

A causal pathway by which genetic variation impacts risk for schizophrenia

Within the realm of neuropsychiatric disorders, there has been great success in identifying common variants impacting risk for multiple disorders (Sullivan et al. 2018; Gratten et al. 2014), yet very few examples explicitly connect genetic loci to causal pathways. This process is significantly more difficult in brain tissues where the specific cell-types, developmental time periods, or brain regions leading to risk for altered behavior are often not known (Kahn et al. 2015). Despite this, progress has been made in several disorders, and notably, over 100 loci have been detected that are associated with risk for schizophrenia (Schizophrenia Working Group of the Psychiatric Genomics Consortium 2014; Pardiñas et al. 2018). Genome-wide association for schizophrenia risk detected the locus of strongest association in a large, multigenic region comprising the major histocompatibility complex (MHC) locus (Schizophrenia Working Group of the Psychiatric Genomics Consortium 2014). Fine-mapping of the MHC locus revealed that the schizophrenia-associated single base pair risk alleles were tagging (or correlated with) a structural variant that increased the copy number of genes *C4A* and *C4B (Sekar et al. 2016)*. Do these extra copies of *C4A* and *C4B* present in the genome influence how much that gene is expressed? An eQTL study in post-mortem human brain tissue demonstrated that increasing copy number of *C4A* and *C4B* was associated with

increased expression of each of these genes (Sekar et al. 2016). Interestingly, C4 acts within the complement cascade involved in synaptic pruning, a process thought to be aberrant in schizophrenia (M. B. Johnson and Stevens 2018; Glausier and Lewis 2013). Such synaptic pruning deficits may explain neuroimaging findings showing an accelerated loss of frontal grey matter in schizophrenia patients (T. D. Cannon et al. 2015). Does modulation of C4 expression impact synaptic pruning? Mice lacking copies of C4 showed fewer synaptic inputs in a visual circuit that normally undergoes synaptic pruning (Sekar et al. 2016), experimentally validating the functional impact of these associations. Adding further causal evidence, a recent study replicated this pruning effect in human cells using patient-derived human neural cultures, and even showed that this mechanism of pathology can be targeted therapeutically (Sellgren et al. 2019). These studies (Sekar et al. 2016; Sellgren et al. 2019) explain a small, yet important part of the causal pathophysiology, including cell-types and biological processes that lead to risk for schizophrenia (Dhindsa and Goldstein 2016), and are particularly exciting as until this point there had been no causal pathophysiology identified for this complex disorder.

The role human neuroimaging of gross brain structure can play in explaining causal pathways

The studies outlined above, and other similar studies not discussed (Musunuru et al. 2010; Thomsen et al. 2018; Roussos et al. 2014), describe how genetic loci have led to a new understanding of the etiology of complex traits and share commonalities in design (**Figure 1**). First, genetic variation has served as an important causal anchor to begin understanding the mechanism leading to complex phenotypes like obesity, type 2 diabetes, or schizophrenia. Second, maps of how genetic variation relates to multiple phenotypes, in multiple tissues, and at multiple developmental time periods allow an inference of the causal chain leading to risk for a disorder. And third, experimental manipulation of genes within model systems, via gene editing in both human cell culture and mice, test the causal predictions generated from the integration of genetic association maps.

An effective starting point for conducting these investigations is measuring the impacts of genetic variation associated with a neuropsychiatric disorder on gene regulation. While caQTLs and eQTLs provide valuable mechanistic evidence proximal to the source of genetic risk, a list of genes impacted by a risk locus is insufficient to describe a complete causal chain that results in behavioral abnormalities. Colocalizing genetic risk loci with QTLs at higher biological levels, like cell morphology and brain structure, allows description of more complete causal pathways. In the example described above concerning a genetic risk locus for obesity, identification of eQTLs was supplemented with observations that the risk locus induced aberrant adipocyte size (Claussnitzer et al. 2015). Together, these lines of evidence explained a mechanism for developing obesity where changes in gene expression shifted a key cell differentiation pathway to fundamentally alter lipid metabolism. We envision that genetic risk loci associated with brain traits can be similarly leveraged to characterize causal pathways in neuropsychiatric disorders at higher biological levels, and that causal hypotheses can be strengthened when this information is integrated with maps of gene regulation QTLs.

Identification of genetic risk loci for neuropsychiatric disorders is accelerating based in large part on the collaborative efforts of psychiatric genetics consortia (Sullivan et al. 2018; SPARK Consortium. Electronic address: pfeliciano@simonsfoundation.org and SPARK Consortium 2018). Mapping how genetic variation impacts multiple levels of biology requires measuring multiple relevant phenotypes (cell or tissue specific chromatin accessibility, cell or tissue specific gene expression, and brain structure) in large, genetically diverse populations. Such maps are being created for chromatin accessibility and gene expression in large samples of post-mortem and stem-cell derived brain cells (Schwartzentruber et al. 2018; GTEx Consortium et al. 2017; Ng et al. 2017). Similar maps of genetic influences on neuroimaging measures serve as another crucial tool for identifying and characterizing links on causal pathways. They allow interpretation of whether genetic variants associated with neuropsychiatric illness are also associated with the structure or function of the human brain within specific regions. Finally,

directed stem cell differentiation protocols producing specific cell types from multiple brain regions and modern genetic engineering techniques allow the experimental validation of predicted causal pathways in a controlled human system (Hoffman and Brennand 2018; Shalem, Sanjana, and Zhang 2015; Di Lullo and Kriegstein 2017; D. V. Hansen, Rubenstein, and Kriegstein 2011; Stein et al. 2014). This review seeks to place maps of genetic variation associated with gross brain structure into context and explain their utility for describing causal pathways impacting risk for neuropsychiatric disorders.

Genetic associations to neuroimaging traits

We note that in our description of the literature going forward, we avoid discussing "candidate gene" studies, despite the fact that they represent the majority of the neuroimaging genetics literature. In a candidate gene study, a researcher selects a limited number of genes of interest and variants near or within these genes, then measures genetic association with phenotypes of interest (brain structure or function measured via MRI) collected in generally small sample sizes (<1000 subjects) without performing strict multiple comparisons correction across all independent variants present in the genome. The premise of these studies is that using our knowledge of genes involved in brain structure, function, and development, we are able to identify individual variants that are likely to impact the brain or risk for neuropsychiatric disorders. To summarize over ten years of work in this field, only an exceedingly small number of those "candidate gene" associations are replicated in much larger sample sizes (Sullivan 2017; E. C. Johnson et al. 2017; Farrell et al. 2015). For example, of 32 candidate gene associations to brain structure or function, zero survived genome-wide significant association levels ($P<5x10^{-8}$) to any subcortical structure or intracranial volume in sample sizes often 100 times larger than the candidate gene association sample size (Hibar et al. 2015). We, as scientists, are remarkably poor at guessing which genetic variants impact any trait, including brain structure. In response, consortia have assembled in order to accumulate large numbers of research participants to gain enough statistical power to identify genetic variants impacting many well measurable traits

without pre-selection and with strict statistical thresholds (Sullivan et al. 2018; Savage et al. 2018; Wood et al. 2014). The Enhancing Neuroimaging Genetics through Meta-Analysis (ENIGMA) consortium (Thompson et al. 2014), the Cohorts for Heart and Aging Research in Genomic Epidemiology (CHARGE) consortium (Bis et al. 2012), and the UK Biobank (Elliott et al. 2018) represent the largest published association studies for neuroimaging traits to date. Strict genome-wide significance thresholds and large sample sizes have led to highly replicable associations not just in brain traits but across many phenotypes (Panagiotou, Ioannidis, and Genome-Wide Significance Project 2012) (see Table 1 for good practices). In imaging genetics, pushback to the ideas of meta-analysis, universally applied strict statistical thresholds, and requirement for replication persists (Bogdan et al. 2017). This resistance stems from an assumption that heterogeneity induced from meta-analysis can dilute or alter effects. Arguing against this point, a recent genetic correlation study measured whether genetic effects are shared between two genome-wide association analyses: the meta-analytic combination of many sites via the ENIGMA consortium and one UK Biobank site for global surface area and thickness (Grasby et al. 2018). The genetic correlations approach one, indicating an almost complete shared genetic basis between meta-analysis and one-site analysis (Grasby et al. 2018). A lack of strict statistical thresholds or requirements for replication have led to many publications without reproducible associations (Mitchell 2018; Flint, Timpson, and Munafò 2014; Flint and Munafò 2013). We make the assertion that brain imaging traits are not special; hence, genetic associations to brain imaging traits are subject to the same statistical thresholds and replication criteria as all other traits. With this in mind, here we focus on imaging genetic findings from large sample sizes reported by consortia. With high confidence consortium-based associations, we discuss how well neuroimaging traits satisfy the previously described criteria of endophenotypes.

Good practices for imaging genetics studies of gross brain structure:
Assess reliability of phenotype measurements prior to conducting association studies to understand noise levels
Conduct unbiased genome-wide association rather than biased selection of candidate genes
Appropriately power an association test based on effect sizes from similar phenotypes (current gross brain structure GWAS suggests ~10,000 samples are needed to detect significant common variant associations)
Apply rigorous statistical thresholds for association across the whole genome ($P<5x10^{-8}$ for common variant associations with more stringent thresholds if multiple phenotypes are tested)
When conducting a genome-wide association meta-analysis to achieve sufficient sample sizes, extensive quality checking of individual site level data is necessary prior to meta-analysis
Attempt replication of significant associations in independent datasets

Table 1.1: Good practices for imaging genetics studies of gross brain structure.

Effect sizes of genetic variants on brain structure

Rare variants can have very large effects on the structure of the human brain. Early genetic associations identified rare, mostly genic, alleles of strong effect that lead to disorders that strongly change the structure of the brain including microcephaly, macrocephaly, polymicrogyria, and cobblestone lissencephaly (Gilmore and Walsh 2013; Mochida and Walsh 2004; Seltzer and Paciorkowski 2014). While rare variants can have large effects, they do not explain the majority of variability in brain structure within a population. To address this, consortia have recently identified hundreds of genome-wide significant common variant loci,

each generally composed of multiple correlated SNPs, that impact human brain structure including intracranial volume (7 loci) (Stein et al. 2012; Adams et al. 2016; Taal et al. 2012; Ikram et al. 2012; Hibar et al. 2015), subcortical volumes (38 loci) (Stein et al. 2012; Bis et al. 2012; Hibar et al. 2015, 2017; Satizabal et al. 2017; van der Meer et al. 2018), ventricular volumes (7 loci) (Vojinovic et al. 2018), cortical surface area and thickness (150 loci) (Grasby et al. 2018; Hofer et al. 2018), and even white matter anatomy (225 loci) (Elliott et al. 2018). No variants have yet been identified impacting brain function as measured through fMRI (Elliott et al. 2018), though a handful of variants reach genome-wide significance for oscillatory brain activity as measured with electroencephalograms (2 loci) (Smit et al. 2018).

Before these large consortia identified replicable genetic associations, it was hypothesized that structural and functional neuroimaging traits were "closer to the underlying biology". Therefore, genetic associations would have a much stronger effect (higher effect size) on quantitative measures of brain structure or function than on heterogeneous and clinically defined disorders (Almasy and Blangero 2001; Meyer-Lindenberg and Weinberger 2006; Kendler and Neale 8/2010; Flint and Munafò 2007). This assumption fueled the low sample size of "candidate gene" association tests, described above. Given recent replicated genetic associations to many different traits, we can now empirically test the higher effect size assumption. SNPs can indeed have a higher effect on some traits as compared to others. For example, individual SNPs can explain well over 50% of the variability of the expression of a gene (Stranger et al. 2007) and therefore are detectable in sample sizes of ~100. No individual SNP has been detected with that level of effect on brain structure or function. However, individual SNPs with slightly higher impact on brain structure (maximum of ~0.8% of phenotypic variance explained for a SNP associated with putamen volume) than for schizophrenia risk (maximum of ~0.2% of phenotypic variance explained for a SNP associated with schizophrenia; see Figure 1.3) have been detected (Franke et al. 2016). So, there are instances where common genetic variation shows a stronger impact on brain structure than on risk for neuropsychiatric disorders. This

gives support to the hypothesis that structural neuroimaging traits are indeed closer to the underlying biology, just not to the degree previously hypothesized in the candidate gene studies. We note that winner's curse, an upward bias in effect sizes in association studies that first discover significant relationships (R. Xiao and Boehnke 2011), could inflate effect sizes discovered in these imaging genetics studies, so the true differences will require further replication samples. Nevertheless, comparing effect sizes in replication samples alone also demonstrates examples of higher effect sizes for brain structure as compared to disease (Franke et al. 2016). Replicable influences of common genetic variation on brain function have been more difficult to detect, indicating that either effect sizes are lower for genetic associations to functional brain traits or that higher noise limits power (Bennett and Miller 2010).

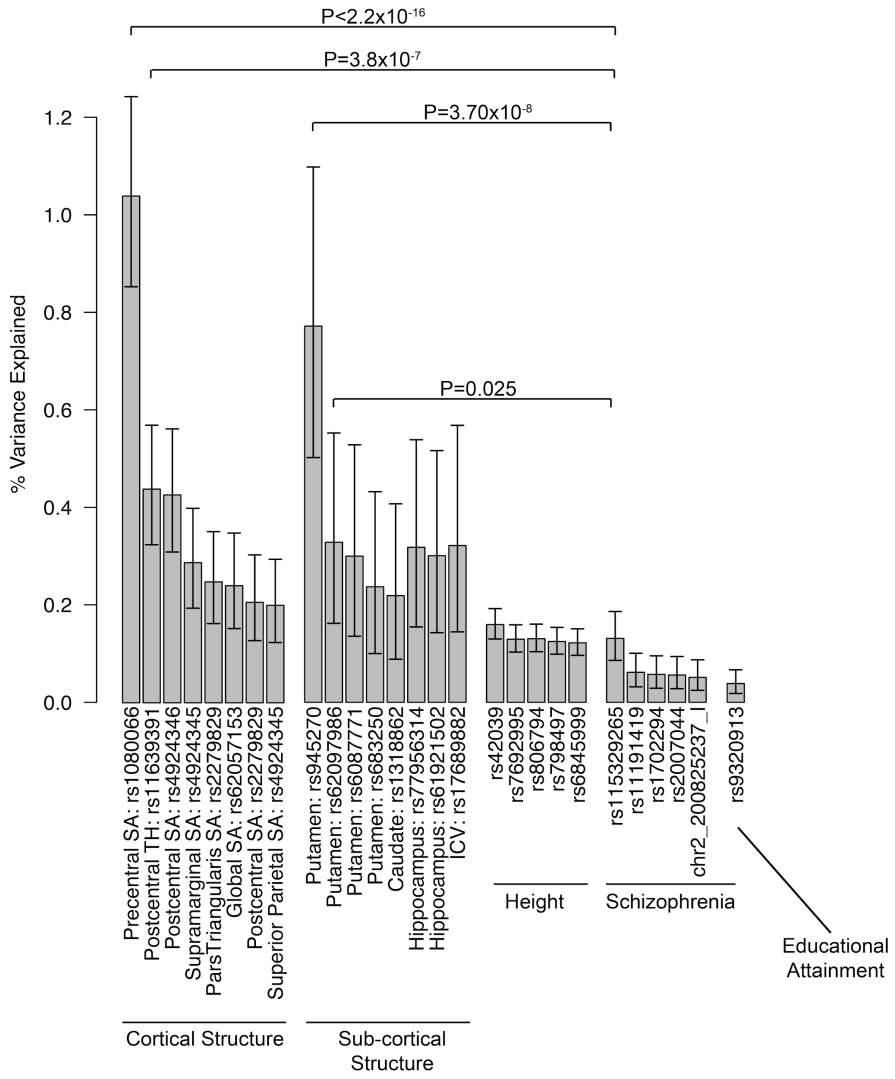

Figure 1.3: Effect size relationships across traits

Each bar corresponds to a common genetic variant, a single-nucleotide polymorphism (SNP), with an association to cortical structure (Grasby et al. 2018), subcortical structure or intracranial volume (ICV) (Hibar et al. 2015), height (Wood et al. 2014), schizophrenia (Schizophrenia Working Group of the Psychiatric Genomics Consortium 2014), and educational attainment (Rietveld et al. 2013). The highest effect size SNPs for each trait are shown. Effect sizes were measured in percent variance explained, the fraction of total trait variance that is accounted for by the genetic variant, (for quantitative traits) or percent variance explained on the liability scale (for disease

categories). Error bars depict 95% confidence intervals. Statistical significance was calculated between the highest effect size SNPs associated with brain structure and the highest effect size SNP associated with schizophrenia. Significance was calculated by transforming effect size to Fisher's Z and calculating the significance of the difference in Z-values. SNPs associated with brain structure traits can account for a greater portion of the total phenotypic variance compared to SNPs correlated with risk for schizophrenia disorder. This figure is extended from previous work (Franke et al. 2016).

Measuring the effect size differences at an individual locus for two different traits determines whether the maximum effect of a variant is higher in one trait than another. Recent studies (Y. Zhang et al. 2018; Holland et al. 2017, 2016) have asked a broader question: if effect size distributions of common variants across the genome are in general stronger for neuroimaging traits than they are for neuropsychiatric disorders. Effect size distributions can be estimated by clustering the effect sizes of LD-independent SNPs across the genomes into one of two general categories: (1) susceptibility SNPs which show some level of non-zero effect sizes (although do not necessarily survive genome-wide significance), and (2) SNPs which have signals so low they cannot be distinguished from no effect. The clustering is applied through a mixture model approach. Effect size distributions are inversely related to polygenicity: the greater the number of susceptibility SNPs, the smaller the effect of each of those SNPs on the trait. Genetic variants impacting psychiatric disorders are amongst the most polygenic studied with an estimated 10,000-50,000 susceptibility SNPs (Y. Zhang et al. 2018), indicating that many genetic variants each of exceedingly small effect size impact risk for these disorders (Y. Zhang et al. 2018; Holland et al. 2017). In comparison, ulcerative colitis or asthma are estimated to have only 1,000-2,000 susceptibility SNPs (Y. Zhang et al. 2018). Within the realm of imaging genetics, the degree of polygenicity of the putamen is over 30 fold less than that of schizophrenia, again indicating a higher effect size distribution of a brain structure trait as

compared to a disorder (Holland et al. 2016). Effect size distributions have not been comprehensively evaluated for all associations to neuroimaging traits and then compared with those from neuropsychiatric disorder risk, although this is an interesting research direction.

While the effect size of genetic variants on brain imaging traits is still modest and generally requires sample sizes close to or over 10,000 subjects to reliably detect any genome-wide significant association (Stein et al. 2012; Bis et al. 2012), current evidence suggests that common variants do have a slightly larger effect on at least some brain structure traits than on risk for neuropsychiatric disorders. Such variants imply that at least some brain structure traits (like putamen volume) are affected by relatively less polygenicity by residing closer to underlying biological processes, thus satisfying the first criteria of an "endophenotype". Associations with these variants are promising starting points for experimental manipulations because they are both detectable with slightly smaller sample sizes and can highlight brain regions and circuitry shouldering the consequences of genetic risk.

Assessing the global shared genetic basis between gross brain structure and risk for neuropsychiatric disorders

How well have neuroimaging traits fulfilled the second usage of 'endophenotype', thereby promoting mechanistic understanding of the effects of genetic risk loci? An initial approach to addressing this question is to ask whether the same genetic variants impact both disorder risk and the gross structure or function of the brain. Using modern statistical genetics techniques, termed genetic correlations, to analyze summary statistics from GWASs (Pasaniuc and Price 2017), it is possible to determine if common risk alleles across the genome are shared between ancestries for the same disorder or between disorders. Strongly positive genetic correlations are observed between schizophrenia in individuals of European descent and of African descent (r_g=0.61), indicating a largely shared common genetic architecture across ancestries (Gratten et al. 2014; Z. Li et al. 2017; de Candia et al. 2013). Perhaps unsurprisingly, risk alleles are shared between schizophrenia, major depressive disorder and ADHD with

positive genetic correlations (r_g>0.2), indicating a shared genetic basis and blurring etiological distinctions between them (Brainstorm Consortium et al. 2018). No significant sharing of risk alleles was detected, however, between Alzheimer's disease and any psychiatric disorder, indicating that they are affected by largely independent genetic variants and have distinct etiologies (Brainstorm Consortium et al. 2018).

Significant genetic correlations observed between alleles influencing brain structure in the population and alleles impacting risk for a neuropsychiatric disorder could help localize brain regions critical for disease pathology. In this spirit, genetic correlations have been performed between hippocampal volume and Alzheimer's disease risk. These demonstrated a significant negative genetic correlation (r_g=-0.15), indicating that alleles associated with decreased hippocampal volume in the general population are also, in part, associated with increased risk for Alzheimer's (Hibar et al. 2017). Giving further credence to this finding, structural deficits in the hippocampus are well known to be associated with Alzheimer's disease (Thompson et al. 2004).

For psychiatric disorders where causally implicated brain regions are not known, genetic correlations may help to identify critical regions involved in the pathology. For example, negative genetic correlations have been observed between the volume of the caudate and nucleus accumbens and bipolar disorder (r_g=-0.17 and r_g=-0.28, respectively) (Satizabal et al. 2017). Other negative genetic correlations have been observed between global cortical surface area and both major depressive disorder (r_g=-0.13) and ADHD (r_g=-0.17) (Grasby et al. 2018). Further supporting the negative genetic correlation between cortical surface area and ADHD, intracranial volume, highly correlated with cortical surface area, is also negatively genetically correlated with ADHD risk (r_g=-0.23) (M. Klein et al. 2017). Positive genetic correlations have been observed between global cortical surface area and both Parkinson's disease (r_g=0.22) and intelligence (r_g=0.22) (Grasby et al. 2018). These studies are notable because they implicate

both the brain regions and the direction of phenotypic effects associated with neuropsychiatric pathologies, thus linking genetics to both disorder and brain structure.

There are some important limitations to the genetic correlation method. It cannot distinguish between causal mediation and a liability index model (Figure 1.2**)**. As described above, in a mediational model, the neuropsychiatric disorder risk alleles impact brain structure which then impacts risk for a neuropsychiatric disorder through a causal pathway. In a liability index model, a risk allele independently impacts both brain structure and risk for a neuropsychiatric disorder (Kendler and Neale 8/2010), indicating pleiotropy instead of causality. To determine which model best fits the data, one needs to experimentally alter brain structure in certain randomly chosen individuals and determine if risk for schizophrenia is altered compared to individuals without alteration in brain structure. If so, this supports the causal mediation model. If not, this supports the liability index model. Of course, experimental manipulation of brain structures is not ethically possible in humans, but our innate genetic differences provide a useful approximation. Assuming that alleles at brain structure associated variants are like treatments randomly assigned in a randomized clinical trial, we can make some causal inferences (given several assumptions detailed in the following references (Pingault et al. 2018; Pickrell et al. 2016)). Using natural genetic diversity in human populations, we can select alleles that are associated with brain structure as a proxy for perturbing brain structure in humans and determine if they also impact risk for neuropsychiatric disorders through a regression framework. If so, this provides support for a mediational model that describes the causal influence of brain structure on risk for neuropsychiatric disorders using a so-called Mendelian randomization (MR) approach. To our knowledge, this method has not yet been applied to neuropsychiatric disorders and brain structure, but has shown that alleles associated with increases in intracranial volume also associated with increased intelligence, putatively showing not just a genetic correlation but also a causal relationship (Savage et al. 2018). Applying this method will be increasingly effective as more loci that impact brain structure are

identified, since the power of MR inferences increases with the number of associated SNPs for the phenotype.

Assessing the local shared genetic basis between gross brain structure and risk for neuropsychiatric disorders

The above methods assess globally, across the genome, whether common variants are associated with both changes in brain structure and risk for neuropsychiatric disorders. In order to determine if the same causal SNP(s) impact both traits at an individual locus, we search for SNPs significantly associated with both phenotypes. However, due to linkage disequilibrium (LD), the correlation between genetic variants, an individual SNP significantly associated with two traits could be the result of two separate causal variants in close proximity on the genome, each independently influencing just one of these two different traits. In this case, the observed significance of a SNP in both traits would be an artifact from decaying significance with LD and could be misinterpreted as the same causal SNP jointly contributing to both traits. To infer if the same causal variant(s) influences two traits, one can determine whether the association statistics follow expected LD patterns driven by a single causal SNP or set of causal SNPs (Z. Zhu et al. 2016; Hormozdiari et al. 2016; Nica et al. 2010; He et al. 2013; Giambartolomei et al. 2014). Colocalization tools have been recently applied to genome-wide association data from schizophrenia and eQTL data from post-mortem brain to identify genes impacting risk for this disorder (Dobbyn et al. 2018). These analyses have identified 40 colocalized signals which provide strong evidence for specific genes whose altered expression is associated with schizophrenia. Although colocalization tools have not yet been formally applied to identify individual loci that impact brain structure and risk for neuropsychiatric disorder, this analysis could identify shared causal variants impacting both brain structure and risk for neuropsychiatric disorders. As such, colocalization analyses will be essential for understanding the causal chains leading to risk for neuropsychiatric disorders.

Importantly, colocalization of signals does not guarantee a causal relationship. For example, if a colocalized SNP affects both brain structure and risk for ADHD, it is not known whether the SNP creates risk for ADHD through changes in brain structure or if the SNP influences ADHD independent of brain structure. This ambiguity makes mechanistic interpretation and subsequent experimental design difficult, as it is not clear whether modification of brain structure will have an effect on ADHD risk. If all data are acquired in the same subjects, it is possible to infer causality at the single locus level using mediation analysis (Schadt et al. 2005; Ng et al. 2017; Y. I. Li et al. 2016). To our knowledge, however, no tools yet exist to prioritize causality on the individual SNP level using summary statistics alone.

The puzzling lack of shared genetic basis between some neuropsychiatric disorders and brain structure

Several well-powered genetic studies of neuropsychiatric disorders, most notably for schizophrenia (Pardiñas et al. 2018; Schizophrenia Working Group of the Psychiatric Genomics Consortium 2014), have so far not demonstrated a significant genetic correlation with any structural or functional brain imaging trait (Franke et al. 2016; Grasby et al. 2018). This indicates that the same common genetic variants associated with many different brain traits are not demonstrably associated with risk for schizophrenia. (Note that we cannot accept the null hypothesis of no genetic correlation, but we do not observe a genetic correlation significantly different than zero in current sample sizes.) Given the observed brain structural differences between individuals with schizophrenia and neurotypical controls (Theo G. M. van Erp et al. 2018; T. G. M. van Erp et al. 2016), as well as the close relationship between structure and function at multiple levels of the brain (Bullmore and Sporns 2009; Holtmaat and Svoboda 2009), why do common genetic variants impacting risk for schizophrenia leave the gross structure of the human brain undetectably changed?

There could be many reasons to explain this puzzling finding. (1) We are underpowered to detect genetic correlations. However, current efforts would set an upper bound on which

genetic correlations would be detected so genetic correlations identified in larger samples must be smaller than those currently observed. (2) Primary causal environmental influences in the absence of genetic effects, for example infection, are driving the observed brain structural differences. However, though environmental influences have been shown to have effects on brain structure and function (Lederbogen et al. 2011; Jha et al. 2019), a primary causal role for these influences in schizophrenia is still difficult to establish (Sutterland et al. 2015; van Os, Kenis, and Rutten 2010). (3) Environmental influences, for example medication, taken in response to schizophrenia diagnosis causes could be driving the observed brain structural differences between cases and controls (Tost et al. 2010). In this case, the observed structural differences are not causing the disorder but are a result of the disorder. (4) Rare variation contributing to schizophrenia risk that is unmeasured in these common variant association studies could be driving the observed brain structural differences. This is unlikely given that common variation, when considered in aggregate, is the greatest contributor to risk for schizophrenia in the population and even individuals harboring a rare mutation also have a polygenic common variant burden (Gratten et al. 2014; Brainstorm Consortium et al. 2018; Tansey et al. 2016). (5) We are measuring genetic influences on brain structure within developmental time periods not critical to disease pathology. Developmental fetal and infant imaging perhaps would detect genetic correlations unobserved in adults (Hazlett et al. 2017; Im and Grant 2018). (6) Brain function, manifesting as the altered behaviors of individuals, could be changed in the absence of structural changes. Given the intimate relationship between brain structure and function (Honey, Thivierge, and Sporns 2010), this seems unlikely. Or, (7) brain changes that predispose to schizophrenia risk happen at the cellular or subcellular level and do not manifest at the gross level at which brain images are taken with MRI. Though many of the above are possibilities, we find the last most compelling and detail further ways in which we can study genetic effects on cellular or subcellular level brain traits.

3D Brain Imaging beyond MRI

Genetic association studies continue to identify both common and rare variants that impact brain structures at the gross anatomical level (H. Stefansson et al. 2014; D. Sun et al. 2018; Martin-Brevet et al. 2018). MRI is suited to measure gross structural traits of intracranial volume and regional phenotypes like hippocampal volume or cortical surface area and thickness (Stein et al. 2012; Adams et al. 2016; Taal et al. 2012; Ikram et al. 2012; Hibar et al. 2015; Grasby et al. 2018; Hibar et al. 2017). These phenotypes can be measured in large numbers of living humans at a relatively affordable cost. While such macroscale imaging is valuable for identifying some affected brain regions and subregions, a typical MRI voxel comprises a brain volume of roughly 1 cubic millimeter: a space that may contain tens of thousands of neurons and millions of synapses (B. Pakkenberg and Gundersen 1997; Bente Pakkenberg et al. 2003; Swanson 1995). So, genetic associations to gross brain structure lack the resolution to explain the cellular or subcellular basis of observed allelic differences. Understanding the cellular and molecular impact of genetic variation demands imaging on microscopic and ultrascopic scales.

For example, if an allele at a particular variant is strongly associated with reduced cortical thickness as measured by MRI in an adult, there are many cellular and circuit changes that could lead to this macroscale alteration. Is the total number of cortical cells reduced, or are they more densely packed? Do neurons in this region have fewer dendritic arborizations? Are relative contributions of specific cell-types altered? Is synaptic density or structure disrupted? Is the spatial architecture and pattern of connectivity within the structure impacted? None of these questions can be adequately addressed with MRI. Measurements of cell numbers, cell types, synapses, circuit connectivity and arrangements of all of these components in 3D space will require both access to post-mortem tissue and image resolution sufficient to capture cellular and molecular features.

We expect that data illuminating these features will be critical to further map causal pathways from genetic risk loci to neuropsychiatric dysfunction, and also may explain why

genetic correlations are not observed at gross brain structural levels with some neuropsychiatric disorders. Measuring phenotypes manifested at the cellular and molecular levels, closer to the effects of a genetic risk factor on the causal chain, will likely be more mechanistically informative and have higher effect sizes - though until association studies are conducted, we will not know the effect sizes. Below, we discuss two emerging imaging technologies that provide cellular resolution or subcellular 3D images of post-mortem human neural tissues, and how they could be applied in a genetically informative design. We describe how modern fluorescence-aided imaging of tissue-cleared samples and high-magnification serial electron microscopy can help to more completely explain the causal mechanisms underlying the genetic risk for disorders of the brain (Figure 1.4).

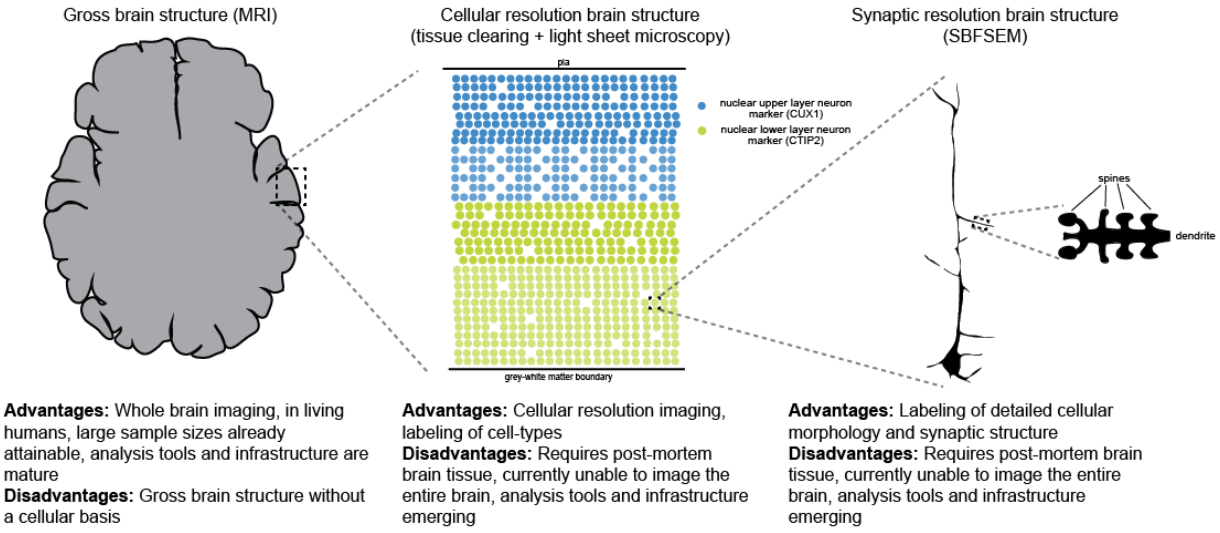

Figure 1.4: Structural brain imaging modalities for the future of imaging genetics

Each of three neuroimaging techniques provides distinct advantages and disadvantages at different biological scales. Neuroimaging of gross brain structures through MRI (leftmost diagram) reveals macro-scale anatomy of specific brain regions at millimeter resolution. The center depicts “micro-scale” imaging achieved by tissue-clearing followed by light sheet microscopy at micrometer resolution. Ultra-scale imaging is possible with serial block-face scanning electron microscopy (SBFSEM) at nanometer resolution.

Combined observations at all three scales using genetically informative experimental designs will facilitate the mapping of causal pathways underlying genetic risk for neuropsychiatric disorders.

Imaging brain structure at cellular resolution with tissue clearing

Our understanding of nervous system function is critically dependent on visualizing the three-dimensional structure of the brain. Cellular resolution volumetric imaging enables interrogations of cell number, density, morphology, and spatial architecture impossible with macroscale imaging, and increases the accuracy and detail of these measurements compared to 2-D image sections. The ability to label and quantify specific cell-types using fluorescence immunohistochemistry in 3-D could help explain the cellular basis of allelic differences in specific brain regions implicated in macroscale imaging genetic studies. For instance, 3-D microscale imaging may reveal cell-type specific spatial disruptions, aberrant cellular morphology, imbalanced numbers of excitatory versus inhibitory neurons, or disorganized cortical lamination.

Cellular resolution optical imaging of post-mortem brain tissue is often restricted to thin 2-D sections due to light's inability to penetrate deeply into the sample. Imaging many serial 2-D sections to reconstruct 3-D images is possible (Stoner et al. 2014), but inefficient and may distort features within the images. Several tissue-clearing techniques have recently been developed to address this problem (Kuwajima et al. 2013; Ertürk et al. 2012; Liu et al. 2016; Aoyagi et al. 2015; Ertürk et al. 2011). These techniques remove light-scattering lipids while preserving cellular spatial arrangements of proteins to yield intact, transparent tissue amenable to light microscopy. Most techniques involve a series of immersions in chemical solvents that dehydrate the sample, dissolve away lipids and induce chemical modifications to create a uniform refractive index, thus minimizing destructive interference (Richardson and Lichtman 2015). In combination with light sheet microscopy for quick image acquisition (Tomer et al.

2015), these methods enable cellular and circuit measurements at micrometer resolution, and are compatible with the use of modern histochemical labeling methods in human tissue. Tissue-clearing approaches are also being scaled and adapted specifically for use on post-mortem human brain tissues, providing a valuable tool for obtaining high resolution volumetric observations of neuropsychiatric pathologies (Lai et al. 2018). As an example, tissue cleared brains from Alzheimer's disease patients showed remarkably detailed 3D measurements of amyloid plaque volume, morphology, and arrangement which varies distinctly across subjects (Liebmann et al. 2016).

These techniques make it possible to design an imaging genetics study of post-mortem brain structure at micrometer resolution. Such a study may be able to directly answer some of the questions posed above about the cellular basis for imaging genetics findings identified with MRI, as well as to identify new genetic influences on cellular level brain structure that were not observable in current association studies given the poor resolution of MRI. In order to design such a study, one needs access to a large set of post-mortem brain samples from genetically diverse and genotyped individuals. Brain banks are therefore a key resource in order to accomplish this goal (Kretzschmar 2009). In addition, genotyping can be completed on existing brain-banked samples and is at this point quite affordable (<$100 USD for arrays which allow genome-wide genotype imputation).

There are of course some barriers to completing such a study. First, post-mortem tissue can be stored either through flash freezing or fixation, and though tissue clearing has been performed on both types, there are limitations: for archival frozen tissue, large chunks may be difficult to fix fully, and for archival fixed tissue, over-fixing may mask the epitopes. Second, it is not known how post-mortem interval affects the degradation of proteins or the ability to label and image them. Third, collecting large sample sizes will likely involve the concerted efforts of multiple different brain banks working together, which can introduce technical variation. Quantifying the degree of technical variation across samples processed at different facilities,

minimizing that technical variation via standard operating procedures, and statistical adjustment for uncontrolled for technical variation has been accomplished for many fields including gene expression via RNA-seq (Lappalainen et al. 2013; 't Hoen et al. 2013), induced pluripotent stem cells (Volpato et al. 2018), and other post-mortem tissue biobanks (Carithers et al. 2015), so will likely be possible in this field as well. Fourth, tissue clearing allows labeling most molecules (assuming an antibody or probe exists and is diffusable within the tissue) with specific expression in a cell-type. It is often not clear which specific cell types are driving an imaging genetic association, so it may be difficult to design the experiment labeling proteins of interest. When trying to explain the specific cell types underlying an observed gross brain structural hit, the proximity on the genome or functional evidence linking to a specific gene may guide cell types to probe (Won et al. 2016). If however, there is no prior hypothesis, studying the most prevalent cell types may be a good place to start, for example labeling upper and lower layer excitatory neurons in the cortex as well as all nuclei. This can lead to future hypotheses about cell fates, spatial architecture and density. Fifth, tissue clearing and light sheet microscopy are not currently possible within an entire intact human brain. Current working distances of light-sheet microscopes allow imaging of chunks of tissue near the size of a mouse brain (10x10x5.6 mm). Given that cortical thickness in humans is on average 2.5 mm (Fischl and Dale 2000), it is possible to image the entire cortical depth of a tissue-cleared sample at a particular location, but covering the entire cortical wall across the ~2500 cm^2 surface area of the cortex would require imaging over 2000 chunks of tissue. Finally, few tools exist for image segmentation, analysis, and storage in large tissue cleared images (Renier et al. 2016; Fürth et al. 2018; Ye et al. 2016). Image segmentation currently works best on features that are sparse and with simple morphology. For example, using a nuclear label for sparse inhibitory neurons in the cortex will be much easier and more accurate to segment than all nuclei. Additionally, computational storage space for images of voxel size ~1x1x4 μm/pixel is around 0.5TB for each channel for an image the size of a mouse brain (or a chunk of the human cortical wall). Raw data

for a sample size of 100 donors for the cortical wall with 4 different types of cells labeled would be 200 TB alone, not including copies of data made in downstream processing. Clearly, large computational resources would be needed to tackle this problem.

By observing tissue-cleared cell populations in brain areas where MRI has identified structural aberrations associated with genetic risk, we can begin to build causal pathways that more explicitly connect genetic risk to brain disorders. When important phenotypes occur in small subcellular structures, such as synapses, electron microscopy techniques that can resolve ultrastructures may be more appropriate, and are discussed below.

Imaging brain structure at subcellular resolution with scanning electron microscopy

Genetic variation may impact synaptic morphology and density, fine-wiring of neuronal processes, axonal myelination and diameter, or other subcellular features. Such ultrastructural phenotypes will be difficult to capture with gross anatomical imaging or optical microscopy. A long standing tool to observe ultrastructures is electron microscopy (EM) which has the power to resolve subcellular organelles, neuronal processes, and the detailed structure of synaptic machinery.

Scanning electron microscopy (SEM) focuses and sweeps a beam of electrons across a fixed and dehydrated biological sample. As the electron beam interacts with molecules within the sample, emitted electrons are detected to create a micrograph image with lateral pixel resolution down to 3.7nm (Horstmann et al. 2012). While SEM micrographs provide an impressive depth of field, traditionally a given image is limited to a single surface of a tissue section. However, modern SEM approaches can reconstruct a 3D volume from a series of two-dimensional images made on thin sections of tissue prepared using a microtome or cryostat (Miranda et al. 2015; Peddie and Collinson 2014). One way this process has been streamlined is via serial block-face scanning electron microscopy (SBFSEM), which combines high-throughput tissue sectioning and subsequent image acquisition (Denk and Horstmann 2004). In this technique, the surface of a tissue block is imaged with repeated passes of Scanning EM as the

top layer of the tissue is shaved away by a microtome to access successively deeper sections. Initial 3D reconstructions using SBFSEM achieved a per-section depth of 50nm with lateral resolution less than 10nm, sufficient to resolve synaptic nanostructures and map circuitry by following axonal paths (Denk and Horstmann 2004). Kasthuri and others employed a similar technique when they captured SEM micrographs of brain volumes serialized using an automatic and tape-collecting microtome to visualize a small volume of mouse cortex with astonishing detail, such that nearly all subcellular elements could be identified with a voxel size of 3x3x30nm (Kasthuri et al. 2015). Their 3D reconstructions clearly resolved axons, dendrites, interactions between glia and neurons, and many subcellular ultrastructures, including synapses, synaptic vesicles, spines, postsynaptic densities, and mitochondria - all features that could play major mechanistic roles in disorders of the brain.

Volumetric ultrascale imaging techniques could be employed to understand the underlying subcellular influences of genetic variation associated with gross brain structure and may identify novel genetic associations structural phenotypes undetectable using tools that are limited to measuring gross brain structure. As an example, let us revisit the study of Sekar and others, who connected a specific genetic locus associated with schizophrenia to the complement immune response and its role in pruning synaptic connections (Sekar et al. 2016). No gross brain structural associations have been detected at this locus to date. However, detailed ultrastructural imaging of synaptic number, morphology, and density in post-mortem samples carrying the C4 risk alleles or protective alleles would provide direct and valuable evidence to support a mechanism of regionally specific synapse loss in schizophrenia. Similarly, SBFSEM could probe cellular hypotheses to explain genetic effects on the volumes of particular brain areas. The volume of a brain structure could be affected by changes in cell size, the density of neuronal processes, rearrangement of spatial architecture, or a mixture of these effects. All of these possibilities could be investigated with ultrascale electron microscopy on samples from the brain region of interest.

There are again limitations to performing such a study, some of which we detail here. Kasthuri et al's impressive saturated reconstructions at 3nm/pixel resolution were performed on just a 40x40x50 μm subset of the tissue block to provide an extremely detailed inventory of one apical dendrite's surroundings. This size represents ~2% of the thickness of the human cortical wall and less than a millionth of total human cortex volume (Toro et al. 2008). In addition, even with expected improvements in acquisition speeds, a 1 mm^3 section of brain can take ~2 months to acquire (Wanner, Kirschmann, and Genoud 2015). Because of this, specific regional hypotheses and/or scaling up imaging acquisitions are needed to apply this technique for imaging genetics studies. With such detailed ultrastructural images, data storage and downstream processing present technical bottlenecks (Wanner, Kirschmann, and Genoud 2015). A single SBFSEM volumetric reconstruction may create an image stack comprising thousands of micrographs (Kasthuri et al. 2015), which can occupy hundreds of gigabytes, and this would represent only a fraction of the data needed to describe the reach of one pyramidal neuron (Peddie and Collinson 2014). For large-scale ultrastructural studies, automated analysis tools and data storage solutions are needed to facilitate the processing of large imaging data sets collected from many individuals across broad swaths of the brain (Kleissas et al. 2017). While obstacles in access to tissue samples, image collection time, and data storage are nontrivial, we highlight these imaging techniques because of their unique potential for providing direct evidence of structural disruptions producing pathology. Further, we hope that appraisal of both the promise and limitations associated with these approaches can accelerate their development and eventual application.

The combination of well-powered genetic studies and gross anatomical imaging of human brain tissues with MRI has provided valuable hints towards the brain regions mediating genetic risk for neuropsychiatric disorders. Microscale and ultrascale imaging genetics will likely identify genetic influences on cellular density, number, arrangement, and synaptic connections

that may be able to both explain the cellular basis of gross imaging genetics associations as well as identifying novel associations to brain structure.

Conclusions

Many loci in the genome have a replicable association with risk for neuropsychiatric disorders. To understand how variation at these loci leads to alterations in cognition and behavior, we need to understand the cell-types, developmental time periods, brain regions, and biological processes impacted by those variants. To do this, we can map webs of QTLs between genetic variation and multiple endophenotypes leading to disorder symptoms. We provide examples of successful integration of multiple lines of genetic association data to explain the basis of genetic risk for other complex traits like obesity and diabetes. We assert that similar approaches augmented by increasingly high-powered and high-resolution genetic associations to brain structure and function will help us understand the causal basis for disorders of the brain. Indeed, MRI measurements have demonstrated significant genetic correlations between certain brain structures and ADHD, major depressive disorder, bipolar disorder and Alzheimer's disease, though the causality of these effects remains to be confirmed. Subsequent modulation of endophenotypes along a causal chain with experiments in model systems can validate the downstream effects of those genetic variants. Layering multiple levels of genetic association with imaging data and experimental validation will generate important mechanistic connections that can illuminate previously dimly-lit causal pathways creating risk for neuropsychiatric illness.

1.2 Challenges in defining genetic mechanisms influencing the expression of brain-related traits

Common genetic variation influences the expression of complex human traits, with SNP-based heritability estimated at an average of 43% among 19 traits (Speed et al. 2017). But, once genetic variants show association with brain traits such as cortical structure or risk for bipolar disorder, how can we map a causal path from variant to trait? A combination of experimental

and analytical approaches must be applied to evaluate molecular mechanisms explaining GWAS loci (X. Xiao, Chang, and Li 2017), which is no small task.

First, each GWAS locus represents a genomic region containing many SNPs, and it is not guaranteed that the lead or index SNP defined by the smallest association P-value in the region is the causal variant. So, which variant(s) at a GWAS trait-associated loci are actually causal? We can prioritize SNPs within a GWAS locus by comparing their varying strengths of association and levels of correlation to the lead or index SNPs. Correlations between SNPs in a region are defined by linkage-disequilibrium patterns based on observed rates of genetic recombination which vary across human populations, and are thus unique to each GWAS cohort. Strong correlation between a GWAS index SNP and nearby SNP is observed as high pairwise LD, and these LD patterns are incorporated into statistical fine-mapping methods that estimate the combined effects of multiple linked SNPs on a trait, narrowing the search for causal variants from perhaps dozens of candidates down to smaller credible set (Schaid, Chen, and Larson 2018).

Still, how can a credible set of GWAS variants prioritized by fine-mapping, identified statistically, be validated experimentally? Unfortunately, direct avenues of validating GWAS variant effects on the expression of complex-traits are intractable. Experimental manipulation of DNA sequences in living humans is unprecedented and unethical. Even if ethics were not an obstacle, experimental validation would require an intractable number of challenging genetic editing events to evaluate even a single GWAS loci harboring many linked and putatively causal SNPs. Furthermore, since GWAS variants may function during development to influence adult phenotypes later on, experiments would not only require risky genetic engineering but also comprehensive longitudinal measurements. The GWAS field must come to terms with the fact that traits and their associated variants reside at opposite ends of a causal chain connected by mechanisms that remain concealed.

One way to side-step this challenge is to study the function of genetic variation on a smaller scale. Instead of interrogating genetic effects scattered across many levels of biology, we might focus specifically on how variants influence gene regulation (Cano-Gamez and Trynka 2020). A hypothetical causal chain leading from a noncoding genetic variant, through gene regulation, to effects on a complex trait may be envisioned as follows:

1. A genetic variant changes the function of a DNA sequence that regulates the transcription or splicing of mRNA from one or more genes.
2. Altered gene expression alters the outcomes of cellular processes such as cell-signaling pathways, proliferation, migration, differentiation, and response to stimuli.
3. Modulation of cellular processes across time, cell- and tissue-types leads to changes in the GWAS-trait of interest.

The research herein focuses on the level of genetic effects described by (1-2) above. At these molecular and cellular levels, effects of genetic variation on the accessibility of DNA itself and the mRNA encoded by that DNA are directly measured. These observations are relatively insulated from complexity introduced by polygenicity and pleiotropy which compounds as genetic effects ripple up through biological levels. Once genetic effects on a reduced scale are characterized, these signals can be colocalized with genetic effects on GWAS traits of interest that ostensibly result from the combined effects of many common variants traversing the various levels of biology. A recent study demonstrated this concept by reporting that up to 50% of GWAS signals were shared with at least one molecular phenotype (Wu et al. 2023). Performing context-specific molecular and cellular QTL studies can nominate specific tissues, cell-types, and cellular states in which GWAS variants actually tune phenotypes.

For example, consider a locus associated with adult risk for bipolar disorder identified via GWAS study. At this locus, a lead or index SNP displaying the most significant P-value of association to the GWAS trait is often reported. However, the locus also harbors several other linked SNPs, which tend to be inherited along with the index SNP due to linkage disequilibrium

(LD). Without other evidence, it is impossible to determine which of the lead or linked SNPs is the true causal variant influencing the GWAS trait. Now consider that tissue or cell-type specific eQTL studies, such as those described by GTEx (GTEx Consortium 2020) or MetaBrain (N. de Klein et al. 2023), evaluated the same locus for genetic effects on gene expression, and found that the lead and/or linked SNPs also showed significant effects on the expression of a nearby gene in particular brain tissues or cell-types. While this still does not pinpoint the causal variant, it prioritizes eQTL SNPs among the potentially causal variants, and importantly assigns genetic effects to the expression of one or more local genes, thus providing functional evidence for a molecular mechanism underlying the association to bipolar disorder risk. This mechanism can then be explored experimentally to better understand how genetic modulation of eGene expression affects downstream cellular processes that in turn exert effects on bipolar disorder risk or other complex traits of interest. While this example describes how eQTL studies can link GWAS variants to gene expression, the same approach can be applied to other molecular QTL approaches such as those characterizing genetic effects on histone decoration, chromatin accessibility, mRNA splicing, or mRNA editing (Aguet et al. 2023).

Still, while eQTL approaches have provided functional characterization of some GWAS loci, many more remain unexplained, begging the question of where the missing regulation mediating GWAS associations is hiding (Umans, Battle, and Gilad 2020)? One reason is that some GWAS variants function only in certain contexts, such as in particular cell types, within developmental windows, or in responses to stimuli. Variants that alter TF binding in a regulatory region, for example, may only affect gene expression in the presence of the relevant TF, which itself may be restricted to specific cell-types, or cell-states, such as the response to a developmental signal. In this way tissue and cell type-specific eQTL mapping studies (GTEx Consortium 2020; Donovan et al. 2020; Bryois et al. 2022), have been useful, but again do not adequately address the missing regulation problem. Recent studies have begun to characterize context-specific molecular QTLs (Alasoo et al. 2018; Kasela et al. 2023; Aygün et al. 2021; Liang

et al. 2021; Panousis et al. 2023; Oelen et al. 2022; Knowles et al. 2018) and allele specific expression (Findley et al. 2021), but dizzying numbers of contexts remain to be explored. This research seeks to use similar approach to considering the contexts of Wnt signaling activation and exposure to mood stabilizing medications in human neural progenitor cells (described in chapters 1.3-1.6).

Another challenge is the fact that most GWAS to date perform genetic associations within samples dominated predominantly by caucasians of European descent. This systemic bias in sample composition fails to represent the diversity of genetic backgrounds within the human population. While most GWAS variants identified in European ancestry populations are generalizable, as many as 25% may show differential directions of effect in other ancestries (Carlson et al. 2013), and there is legitimate concern that polygenic risk scores derived from one ancestry group may not accurately predict phenotypes in others (Martin et al. 2019). Both GWAS and molecular QTL studies should expand sampling underrepresented ancestries to maximize discovery and applicability.

1.3 Primary human neural progenitors: a cell-type specific model for exploring genetic effects on human fetal brain development

Mechanistic understanding of complex traits like psychiatric disorder risk requires cell-based models that provide experimental tractability and access to diverse genetic backgrounds (Brennand et al. 2012). These models strive to disentangle often complex symptomatology into cellular endophenotypes that can be readily studied *in vitro*.

Which cells should be studied? While every cell in an individual has the same genome, the information usage of that genome is cell-type specific and observable as distinct patterns of epigenomic organization (Preissl, Gaulton, and Ren 2023) and gene expression (Arendt et al. 2016). Dysfunction of cell-type specific genomic regulation explains why heritable traits and diseases may manifest only within certain tissues or cells (Hekselman and Yeger-Lotem 2020). Therefore, in order to understand the expression of complex traits and the basis for inherited

disease risk, we must characterize the effects of genetic variation in specific cell populations. Tissue- and cell-type resolution molecular QTL studies have begun to address this (GTEx Consortium 2020; Preissl, Gaulton, and Ren 2023; Gaulton, Preissl, and Ren 2023), including within subregions of the cerebral cortex (N. de Klein et al. 2023). These studies have predominantly relied on samples of adult bulk postmortem tissues where cell-types are resolved using single-cell sequencing approaches. However, some genetic effects on gene regulatory mechanisms may not be present in adult tissues, instead exerting their effects during temporal windows such as fetal development. This may in part explain the limited ability of existing QTL studies to explain genetic effects on GWAS traits (Umans, Battle, and Gilad 2020). By targeting a specific cell-type and developmental time-period we can capture novel genetic effects on both molecular and cellular phenotypes that will improve understanding of complex trait expression(Liang et al. 2021; Aygün et al. 2021). Not only can molecular QTLs be characterized in specific cell-types and developmental states, data capture can be conducted in cultured cells. In addition to the benefit of phenotyping living (versus postmortem) cells, the experimental tractability of cultured cells affords new opportunities, including: 1) cellular assays can be conducted to evaluate genetic effects on biological processes, 2) cells can be exposed to stimuli to evaluate context-specific genetic effects, and 3) cell-lines can be cultured in replicates to improve reproducibility.

So, targeting an appropriate cell-type and developmental time-point is crucial for applying a cell culture-based QTL study toward understanding genetic influences on complex brain traits and NPD risk. This research utilized human neural progenitor cell-lines derived from fetal dorsal telencephalic tissue ranging from gestation weeks 14-21. During this period, multipotent neural progenitor cells, or radial glia, proliferate via symmetric cell divisions. These radial glia comprise a neurogenic pool of progenitors that soon give rise to the cerebral cortex by differentiating into neurons that migrate into their final positions within the cortical laminae (Bystron, Blakemore, and Rakic 2008). The potent influence of radial glia on the resulting

neocortex is described by the radial unit hypothesis, which posits that increased proliferation of neural progenitors along the ventricular zone creates more columnar "radial units" that later undergo asymmetric cell divisions to generate increased numbers of differentiated cortical cell-types including both neurons and glia (P. Rakic 1988). The impact radial glia have on the brain is demonstrated by studies showing that genetic variation associated with cognition, risk for neuropsychiatric disorders, and inter-individual differences in cortical structure is enriched within regulatory elements of fetal brain tissue from the NPC-rich ventricular zone (de la Torre-Ubieta et al. 2018). Developing primary human neural progenitor cells (hNPCs) are thus an appropriate cell-type in which to explore how genetic regulation influences the expression of complex brain-traits. Subsequent sections describe how these cells were utilized for context-specific molecular and cellular to this end.

1.4 Exploring gene regulation using context-specific chromatin accessibility and gene expression

Mapping causal pathways that link genotypes to phenotypes requires characterization of both how DNA information is regulated and how it is expressed. Only about 2% of the human genome's DNA sequence represents genes that encode information used for directing the synthesis of proteins. In contrast, the vast majority of DNA sequences are noncoding, where they are thought to serve a regulatory function by directing the transcription of genes, direct the transcription of non-protein-coding RNA molecules, or perhaps perform no known function (ENCODE Project Consortium et al. 2020). Most trait-associated variants identified by GWAS reside within non-coding genomic regions, posing a challenge for functional characterization (M. E. Cannon and Mohlke 2018; Elkon and Agami 2017).

Let us first consider the regulation of DNA sequences. Genomic regions that are ostensibly engaged in some functional regulatory mechanism can be inferred by measuring chromatin accessibility (Klemm, Shipony, and Greenleaf 2019). Chromatin accessibility indicates which portions of the genome are available for participation in regulatory interactions

with other DNA sequences, proteins, or non-coding RNA. In contrast, inaccessible chromatin is thought to be prohibited from regulatory interactions due to nucleosomal packaging of DNA, where functional sequences are obscured by tight association with histones. A number of methods are available to profile accessible chromatin (Minnoye et al. 2021); research chronicled here relied on the assay for transposase-accessible chromatin, or ATAC-seq (Grandi et al. 2022). ATAC-seq relies on the preferential activity of the Tn5 transposase enzyme to cut and insert sequencing adapters at regions of open chromatin where DNA sequences are free of nucleosomes (Buenrostro et al. 2013). Open chromatin profiles obtained via ATAC-seq identify putative regulatory elements, which typically include transcriptional start sites, promoters, and enhancers. All of these elements likely influence gene expression through DNA sequences capable of binding TFs which convey regulatory complexity via interactions with other TFs, other DNA, or transcriptional machinery.

The complex regulatory logic emerging from the dynamic interplay between enhancers, promoters, and TFs ultimately controls which genes are expressed and when. Open chromatin provides a snapshot of the regulatory landscape, but to understand how this regulation is being utilized, the transcriptional product, mRNA, must be quantified. This work applied standard total RNA-seq methods (Ozsolak and Milos 2011) to profile hNPC gene expression. By capturing ATAC-seq and RNA-seq data from the same batches of cultured hNPCs at the same time-point, the regulatory and gene expression profiles can be integrated to infer functional gene regulatory mechanisms.

During cortical development, gene regulation is a highly dynamic process at the level of both chromatin accessibility and mRNA transcription (Trevino et al. 2021). Chromatin accessibility dynamics alter which regulatory elements are available for interactions with TFs and other chromatin regions, which in turn shapes transcriptional output. 3D interactions between accessible chromatin regions observed by chromatin conformation capture methods like Hi-C reveal major differences between human fetal brain cells from the ventricular zone

(progenitor-rich) versus cells from the cortical plate (neuron-rich) (Won et al. 2016), illustrating that epigenomic overhaul is a distinguishing feature of cortical development. Developmental changes in the epigenome underlie changes in gene expression producing major consequences for cell-type identity and function. For example, gene regulatory dynamics mediate radial glia's fate decisions, determining whether a cell will proliferate via symmetric division to maintain the progenitor pool in the ventricular zone, or differentiate via asymmetric division to generate intermediate progenitors and/or neurons that migrate up through the cortical plate where they form functional synaptic connections (Ohtaka-Maruyama and Okado 2015).

Epigenomic and transcriptomic shifts during development are orchestrated by a complex interaction of both extracellular and intracellular signaling, with molecules such as Sonic Hedgehog, Notch, and Wnt playing major roles in patterning the telencephalon and directing the cell-fate decisions of neural progenitors (Hébert and Fishell 2008; Kageyama et al. 2009; Harrison-Uy and Pleasure 2012). Because in vivo cortical development depends on these and other signals, modeling this process in vitro without taking into account these cellular contexts provides an incomplete picture of a dynamic gene regulatory landscape. A major advantage of studying developing hNPCs in vitro is that cells can be stimulated by these or other molecules under controlled experimental conditions preceding preparation of ATAC-seq and RNA-seq samples. Context-specific epigenomic and transcriptomic dynamics can then be characterized by comparing unstimulated or baseline cellular states against stimulated cellular states. This research took advantage of the experimental tractability of cultured hNPCs to evaluate gene regulatory changes induced by exposure to Wnt-activating compounds, lithium, or valproic acid (described in detail in the following sections).

Lastly, in vitro epigenomic and transcriptomic analyses can be performed on genetically distinct hNPC cell-lines. Comparing chromatin accessibility and gene expression across the entire cohort of hNPCs (n_{max}=82) enables evaluation of common genetic effects on these molecular phenotypes (caQTLs and eQTLs). Combined with GWAS variants, genetic effects on

gene regulation can prioritize variants, regulatory elements, and genes that may go on to influence trait expression.

1.5 The Wnt signaling pathway, brain development, and neuropsychiatric disorders

Molecular phenotyping of chromatin accessibility and gene expression in genetically diverse cultured hNPCs provides an opportunity to understand genetic effects on gene regulation that may tune neurodevelopment, and in turn, complex structural and functional brain traits. However, this dynamic process does not occur in a vacuum; myriad chemical signals cause epigenetic and/or transcriptional changes that drive development. A major portion of this research focused on molecular and cellular effects induced by activation of the canonical Wnt signaling pathway.

Wnt signaling components are conserved across all metazoan organisms, underscoring their vital roles in embryogenesis, patterning, and cellular differentiation (Holstein 2012). The canonical Wnt signaling cascade is initiated by the binding of secreted Wnt ligands to membrane-bound Frizzled-LRP5/6 receptors. In the absence of Wnt ligand, the cytoplasmic protein β-Catenin is phosphorylated by GSK3β, targeting it for proteasomal degradation by a destruction complex composed of Axin, APC, CK1, and DVL. In the presence of Wnt ligand, the destruction complex is disassembled, allowing β-Catenin to elude phosphorylation and targeting by the proteasome. With the destruction complex inactivated, β-Catenin accumulates in the cytoplasm and translocates into the nucleus, where it binds TCF/LEF family proteins and recruits transcriptional coactivators that bind DNA-sequences at the promoters of Wnt target genes to promote the initiation of transcription (Bengoa-Vergniory and Kypta 2015). (see fig 2.1A in data chapter 2)

In the developing forebrain, Wnt ligands are secreted from cells of the cortical hem where they stimulate radial glia proliferation through symmetric cell divisions, increasing the neurogenic pool (Harrison-Uy and Pleasure 2012). As development continues, Wnt activation

wanes, shifting radial glia fate decisions towards asymmetric divisions which generate both intermediate progenitor cells and radial glia (Bielen and Houart 2014). Intermediate progenitor cells continue to respond to Wnt, but instead of stimulating self-renewal, Wnt promotes neural differentiation (Munji et al. 2011) and directs neural migration (W. J. Nelson and Nusse 2004). Wnt's influence appears to extend into adulthood, where it maintains the potency of neural progenitors in the hippocampus (Wexler et al. 2009).

Because of these critical roles, aberrant Wnt signaling is connected to both developmental and neurospychiatric disorders (Freese, Pino, and Pleasure 2010; Bem et al. 2019). As an illustrative example, a constitutively active β-catenin transgene induces prominent cortical hyperexpansion in mice (Chenn and Walsh 2002). Genetic effects on canonical Wnt signaling are associated with the expression of complex brain traits. For example, rare variants affecting Wnt pathway genes are associated with ASD (Krumm et al. 2014; Caracci et al. 2021), common genetic variants associated with brain structure or neuropsychiatric disorders are enriched near Wnt pathway genes (Grasby et al. 2020; Mulligan and Cheyette 2017), and transcriptional dysregulation of Wnt-related genes is observed in schizophrenia and bipolar disorder (Hoseth et al. 2018).

Elucidating Wnt-related disease mechanisms motivates functional characterization of both the upstream factors affecting the signaling cascade, and the downstream effects on cellular processes. Studying the Wnt pathway in cultured primary hNPCs unlocks experimental opportunities to achieve to do so. Because each hNPC line is genetically unique, any experimental measurement can be stratified by genotype to understand the impact of common genetic variation. Multi-omic profiling of each hNPC line enables molecular QTL mapping, as introduced previously. In this thesis research, we stimulated the Wnt pathway prior to profiling chromatin accessibility and gene expression, providing a genome-wide view of the effects of Wnt activation on gene regulation. We then use hNPC genotypes alongside these molecular phenotypes to discover context-specific QTLs, which describe genetic effects that are only

functional in the context of Wnt signaling activation. Wnt-stimulated hNPCs are also amenable to cellular assays, and cellular-QTL mapping. Here, a beta-catenin responsive luciferase assay reported canonical Wnt activation across available hNPC lines. Additionally, we measured cellular proliferation using EdU-incorporation assays in Wnt-stimulated hNPCs. As with the molecular phenotypes, context-specific genotypic effects on these cellular phenotypes of Wnt-activation and proliferation were then characterized as cellular-QTLs. Together, these molecular and cellular phenotypes outline a path from gene regulation, through Wnt-signaling, to effects on radial glia proliferation. Furthermore, common genetic effects on this chain of events provide functional interpretation of genomic loci implicated by brain structure and neuropsychiatric disorder GWAS, further highlighting the importance of Wnt signaling in both brain development and function.

1.6 Pharmacogenomics in a dish

Pharmacogenomics is the application of genetic information towards improving clinical treatment outcomes, a major promise of precision medicine (Roden et al. 2019; Zeggini et al. 2019). The rapid expansion of genomic profiling has shown promise for pharmacogenomic predictions for neuropsychiatric medications (Pardiñas, Owen, and Walters 2021), including those for bipolar disorder, schizophrenia, major depression and autism spectrum disorder (Shani Stern et al. 2018). Despite this promise, both defining molecular profiles that differentiate responders and non-responders, and implementing appropriate clinical interpretations has been challenging (Krebs and Milani 2019). One issue is that current efforts to understand genetic influences on clinical responses are limited by sample-size, polypharmacy, and varied compliance, duration, and dosing across participants (McInnes et al. 2021). The underwhelming discovery of genetic variants that predict clinical responses to psychiatric treatment illustrates these limitations. We need high throughput interpretable pharmacogenomics experiments to make good on these promises.

This research leverages genotypic information, molecular and cellular profiling, and the experimental tractability afforded by hNPC cell culture to explore pharmacogenomic effects underlying responses to Lithium and valproic acid/valproate (VPA). These widely prescribed mood stabilizers treat manic symptoms associated with bipolar disorder (BD), an illness contributing a substantial global health burden by afflicting as much as 2.5% of the population (Crapanzano et al. 2022; Vigo, Thornicroft, and Atun 2016; Kato 2007). However, these treatments are only effective at preventing relapse of manic episodes in 40-60% of individuals, indicating a high degree of variability in clinical response (Tohen et al. 2005; BALANCE investigators and collaborators et al. 2010; Viguera, Tondo, and Baldessarini 2000). High heritability estimates for BD as revealed by twin studies (80% broad sense heritability) and case-control GWAS (25% SNP-based heritability) suggest that translational genomics approaches to understand disease etiology hold promise (C. Zhang et al. 2021). GWAS on clinical responses to lithium and VPA are beginning to reveal genomic loci underlying variance in treatment outcomes. Several studies have identified loci associated with lithium responses in BD, including variants within genes GADL1 and SESTD1 (Hou et al. 2016; C.-H. Chen et al. 2014; Song et al. 2016). For VPA, polymorphisms in specific pharmacodynamic genes affect clinical responses (Goey et al. 2016; M.-M. Zhu et al. 2017), but GWAS approaches have struggled to identify genome-wide significant loci (Wolking et al. 2020, 2021). So far, results from clinical response GWAS for lithium and VPA are hindered by small sample sizes and difficulties phenotyping complex outcomes. Furthermore, the function of noncoding variants associated with clinical responses is unclear.

This research aimed to phenotype the response to lithium or VPA on both molecular and cellular levels in genetically diverse cultured hNPCs, and to identify common genetic variation that influences these phenotypes. The precise phenotyping afforded by ATAC-seq, RNA-seq, and cellular assays is expected to enhance discovery of genetic effects in smaller sample sizes than would be needed to conduct adequately powered clinical response GWAS. Human cell culture-

based methods offer an opportunity to interrogate pharmacogenomic effects under experimentally controlled conditions. A number of studies illustrate the efficacy of cell-based models by finding differences in excitability and transcription, including of Wnt-related genes, in iPSC-derived neurons from lithium-responsive versus lithium-non-responsive BD patients (Mertens et al. 2015; Shani Stern et al. 2020; Santos et al. 2021; Niemsiri et al. 2022). Since many genetic effects may exclusively function in specific cell types or contexts, comparison of molecular and cellular QTLs captured in baseline (vehicle) versus Lithium- or VPA-stimulated states will identify regulatory elements and genes that respond dynamically to these BD treatments. Colocalization of context-specific QTLs with current and future clinical response GWAS will provide gene-regulatory hypotheses that may underlie variance in treatment responses and can be investigated by follow-up experiments. Additionally, context-specific genetic effects stand to enhance functional interpretations of disease-associated loci, as outlined above.

A pharmacogenomics in a dish approach represents a powerful and flexible cell-based model to explore treatment effects and mechanisms. If enough genetically distinct cell-lines are available, genetic effects on molecular and cellular treatment responses can be characterized that can act as footholds to interpret clinical response GWAS loci. Experiments described here utilized up to 82 hNPC lines which included diverse genotypes from population groups typically underrepresented in genetic studies, including samples from admixed ancestry (See supplementary figure 2.1: Multidimensional scaling analysis of genotype data). Diverse hNPC genotypes will expand the translatability of pharmacogenomic results to historically underserved populations (Wojcik et al. 2019; Peterson et al. 2019; Ju et al. 2022).

CHAPTER 2: WNT ACTIVITY REVEALS CONTEXT-SPECIFIC GENETIC EFFECTS ON GENE REGULATION IN NEURAL PROGENITORS

2.1 Introduction

Common genetic variants associated with brain-relevant traits and risk for neuropsychiatric disorders have been identified and replicated, providing a molecular basis for understanding inter-individual variation in brain structure, function, and behavior (Sullivan and Geschwind 2019; Grasby et al. 2020). However, brain-trait associated loci are mostly found in non-coding regions without clear mechanisms of action. Gene regulatory mechanisms of non-coding loci are inferred using datasets mapping the effects of genetic variation on regulatory element activity, marked by accessible chromatin peaks (chromatin accessibility quantitative trait loci or caQTL), or gene expression (eQTL) (Lappalainen and MacArthur 2021). Gene regulatory associated loci (ca/eQTLs) measured in bulk post-mortem tissue have explained mechanisms for a subset of brain-trait associated loci through sharing, or colocalization, of causal variants (Dong et al. 2022; Zeng et al. 2022; N. de Klein et al. 2023). Yet, many brain-trait associated variants do not have detectable gene regulatory function in bulk post-mortem brain tissue, leading to the question of where the 'missing regulation' linking trait-associated variants to gene expression lies (Connally et al. 2022; Umans, Battle, and Gilad 2020; N. de Klein et al. 2023).

One potential solution is that variants impact the accessibility of regulatory elements or the expression of target genes only in specific contexts or when activated by certain stimuli, and therefore are unlikely to be observed in bulk post-mortem tissue (Alasoo et al. 2018). The context specificity of genetic variant function, despite identical genetic sequence (excluding somatic mutations) being present in every cell, may be explained in part through the action of

transcription factors only expressed, activated, or translocated to the nucleus within certain cell-types or during stimulation. Context-specific genetic effects on gene expression are consistent with the observation that only a subset of genetic variants affecting unstimulated chromatin accessibility also affect gene expression, suggesting that some regulatory elements are primed to impact gene expression when a stimulus leads to the activation of additional transcription factors (Liang et al. 2021; Alasoo et al. 2018). Recent studies characterizing cell-type specific ca/eQTLs highlight the importance of cellular context by revealing novel brain trait colocalizations undetected in bulk tissues (Liang et al. 2021; Aygün et al. 2021; Bryois et al. 2022; Kosoy et al. 2022). We hypothesized that the stimulation of a developmental signaling pathway in a homogeneous neural cell type would reveal previously undetected functions of genetic variation and explain some of the 'missing regulation' for brain-trait associated loci.

We evaluated context-specific effects of genetic variation in a population of primary human neural progenitor cells (hNPCs), a developmental cell type with regulatory elements enriched with genetic association signals for multiple-brain related traits and neuropsychiatric disorders (Liang et al. 2021; Aygün et al. 2021; de la Torre-Ubieta et al. 2018). We measured chromatin accessibility and gene expression in hNPCs following stimulation of the canonical Wnt pathway. Wnt stimulation stabilizes cytoplasmic β-catenin, allowing it to translocate into the nucleus where it opens chromatin by displacing the repressor Groucho at TCF/LEF binding sites and promotes the expression of Wnt target genes (Fig. 1A) (Mosimann, Hausmann, and Basler 2009). Wnt signaling influences the patterning and development of the cerebral cortex by regulating proliferation and fate decisions of cortical progenitor cells (Pasko Rakic 2009; Harrison-Uy and Pleasure 2012). As an illustrative example, a constitutively active β-catenin transgene induces prominent cortical hyperexpansion in mice (Chenn and Walsh 2002). Genetic effects on canonical Wnt signaling are associated with the expression of complex brain traits. For example, rare variants affecting Wnt pathway genes are associated with ASD (Krumm et al. 2014; Caracci et al. 2021), common genetic variants associated with brain structure or

neuropsychiatric disorders are enriched near Wnt pathway genes (Grasby et al. 2020; Mulligan and Cheyette 2017), and transcriptional dysregulation of Wnt-related genes is observed in schizophrenia and bipolar disorder (Hoseth et al. 2018). Lastly, iPSC-derived neural cells from individuals with neuropsychiatric disorders show alterations in expression of Wnt pathway genes (Evgrafov et al. 2020; Topol et al. 2015; Marchetto et al. 2017). Our results characterize context-specific genetic effects in hNPCs that provide insights into neurodevelopmental gene regulatory mechanisms underlying brain trait-associated loci.

2.2 Results

Wnt stimuli impact gene regulation

We interrogated gene regulation in the context of Wnt stimulation in a population of previously genotyped multi-ancestry hNPC donors that we cultured and maintained as proliferative neural progenitors (Stein et al. 2014; Liang et al. 2021) (Fig. 1B, fig. S1). To optimize activation of canonical Wnt signaling, we exposed hNPCs to various concentrations of either the WNT3A ligand, CHIR (CHIR99021, also known as CT99021), a potent GSK3β inhibitor and Wnt activator, or vehicle, for 48 hours (Bain et al. 2007). We evaluated the effect of each stimulus on canonical Wnt-signaling using a β-catenin-responsive luciferase reporter assay (Biechele, Adams, and Moon 2009) and the influence on hNPC proliferation using an EdU incorporation assay (fig. S2). Guided by the results from these assays, we selected 5nM WNT3A because it maximized both Wnt activity and proliferation. While CHIR exposure exceeding 2.5μM increased Wnt pathway activation, we selected this concentration based on its ability to maximize hNPC proliferation (fig. S2). Following 48h stimulation by 5nM WNT3A, 2.5μM CHIR, or vehicle, we performed ATAC-seq and RNA-seq for all samples, including 2-6 replicates for each of six randomly selected donors to evaluate technical reproducibility (fig. S3-5). After quality checks and selection of one technical replicate from each donor-condition pair (see Methods), we detected expression of 15,762 protein-coding genes and 7,695 lncRNAs from 242

RNA-seq samples ($n_{vehicle}$=79, n_{WNT3A}=82, n_{CHIR}=81) and chromatin accessibility at 172,887 peaks from 222 ATAC-seq samples ($n_{vehicle}$=76, n_{WNT3A}=68, n_{CHIR}=78).

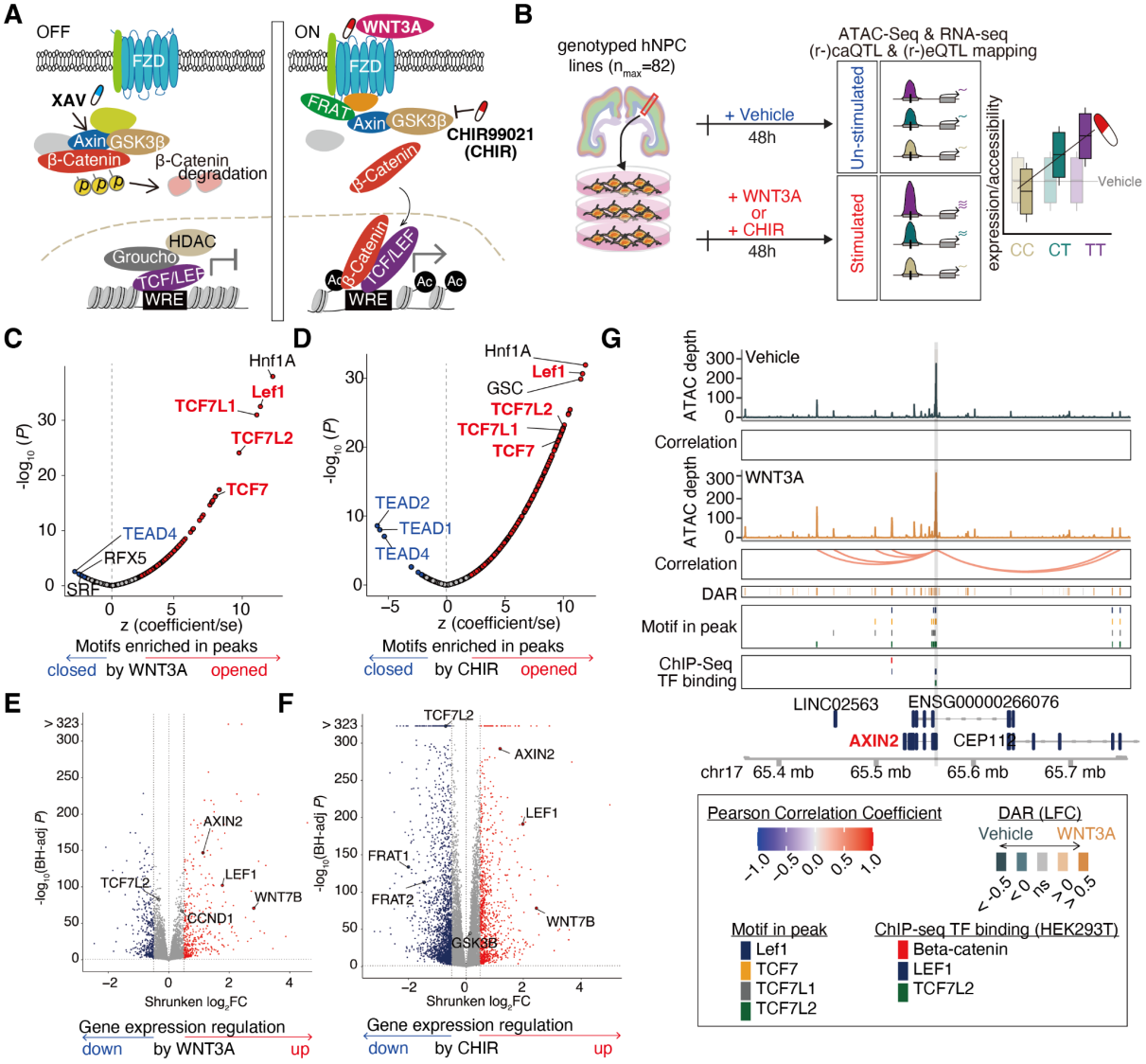

Figure 2.1: Gene regulatory changes induced by WNT stimulation

(A) Cartoon of the canonical WNT signaling pathway. (B) Schematic of study design. Enrichment of TF motifs in WNT3A-responsive (C) or CHIR-responsive (D) chromatin accessibility peaks. Z-scores reflect scaled enrichment scores (x-axis), and -log10(P-values) depict the significance of enrichment (y-axis). TFBS motifs significantly enriched in peaks opening or closing due to the stimulus are represented by red and blue points, respectively. Volcano plots show gene expression changes induced by exposure to

WNT3A (E) or CHIR (F). Genes with significantly increased or decreased expression (DEGs) are represented by red and blue points, respectively. (G) WREs significantly correlated to AXIN2 expression during WNT3A stimulation. DAR: Differentially accessible chromatin regions measured by ATAC-seq. DARs and TSSs in the region overlap TCF/LEF motifs and Wnt-relevant TF binding from previous ChIP-seq experiments (Doumpas et al. 2019).

To determine the gene regulatory impacts of Wnt stimulation on human neural progenitors, we performed differential analyses of chromatin accessibility and gene expression between WNT3A- or CHIR-stimulated conditions compared to vehicle control. Stimulation by WNT3A or CHIR revealed 21,383 unique differentially accessible chromatin regions (Wnt-responsive elements or WREs; FDR Benjamini-Hochberg-adjusted $P < 0.1$, shrunken $|LFC| > 0.5$; WNT3A vs Vehicle (62 pairs): 4,819 WREs; CHIR vs Vehicle (72 pairs): 20,179 WREs; fig. S6A, table S1). We anticipated Wnt stimulation would increase chromatin accessibility at TCF/LEF binding sites as β-Catenin displaces the chromatin condenser Groucho (Mosimann, Hausmann, and Basler 2009). Consistent with these expectations, WREs opening due to Wnt stimulation were strongly enriched with TCF7, TCF7L1/2, and Lef1 motifs (Fig. 1C-D, table S2). β-Catenin, Lef1, and TCF7L2 binding sites defined by ChIP-seq in HEK293T cells (Doumpas et al. 2019) also overlapped WREs opened by Wnt stimulation significantly more than WREs closed by Wnt stimulation (fig. S7). Additional enrichment of HNF1a motifs within WREs (Fig. 1C-D) implies a coregulatory relationship with TCF/LEF, as has been previously described in cancer cells (Hatzis et al. 2008). Interestingly, binding motifs of non-canonical Wnt signaling such as TEAD4 (Park et al. 2015) were enriched in WREs that closed in response to Wnt stimulation (Fig. 1C-D), suggesting an antagonistic relationship between canonical and non-canonical WREs. These results show that Wnt stimulation in human neural progenitors

modulates known downstream DNA-binding protein effectors in expected directions and defines a set of human brain-developmental WREs.

We detected a total of 3,254 unique Wnt-responsive differentially expressed genes (DEGs) across the two Wnt-stimulating conditions (DEGs, FDR-adjusted $P < 0.1$; $|LFC| > 0.5$; WNT3A vs Vehicle (75 pairs): 762 DEGs; CHIR vs Vehicle (74 pairs): 3,031 DEGs; Fig. 1E-F, fig. S6B, table S3). DEGs included known components of the Wnt pathway such as LEF1 and AXIN2, confirming that Wnt stimulation leads to autoregulation of the Wnt pathway (Nusse and Clevers 2017; Kunz et al. 2004). Pathway enrichment analysis of DEGs showed that those upregulated in response to Wnt stimulus were over-represented in Wnt-related pathways such as "TCF dependent signaling in response to WNT" (FDR-adjusted $P = 3.81 \times 10^{-7}$ and 4.69×10^{-7}, for WNT3A vs Vehicle, or CHIR vs Vehicle, respectively), as expected (table S3-4). The Wnt pathway is also known to increase proliferation (fig. S2), and indeed, upregulated DEGs were enriched in "Cell Cycle [REAC]" related genes (FDR-adjusted $P = 7.17 \times 10^{-51}$ and 7.97×10^{-45}, for WNT3A vs Vehicle, or CHIR vs Vehicle, respectively) (Niehrs and Acebron 2012). Additionally, Cyclin D1 (CCND1), a known target gene of WNT stimulation and a key factor regulating cell cycle progression (Shtutman et al. 1999), was significantly upregulated under WNT3A stimulation (LFC = 0.44, FDR-adjusted $P = 1.63 \times 10^{-67}$, Fig. 1E).

Wnt stimulation recruits novel regulatory elements

Activation of the Wnt-signaling pathway alters gene expression patterns that modulate NPC cellular behaviors such as proliferation and differentiation to shape brain development (Hur and Zhou 2010; Bielen and Houart 2014). To link novel WREs to genes they putatively regulate, we estimated the correlation between chromatin accessibility and gene expression for proximal gene-peak pairs (+/-1Mb from the transcription start site (TSS)). We found that across stimulation and vehicle conditions, over 5% of peaks are significantly correlated with nearby genes and over 12% of genes are significantly correlated with nearby peaks (FDR-adjusted $P < 0.1$, median peak-TSS distance ~120 kb, fig. S9, table S5-6). Over 80% of gene-peak pairs showed a

positive correlation, supporting the idea that opening chromatin usually increases, while restricting chromatin accessibility usually decreases, the expression of target genes. Wnt stimulation revealed 12,643 enhancer-gene pairs not detected in the vehicle condition, while 6,461 were lost (fig. S8). For example, *AXIN2*, a gene known to be upregulated by canonical Wnt signaling across tissues (Mosimann, Hausmann, and Basler 2009; Jho et al. 2002), linked to 11 or 8 peaks each harboring TCF/LEF binding sites under WNT3A or CHIR condition, respectively, yet had no significantly correlated peak-gene links found in the vehicle condition (Fig. 1G). These data suggest that new regulatory elements are recruited to regulate gene expression during Wnt stimulation.

Distinct effects of Wnt stimulation or inhibition with XAV

Because WNT3A and CHIR stimulate the Wnt pathway through separate mechanisms, we anticipated a combination of shared and distinct effects on gene expression. Indeed, CHIR yielded considerably more WREs and DEGs as compared to WNT3A, suggesting that this potent small molecule inhibitor of GSK3β induces more gene regulatory changes as compared to the endogenous ligand at their respective concentrations. This difference possibly occurs because CHIR acts downstream of WNT3A where it may more directly affect target gene expression, though concentration differences between the two stimuli make direct comparisons difficult (Fig. 1E-F; fig. S6). The expression level of *GSK3β* is upregulated in progenitor cells stimulated with CHIR (LFC = 0.15, FDR-adjusted $P = 4.64 \times 10^{-46}$), but not WNT3A (LFC = 0, FDR-adjusted P = 0.97; differential impact estimated by interaction term = 9.14×10^{-26}). This suggests that GSK3β inhibition by CHIR triggers a compensatory gene expression response that is not induced by Wnt signaling activated via the recombinant version of the endogenous ligand (Fig. 1A)(Bengoa-Vergniory and Kypta 2015).

To provide additional evidence confirming that our experimental design was stimulating the canonical Wnt pathway, we compared gene expression during simultaneous activation and downstream inhibition of the pathway (WNT3A + XAV(S.-M. A. Huang et al. 2009)) with WNT3A

activation alone in 6 hNPC donor lines (fig. S10A). Little endogenous Wnt activity is observed in unstimulated neural progenitors (fig. S2B-C), so we hypothesized that simultaneous stimulation and downstream inhibition of the Wnt pathway would reduce any Wnt-related transcriptional changes. As expected, inhibition of the Wnt signaling pathway suppressed expression of genes upregulated by Wnt stimulation as compared to vehicle ($r = -0.59$; $P < 1 \times 10^{-323}$; fig. S10B). For example, *LEF1* expression increased in response to WNT3A stimulation, and decreased following inhibition of the WNT pathway. These opposing effects provide further support that the observed gene expression changes are caused by induction of canonical Wnt signaling.

Wnt-responsive genes and regulatory elements contribute to inter-individual differences in brain traits.

Wnt-responsive genes and regulatory elements contribute to inter-individual differences in brain traits

Previous studies suggest that genes related to the Wnt pathway are mutated or differentially expressed in individuals with neuropsychiatric disorders (Evgrafov et al. 2020; Topol et al. 2015; Marchetto et al. 2017; Krumm et al. 2014; Caracci et al. 2021). We sought to determine whether Wnt-responsive genes further support these associations by testing for enrichment of Wnt-responsive DEGs in sets of brain-related disease-associated genes using curated gene-disease information from the DisGeNET database (Piñero et al. 2020). We found enrichment of Wnt-responsive DEGs among schizophrenia and ASD risk genes (Fig. 2A, table S7), while genes not significantly differentially expressed after Wnt stimulation did not show a detectable enrichment among brain-related disease associated genes (Packer 2016). This implies that alteration in the function of Wnt-responsive genes contributes to risk for neurodevelopmental disorders.

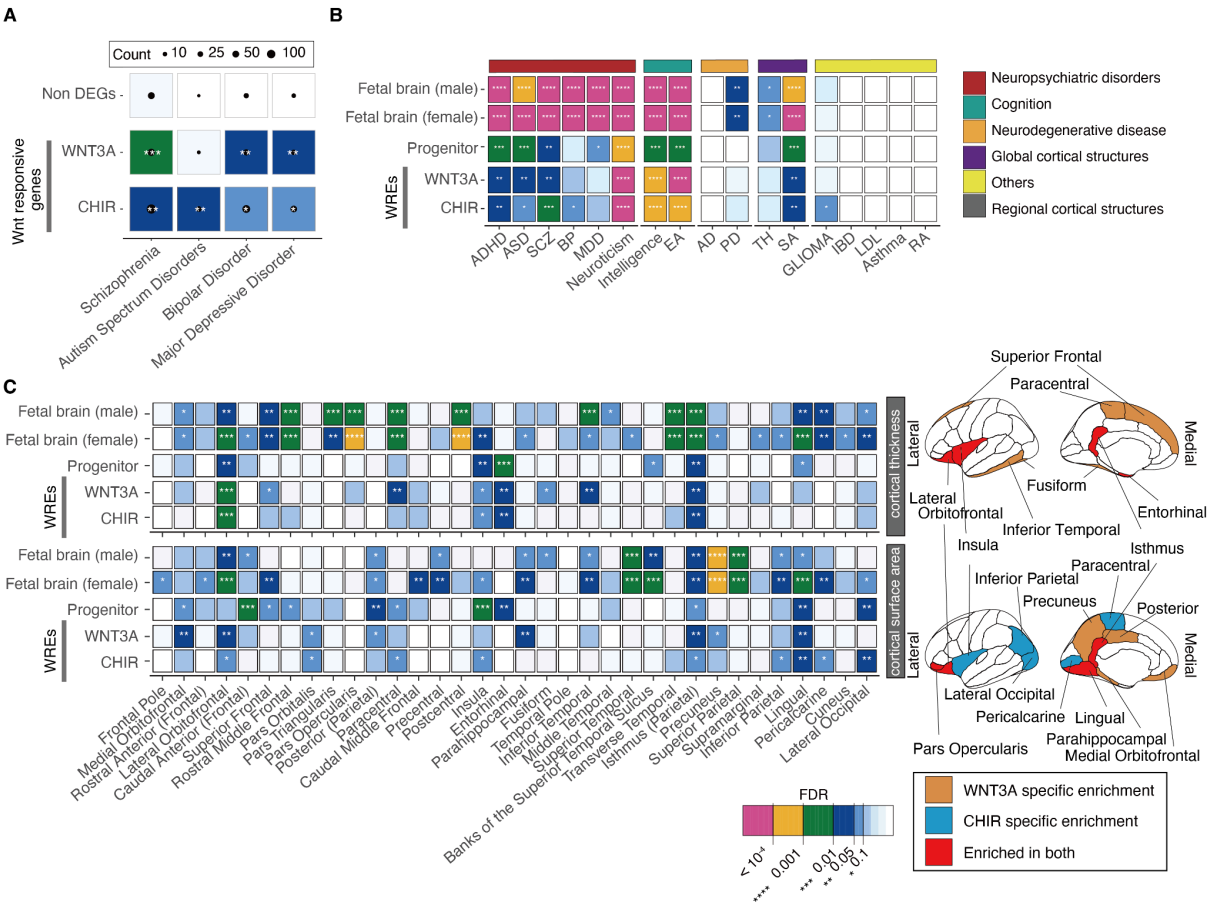

Figure 2.2: Contribution of Wnt-responsive regulatory elements to the heritability of brain traits

(A) Enrichment of Wnt-responsive genes within neuropsychiatric disorder risk gene sets from the DisGeNET database41. Size of dot indicates overlapped gene counts in disease data sets. (B) Contribution of WREs to brain-related trait heritability evaluated by S-LDSC. Traits are grouped by category. (C) Contribution of WREs to the heritability of adult cortical thickness and cortical surface area traits across regions (left). Brain regions with significant enrichment of cortical thickness (top) or cortical surface area (bottom) traits within WREs (right). The P values indicated by color in (B-C) denote whether the WREs contribute significantly to SNP heritability after controlling for other annotations including elements in baseline model and/or non-WREs. * indicates enrichments with FDR < 0.1. ADHD: Attention deficit hyperactivity disorder, ASD: Autism spectrum

disorder, SCZ: Schizophrenia, BP: Bipolar disorder, MDD: Major depressive disorder, EA: Educational attainment, AD: Alzheimer's disease, PD: Parkinson's disease, TH: Average cortical thickness, SA: Cortical surface area, IBD: Inflammatory bowel disease, LDL: low-density lipoprotein, RA: Rheumatoid arthritis (see table S8 for references).

We next explored whether common genetic variants within WREs contribute to brain-related traits (table S8). By performing stratified LD score regression (S-LDSC) accounting for the baseline-model (Bulik-Sullivan et al. 2015; Finucane et al. 2015), we replicated previous findings that regulatory elements in fetal brain tissues or hNPCs contribute to the heritability of neuropsychiatric disorders and brain-related traits (Liang et al. 2021; de la Torre-Ubieta et al. 2018) (FDR-adjusted $P < 0.1$; Fig. 2B, table S9). We then applied S-LDSC to WREs and found that they contribute to the heritability of schizophrenia, ADHD, ASD, and glioma, as well as inter-individual differences in intelligence, even when controlling for the effects of non-differentially accessible peaks (Fig. 2B, table S9). We also found that common variants within WREs significantly contribute to inter-individual differences in global cortical surface area, but not average cortical thickness, consistent with Wnt regulating progenitor proliferation and the predictions of the radial unit hypothesis (Chenn and Walsh 2002; P. Rakic 1988). We further estimated partitioned heritability enrichment for regional cortical surface area and thickness traits. We observed regional specificity where heritability was enriched in WREs for the surface area of medial regions close to the cortical hem, where WNT3A is secreted (Fig. 2C). The heritability of cortical thickness was also enriched in WREs within regions including lateral orbitofrontal and the isthmus of the cingulate. We did not detect partitioned heritability enrichment for neurodegenerative disorders (Alzheimer's disease and Parkinson's disease) or non-brain related traits (Irritable Bowel Disease, Low-Density Lipoprotein, Asthma, and Rheumatoid Arthritis), showing the specificity of these enrichments. In summary, common

variants within Wnt-responsive genes and regulatory elements contribute to inter-individual differences in brain structure, neuropsychiatric disease risk, and cognitive ability.

Context-specific genetic effects on chromatin accessibility and gene expression

Because Wnt-responsive gene expression and regulatory elements contribute to inter-individual differences in brain traits, we sought to identify common single nucleotide polymorphisms (SNPs) and indels affecting gene regulation during Wnt-stimulation. We mapped chromatin accessibility and expression quantitative trait loci (ca/eQTL) using stringent control for known and unknown confounding and use of a hierarchical multiple testing correction (Methods). We identified over 43,000 caQTLs (caSNP-caPeak pairs) in each condition regulating 36,423 unique caPeaks (FDR-adjusted P < 0.1; number of caQTL pairs = 43,664 Vehicle; 57,718 WNT3A; 57,581 CHIR; Fig. 3A-B). We also identified ~2,000 eQTL (eSNP-eGene pairs) in each condition regulating 3,089 unique eGenes (FDR-adjusted $P < 0.1$; number of eQTL pairs = 2,025 Vehicle; 2,075 WNT3A; 1,961 CHIR) (Fig. 3C-D, tables S10-11). The observed effect size of vehicle ca/eQTLs in this study strongly correlated with ca/eQTL effect sizes using largely overlapping hNPC samples cultured during previous studies (Liang et al. 2021; Aygün et al. 2021), indicating our findings are highly reproducible (caQTL r = 0.87, $P < 1 \times 10^{-323}$; eQTL r = 0.89, $P < 1 \times 10^{-323}$; fig. S11). The majority of caSNPs (mean of 74% across conditions) show experimentally validated effects on TF binding via the SNP-SELEX assay (Yan et al. 2021) (fig. S12), providing further validation of the associations discovered here. When the same SNP was identified as both a caQTL and an eQTL for a given stimulus, we observed strong positive correlation between effect sizes on chromatin accessibility and gene expression, also as found in our previous work (fig. S13, table S17), showing that alleles increasing chromatin accessibility generally lead to increased gene expression.

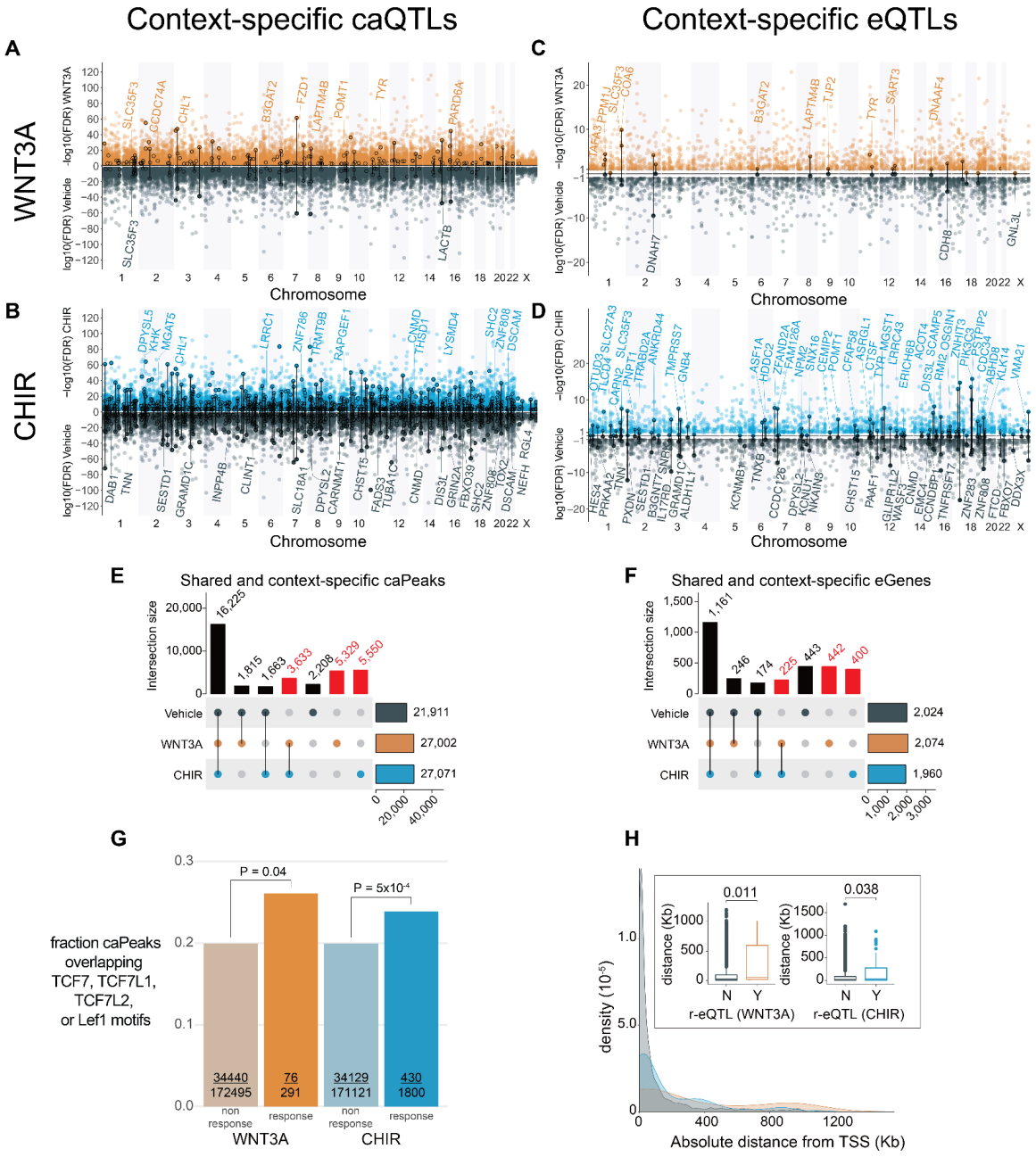

Figure 2.3: Context-specific genetic effects on chromatin accessibility and gene expression

Miami plots depict significant caQTLs (A, B) or eQTLs (C, D) detected under WNT3A (orange) (A, C), CHIR (blue) (B, D) or vehicle conditions (gray) across the genome. Circled variants denote significant genotype-by-condition interaction effects (r-QTLs). A subset

of protein-coding eGenes overlapping r-caQTLs and eGenes are labeled. The number of context-specific caPeaks (E) or eGenes (F) shared across vehicle, WNT3A, and CHIR conditions. Columns labeled in red represent caPeaks or eGenes only detected in Wnt-stimulated conditions. (G) Fraction of response-caQTL-regulated caPeaks vs all other caPeaks containing TCF7, TCF7L1, TCF7L2, or Lef1 motifs. *P*-values denote significance of the difference in proportions of response and non-response caPeaks containing a TCF/Lef motif, evaluated by logistic regression. (H) Distributions of absolute genomic distances between eQTLs and their target gene's transcriptional sites (TSS). Boxplots summarizing these distances are shown in the inset.

We observed a 66.2% increase in caPeaks and a 52.7% increase in eGenes detected in the Wnt stimulated states as compared to vehicle (Fig. 3E-F). Though stimulus-specific caPeaks and eGenes were not statistically evaluated for different genetic effects across conditions, we found the majority of these caPeak/eGenes were also novel when when comparing the stimulated condition with a previous unstimulated ca/eQTL dataset within the same cell type (Aygün et al. 2021; Liang et al. 2021) (fig. S11). While we applied FDR-adjusted $P < 0.1$ thresholding to QTL discovery, these conclusions were robust to a more stringent FDR-adjusted $P < 0.01$ threshold (fig. S14). These results bolster confidence in the novel detection of genetically regulated elements under stimulated conditions, and show that Wnt stimulation reveals stimulus-specific genetic effects on gene regulation previously undetected in unstimulated cells.

Together, stimulus-specific caQTLs and eQTLs enable inference of enhancer priming, where a genetic variant is associated with chromatin accessibility in both unstimulated and stimulated conditions, but only leads to changes in gene expression in the stimulated condition. In this way, enhancers are primed to drive gene expression upon recruitment of additional stimulus-specific TFs. In total, we detected 397 primed regulatory elements. Primed regulatory elements were significantly enriched for a variety of genomic annotations from the fetal brain

called by chromHMM, including transcription start sites, enhancers, and bivalent enhancers, but not heterochromatin, quiescent or transcribed regions (Fig. 4A-B). Surprisingly, we found that primed elements were not more enriched in bivalent enhancers as compared to non-primed elements. Instead, primed caPeaks showed greater enrichment near active transcription start sites than did non-primed caPeaks (Fig. 4A-B). Because primed caPeaks are defined by their proximity to stimulation-specific eQTLs, this enrichment may in part be driven by the tendency of eQTLs themselves to be located near promoter regions (GTEx Consortium 2020). One example of a primed peak was found at a caPeak 53kb from the TSS of *CLINT1*, where we detected two high LD SNPs within the peak strongly associated with chromatin accessibility in both vehicle and under CHIR stimulation, one of which disrupts the CTCF motif (table S12). But, this locus was only associated with gene expression under CHIR stimulation, presumably due to the recruitment of β-catenin to TCF/LEF motifs present in this peak (Fig. 4C-E). CLINT1 protein interacts with clathrin to mediate endocytosis, a process important for both secretion of WNT ligands and WNT-induced accumulation of β-catenin in the nucleus (Brunt and Scholpp 2018; Blitzer and Nusse 2006).

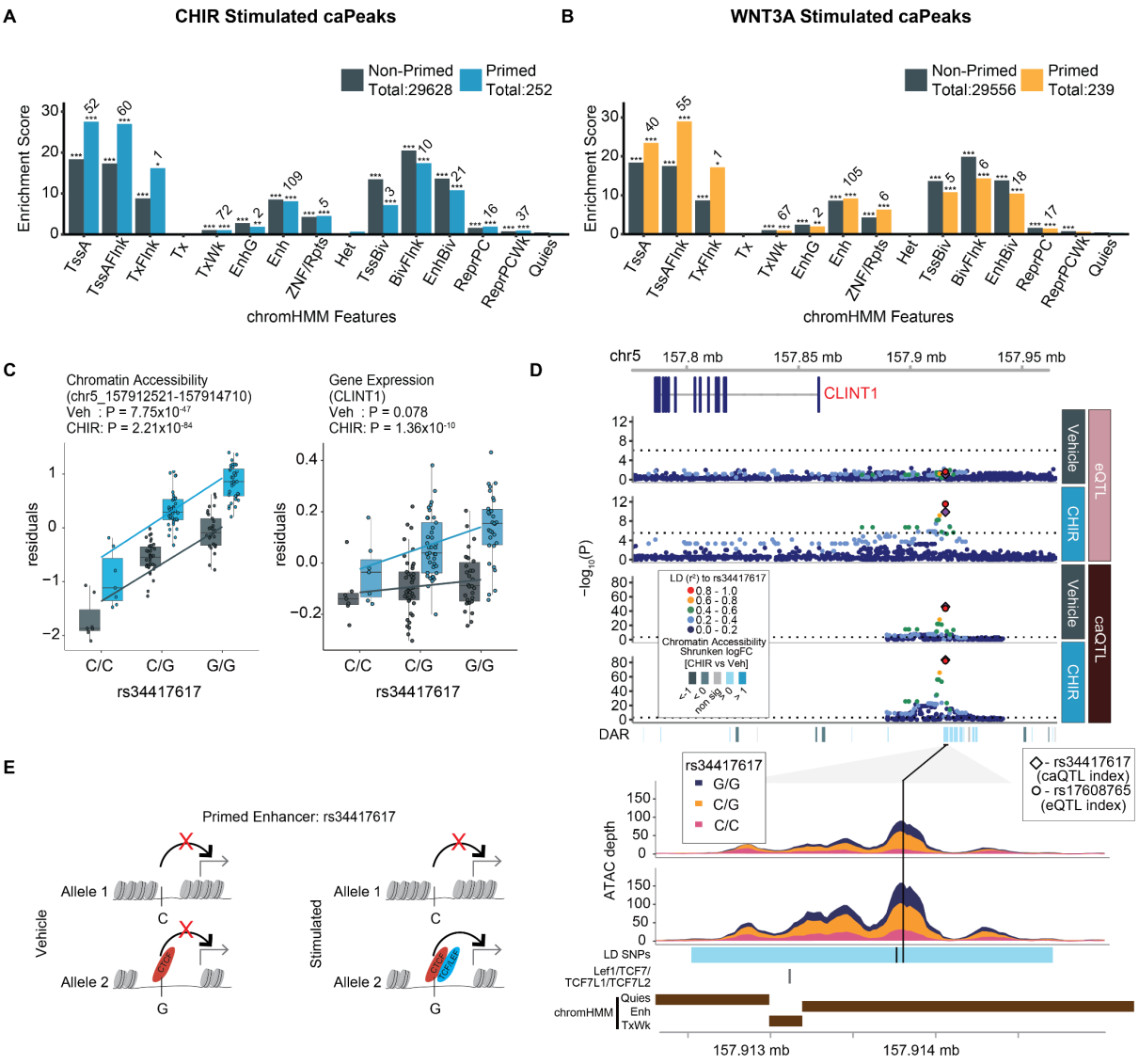

Figure 2.4: Enhancer priming identified through context-specific molecular QTLs

Enrichment of primed and non-primed CHIR (A) and WNT3A (B) caPeaks within chromHMM states defined in the fetal brain. *, **, *** indicate enrichments with *P*-values < 0.05, .01 and .001, respectively. Numeric labels indicate overlap count of a caPeak with a given annotation. (C) Allelic effects of rs34417617 on chromatin accessibility of WRE (chr5:157912521-157914710) (left) and *CLINT1* expression (right). (D) Regional association plots at the *CLINT1* locus. From top to bottom: Genomic coordinates, gene models, eQTL and caQTL *P* values for vehicle and CHIR-stimulated conditions, ATAC-seq coverage showing differential chromatin accessibility, with SNPs linked by LD ($r^2 > 0.8$),

TCF/LEF elements annotated, and chromHMM features. (E) Putative mechanism for rs34417617 regulating chromatin accessibility and gene expression in the vehicle and stimulated conditions.

To identify whether Wnt activation alters the function of a genetic variant in regulating chromatin accessibility or target gene expression, we performed a genotype by condition interaction test which statistically assesses the impact of stimulation on the genotypic effect compared to vehicle. We labeled the significant results as r-QTLs, which are complementary to the stimulus-specific QTLs defined above, though are not expected to be identical. For example, a genetic variant with effects on gene expression only in the vehicle condition, but not in the stimulated condition, would be an r-eQTL, but not a stimulus-specific eQTL. We detected 291 and 1,800 r-caQTLs, and 22 and 102 significant r-eQTLs in WNT3A, CHIR, respectively (labeled with circles in Fig. 3A-D, fig. S15, tables S13-14). The directionality and magnitude of QTL effect sizes were generally consistent between stimulated and unstimulated conditions, but r-QTLs exhibited differential effects in the stimulated condition (fig. S15). Chromatin accessibility peaks regulated by r-caQTLs were enriched in specific transcription factor binding site (TFBS) motifs as compared to all other caPeaks (table S15). For example, significantly more TCF7, TCF7L1/2, and Lef1 motifs were found within CHIR or WNT3A response peaks as compared to non-response peaks (Fig. 3G), suggesting that these Wnt-stimulation-specific TFs lead to context-dependent genetic effects on chromatin accessibility. Interestingly, the transcription factor motif most significantly associated with response-caPeaks, ARID3A, is involved in neural fate specification (Yao et al. 2017; Pavlaki et al. 2022), and interacts with TCF7 to co-bind regulatory elements in murine T cell progenitors (Astori et al. 2020). Response caPeaks were enriched within several chromHMM genomic annotations including active TSS, enhancers, and bivalent enhancers. Response caPeaks were significantly less enriched for active TSS and enhancers as compared to non-response caPeaks, perhaps because these response caPeaks flag novel condition specific enhancers not annotated in

post-mortem fetal brain tissue (fig. S16). We also observed that r-eQTLs were more distal to the TSS of the regulated eGene as compared to non-r-eQTLs (Fig. 3H). This finding is consistent with the idea that context-dependent regulatory elements are farther from the genes they regulate than are non-context-dependent regulatory elements (Dimas et al. 2009).

Genomic regions undergoing rapid human-specific evolution are enriched in caPeaks

Non-coding genomic regions likely contributed to the expansion of the cerebral cortex along the human lineage, but it has been difficult to identify specific evolutionarily relevant regulatory elements involved in brain development (Sousa et al. 2017). Human accelerated regions (HARs) and human ancestor quickly evolved regions (HAQERs) are largely non-overlapping sets of genomic regions that have acquired many mutations since the divergence of chimpanzees and humans (Capra et al. 2013; Mangan et al. 2022). HARs have the constraint of being highly conserved until the divergence of humans and chimpanzees, so likely represent ancestral regulatory elements with altered function in humans; whereas HAQERs do not have this constraint so could represent new regulatory elements generated from previously non-functional sequences along the human lineage. Many HARs have been shown to act as neurodevelopmental enhancers and HAQERs are highly enriched within bivalent chromatin states in the developing human brain, sites which are thought to regulate expression of context-responsive, developmentally relevant genes (Girskis et al. 2021; Mangan et al. 2022). We found 123 HARs and 37 HAQERs (out of 2,751 and 1,581 that were defined, respectively) overlapped caPeaks, yielding a highly significant enrichment both across and within stimulated and unstimulated conditions (Fig. 5A-D, table S16). Interestingly, Wnt stimulation led to a higher overlap of caPeaks with HARs/HAQERs compared to unstimulated cells (48% and 60% increase in HAR and HAQERs, respectively), consistent with the idea that these genomic elements have gained Wnt-responsive developmental function that sets human cortical development apart from our recent non-human primate ancestors.

A notable HAR-caPeak overlap was found at a previously validated distal enhancer of the Wnt ligand receptor gene *FZD8*, where the human, but not chimpanzee, enhancer ortholog has been shown to expand the cerebral cortex in transgenic mouse models (Boyd et al. 2015). Here, we found that this HAR overlapped a caPeak where Wnt stimulation led to significantly decreased chromatin accessibility. The peak also contained a common variant with consistent effects on chromatin accessibility across stimulation conditions that overlapped a Lef1 binding motif (Fig. 5E-F). Though we found strong genetic regulation of chromatin accessibility at this HAR, we did not find evidence that *FZD8* expression was genetically regulated by the same locus. Our results provide additional support that this evolutionarily relevant region is a functional Wnt-sensitive regulatory element in human neural progenitors and that common genetic variation influences its chromatin accessibility.

Additionally, we highlight two HAQER-caPeak overlaps near *PAX8/PSD4* and the promoter region of HAR1A/B that exhibit Wnt-responsive genetic effects on chromatin accessibility (fig. S17-18). Together, HAR/HAQER-caPeak overlaps show that some non-coding genetic elements with evidence of positive selection along the human lineage harbor common variation that alters chromatin accessibility in response to Wnt stimulation in developing neural progenitor cells.

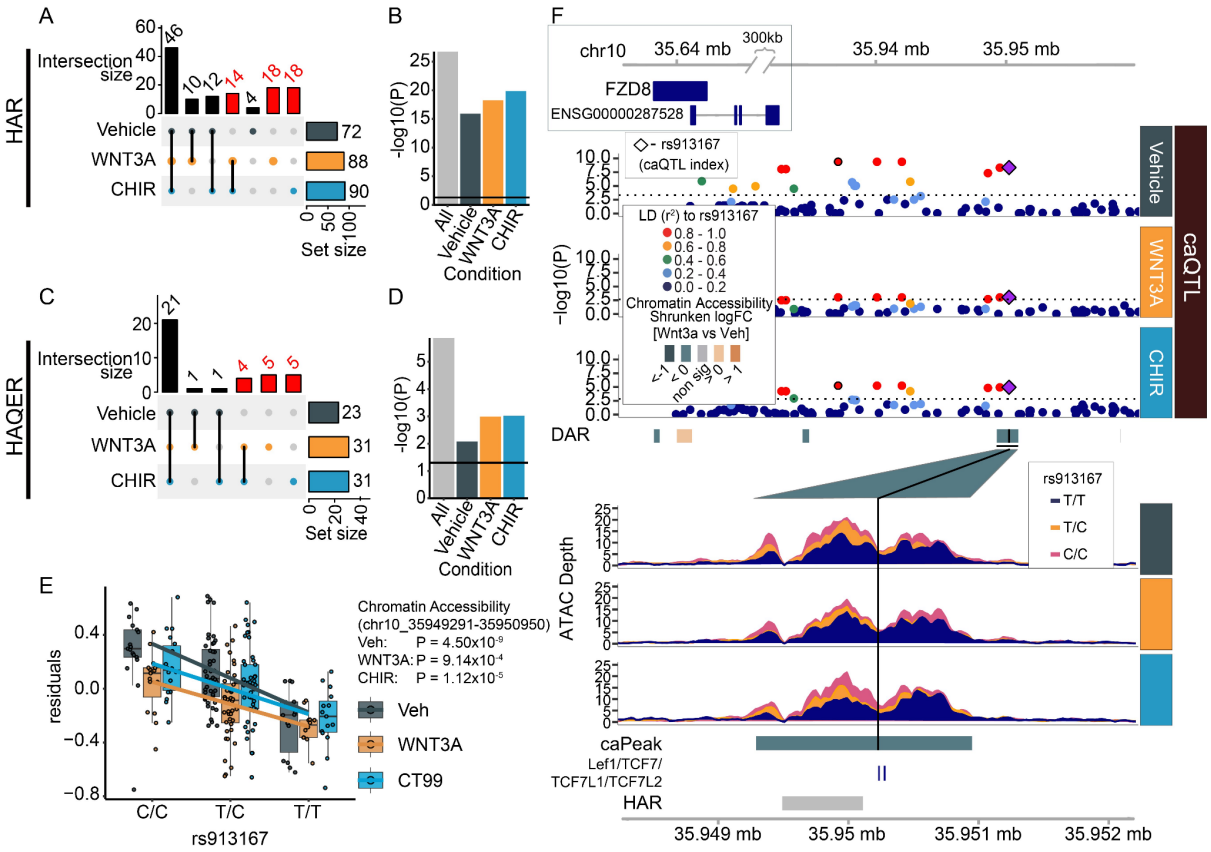

Figure 2.5: caPeaks overlap with regions undergoing rapid human-specific evolution

(A, C) The number of caPeaks overlapping HARs and HAQERs, respectively, across vehicle, WNT3A, and CHIR conditions. Columns labeled in red represent overlaps only detected in Wnt-stimulated conditions. (B, D) Enrichment -log10(P) values of HARs and HAQERs, respectively within unique caPeaks across all conditions and within each condition. (E) Allelic effects of rs913167 on chromatin accessibility (chr10:35949291-35950950). (D) Regional association plots at rs913167, the index SNP for a caPeak-HAR overlap. From top to bottom: Genomic coordinates, gene models where the boxed region shows the location of *FZD8* ~300kb away from the caPeak, caQTL P-values for vehicle, WNT3A, and CHIR-stimulated conditions, ATAC-seq coverage showing differential chromatin accessibility, TCF/LEF elements annotated, and HAR location.

Identifying context-dependent gene regulatory loci shared with brain-related GWAS traits

Partitioned heritability analysis revealed that GWAS loci associated with neuropsychiatric disorder risk and brain structures are enriched at WREs, demonstrating that these elements contribute broadly to brain phenotypes (Fig. 2). However, enrichments do not nominate specific genes and variants underlying these contributions. In order to identify variants and putative gene regulatory mechanisms to explain brain trait GWAS loci including brain structure, function, neuropsychiatric disorders, and cognitive ability, we examined caQTLs and eQTLs with LD-overlap to GWAS loci (table S8). Based on this analysis, we identified 1,684 regulatory elements and 169 genes involved in brain-traits in the vehicle condition (Fig. 6A). The use of stimulated conditions increased the number of brain-trait associated peaks by 72.2% and genes by 57.3% (Fig. 6B), demonstrating that they may explain some of the 'missing regulation' underlying GWAS loci. 6,965 caQTL-GWAS pairs and 1,189 eGene-GWAS pairs were unique to stimulated conditions (Fig. 6C, table S18-19). 27% of eGenes regulated by any eQTL detected in our study that overlapped GWAS loci represent novel overlaps specific to developing hNPCs not previously reported as eQTLs detected in bulk postmortem human brain frontal cortex (GTEx Consortium et al. 2017). Of these eGenes detected only in WNT3A- or CHIR-stimulated conditions, 30% were not identified as eQTLs in adult bulk postmortem frontal cortex from GTEx, showing that stimulus specific eQTLs reveal novel mechanisms underlying GWAS loci undetected without stimulation (table S19).

Among GWAS colocalized regions, 45 caPeaks (7 WNT3A, 38 CHIR) and 5 eGenes (1 WNT3A, 4 CHIR) are regulated by r-QTLs. We highlight two context-dependent colocalizations with r-e/ca-QTLs that we confirmed by conditional analysis. First, a CHIR r-eQTL modulating expression of *ANKRD44* (rs979020-T, Fig. 6D, fig. S19A) colocalized with schizophrenia GWAS and the volume of the left presubiculum body hippocampal subfield (Trubetskoy et al. 2022; Smith et al. 2021). *ANKRD44* encodes an ankyrin repeat domain functioning as a regulatory subunit of protein phosphatase-6 (PP6), an enzyme that regulates the cell cycle and suppresses

NF-kB signaling, a pathway known to engage in cross-talk with Wnt signaling (B. Stefansson et al. 2008; Bastians and Ponstingl 1996; Ziembik et al. 2017; Du and Geller 2010). The T allele of rs979020 is associated with increased expression of *ANKRD44*, decreased risk of schizophrenia, and reduced volume of the hippocampal presubiculum. This colocalization underscores the connection between decreased hippocampal volume and schizophrenia (Roeske et al. 2021; Sasabayashi et al. 2021) and suggests Wnt-responsive regulation of *ANKRD44* in neural progenitors plays a role in the expression of these traits. A second example is the colocalization of a CHIR r-caQTL (rs1992311; Fig. 6E, fig. S20) with a CHIR-responsive *DPYSL5* eQTL signal and a GWAS of average thickness of the isthmus cingulate region. *DPYSL5*, also known as *CRMP5*, has shown to be a negative regulator of neural progenitor proliferation (Veyrac et al. 2011). A Pou5f1::Sox2 motif is predicted to be disrupted by the caSNP in this caPeak (rs4665363-G; fig. S20E) which is likely modulated in the stimulation condition by TCF/LEF binding to motifs present in the same peak. This suggests that rs4665363 is a putative causal variant altering chromatin accessibility and downregulating *DPYSL5* expression, which may lead to increase of average thickness of the isthmus cingulate. We also observed stimulus-specific colocalizations supported by eCAVIAR (fig. S21), including *FADS3* with bipolar disorder (Mullins et al. 2021), and *ENO4* with variants associated with regional cortical surface area including insula (Grasby et al. 2020) (figs. S22-S23). These results highlight that fine-mapping via integrating r-QTLs and GWAS traits support putative regulatory mechanisms that impact brain-related GWAS traits.

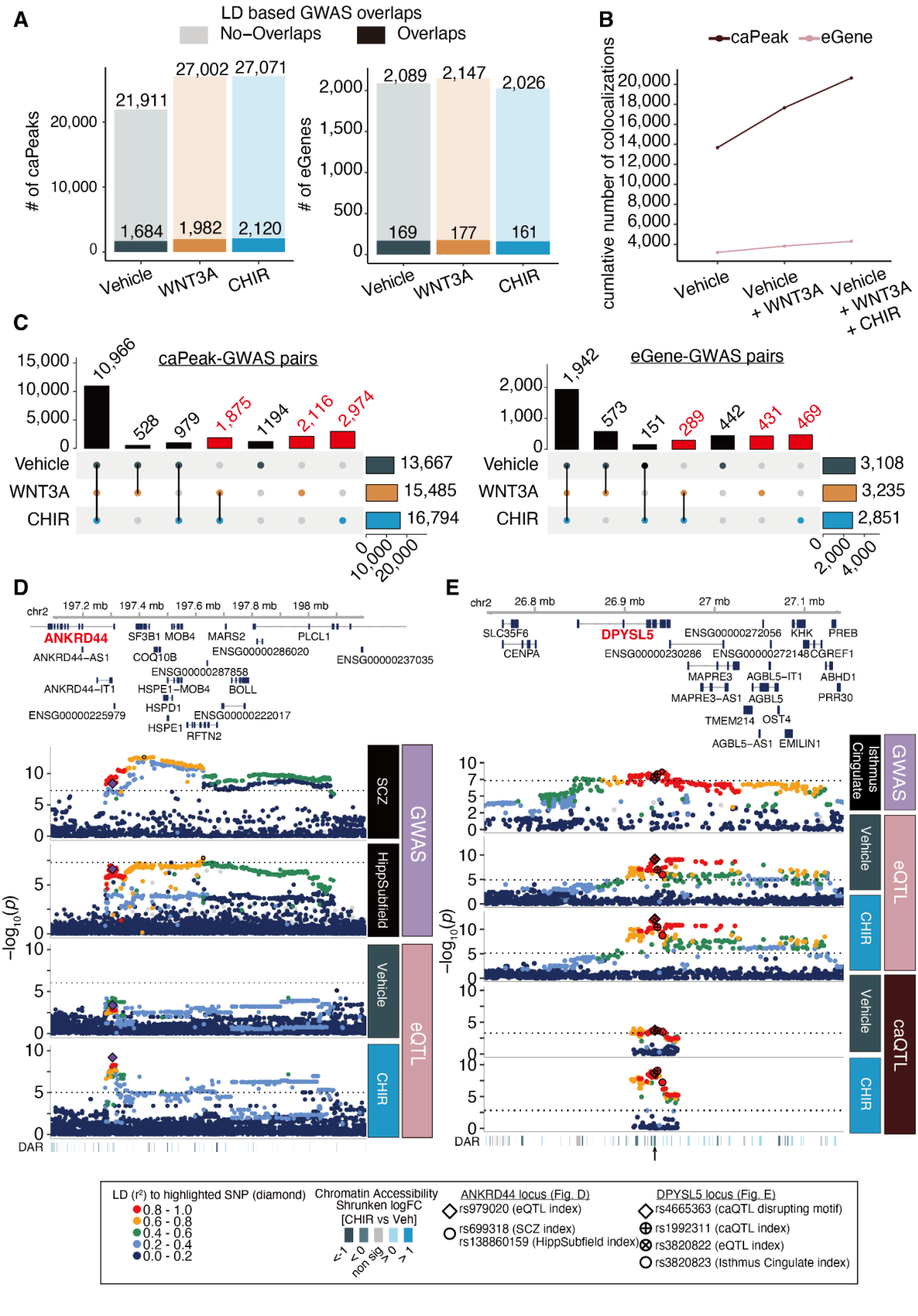
A
LD based GWAS overlaps
No−Overlaps
Overlaps
# of caPeaks
21,911
27,002
27,071
1,684
1,982
2,120
Vehicle
WNT3A
CHIR
# of eGenes
2,089
2,147
2,026
169
177
161
B
caPeak
eGene
cumlative number of colocalizations
Vehicle
Vehicle + WNT3A
Vehicle + WNT3A + CHIR
C
caPeak-GWAS pairs
10,966
528
979
1,875
1,194
2,116
2,974
Vehicle
WNT3A
CHIR
13,667
15,485
16,794
eGene-GWAS pairs
1,942
573
151
289
442
431
469
3,108
3,235
2,851
D
chr2
197.2 mb
197.4 mb
197.6 mb
197.8 mb
198 mb
ANKRD44
SF3B1
MOB4
MARS2
PLCL1
ANKRD44−AS1
COQ10B
ENSG00000286020
ENSG00000237035
ENSG00000287858
ANKRD44−IT1
HSPE1−MOB4
BOLL
HSPD1
ENSG00000225979
ENSG00000222017
HSPE1
RFTN2
SCZ
HippSubfield
Vehicle
CHIR
GWAS
eQTL
−log10(p)
DAR
E
chr2
26.8 mb
26.9 mb
27 mb
27.1 mb
SLC35F6
DPYSL5
ENSG00000272056
KHK
PREB
CENPA
ENSG00000230286
ENSG00000272148
CGREF1
MAPRE3
AGBL5−IT1
ABHD1
MAPRE3−AS1
AGBL5
PRR30
TMEM214
OST4
AGBL5−AS1
EMILIN1
Isthmus Cingulate
Vehicle
CHIR
GWAS
eQTL
caQTL
−log10(p)
DAR
LD (r²) to highlighted SNP (diamond)
0.8 - 1.0
0.6 - 0.8
0.4 - 0.6
0.2 - 0.4
0.0 - 0.2
Chromatin Accessibility Shrunken logFC [CHIR vs Veh]
<−1
<0
non sig
>0
>1
ANKRD44 locus (Fig. D)
rs979020 (eQTL index)
rs699318 (SCZ index)
rs138860159 (HippSubfield index)
DPYSL5 locus (Fig. E)
rs4665363 (caQTL disrupting motif)
rs1992311 (caQTL index)
rs3820822 (eQTL index)
rs3820823 (Isthmus Cingulate index)

Figure 2.6: Using WNT context-dependent gene regulation to inform mechanisms underlying complex brain traits

(A) The number of caPeaks (left) or eGenes (right) overlapping brain-related GWAS loci defined by moderate LD (r^2 > 0.6 in either 1KG EUR population or our study) across vehicle, WNT3A and CHIR conditions. (B) The cumulative number of colocalized caPeaks or eGenes increases across stimulation conditions. (C) Shared or condition-specific caPeaks (left) or eGenes (right) colocalized with brain-related GWAS traits in each condition. Columns labeled in red indicate colocalizations only detected in Wnt-stimulated conditions. (D) Regional association plot depicting colocalization of schizophrenia (top panel) and the volume of a hippocampal subfield (presubiculum body, left hemisphere) GWAS with a CHIR-responsive eQTL modulating *ANKRD44* expression (rs979020-T, CHIR vs vehicle interaction FDR-adjusted *P* = 0.09). From top to bottom: Genomic coordinates and gene models, *P* values for brain-related GWAS, *P* values for condition-specific QTLs discovered in this study, and differentially accessible regions (DAR) within the locus. Differences in the patterns of association are likely due to population differences in LD between the GWAS and QTL studies. (E) Regional association plot depicting colocalization of average thickness of isthmus cingulate GWAS with a CHIR-responsive eQTL modulating *DPYSL5* expression and a CHIR-responsive caQTL (rs1992311, interaction FDR-adjusted *P* = 0.041; chr2:26932281-26934470, in an intron of *DPYSL5*), arranged as in (D).

2.3 Discussion

In this study, we stimulated the Wnt pathway in a library of human neural progenitor cells and measured chromatin accessibility and gene expression across the genome. Wnt stimulation robustly altered chromatin accessibility and gene expression including opening of chromatin at TCF/Lef motifs, and increased expression of known Wnt-pathway target genes including those associated with cell cycle (Nusse and Clevers 2017) (Fig. 1A-F). We defined a

comprehensive set of Wnt-responsive regulatory elements present in human neural progenitor cells, and show that these elements are recruited during stimulation to regulate Wnt-responsive genes, like AXIN2 (Fig. 1G). WREs strongly contribute to heritability for a variety of psychiatric disorders, brain structure, and cognitive traits, implying that these brain-trait associated variants function during patterning of neural progenitors in fetal development and contribute to inter-individual differences in adult brain traits (Fig. 2). Inherent genetic variation in this hNPC library led to significant differences in chromatin accessibility at over 30,000 regulatory elements, and significant differences in gene expression at over 3,000 genes (Fig. 3). Interestingly, Wnt stimulation impacted regulatory elements and genes that were undetected in unstimulated states, and enabled inference of stimulation-specific gene regulatory relationships. Our results show that genetic variation has context-dependent function, even within a single cell-type (Fig. 3,4). Some genetically influenced regulatory elements show evidence of positive selection along the human lineage, indicating they are context-dependent regulatory elements important for the evolution of the human brain (Fig. 5). In addition, genetically influenced regulatory elements and genes revealed additional mechanisms underlying GWAS signals, providing regulatory elements, genes, cell types, and cell states that impact psychiatric disorder risk and other brain-related traits that are candidates for future functional testing (Fig. 6).

These results demonstrate that the function of some genetic variants are dependent on environmental stimuli. New genetic variant function can be revealed through stimulation, where no detectable effect on gene regulation is observed in unstimulated states (Fig. 3,6D). Conversely, genetic variant function can be hidden during stimulation but only revealed in unstimulated states (Fig. 3). Another possibility is that genetic variants can have an effect in both unstimulated and stimulated states, but a stronger effect in one condition showing that the stimulus modulates a variant's effect (Fig. 3,6E). All scenarios indicate that stimulation alters the function of genetic variation and are detectable through interaction analyses, but future

development of statistical tools that can separate these possibilities will aid biological interpretations.

Common genetic variants associated with complex brain traits have low effect sizes individually, but represent an important causal foothold to understand mechanisms underlying neuropsychiatric disorder risk and inter-individual differences in brain traits (Sullivan and Geschwind 2019). Most research focusing on understanding the regulatory function of non-coding genetic variation relies on bulk adult post-mortem tissue which cannot respond to external stimuli and lacks cell-type specificity. Our study addresses this limitation and reveals novel mechanisms underlying GWAS traits, where some colocalizations were undetected by bulk adult post-mortem eQTLs (GTEx Consortium et al. 2017). 30% of unique Wnt stimulus-specific eGenes overlapping brain-trait GWAS, and 57% of genes regulated by primed enhancers were novel compared to post-mortem frontal cortex GTEx eQTLs. While increasing sample sizes using large multi-site consortia-based bulk post-mortem molecular QTLs may also capture some context-specific genetic effects, still 11% of stimulus-specific eGenes overlapping brain-trait GWAS were regulated by novel eQTLs undiscovered by Metabrain, which has >12 times the sample size of GTEx (N. de Klein et al. 2023). These context-specific gains are similar to those reported in a recent study characterizing response-eQTLs in a similar sample size which found 39% novel disease-colocalized eGenes compared to GTEx (Panousis et al. 2023). This suggests that context-specific QTL approaches will yield additional colocalizations relative to post-mortem brain QTLs, which are unable to model stimulus response (Umans, Battle, and Gilad 2020) A growing number of novel context-specific signals underscores that consideration of stimulus, cell-type, and developmental time illuminates some of the 'missing regulation' linking genetic variants to the expression of GWAS traits.

Previous work from our group and others has found that brain-trait associated genetic variants are enriched in regulatory elements present in the fetal brain (Grasby et al. 2020; M. Li et al. 2018; Warrier et al. 2023; Liang et al. 2021; de la Torre-Ubieta et al. 2018). Here, we

extend this work using a study design that employed prenatally-derived primary human neural progenitor cells stimulated with a potent developmental signaling pathway involved in cell proliferation and brain patterning. Our results imply that genetic variants exert context-dependent effects during early neurodevelopment that can lead to differences in adult brain and behavioral traits.

Paired chromatin accessibility and gene expression QTLs allowed us to detect 397 gene regulatory relationships indicative of enhancer priming, where genetic effects on chromatin accessibility are present in both unstimulated and stimulated conditions, but genetic effects on gene expression require a stimulus (Alasoo et al. 2018) (Fig. 4). Bivalent elements are defined as those with both active and repressive chromatin marks. These elements are posited to poise regulatory elements for quick activation of target genes, though little support for this function has been described (Kumar et al. 2021; Macrae, Fothergill-Robinson, and Ramalho-Santos 2023). We found that primed enhancers were less enriched in regions with bivalent chromatin than non-primed elements. While this could be due to differences in eQTL detection power, another possibility is that priming and poising are not necessarily overlapping mechanisms. We hypothesize that bivalent enhancers tend to regulate gene expression that establishes commitment to cell fate decisions and operate on a relatively slower time-scale that requires editing of chromatin modifications (Macrae, Fothergill-Robinson, and Ramalho-Santos 2023). In contrast, primed enhancers may regulate genes in a relatively faster and more plastic manner dependent on binding of stimulus specific transcription factors and do not require both active and repressive chromatin marks.

We noted significant overlap between our caPeaks and regions of rapid evolution in human ancestors defined by cross-species sequence comparisons (HARs/HAQERs) (Mangan et al. 2022; Capra et al. 2013) (Fig. 5). These overlaps provide further evidence that at least some HARs/HAQERs are indeed functional stimulus-specific regulatory elements active during brain development. Most previous research to understand the function of these regions has been

conducted in post-mortem tissue or unstimulated cells, but here we show that consideration of developmentally relevant cell-types and stimuli can identify undiscovered functions of regulatory elements important for human-specific evolution (Girskis et al. 2021; Won et al. 2019; Mangan et al. 2022). A striking example was identified at an overlap of the HARE5 distal enhancer of FZD8, where the human ortholog has been shown to drive brain enlargement by accelerating the cell cycle in neural progenitor cells when expressed as a transgene construct in mice (Boyd et al. 2015). Here, we were able to additionally confirm that this HAR has regulatory function in the endogenous human genome within neural progenitor cells and is Wnt sensitive. Interestingly, this HAR-overlapping caPeak also harbors common genetic variation within a Lef binding site that alters its chromatin accessibility, showing that HARs tolerate functional variation. Similarly, HAQERs are highly mutable and enriched for common genetic variants associated with a variety of neuropsychiatric disorders, further supporting that genetic variation within evolutionarily relevant hot-spots influences the expression of complex brain traits (Doan et al. 2016). Because common genetic variants within both HARs and HAQERs can influence local chromatin accessibility, we speculate that these annotations represent functional regulatory elements that affect hNPC developmental fate decisions driving human-specific cortical expansion and in turn may influence brain-related traits.

caQTL and eQTL mapping revealed novel effects of common genetic variants undetected in unstimulated states. While sample size limits QTL discovery, and especially response-QTL power, we discovered thousands of Wnt stimulus-specific caPeaks and eGenes. Genetic effects detected under unstimulated conditions replicated those found in previous studies of unstimulated hNPC QTLs, underscoring the robustness of in vitro QTL study design. We focused on studying genetic variation during stimulation of the well-studied and developmentally important Wnt signaling pathway, because alterations in this pathway have been associated with risk for neuropsychiatric disorders, all brains are exposed to this stimulus during development, activators and inhibitors are available, and the downstream effectors of the

signaling pathway on gene expression are well-characterized (Chenn and Walsh 2002; D. V. Hansen, Rubenstein, and Kriegstein 2011; Harrison-Uy and Pleasure 2012; Grasby et al. 2020; Evgrafov et al. 2020; Topol et al. 2015; Marchetto et al. 2017; Krumm et al. 2014; Caracci et al. 2021; Pasko Rakic 2009). Expansion of this approach in large populations of primary human neural progenitor cells or induced pluripotent stem cells can investigate other gene-by-environment interactions in a dish. Specifically, similar study designs evaluating stimulation for different durations, stimulation of additional signaling pathways relevant to brain development (T. Sun and Hevner 2014), exposures to environmental insults (Jerber et al. 2021), responses to clinically useful drugs (Wolter, Le, et al. 2022) or modulation of neuronal activity (Boulting et al. 2021), may reveal additional genetic effects that are masked in QTL studies conducted in bulk post-mortem tissue.

2.4 Materials and Methods

Ethics statement for human tissue-derived cell-lines

This study followed IRB regulations to derive human NPC cell-lines from prenatal tissue collected at the UCLA Gene and Cell Therapy facility following voluntary termination of pregnancy.

Generation of hNPC lines

Fetal brain tissue visually consistent with dorsal telencephalon morphology (flat and sheet-like) was collected at 14-21 gestation weeks from presumed neurotypical donors to derive primary human NPCs as previously described (Aygün et al. 2021; Stein et al. 2014; Liang et al. 2021). To summarize, tissue was dissociated into single cells which were cultured as neurospheres before transfer to fibronectin (Sigma F1141) and Poly-L-Ornithine (Sigma P3655) coated plates. Neuronal differentiation was suppressed to maintain NPCs in a proliferative state by following previously established culture methods (Liang et al. 2021). After 2-3 passages, NPC lines were cryopreserved and transferred to UNC Chapel Hill. NPC media: Neurobasal A (Life Technologies 10888-022) supplemented with 100 μg ml^{-1} primocin (Invivogen ant-pm-2), 10% BIT 9500

(Stemcell Technologies 09500), 1% glutamax (100x; Life Technologies 35050061), 1 $\mu g\ ml^{-1}$ heparin (Sigma-Aldrich H3393-10KU), 20 $ng\ ml^{-1}$ EGF/FGF (Life Technologies PHG0313/PHG0023), 2 $ng\ ml^{-1}$ LIF (Life Technologies PHC9481) and 10 $ng\ ml^{-1}$ PDGF (Life Technologies PHG1034).

hNPC cell culture and WNT-stimulation

We cultured cryopreserved hNPCs in batches of 8 cell lines per week, pseudo-randomizing each experimental group for biological variables (sex and donor gestation week), and technical variables (passage number). Following a two-week expansion period, we plated 400k NPCs per well of a 6-well plate for each cell-line. Next, we exposed each well to either vehicle (Neurobasal A media supplemented with PBS+0.1%BSA and DMSO), 5nM WNT3A in PBS+0.1% BSA, or 2.5uM CHIR in DMSO for 48h. All exposures were prepared such that equal volumes were applied for each stimulated condition, including a "balancer" solution composed of culture media, PBS+0.1% BSA, DMSO, and water in order to standardize diluents across all exposures. We focused on this time-point because Wnt target gene expression was maximized in hNPCs after 48h exposure to 10uM CHIR in previous experiments (Wolter, Le, et al. 2022). The well-position of each exposure was rotated every week of the experiment to minimize the potential effects of plate position. After 48h exposure to stimuli or vehicle, cells were lifted with Accutase (Thermo Fisher Scientific A1110501) for preparation of ATAC-seq and RNA-seq libraries. We generated 2-6 separately cultured replicates for each of 6 randomly selected donors to measure technical variation across the experiment. We utilized cell culture media, growth factors, additives, and WNT-stimulating exposures from the same manufacturer lots across the entire experiment, whenever possible, to mitigate potential batch effects. When it was not possible to use the same lot of reagent, this information was recorded. One individual (JMV) performed all hNPC cultures and exposures to stimuli to minimize variance in handling effects. The investigators were not explicitly blinded to the donor during cell culture or library preparation. However, the

investigators did not have knowledge of donor genotype when performing cell culture or library preparation. Regular pre-assay screening detected no mycoplasma contamination (ATCC 30-1012K).

hNPC Wnt activity luciferase assays

Canonical Wnt pathway signaling activity was measured via a luciferase reporter assay (fig. S2A-C). After two weeks of hNPC culture expansion as described above, we lifted cells with 0.05% trypsin (Gibco 25300062) and plated 10k cells counted by hemocytometer per well of 96-well plates (Corning 07-200-91). Cells were transduced with 10uL lentivirus carrying BAR:Luciferase and Tk:Renilla constructs 24 hours after plating. Plasmids were generous gifts from the lab of Ben Major (Major et al. 2007) and lentivirus was generated as previously described (Wolter, Le, et al. 2022) . After a two-day incubation, cells were exposed with either vehicle, CHIR, or WNT3A as described above. 48 hours later, cell lysates were collected and luminescence measured using the Dual-Glo luciferase system (Promega E2920) on the GloMax Discover plate reader (Promega). β-Catenin induced BAR:Luciferase signal was normalized by Renilla luminescence from the constitutively active Tk promoter.

hNPC proliferation assays

After two weeks of hNPC culture expansion as described above, we lifted cells with 0.05% trypsin (Gibco 25300062), and plated 12.5k cells counted by hemocytometer per well of 96-well plates (Corning 3610). We generated 4 technical replicate wells for each concentration of Wnt-activating stimulus or vehicle, and 8 technical replicate wells for vehicle exposures per hNPC donor cell-line, distributing replicates across each culture plate to mitigate potential artifacts introduced by plate position. One day later, vehicle or Wnt activating stimuli were applied, as described above. 46 hours later, we exposed cells with 10 μM EdU with a 10% media addition for 2 hours. hNPCs were collected and fixed via a 10-minute incubation in 4% paraformaldehyde in phosphate-buffered saline. On these cells, we labeled total DNA content with FxCycle Far Red dye (Thermo Fisher Scientific F10347) and performed Click-iT EdU-incorporation assays (Thermo

Fisher Scientific C10337) according to the manufacturer's protocols. We quantified EdU and FxCycle signals using the Attune NxT 96-well Flow Cytometer (Thermo Fisher Scientific) (fig. S2D-F), or via high content imaging on the Nikon Eclipse Ti2 microscope followed by manual quantification with Fiji (fig. S2G-H). Flow cytometry data was processed with FlowJo v10.7.1 and cell-cycle populations defined by automated gating with FlowDensity software (Malek et al. 2015). Detailed methods for analysis of flow cytometry can be found in previous work (Wolter, Le, et al. 2022).

ATAC-seq Library preparation

Cells were lifted and counted to isolate 50k cells per sample to be used as input for the Omni-ATAC protocol for library preparation (Corces et al. 2017). To summarize, 50k nuclei from fresh NPCs were counted via hemocytometer and tagmented using TDE1 enzyme (Illumina 20034198) and tagmentation buffer composed of 20mM Tris-HCl pH 7.6, 10mM $MgCl_2$, and 20% Dimethyl Formamide. All libraries were PCR amplified (NEB M0544S) for 5 cycles, and then each library was further amplified for a sample-specific additional number of cycles (average 2 additional cycles across all samples) determined by a qPCR side reaction to avoid overamplification. Nextera-compatible unique dual-indexing primers barcoded each sample during amplification (Illumina 20027213). We purified libraries to remove primer dimers and eliminate fragments over 1000bp (Roche 07983298001). We validated ATAC-seq library quality before sequencing for a subset of samples by observing appropriate nucleosomal banding patterns via capillary gel electrophoresis on an Agilent 4150 TapeStation system (Agilent 5067-5584). We then pooled ~70 ATAC-seq libraries with unique barcodes in each of four pools, and sent pooled libraries for multiplexed sequencing. One individual (BDL) generated all ATAC-seq library preparations in order to minimize batch effects introduced by handling variance.

RNA-seq Library Preparation

Total RNA was isolated from each hNPC line and condition using all cells remaining (average 1.1M cells per sample) after removing 50k cells for ATAC-seq library preparation as

described above. For each experimental week, hNPCs were lifted with Accutase (Thermo Fisher Scientific A1110501), lysed, and stored in TriZol (Thermo 15-596-026) at -80C for subsequent purification of total RNA using RNeasy Mini Kits and on-column DNase digestion (Qiagen 74106, 79256). All RNA extractions were performed by the same individual (JTM) to minimize potential batch effects introduced by handling. We quantified RNA isolates using fluorescence-based Quant-iT RNA assay kits (Thermo Q33140). Mean RNA integrity number (RIN) across all samples was 9.86 (SD = 0.39). Library preparation was performed using a stranded total RNA kit (KAPA KR0934) after samples were depleted of ribosomal RNA (KAPA KR1151).

Sequencing of ATAC-seq and RNA-seq libraries

ATAC-seq libraries were sequenced at the NYGC to an average read depth of 49M (SD = 13.6M) paired-end reads (2x100bp) per sample on the Illumina Novaseq platform. Total RNA-seq libraries were sequenced at the NYGC to an average sequencing depth of 55M (SD = 13M) paired-end reads (2x100bp) per sample on the Illumina Novaseq platform.

Genotyping and imputation

hNPC genotypes were obtained from genomic DNA isolated with DNeasy Blood and Tissue Kit (QIAGEN 69504) using Illumina's HumanOmni2.5 platform. Additional variants were imputed using the TOPMed freeze 5 reference panel (Taliun et al. 2021) with minimac4 software (Das et al. 2016) on the University of Michigan Imputation server. We performed quality control, pre-processing, and filtering of SNPs with PLINK v1.9 (Chang et al. 2015) as previously described (Liang et al. 2021) based on Hardy-Weinberg equilibrium, minor allele frequency, individual missing genotype rates, and variant missing genotype rate (plink --hwe 1e-6 --maf 0.01 --mind 0.1 --geno 0.05).

ATAC-seq data preprocessing

FastQC (v0.11.9) ("Babraham Bioinformatics - FastQC A Quality Control Tool for High Throughput Sequence Data" n.d.) and MultiQC (v1.7) (Ewels et al. 2016) software performed quality control for all ATAC-seq libraries before and after trimming sequencing adapters with

BBMap (v38.98) ("BBMap" 2022). We then mapped ATAC-seq reads to the hg38 reference genome with the Burrows-Wheeler Alignment tool (BWA-MEM v0.7.17) (H. Li and Durbin 2009). We then refined alignments to minimize mapping bias at sites where ATAC-seq reads overlapping bi-allelic SNPs using imputed genotypes by re-mapping and removing duplicate reads with WASP (v0.3.4) (van de Geijn et al. 2015). Samtools (v1.16) (Danecek et al. 2021) then removed unmapped or mitochondrial reads and bedtools (v2.3) (Quinlan and Hall 2010) removed reads mapped to genomic blacklist regions as defined by ENCODE (Luo et al. 2020). ATAC-seq read metrics during and following preprocessing were calculated using picard (v2.21.7) ("Picard" n.d.) and ataqv software (v1.0.0) (Orchard et al. 2020) (fig. S4). We evaluated cross-sample contamination using verifyBAMID (Jun et al. 2012), and omitted samples with FREEMIX or CHIPMIX scores greater than 0.02. We also omitted samples with low transcriptional start site enrichment (TSSe < 5) and aberrant short read/mononucleosomal read ratios (S/M <1 or S/M > 7). In total, 51 samples were omitted by these criteria. Principal component analysis (PCA) on ATAC-seq samples separated samples by stimulus condition, and not by sex or other biological or technical variables in the first two principal components (PCs) of variance (fig. S5). Sex and Donor ID, which captures cell-line intrinsic effects for each hNPC showed some correlation with other PCs, leading us to include these variables in QTL models described below and use residualized data following regression of PCs 1-10.

Chromatin Accessibility Peak Calling

After selecting a single ATAC-seq replicate for each donor-condition pair based first on whether stimulated conditions and vehicle were cultured in the same plate, and subsequently on on QC metrics, we called chromatin accessibility peaks from ATAC-seq reads using all samples excluding technical replicates with CSAW's (v1.28) (Lun and Smyth 2016) *windowCounts* function with the options (ext = *mean length of fragments*, filter = *5 * sample number* spacing = *10*, param = pe.param) where pe.param were *max.frag = 1500, pe='both', minq=20*. Windows within 100bp were merged with the *mergeWindows* function. Read counts were normalized

accounting for GC-content via conditional quantile normalization with cqn software (K. D. Hansen, Irizarry, and Wu 2012).

Differential chromatin accessibility analysis

We ran DEseq2 for the read counts described above to identify peaks with differential accessibility due to stimulus condition, called WREs. The comparisons were performed as paired tests within donor, hence, the model was set to *Peak Accessibility ~ Donor ID + stimulus_condition*, where Donor ID and stimulus condition were factor variables. We repeated this analysis for each WNT stimulus condition vs vehicle pairs (e.g. WNT3A vs Vehicle and CHIR vs Vehicle) or WNT3A+XAV vs WNT3A. FDR-adjusted $P < 0.1$ was used as the significance threshold.

RNA-seq data pre-processing and analysis

Similar to the preprocessing of ATAC-seq data described above, we initially screened RNA-sequencing libraries using FastQC and MultiQC. We then trimmed sequencing adapters and mapped reads to genes as annotated by Ensembl v104 for the hg38 reference genome using the STAR aligner (v2.7.7a) (Dobin et al. 2013). We filtered samples with (1) low RIN score (<7), (2) low unique mapped rate (< 80%), (3) high mismatched rate (>50%), (4) high multi-mapping rates (>8%), (5) high duplicated read rates (> 30%), or (6) FREEMIX or CHIPMIX scores from verifyBAMID greater than 0.02. QC filtering by these criteria removed 27 samples, and retained a total of 242 samples. Transcripts were collapsed using collapse_annotation.py (https://github.com/broadinstitute/gtex-pipeline/tree/master/gene_model) into a single gene model and gene-level reads were summarized for each sample using featureCounts from Rsubread (v2.8.2) (Liao, Smyth, and Shi 2019). As with the ATAC-seq samples, we performed PCA and found that the RNA-seq samples clustered according to stimulus condition and not sex, RIN, or other variables in PC1 vs PC2 plots (fig. S5). Again, some PCs correlated with hNPC donor sex and RIN, indicating that we should include these variables in the QTL models described below for data corrected for PCs 1-10. Significantly higher pair-wise correlations within RNA-seq sample

technical replicates generated for the same hNPC donor and condition ("within donor") compared to correlation across distinct donors (Evaluated by the Welch two sample t-test) supports the technical reproducibility of the RNA-seq dataset (fig. S3).

After selecting a single RNA-seq replicate for each donor-condition pair based first on whether stimulated conditions and vehicle were cultured in the same plate, and subsequently on QC metrics, DESeq2 (Soneson, Love, and Robinson 2015) was used to assess differential gene expression from RNA-seq reads mapped to protein-coding genes or lncRNA where at least 1% of samples in either condition show at least 10 normalized counts. We evaluated the model *RNAseq Count ~ RIN + Donor ID + stimulus_condition* to identify DEGs. In this model, we represented RIN as a numeric variable and Donor ID and stimulus condition as factor variables. Shrunken log2 fold change (LFC) (Love, Huber, and Anders 2014) was used for estimating dispersions and FDR-adjusted *P*-value < 0.1 was used as significance threshold.

Pathway enrichment analysis on differentially expressed genes

To determine pathways enriched in DEGs, we first obtained up-/ down-regulated genes in WNT stimulus condition as compared to vehicle (shrunken LFC > 0, < 0, respectively; and FDR-adjusted $P < 0.1$). All genes included in DEG analysis were used as the background. For both DEG and background genes, we restricted the analysis to protein-coding genes located outside the MHC region (chr6:28,510,120-33,480,577). Analysis was run by g:COSt from g:profiler (Reimand et al. 2007) for KEGG and REACTOME pathways (Ogata et al. 1999; Croft et al. 2011). FDR-adjusted $P < 0.1$ was used as the statistical significance threshold.

Motif Enrichment Analysis

We tested differential transcription factor (TF) motif enrichment within WREs, primed-caPeaks, or response-caPeaks for 841 predicted human TFs in JASPAR 2022 (Castro-Mondragon et al. 2022) core database (taxonomic group = vertebrates), using data downloaded from http://expdata.cmmt.ubc.ca/JASPAR/downloads/UCSC_tracks/2022/hg38/ (data access date: May 4th 2022). We restricted analysis to TFBS motifs within conserved regions, defined by 100-

way phastCons scores > 0.4 downloaded from UCSC Genome Browser in regions ≥ 20bp (Pollard et al. 2010). For WREs, estimated TFBS motif enrichment within the top 2,000 chromatin accessibility peaks representing chromatin regions gained or lost in each stimulus condition (|LogFC| at FDR-adj $P < 0.1$ as compared to vehicle) to avoid bias introduced by the different number WREs across conditions. We ran a logistic regression to identify TF motifs observed more often in opened vs. closed peaks or response vs. non-response peaks while accounting for differences in peak width and percentage of peaks in conserved regions using the following model: *glm(TFBS ~ peaktype + peadkwidth + conservedbppercent, family ='binomial'),* where *TFBS* is a binary outcome that indicates whether each differentially accessible peak overlaps with TF binding sites, *peaktype* indicates open/closed WREs, or response/non-response caPeaks for each stimulus condition, *peadkwidth* indicates window size of peak and *conservedbppercent* indicates percentage of conserved regions (*conserved bp / peak width*). We considered estimated effects of *peaktype* on TFBS motif presence with FDR-adjusted $P < 0.1$ as statistically significant.

Correlation between chromatin accessibility and gene expression

We estimated Pearson's correlation between chromatin accessibility and gene expression using variance stabilizing transformation (VST) normalized ATAC-seq and RNA-seq read counts residualized by 10 global chromatin peak or gene expression PCs, respectively. For each condition, we tested all peaks located within 1Mb from the transcription starting site (TSS) of each gene. FDR-adjusted $P < 0.1$ was used for the statistical significance threshold.

Disease enrichment analysis using differentially expressed genes

We performed disease enrichment analysis for each DEG category (all-regulated/non-DEGs) using disease_enrichment() function implemented in disgenet2r (Piñero et al. 2020). Disease enrichments referenced "CURATED" genes from 4,254 diseases from the DisGeNET database (Piñero et al. 2020), and we classified results with FDR-adjusted $P < 0.1$ generated by the disease_enrichment() function as significant. Due to limited space, we only presented diseases

if disease_semantic_type is either “Mental”, “ Behavioral Dysfunction”, “Individual Behavior” or “Mental Process” in Fig. 2. Full lists are provided in table S7.

Partitioning GWAS heritability by WREs

We first assessed the contribution of regulatory elements including tissue-type-specific or cell-type-specific regulatory annotations to the overall heritability of brain-related and other traits (table S8). Analyses were performed using Stratified LD Score regression (S-LDSC) (Finucane et al. 2015; Gazal et al. 2017) (v1.0.0) including the baseline-LD model (v1.2). Annotations included (1) Active enhancer or promoter states in fetal brains (female/male). Active enhancer and promoter regions were defined based on chromatin states predicted by chromHMM (Ernst and Kellis 2012) and included: ‘active transcription start site’, ‘flanking active TSS’, ’genic enhancers’, and ’enhancers’ in the core 15-state model (https://egg2.wustl.edu/roadmap/web_portal/chr_state_learning.html). (2) Progenitor-specific chromatin accessible regions were defined as logFC > 0 and FDR-adjusted $P < 0.1$ as a comparison to differentiated neuronal cells. ATAC-seq data were obtained from our previous work (Liang et al. 2021). (3) Open or closed chromatin accessible regions by stimulus condition compared to vehicle conditions were defined by logFC > 0 or logFC < 0, FDR-adjusted $P < 0.1$ and identified in the current study as WREs. For (3), we included non-WREs (FDR-adjusted P > 0.1) in the model to test the specificity of WREs. We obtained publicly available GWAS summary statistics for testing partitioned heritability. The details of GWAS are provided in table S8. For each GWAS summary statistics, SNPs were filtered to those found in HapMap3 (The International HapMap 3 Consortium 2010) using munge_sumstats.py provided by LDSC. The pre-computed LD scores for the European population from the 1,000 Genome Project Phase 3 (1KG) (1000 Genomes Project Consortium et al. 2015) were downloaded from https://data.broadinstitute.org/alkesgroup/LDSCORE/eur_w_ld_chr.tar.bz2. Enrichment was assessed using *P*-values calculated by the annotation's standardized effect size (tau) that was conditioned on other annotations included in the model. FDR-adjusted $P < 0.1$ was used for

statistical significance threshold. We note that we also performed this analysis with a more stringent threshold (FDR-adjusted $P < 0.01$) for defining WREs, which was then used to perform S-LDSC partitioned heritability enrichments. The correlation of results from these two different thresholds was high ($r > 0.85$) (fig. S14).

caQTL and response-caQTL mapping

caQTL analyses within each condition (Vehicle, WNT3A, CHIR) were performed using the joint model implemented in RASQUAL (Kumasaka, Knights, and Gaffney 2016) which integrates both between-individual signals and allele-specific signals within individuals. Previously described cqn normalization factors were used as sample specific offsets. Covariates were included consisting of 10 count-based principal components and 10 multidimensional scaling (MDS) genotype components to reduce the confounding effects of technical factors and population structure, respectively. Variants were tested according to the following criteria (1) in a given accessible region or within +/- 25kb (2) minor allele frequency (MAF) ≥ 1% (3) Hardy-Weinberg equilibrium < 0.000001 (4) imputation quality ≥ 0.3 (5) at least two individuals have minor homozygous allele or heterozygous allele. Multiple testing correction followed a hierarchical correction procedure (Aygün et al. 2021; Q. Q. Huang et al. 2018) consisting of (1) adjusting nominal *P*-values of all SNPs for each peak separately using the eigenMT method (Davis et al. 2016) (2) BH procedure was then applied to these locally adjusted *P*-values to determine globally adjusted *P*-values lower than 0.1 (3) To determine other independent SNPs for each peak, the maximum nominal *P*-value from step 1 corresponding to a globally adjusted *P*-value of 0.1 was used as a significance threshold. Due to limitations of RASQUAL, conditional analysis, where the top caSNP was controlled for in the association model to find additional independent signals, was not possible. To determine signals most likely to be distinct from the lead for each peak a LD threshold of < 0.2 was used iteratively until no additional significant caQTL remained. Response caQTL interaction analyses between vehicle and each WNT-stimulus condition (WNT3a or CHIR)

used the R package lme4 to evaluate the following linear mixed model for all index caQTL with main effects (n_{caSNP} = 136,163 (WNT3A_Vehicle pairs), 136,641 (CHIR_Vehicle pairs)):

$$adjCounts = SNP + condition + condition{:}SNP + covariates + (1|Donor)$$

where condition = 0 or 1 (Veh or WNT activators, respectively). The first 10 count-based PCs were used as covariates. We compared the fit of the model above with and without the condition:SNP interaction term to assess significance. BH was then used to adjust for multiple testing (FDR-adjusted $P < 0.1$). We also ran this analysis with a more stringent threshold (FDR-adjusted $P < 0.01$) and our conclusions remain robust to the choice of threshold (fig. S14).

cis-eQTL and response-eQTL mapping

Cis-eQTL analyses within each condition (Vehicle, WNT3A, CHIR) were performed using a linear mixed model implemented in limix_qtl (Cuomo et al. 2021) (https://github.com/single-cell-genetics/limix_qtl), an optimized version of limix (Casale et al. 2015). The following genes and SNPs were tested: *Gene*: (1) at least 1% of samples in the condition have at least ≥ 10 normalized counts; (2) protein-coding gene or lncRNA; SNP: (1) located in gene body or within +/- 1Mb from gene body. (2) minor allele frequency (MAF) ≥ 1% (3) Hardy-Weinberg equilibrium < 0.000001, (4) imputation quality ≥ 0.3, (5) at least two individuals have minor homozygous allele or heterozygous allele). We used the following model:

$$adjE = SNP + \varepsilon$$

where *adj*E is VST-normalized gene read count and further corrected with 10 principal components across the gene expression matrix, that were chosen to maximize the number of eQTLs (fig. S24), SNP is a genotype (0/1/2), ε is an error term with $cov(\varepsilon) = (\sigma^2_u u_K + \sigma^2_e I)$ where u_K is the kinship matrix, σ^2_u Is the variance attributable to genetic relatedness, and σ^2_e is the variance attributable to random noise. The kinship matrix was generated by pcrelate() function in GENESIS (v2.14.1) (Conomos et al., n.d.; Gogarten et al. 2019) with 10 PCs to control ancestry population structure.

Gene-level multiple corrections were done for each gene by permutation test implemented in limix_qtl, then applied BH-FDR for global correction. eSNP-eGene pairs with FDR-adjusted $P < 0.1$ were considered as statistically significant eQTLs. The impact of using a more stringent significance threshold (FDR-adjusted $P < 0.01$) is provided in the fig. S14D. Those eGenes were further tested for independent signals through conditional testing, whereby the index eSNP is included as a covariate in the association model. For visualization purposes, we set the significance line threshold for loci with no significant eQTL in the condition as follows. First, we obtained the maximum permutation test *P*-value satisfying FDR-adjusted $P < 0.1$ (max_permP). Then, we estimated the median of the maximum raw *P*-value less than max_permP across eGene as the significant line threshold.

Response eQTL interaction analyses between vehicle and each WNT-stimulus condition (WNT3A or CHIR), were also performed by limix_qtl for all index eQTLs with main effects (n_{eSNP} = 2,966 (WNT3A_Vehicle pairs), 2,906 (CHIR_Vehicle pairs)). The interaction term for the model:

$$adjE = SNP + condition + condition{:}SNP + \varepsilon$$

was tested to identify interaction effects between SNP and condition where condition = 0 or 1 (Vehicle or WNT activators, respectively), and ε is defined as above. We used BH to adjust multiple testing (FDR-adjusted $P < 0.1$).

Effects of ca/eQTLs on transcription factor binding sites

We used motifBreakR (v.2.6.1) (Coetzee, Coetzee, and Hazelett 2015) to assess the impact of genetic variants within peaks on TF binding motifs surrounding significant caSNP-caPeak associations (parameter setting, threshold of $1x10^{-4}$) (Touzet and Varré 2007) (**table S12**). Annotated motifs (839 total TF motifs) from JASPAR2022 vertebrate were used in MotifDb (v1.37.1) (Shannon and Richards 2022). Relative entropy (parameter setting method, 'ic') for both reference and alternative allele was calculated and only TFBSs strongly affected by the SNPs (parameter setting effect, 'strong') were retained.

Support for context-specific caQTLs from SNP-SELEX experiments

Experimental SNP-SELEX data (Yan et al. 2021) was downloaded from https://renlab.sdsc.edu/GVATdb/ and used to evaluate whether caSNPs from our study altered TF-binding. Because the SNP-SELEX study only evaluated a subset of the SNPs we tested for genetic effects on chromatin accessibility, we considered all local SNPs with linkage disequilibrium $r^2 > 0.6$ from the index caSNP in our study. The percentage of caQTL loci with caSNPs altering TF binding was calculated by dividing the number of those caQTL loci where at least one linked caSNP had a significant protein-binding score (PB score) by the total number of caQTL loci with at least one linked caSNP tested via SNP-SELEX. After evaluating the level of experimental support for the top 1000 significant caQTLs (and the surrounding linked caSNPs) with the smallest *P*-values in each condition, we compared this to the mean level of support for 100 random samples of 1000 non-significant caSNPs and their surrounding linked caSNPs (fig. S12).

Determining Primed Enhancer Candidates

caPeaks sites were assessed for patterns indicative of priming or stimulus-specific signals within each Vehicle-WNT stimulus pair. caPeak and eGene overlaps were determined where a caPeak was within 1Mb of an eGene and at least 1 significant SNP in both datasets were in LD $r^2 \geq 0.8$ (table S17). Priming signals were called based on: (1) significant caPeaks common to both Vehicle and WNT stimulus condition, (2) only those loci which overlapped an eGene signal, and (3) a significant eGene was found specifically in the WNT stimulated condition. Stimulus-specific signals were assessed following the same criteria but filtering to significant caPeaks specific to the WNT stimulus.

Genomic Feature Enrichment Analysis

Primed and non-primed caPeaks were evaluated for overlaps within each Vehicle-WNT stimulus pair for overlaps with the 15 core chromHMM states defined in fetal brain male (E081) (Roadmap Epigenomics Consortium et al. 2015). All unique caPeaks across both WNT stimulated

conditions were subset into response and non-response sets and overlapped with the same chromHMM states. HAQERs (1,581 total) and HARs (2,751 total after liftover from hg17 to hg38) were downloaded from previous papers and were also assessed for overlaps with genetically regulated caPeaks within each condition (Mangan et al. 2022; Capra et al. 2013). Significance of enrichment of overlaps with previously annotated genomic features within each of these datasets were then assessed using a binomial test (McLean et al. 2010). The method determines if the number of evolutionarily annotated genomic regions falling into the proportion of the genome annotated as caPeak/eGene is beyond that expected by chance, using a binomial test. Neighborhood enrichment scores were calculated using a previously defined method (Roadmap Epigenomics Consortium et al. 2015). The differences in enrichment between two annotations was calculated with Fisher's exact test.

Shared eSNPs/caSNPs and GWAS SNPs

We assessed colocalization between all ca/e-QTL variants identified in our study and GWAS signals in brain-related traits (tables S8, S18 and S19) through a three-step process. First, we extracted all GWAS lead ($P < 5x10^{-8}$) SNP-ca/eQTL pairs located within 1Mb from each other. Second, we selected GWAS-QTL pairs for which index SNPs are in LD ($r^2 > 0.6$) in either population (1KG EUR or samples used in this study). To consider the possibility of undefined secondary GWAS signals, we also selected GWAS-QTL pairs for which at least one non-index but genome-wide (GW) significant ($P < 5 \times 10^{-8}$) GWAS SNP was in LD with an ca/eQTL index SNP. We tested two colocalization approaches and reported if either approach suggested colocalization. As the first approach, we estimated residual GWAS association statistics after conditioning ca/eQTL index SNPs. We performed approximate conditional analysis using default GCTA settings on variants within 1Mb of those variants (Yang et al. 2011, 2012). We used a subset of 40,000 European-ancestry UKBB participants for the LD reference panel (https://www.ukbiobank.ac.uk/). We excluded variants from GCTA output if the frequency of effect allele differed by >0.2 between UKBB and GWAS summary results, and masked

approximate conditional results if variants exceeded a collinearity threshold of 0.9 with the ca/eQTL index SNP. The second approach was to use eCAVIAR (Hormozdiari et al. 2016). We calculated SNP-level colocalization posterior probability (CLPP) for each SNP in a locus that passed the previous two steps. CLPP was estimated by eCAVIAR (Hormozdiari et al. 2016) for SNP at P < 0.05 in both GWAS and QTL. We considered any locus with CLPP > 1% and r^2 between causal SNP and at least one of GW SNPs in the region > 0.8 as evidence of colocalization in this approach. False positives for QTL condition-specificity could occur due to insufficient power limited by sample size. Thus, we repeated eCAVIAR to salvage potentially shared eGene/caPeak-GWAS pairs that failed to meet FDR-adjusted significance thresholds ($P < 0.1$), but passed the raw significance threshold ($P < 10^{-6}$) for QTL mapping under a particular condition, and showed shared caPeak/eGene-GWAS pairs under a separate condition. To evaluate the novelty of context-specific eQTL signals, we asked whether eQTLs regulating unique eGenes discovered in this study and their locally linked SNPs (LD $r^2 < 0.6$) were significant in frontal cortex GTEx v8 (GTEx Consortium 2020) or MetaBrain (N. de Klein et al. 2023) eQTL data.

2.5 Supplemental Figures

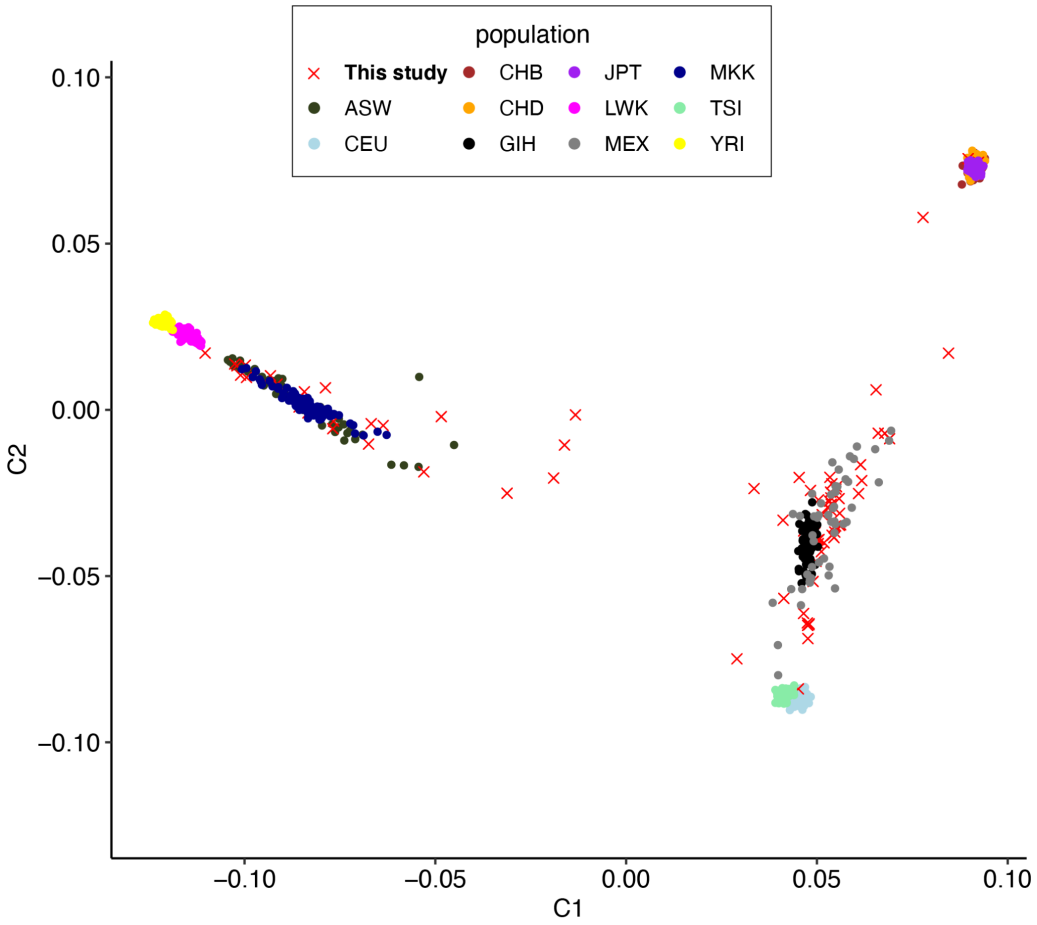

Supplementary Figure 2.1: Multidimensional scaling analysis of genotype data

Multi-dimensional scaling (MDS) plot shows the first two components of genetic similarity for all HapMap populations and donors in this study, allowing inference of genetic ancestry. Multiple ancestries of donors are present in this population.

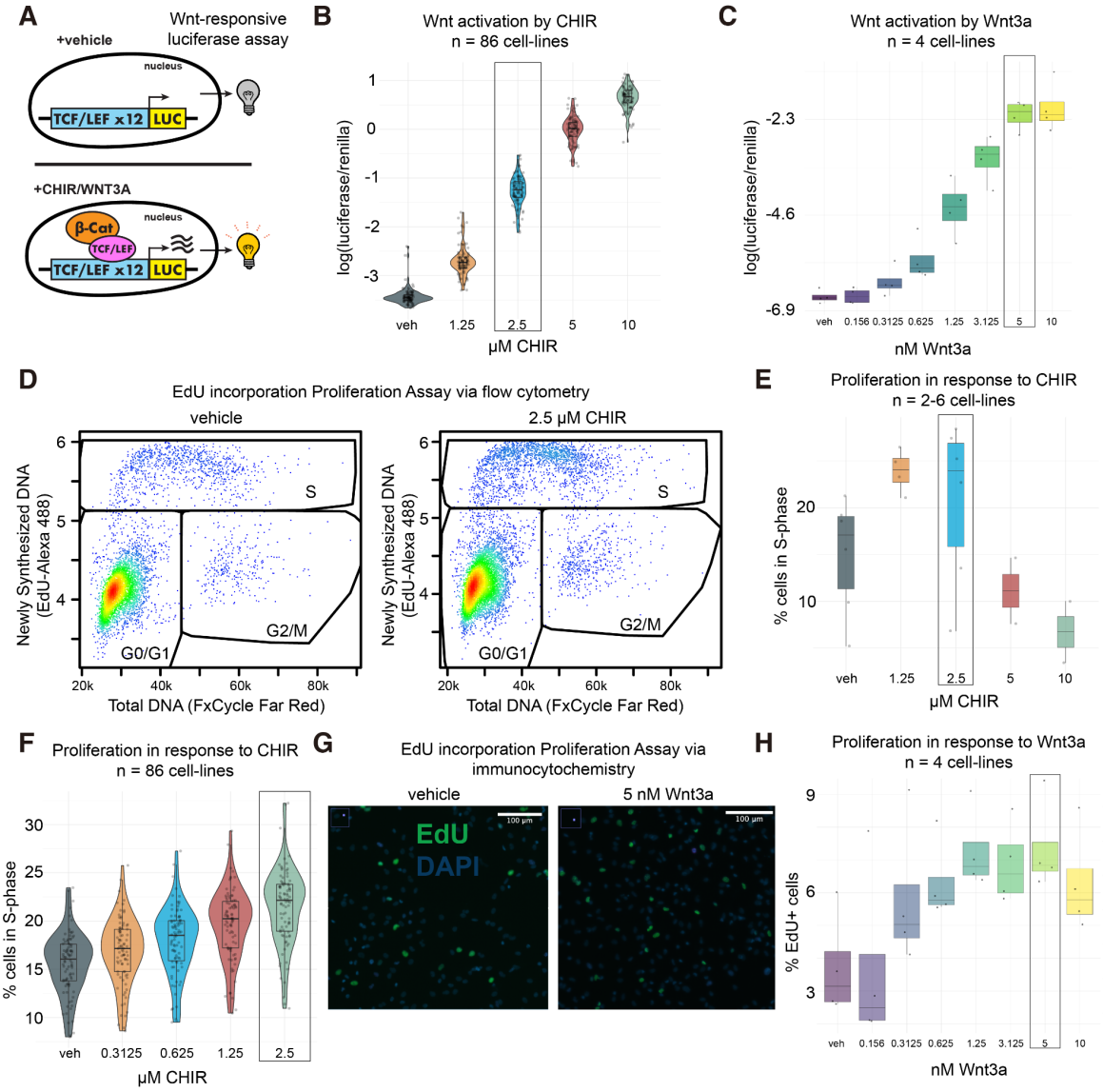

Supplementary Figure 2.2: Effects of CHIR and WNT3A on proliferation and Wnt activity

Cellular assays show that WNT3A and CHIR stimulation increase canonical Wnt pathway signaling and hNPC proliferation. Diagram of luciferase reporter assay measuring β-catenin mediated Wnt pathway activation by CHIR or WNT3A (A). Effects of 48h CHIR (B) or WNT3A (C) exposure on Wnt pathway activation, reported as the log of luciferase luminescence (activated by Wnt stimulation) normalized by renilla luminescence (from a constitutively active reporter transgene). We focused on this time-point because Wnt target gene expression was

maximized in hNPCs after 48h exposure to CHIR in previous experiments (Wolter, Le, et al. 2022). Representative flow cytometry scatter plots from proliferation assays depict newly synthesized DNA from a 2h hr EdU pulse vs total DNA content following 48h vehicle (left) or 2.5uM CHIR (right) exposure (D). Percentage of cells in S-phase (%EdU+) exposed to vehicle or increasing doses of CHIR for 48h as measured by flow cytometry in a subset of cell-lines (E), and in all cell-lines used for ATAC-seq and RNA-seq in this study (F). Representative immunocytochemistry images from proliferation assay of hNPCs following 48h vehicle (left) and 5nM WNT3A (right) exposure (G). Green (GFP) labels cells in S-phase during the EdU pulse, and blue (DAPI) stains all nuclei. Percentage of cells in S-phase (%EdU+) exposed to vehicle or increasing doses of WNT3A for 48h as measured by flow cytometry in a subset of cell-lines (H). CHIR and WNT3A concentrations (boxed) that maximize Wnt activation and proliferative responses were used in this study for ca/eQTL mapping.

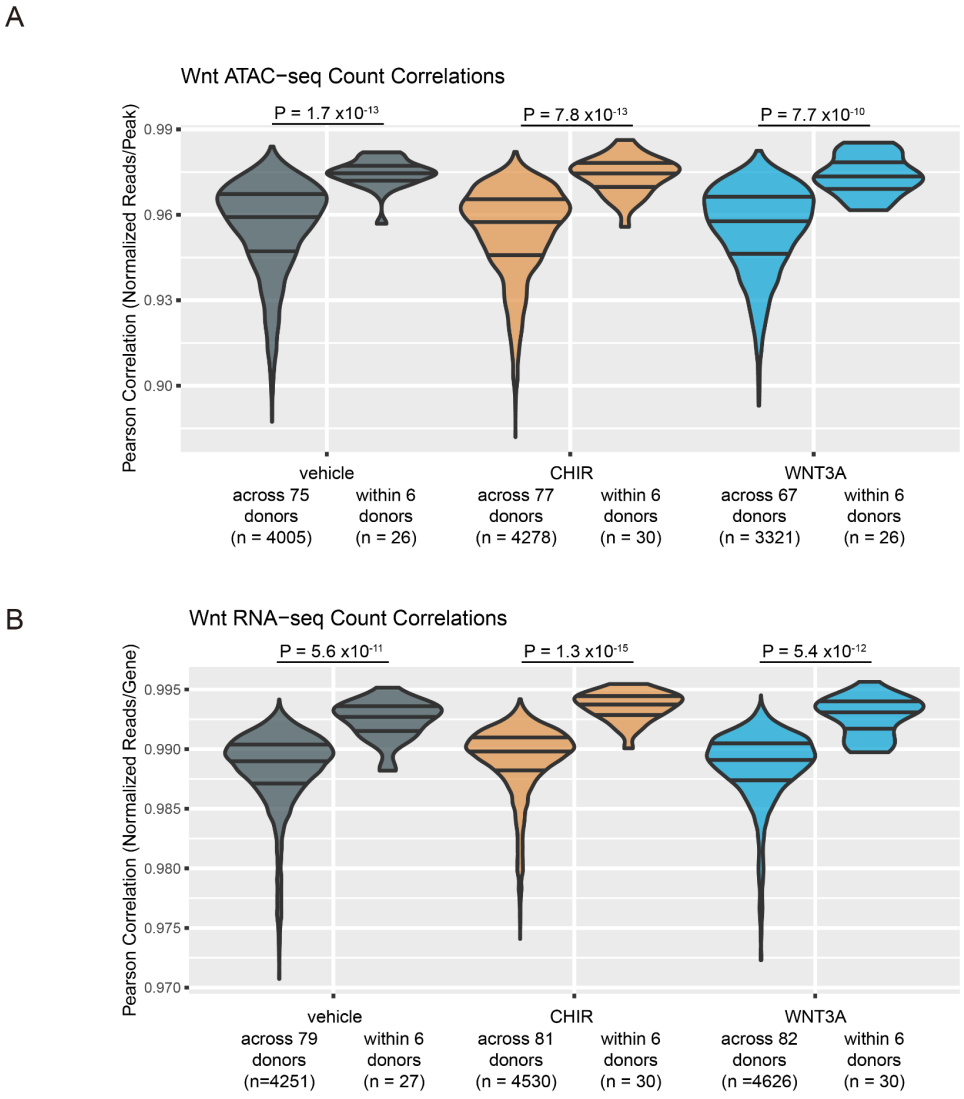

Supplementary Figure 2.3: Technical reproducibility of RNA-seq and ATAC-seq

Pairwise correlations normalized sequencing counts from technical replicates across open chromatin peaks measured by ATAC-seq (A) or genes measured by RNA-seq (B). Higher correlations for within donor vs across donor pairs indicates robust reproducibility of measurements for a given donor and condition. Violin plots represent the distribution of Pearson correlation coefficients calculated between a pair of genotypically distinct donors ("across donor") or between two technical replicates of the same donor cultured at different times ("within donor").

Top and bottom horizontal lines within violin plots represent the interquartile range of the data, and the middle bar represents the median. P-values report significant differences between the across vs. within donor correlations following Fisher's Z transformation and evaluated with the Welch two sample t-test. The total number of cell-lines and pairwise correlations (n) for each experimental condition is reported along the x-axis.

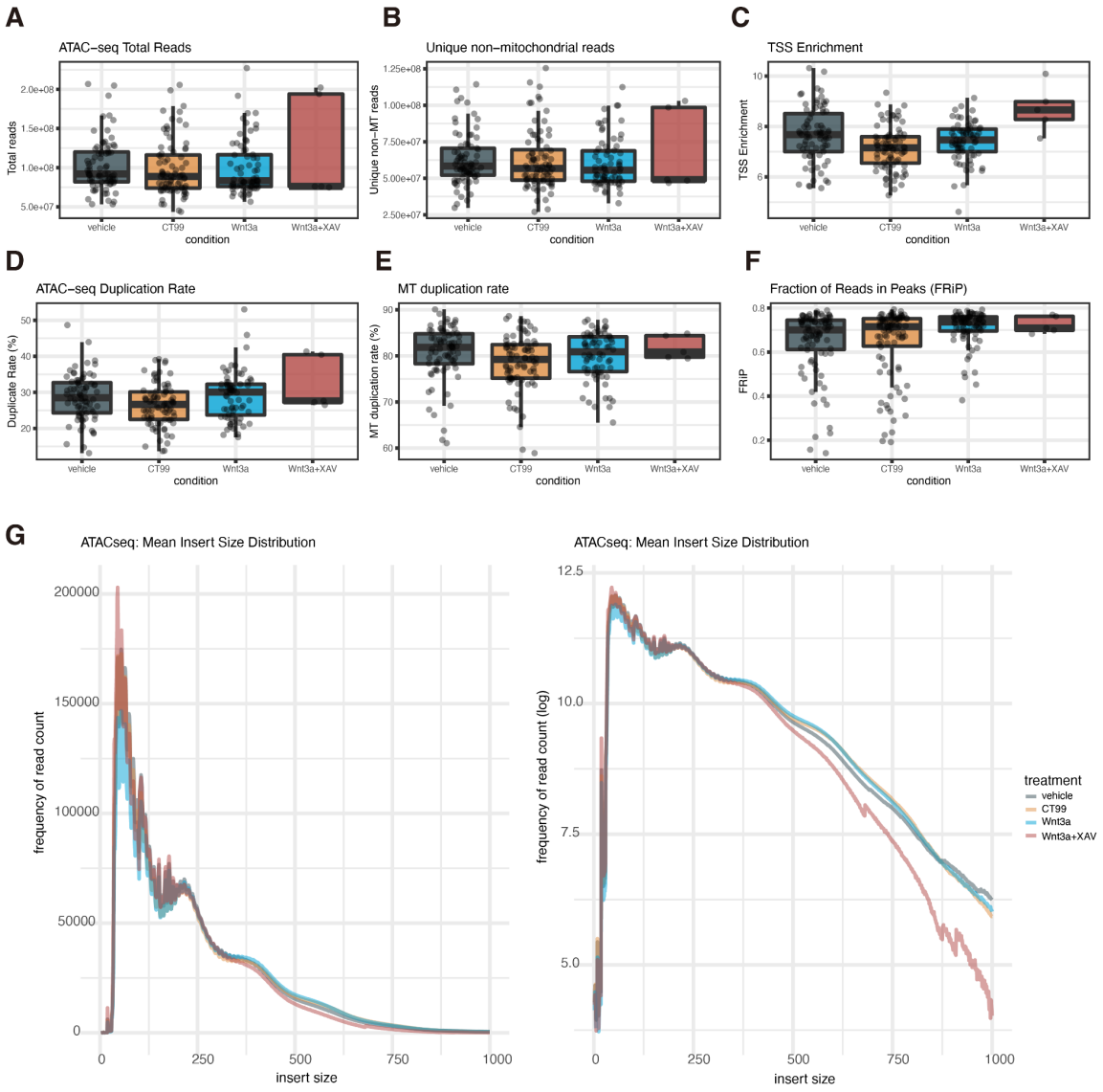

Supplementary Figure 2.4: ATAC-seq Quality Control

Total ATAC-seq reads (A), unique non mitochondrial reads (B), transcription start site (TSS) enrichment (C), total read duplication rate (D), mitochondrial read duplication rate (E), and fraction of reads within chromatin accessibility peaks (FRiP) (F) across stimulus conditions. Mean insert size distributions in base pairs across all samples colored by stimulus condition (G) exhibit a nucleosomal phasing pattern; right: insert size distribution plotted on log- scale. Mean TSS enrichments (> 7) and FRiP scores (>0.3) exceed the “ideal” metrics for ATAC-seq libraries

defined by the ENCODE project (Luo et al. 2020). Together, these measurements validate the quality of ATAC-seq samples used in this study.

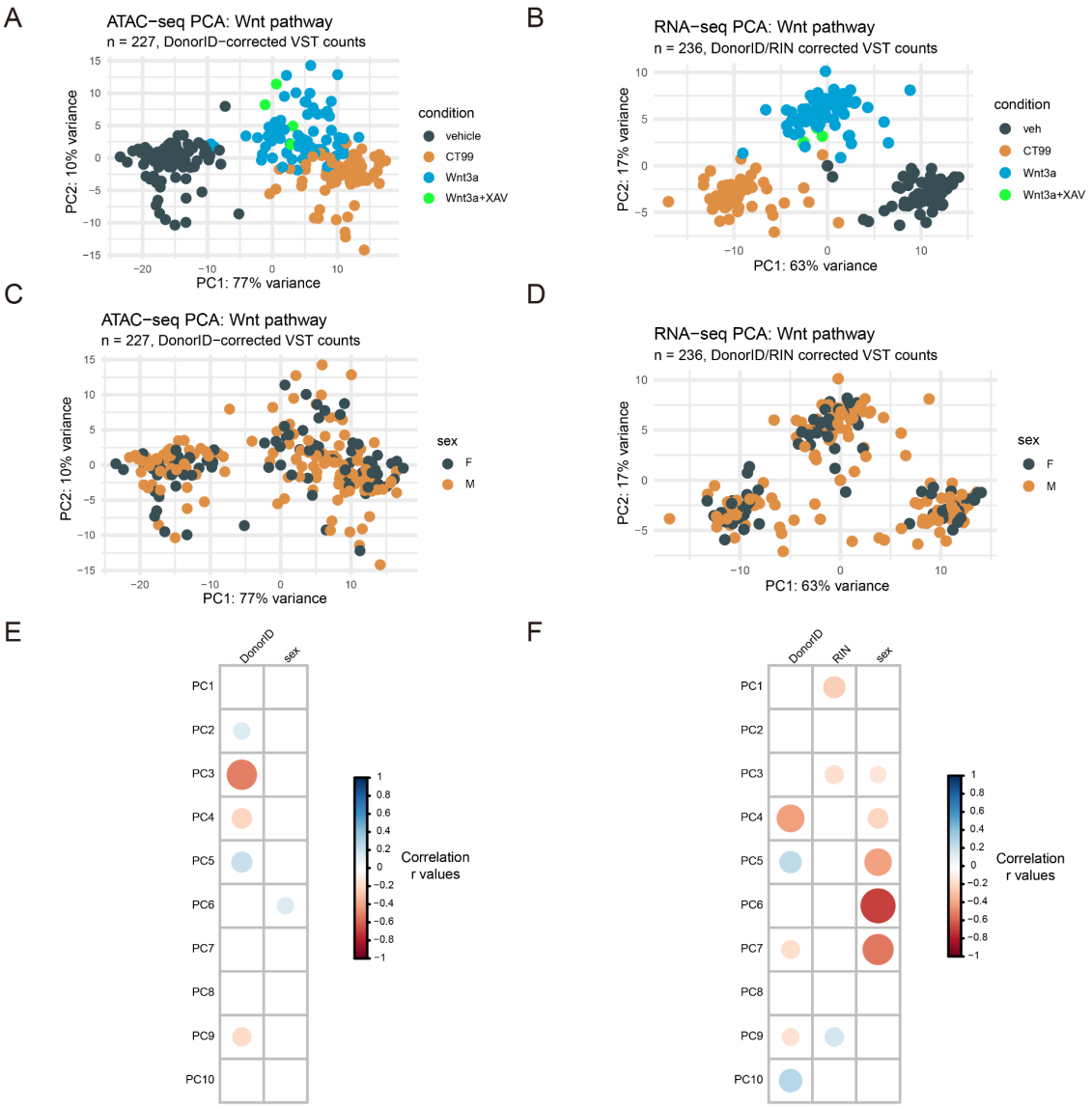

Supplementary Figure 2.5: Global gene expression and chromatin accessibility patterns

Principal component analysis (PCA) of ATAC-seq (A, C) and RNA-seq (B, D) data after batch correction for technical variables included in differential accessibility or expression models, respectively. Samples are labeled by condition (A, B), or sex (C, D). Variance in global gene expression and chromatin accessibility profiles across the first two PCs is driven by stimulation

condition, but not by sex. Correlation matrix of ATAC-seq (E) or RNA-seq (F) principal components 1-10 with technical (RIN) and biological variables (donor and sex). We performed linear regression to remove effects of PCs 1-10 and the residualized sequencing count data was used as QTL model input to account for measured and unmeasured confounding.

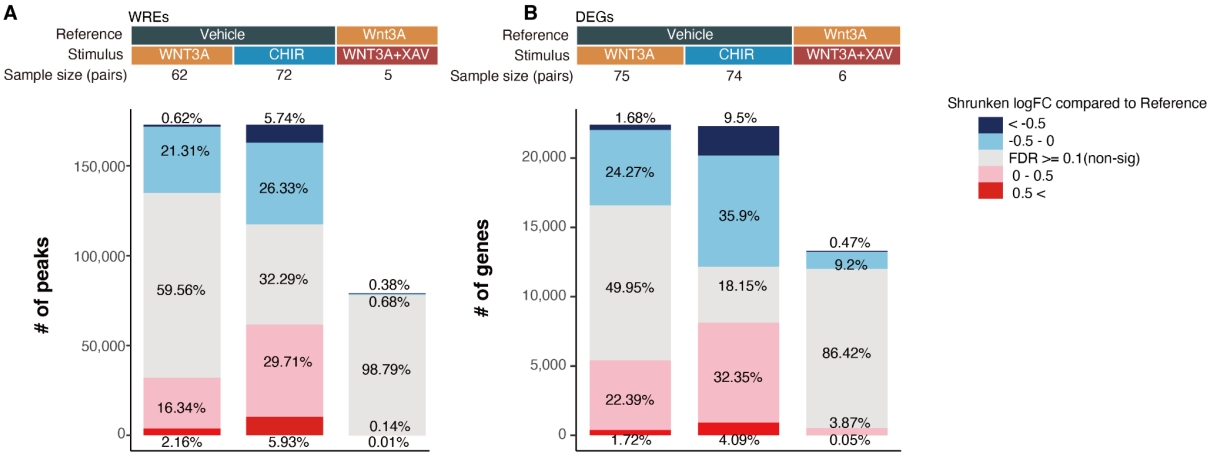

Supplementary Figure 2.6: Number of differentially accessible regions and differentially expressed genes

Barplots showing the number of differentially accessible regions (WREs) (A) and differentially expressed genes (DEGs) (B). The reference indicates referenced condition (either vehicle or WNT3A). Sample size indicates paired samples between conditions. Percentage of increased (shrunken log2FC > 0.5 in dark blue, shrunken log2FC > 0 in blue) or decreased (shrunken log2FC < -0.5 in red, shrunken log2FC < 0 in pink) accessibility or expression are shown for each category. Nonsignificant peaks and genes (FDR-adjusted P >=0.1) are colored gray. Greater changes were observed in both chromatin accessibility and gene expression for CHIR, a potent Wnt activator, as compared to WNT3A, an endogenous Wnt ligand. Simultaneous WNT3A activation and inhibition via XAV as compared to WNT3A activation yielded few differentially expressed genes and chromatin elements, likely due to the low sample size. We also note that 93,853 peaks and 9,890 genes were filtered out (adjusted *P* value were set to *NA*) by DESeq2 (Bourgon, Gentleman, and Huber 2010; Love, Huber, and Anders 2014) as those have low mean read counts.

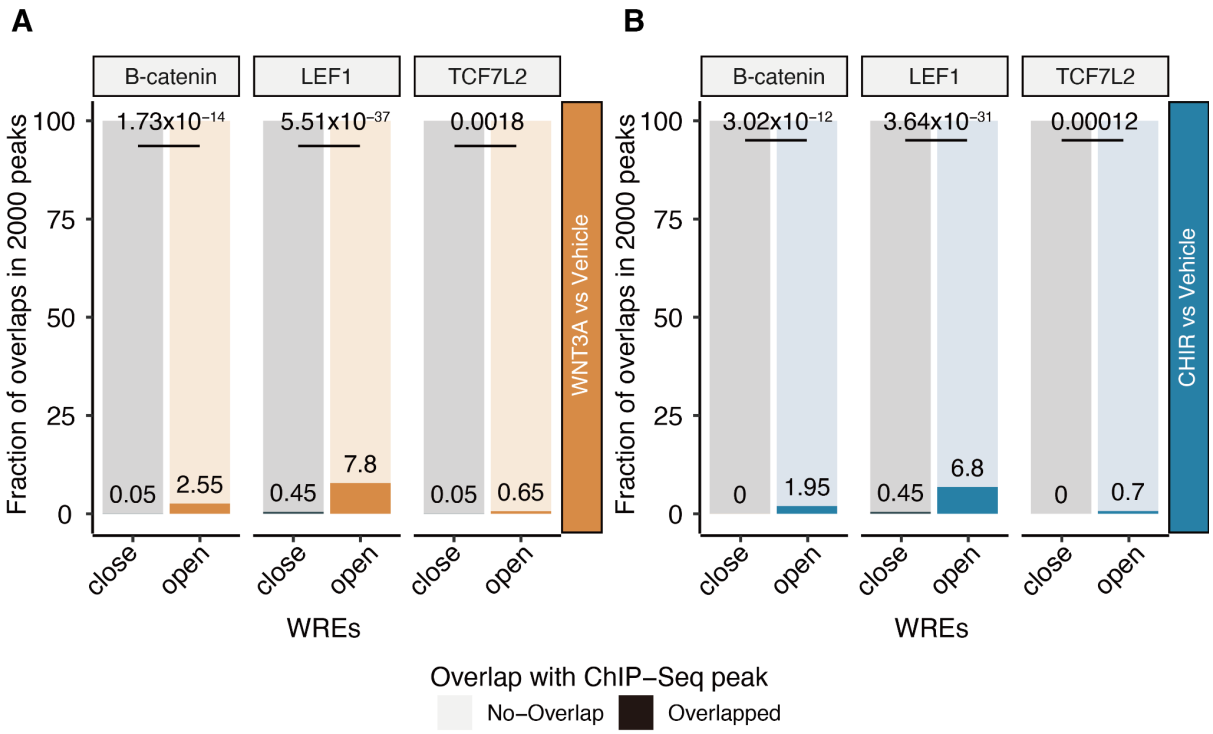

Supplementary Figure 2.7: Wnt-pathway related transcription factor binding sites are enriched in upregulated WREs

The canonical Wnt-pathway downstream effectors, ß-catenin, LEF1, and TCF7L2 binding sites previously identified by ChIP-seq experiments in HEK cells (Doumpas et al. 2019; Luo et al. 2020) are more often overlapped with WREs opening due to WNT3A (A) or CHIR (B) than closing WREs. The figures show the percentage of overlaps with the indicated TF binding sites in either the 2,000 most upregulated peaks or the 2,000 most downregulated peaks based on shrunken logFC. Statistical significance was estimated using Fisher's exact test on the number of overlaps.

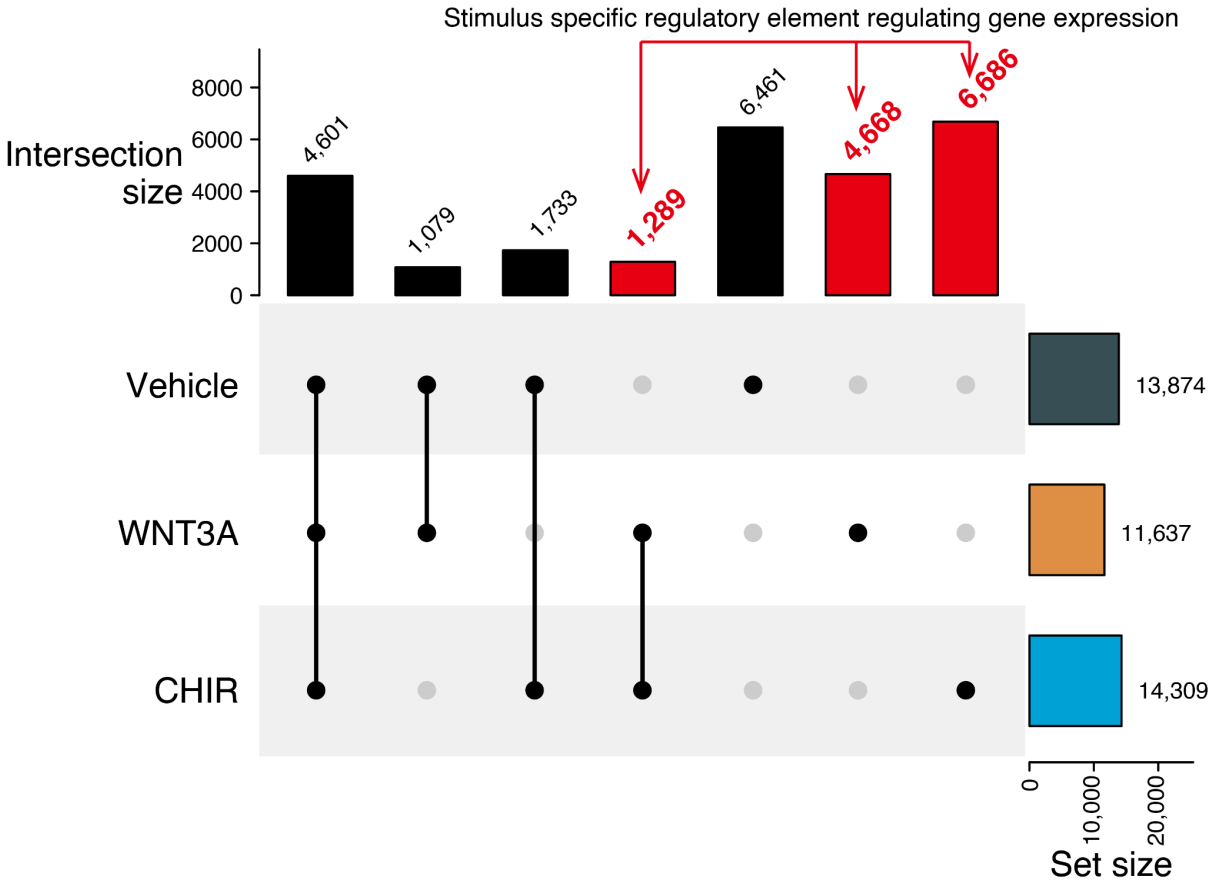

Supplementary Figure 2.8: Stimulus-specific regulatory element-gene correlation

We identified stimulus-specific regulatory elements which regulate gene expression by correlating expression with chromatin accessibility. The number in the plot indicates significant and positively correlated peak-gene pairs. In total, 12,643 peak-gene pairs are detected only under the stimulus condition (highlighted in red), demonstrating new stimulus-specific regulatory elements.

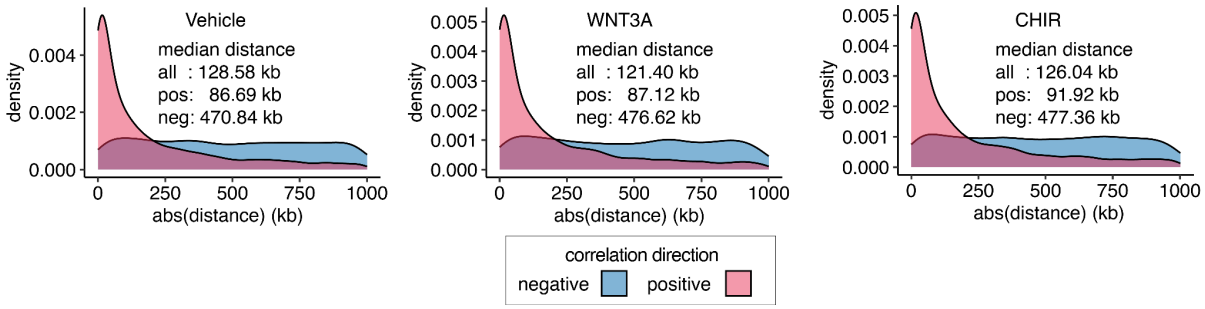

Supplementary Figure 2.9: Absolute distance from TSS of correlated genes

Distribution of absolute peak distance to TSS of correlated gene are shown for Vehicle (left), WNT3A (middle), and CHIR (right). Color represents the sign of correlation coefficient (pos: pink, neg:blue).

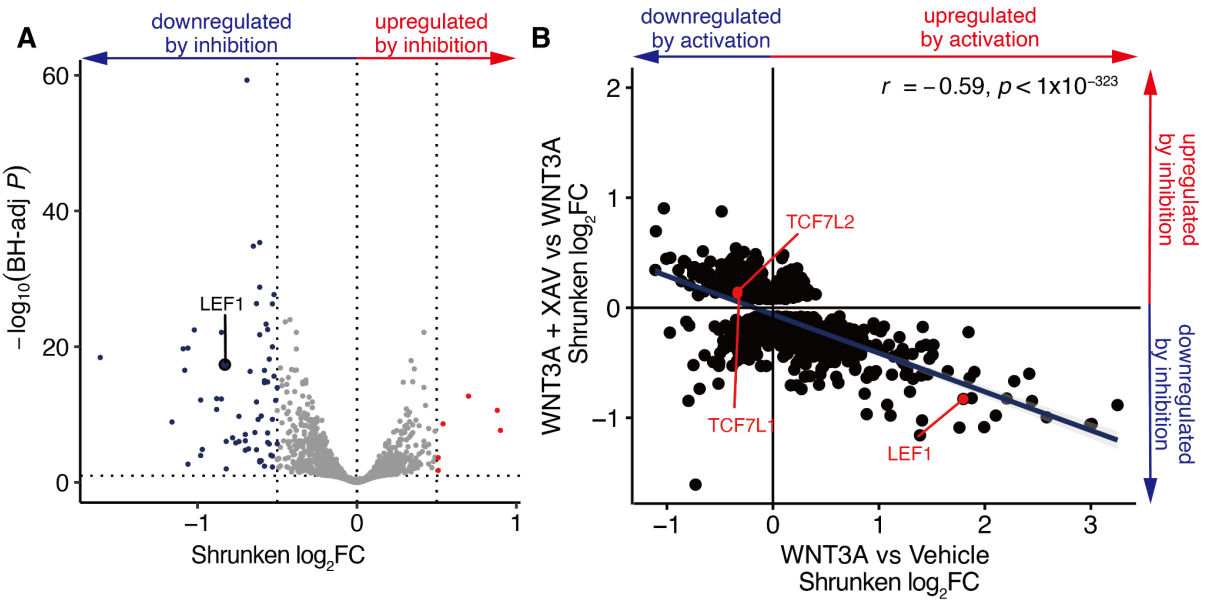

Supplementary Figure 2.10: Opposing gene regulation by WNT pathway inhibition

(A) Volcano plot showing differential expressed genes between simultaneous excitation and inhibition of WNT3A (WNT3A+XAV) as compared to WNT3A stimulus alone. Note that LEF1, a downstream effector of the Wnt pathways, has decreased expression under inhibition of the Wnt pathway. (B) Among 1413 genes that are differentially expressed at BH-adj P < 0.1 in both comparisons (WNT3A+XAV vs WNT3A (6 pairs) and WNT3A vs Vehicle (75 pairs)), 70.8% (1001

genes), opposing changes in gene expression were observed. This result is consistent with most gene expression changes being caused by the stimulus of the Wnt pathway.

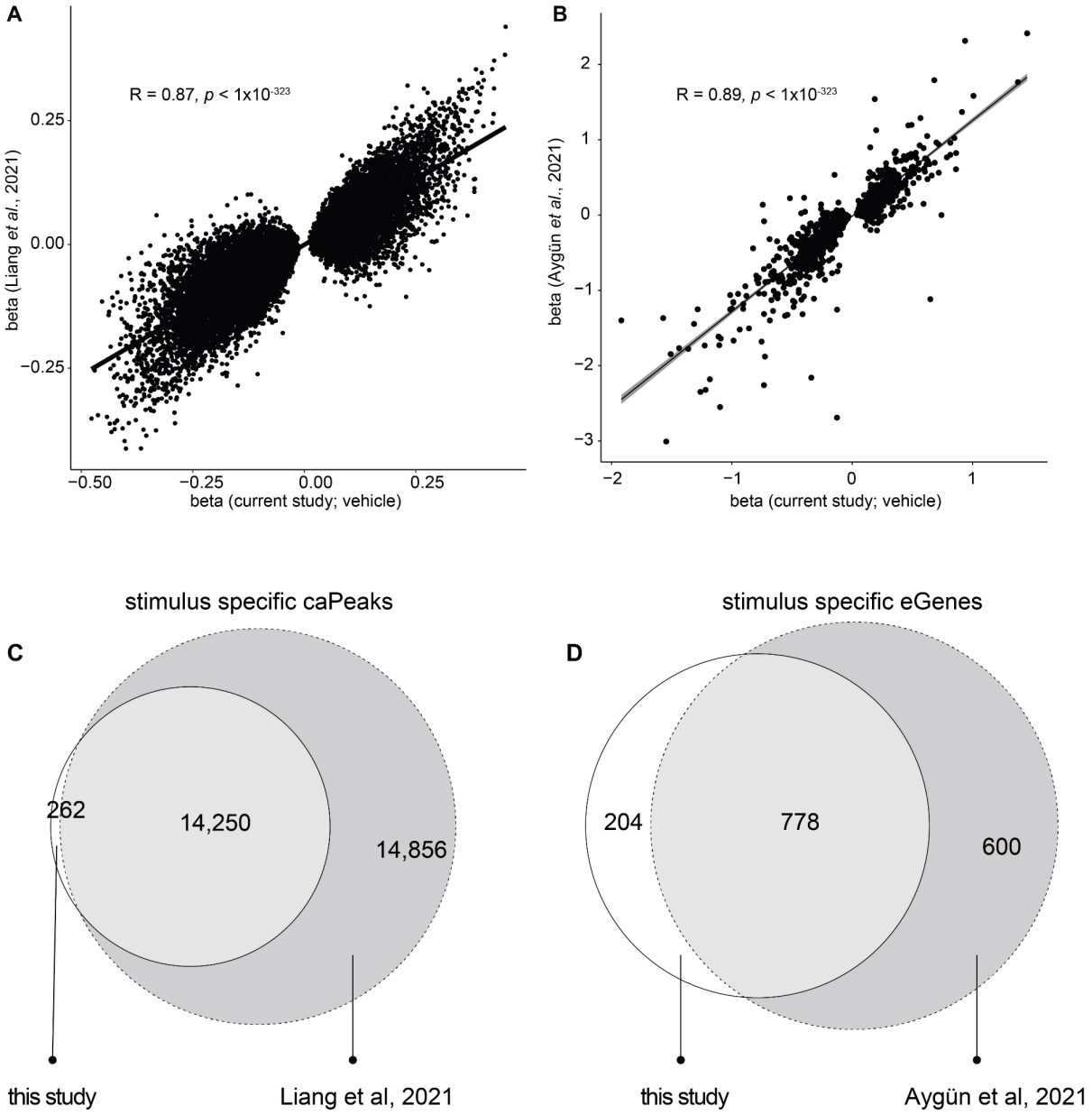

Supplementary Figure 2.11: ca/eQTL discovery and effect sizes compared to previous data

We compared the effect size of ca-QTL (A) and eQTL (B) in vehicle condition to previous studies using the same hNPC cell lines with slightly larger sample size (Liang et al. 2021; Aygün et al. 2021). Strongly correlated effect sizes for unstimulated ca/eQTLs were found between the two

datasets. One SNP showed opposite effect directionality across the caQTL datasets between the current and previous datasets (rs2076179). We suspect this was due to an error in allele assignment for that SNP in the previous analysis caused by sampling differences incorrectly changing the labeled minor allele for a SNP with allele frequency close to 0.50. We corrected this error for the one SNP prior to plotting. (C) caPeaks identified in WNT3A or CHIR stimulated conditions but not in vehicle (this study) were compared with caPeaks identified in WNT3A or CHIR stimulated conditions but not in a previous caQTL study using the same cell lines (Liang et al., 2021). (D) eGenes identified in WNT3A or CHIR stimulated conditions but not in vehicle (this study) were compared with eGenes identified in WNT3A or CHIR stimulated conditions but not in a previous eQTL study using the same cell lines (Aygün et al., 2021). Overall, the vast majority of stimulus-specific caPeaks/eGenes were shared regardless of the unstimulated dataset used, providing confidence in the context specificity of the caPeak/eGenes.

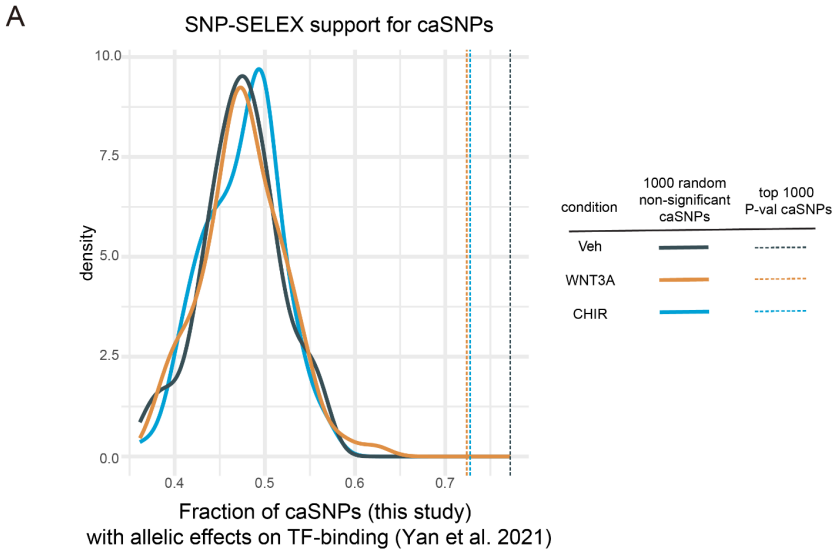

Supplementary Figure 2.12 : Support for context-specific caQTLs from SNP-SELEX experiments

(A) The fraction of caSNPs discovered in this study tested by SNP-SELEX experiments (Yan et al. 2021) that were determined to have allelic effects on TF-binding. Solid line curves represent the

frequency distribution of SNP-SELEX support for 100 random samples of 1,000 non-significant caSNPs for each of the Vehicle, WNT3A or CHIR conditions. Dashed lines mark the level of SNP-SELEX support for the top 1,000 most significant caSNPs in each condition.

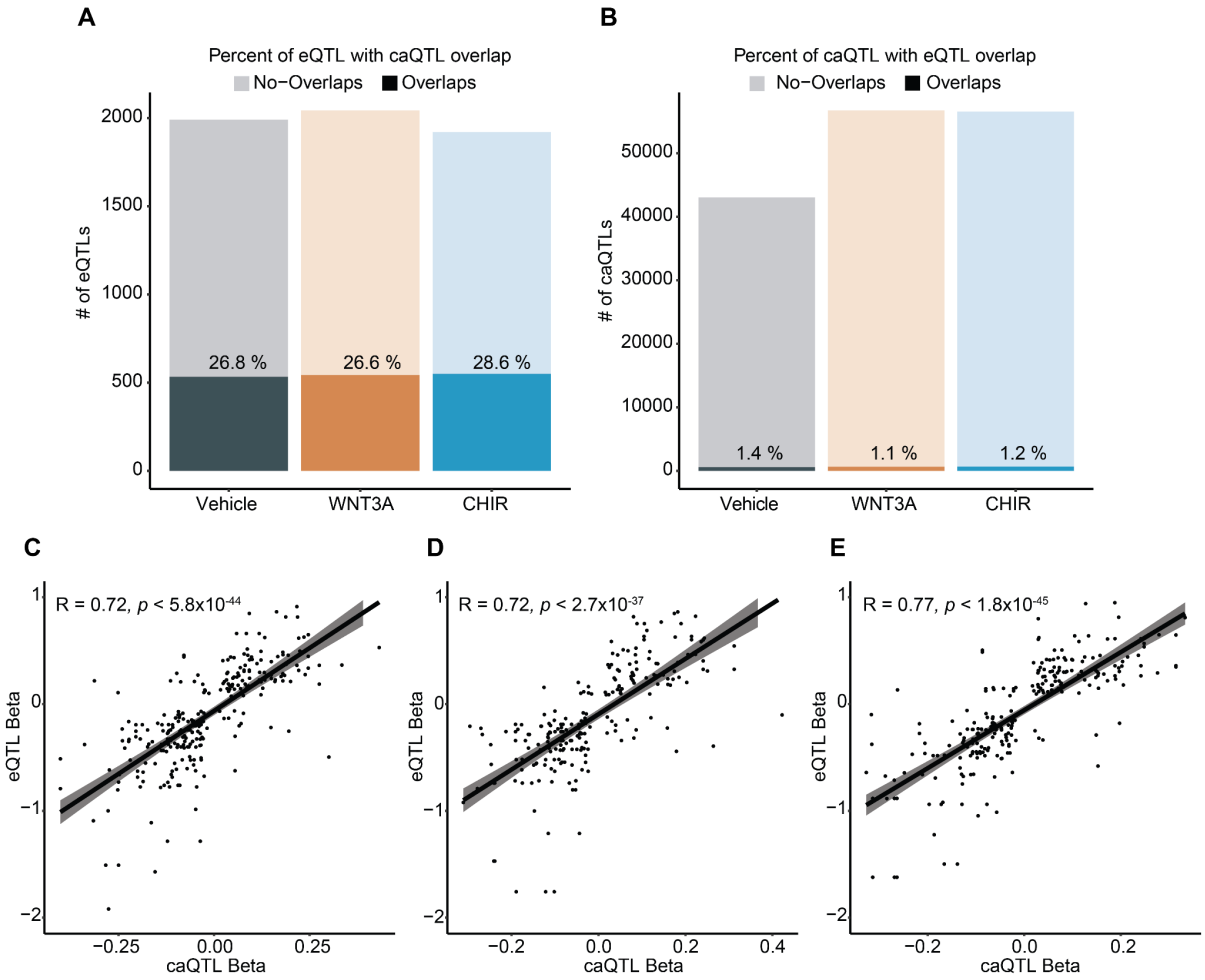

Supplementary Figure 2.13: eQTL-caQTL overlaps

Overlaps between caQTLs and eQTLs were called where a caSNP was within 1Mb of an eGene and at least 1 significant SNP in both datasets were in LD $r^2 \geq 0.8$. The percentage of eQTLs (A) and caQTLs (B) overlapped within vehicle and WNT stimulus conditions are shown. The effect size of caQTL-eQTL sites which shared the same SNP position were compared within vehicle (C) and WNT stimulus conditions (WNT3A and CHIR shown in D and E respectively). SNPs selected to influence chromatin accessibility had relatively little overlap with those influencing gene

expression likely because genetic variation affecting chromatin accessibility often does not lead to changes in gene expression (about <2% of caQTLs had a shared eQTL based on LD overlap (r^2 >= 0.8). However, SNPs selected to influence gene expression more often also influence chromatin accessibility in that ~27% of eQTLs have a shared caQTL within condition, a comparable number observed in our previous study (34.9% caQTL-eQTLs overlap (Liang et al. 2021)).

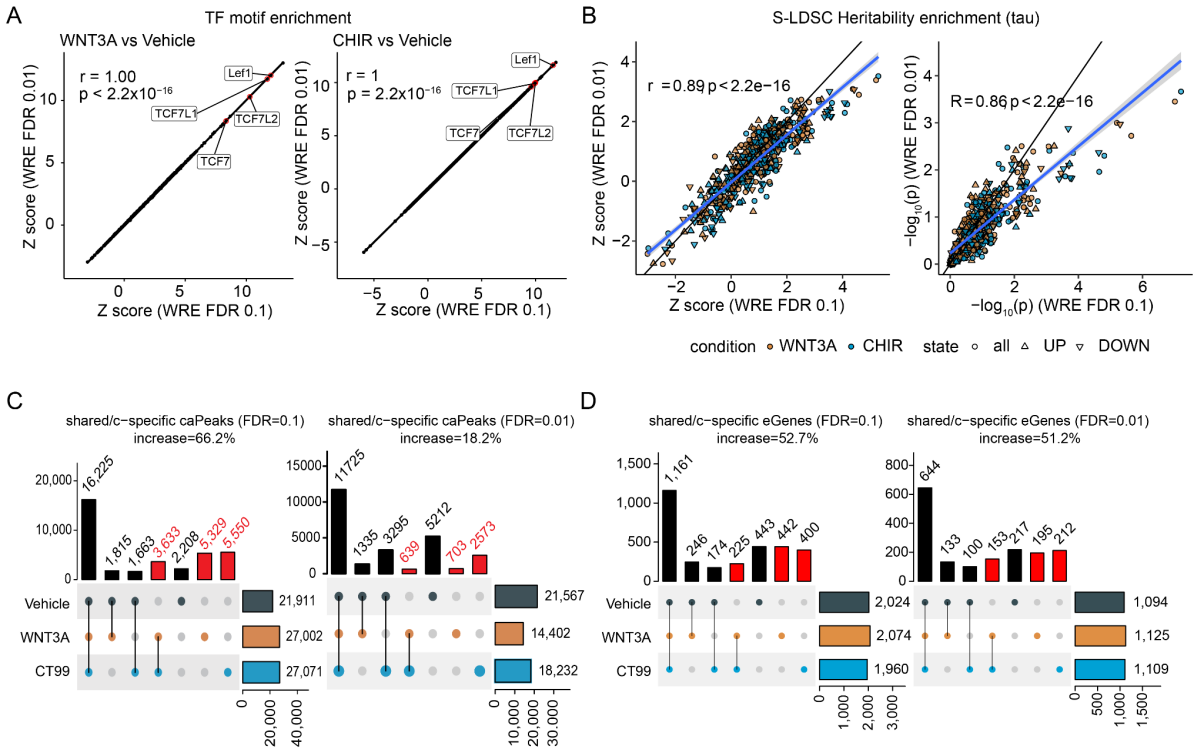

Supplementary Figure 2.14: Conclusions remain robust to varying FDR thresholds

We evaluated how varying FDR thresholds (FDR < 0.01 or 0.10) impacted our conclusions for TF motif binding site enrichment analysis (A), S-LDSC heritability enrichment analysis (B), and ca/e-QTL mappings (C) and (D). TF motif enrichment based on differentially accessible peaks due to Wnt stimulation are almost identical when using FDR < 0.01 or FDR < 0.10 thresholds, due to use of the top 2,000 opened or closed peaks as compared to vehicle (A). Partitioned heritability enrichment is highly similar based on defining WREs using a FDR < 0.01 or FDR < 0.10 threshold (B). We do observe a smaller Z score in the FDR < 0.01 threshold, likely due to

lower power because less of the genome was annotated as a WRE, but the correlation between results from the two thresholds is very high ($r > 0.85$). We also called e/caQTLs at a more stringent FDR < 0.01 threshold (C, D). As expected, we observed a decrease in the number of QTLs found at FDR < 0.01 compared to FDR < 0.10. But the conclusion, that stimulation enables us to identify more caPeaks/eGenes as compared to the vehicle condition alone, remains the same.

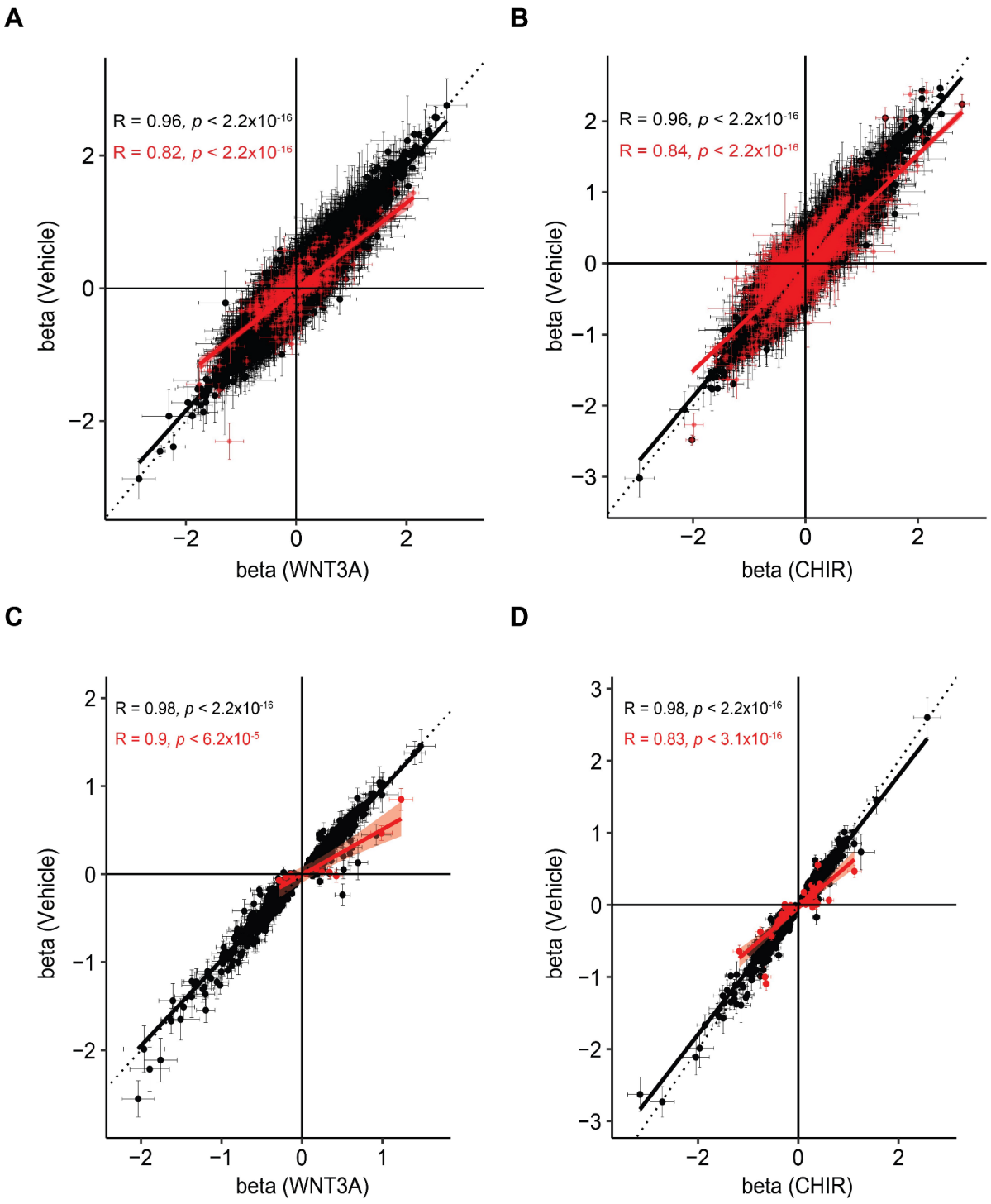

Supplementary Figure 2.15: Effect size differences across conditions

We compared effect sizes of index caQTLs (A-B) / eQTLs (C-D) in stimulated conditions versus vehicle conditions (WNT3A or CHIR in (A,C) and (B,D), respectively). Dots in red indicate significant interaction effects were observed (r-QTLs). Error bars are standard errors of beta. We

observed lower correlation in r-QTLs as compared to non-r-QTLs. We note that some SNPs are not tested for a baseline model due to low expression thus could not be plotted because no beta value was calculated.

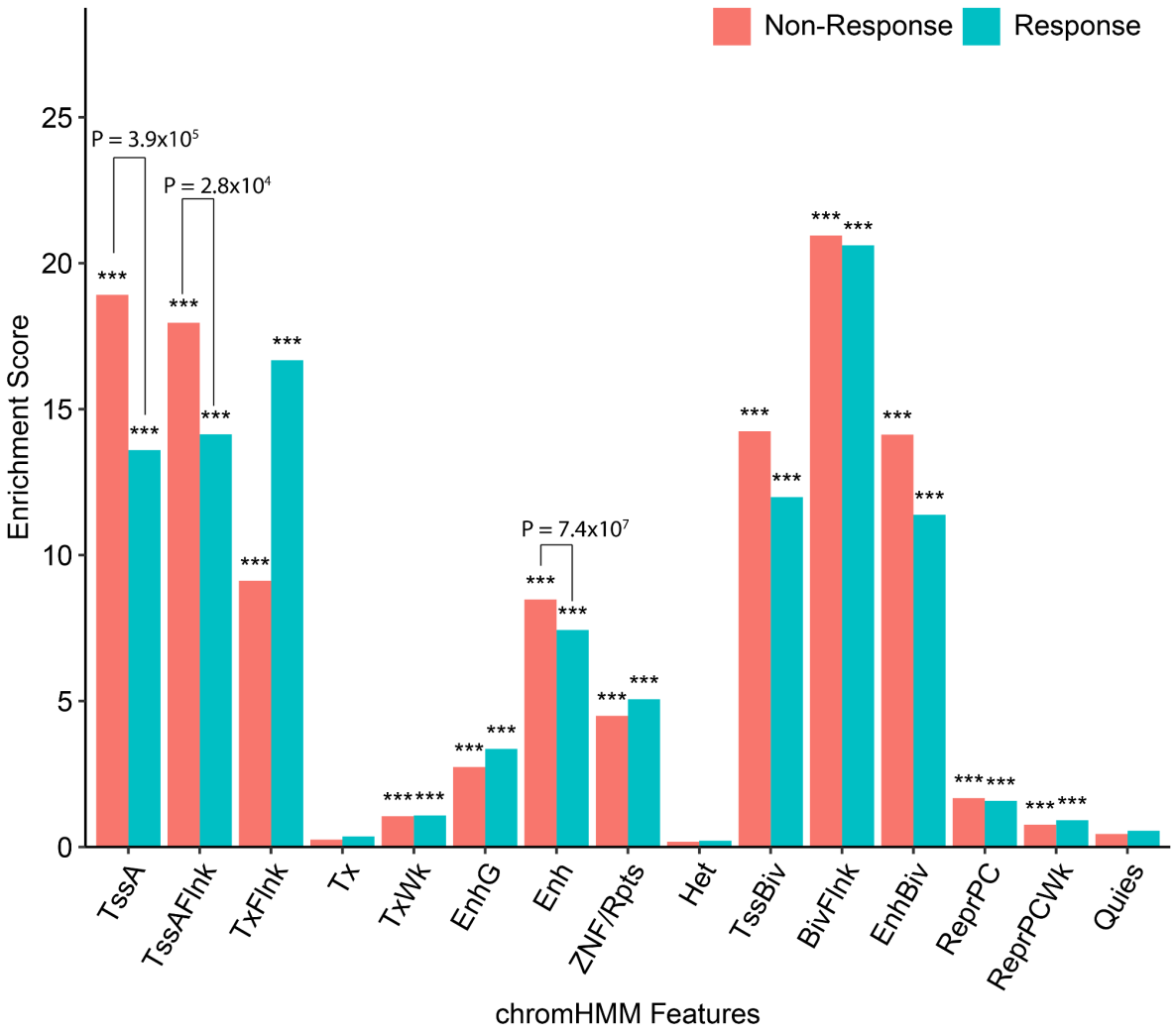

Supplementary Figure 2.16: Response and Non–Response caPeaks enrichment within chromHMM Annotations

Enrichment of response and non-response caPeaks within chromHMM states defined within fetal brain male (E081) (Roadmap Epigenomics Consortium et al. 2015). *, **, *** indicate enrichments of overlaps relative to the entire genome, evaluated with a binomial test, similar to the GREAT test (McLean et al. 2010), with *P*-values < 0.05, .01 and .001, respectively. We observed a significant enrichment of both response and non-response caPeaks within promoters,

enhancers, and bivalent regions. TssA, TssFlnk, and Enh states showed a significant difference in overlap counts between response and non-response caPeaks (P = $3.9x10^{-5}$; $2.8x10^{-4}$; $7.4x10^{-7}$, respectively), as evaluated with Fisher's exact test. There was significantly less enrichment of response caPeaks in active TSS and enhancers as compared to non-response caPeaks, perhaps because these response caPeaks flag novel condition specific enhancers not annotated in post-mortem fetal brain tissue.

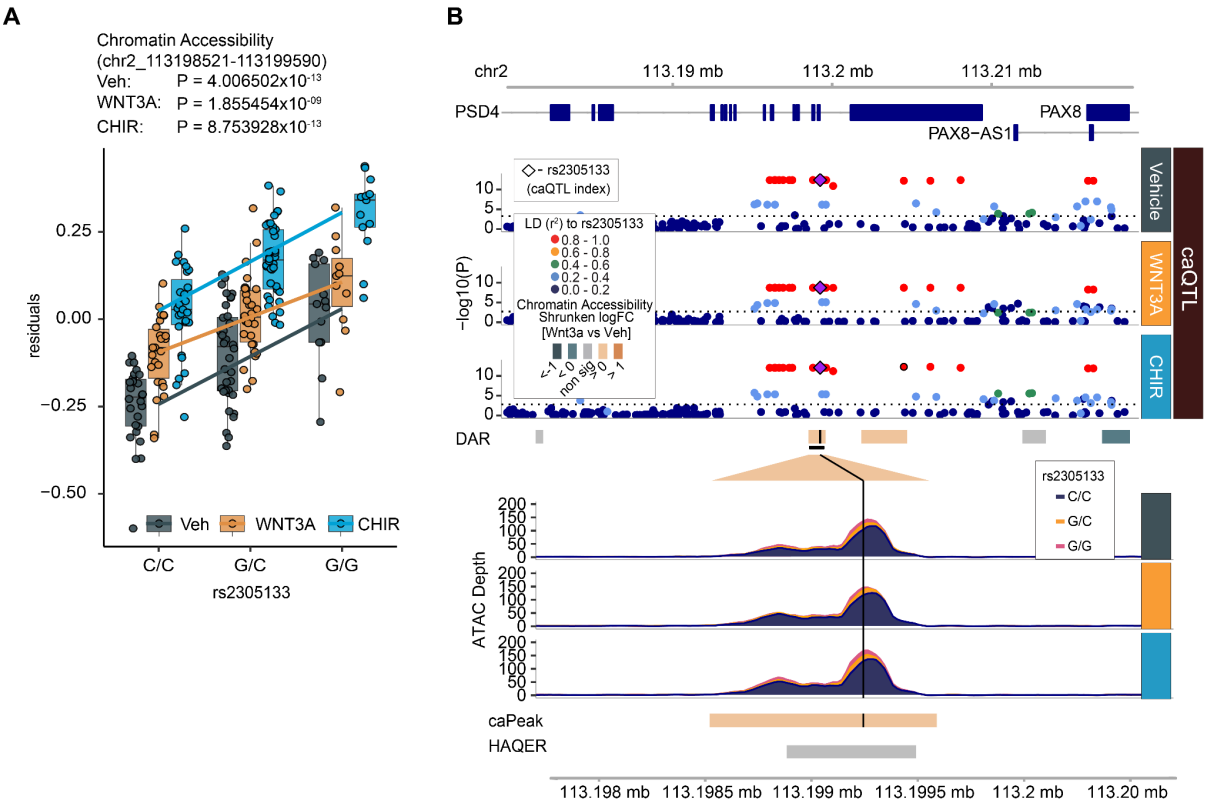

Supplementary Figure 2.17: Wnt responsive caPeak overlaps HAQER near PAX8

(A) Allelic effects of rs2305133 on chromatin accessibility (chr2:113198521-11319959). (B) Regional association plots at rs2305133, the index SNP for a caPeak-HAQER overlap. From top to bottom: Genomic coordinates, gene models, caQTL P-values for vehicle, WNT3A, and CHIR-stimulated conditions, ATAC-seq coverage showing differential chromatin accessibility and HAQER location.

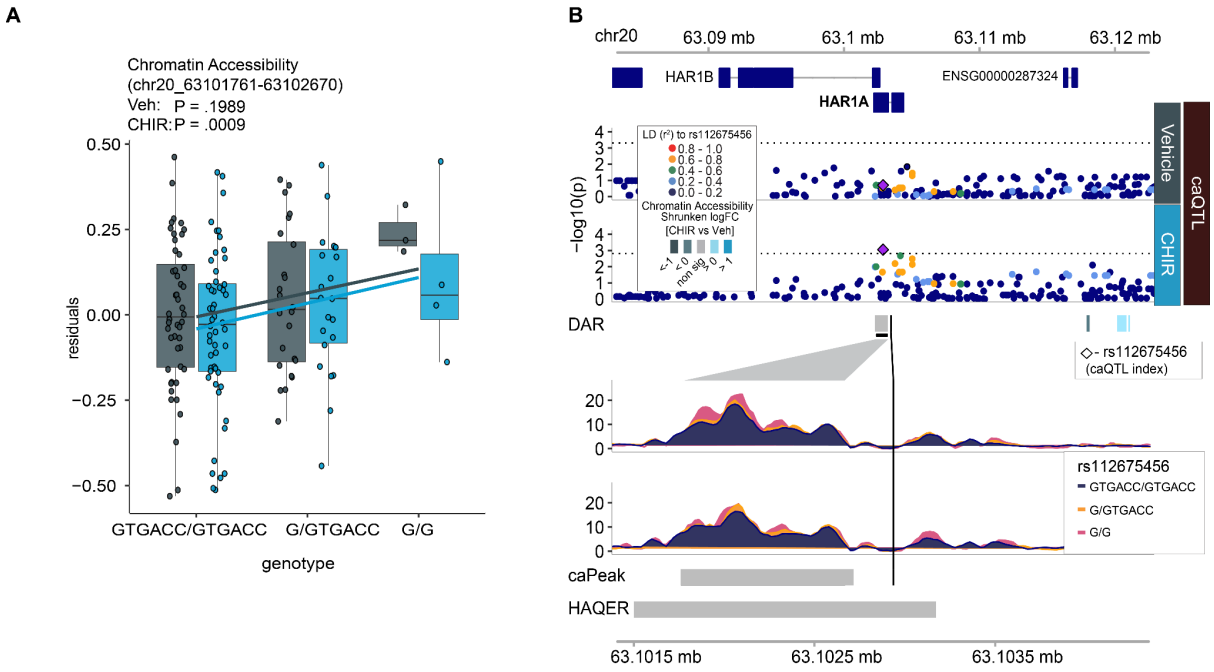

Supplementary Figure 2.18: Stimulus-specific caPeak overlaps HAQER near HAR1A/B

(A) Allelic effects of rs112675456 on chromatin accessibility (chr20:63101761-63102670), reveal a caQTL significant in CHIR stimulated condition but not vehicle. (B) Regional association plots at rs112675456, the index SNP for a caPeak-HAQER overlap near the transcription start sites of HAR1A/B. From top to bottom: Genomic coordinates, gene models, caQTL *P* values for vehicle and CHIR-stimulated conditions, ATAC-seq coverage showing differential chromatin accessibility, and HAQER.

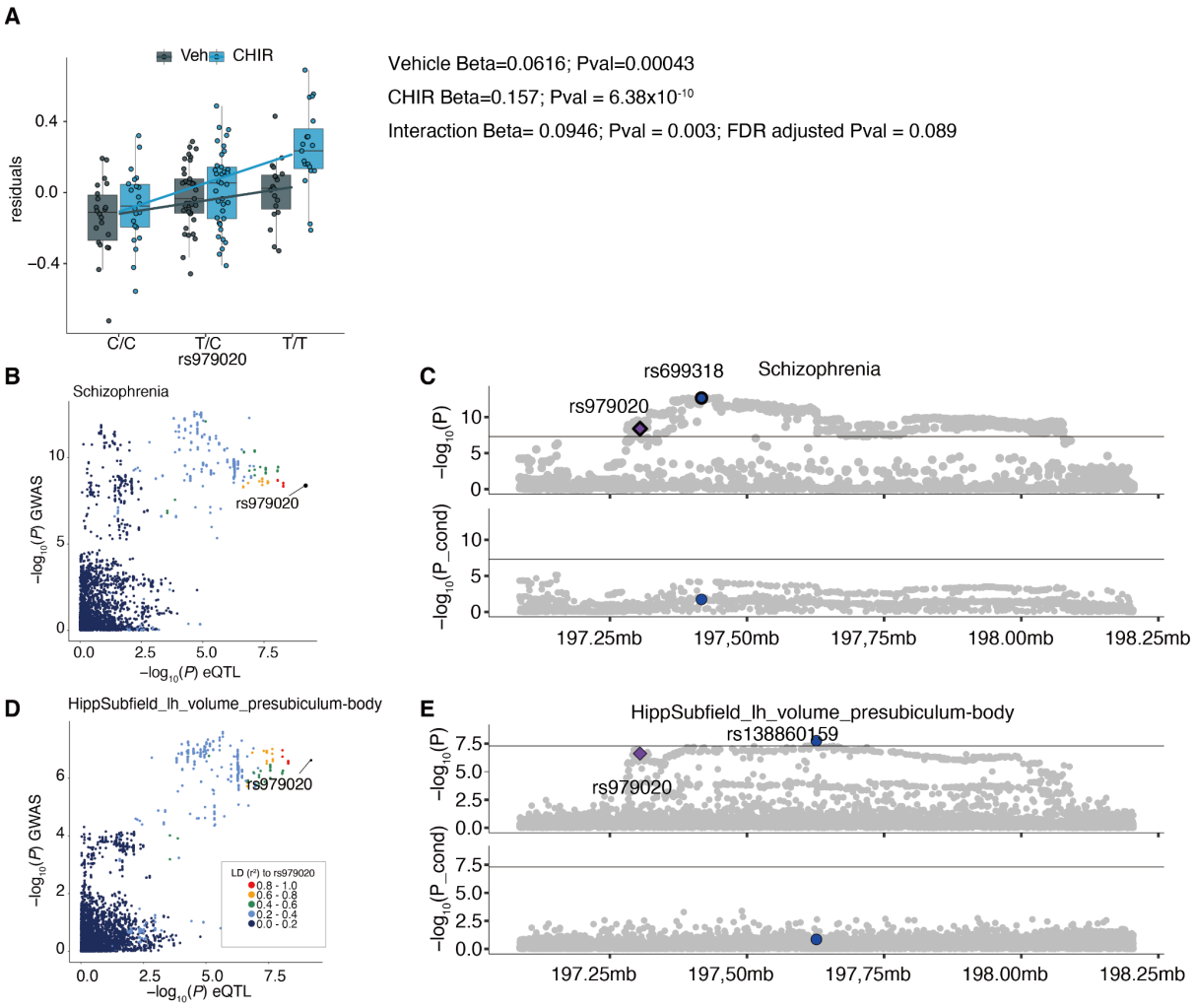

Supplementary Figure 2.19: Colocalization of ANKRD44 r-eQTL, schizophrenia, and the volume of a hippocampal subfield (presubiculum body)

(A) Boxplot showing increased ANKRD44 gene expression by rs979020-T and the SNP a significant interaction effect. (B) P-P plot from schizophrenia GWAS vs eQTL colored by r^2 in this study population to rs979020, providing evidence for a colocalization. (C) Conditional analysis of schizophrenia GWAS was performed using GCTA-cojo tool with LD from the UKBB reference panel (White British). GWAS *P* value (upper panel) and post-conditional analysis *P* value (bottom panel) are shown. An absence of GWAS signal after conditioning on the r-eQTL index provides evidence for colocalization. (D, E) Similar to (B, C) but using GWAS for volume of a hippocampal subfield (presubiculum body; left hemisphere).

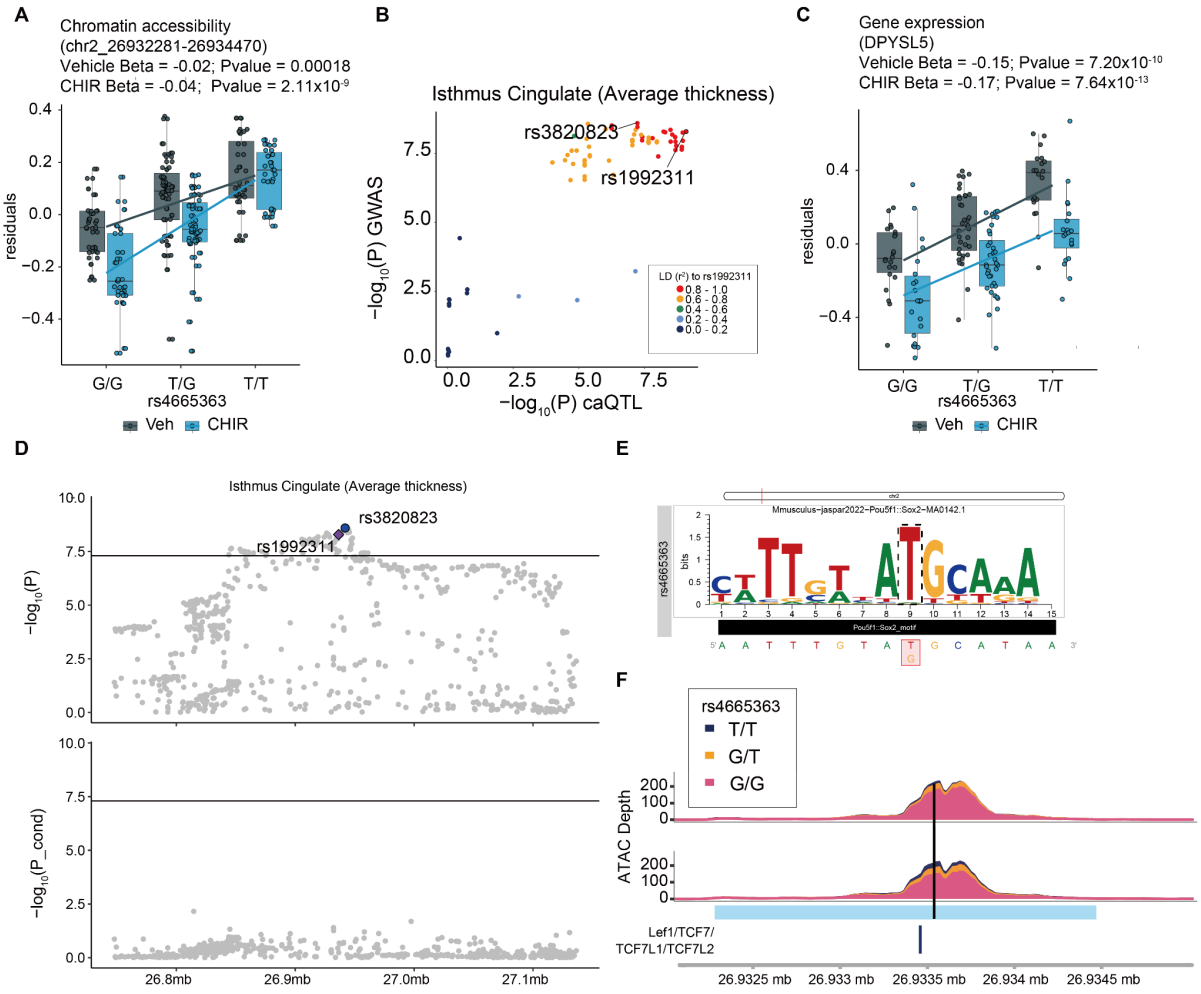

Supplementary Figure 2.20: Colocalization of an r-caQTL in DPYSL5 region and average thickness of the isthmus Cingulate

(A) We detected an r-caQTL at rs1992311 (FDR-adjusted *P* value = 0.04). We present boxplots showing differential genetic effects on chromatin accessibility in stimulated versus vehicle conditions in a linked SNP within the peak that disrupts a motif (rs4665363-G). (B) P-P plot for isthmus Cingulate GWAS (Grasby et al. 2020) vs caQTL colored by r^2 in our population to rs1992311, providing evidence for colocalization. (C) Boxplot showing decreased *DPYSL5* expression by rs4665363-G. (D) Conditional analysis on GWAS for average thickness of Isthmus Cingulate was performed using the UKBB reference panel (White British). GWAS *P* value (upper panel) and post-conditional analysis *P* value (bottom panel) are shown. GCTA-cojo identified collinearity between rs4665363 and rs3820823 (r^2>0.9) thus both SNPs are not shown in the

bottom panel. A decrease in GWAS signal after conditioning on the r-caQTL provides evidence for colocalization. (E) Logo plot predicting disruption of the Pou5f1::Sox2 motif by rs4665363-G. (F) Coverage plots of the peak showing the location of rs4665363 and a TCF/LEF motif present in the peak.

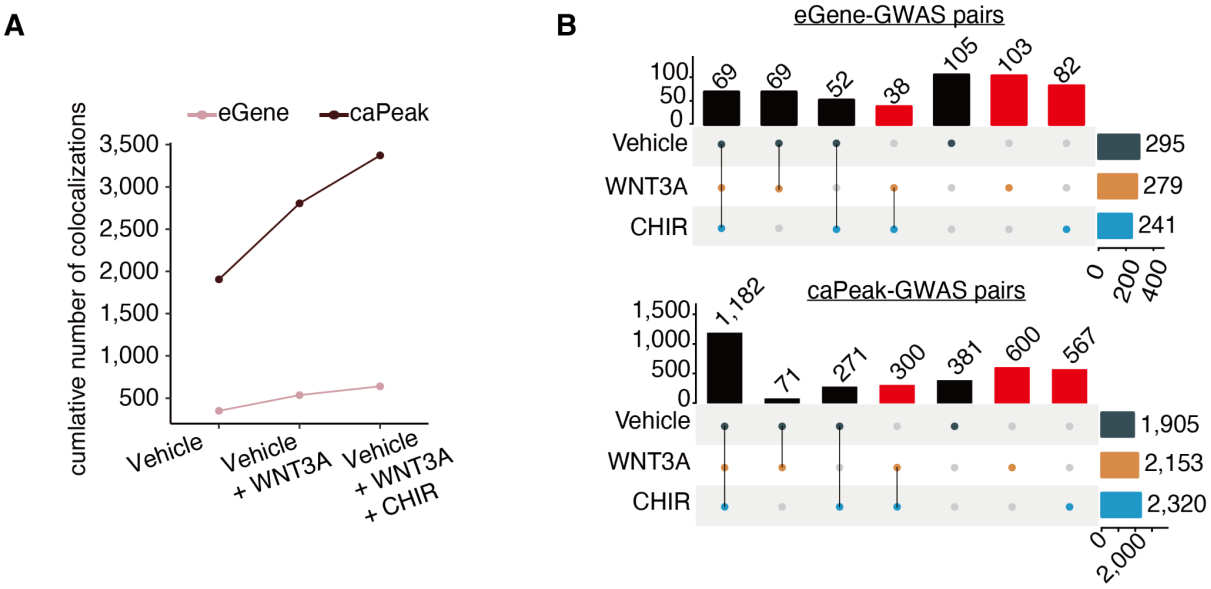

Supplementary Figure 2.21: Shared and context-specific QTL GWAS overlaps confirmed by eCAVIAR

Colocalization of eQTLs/caQTLs and brain-related GWAS phenotypes tested by eCAVIAR. (A) A cumulative number of colocalized eGenes/caPeaks after colocalization analysis by eCAVIAR and (B) shared/distinct colocalization in each condition. The use of stimulated conditions increased the number of brain-trait associated genes by 75.6% and peaks by 77.0%.

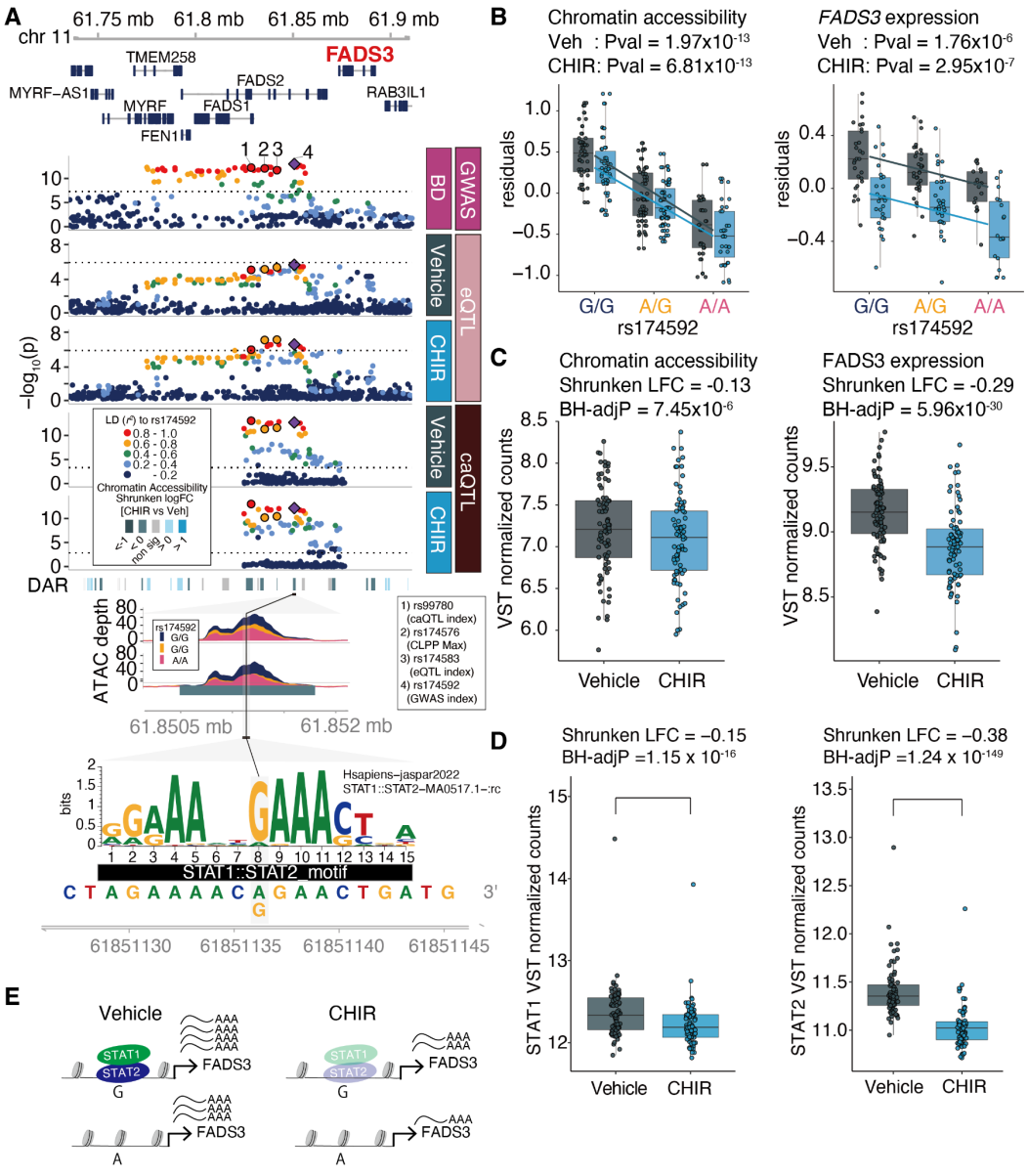

Supplementary Figure 2.22: Stimulus-specific GWAS colocalization of *FADS3* and Bipolar disorder

(A) GWAS and QTL locus plots in the region of *FADS3*. GWAS index SNP rs174592-A (protective allele) of bipolar disorder (BP) is in high LD with index caQTL (rs99780, r^2 = 0.86 in EUR, 0.85 in this study population) for RE (chr11:61850491-61851800) and *FAD3* index eQTL (rs174583, r^2 = 0.89 in EUR, r^2 = 0.78 in this study population). Rs174592-A is located within the peak and predicted to disrupt a STAT1::STAT2 transcription factor binding site motif. (B) Rs174592-A decreases chromatin accessibility of this WRE (Beta = -0.10; P = 6.81 x 10^{-13}, left), and expression

of *FADS3* (Beta = -0.13 P = 2.95 x 10^{-7}, right) in CHIR condition. (C) Differential chromatin accessibility and *FADS3* gene expression between CHIR and Vehicle. (D) VST normalized expression counts of STAT1 and STAT2 are shown. Shrunken LFC and FDR-adjusted P values were estimated for 78 pairs. In the boxplots, chromatin accessibility or gene expression are colored by condition (gray: vehicle, blue:CHIR). (E) Schematic of FADS3 regulation through STAT1::STAT2 binding. Our data suggests characterization of the colocalized putative BP risk SNP (rs174592) as a functional variant regulating *FADS3* expression through differences in STAT1::STAT2 binding, which is inhibited during Wnt stimulation.

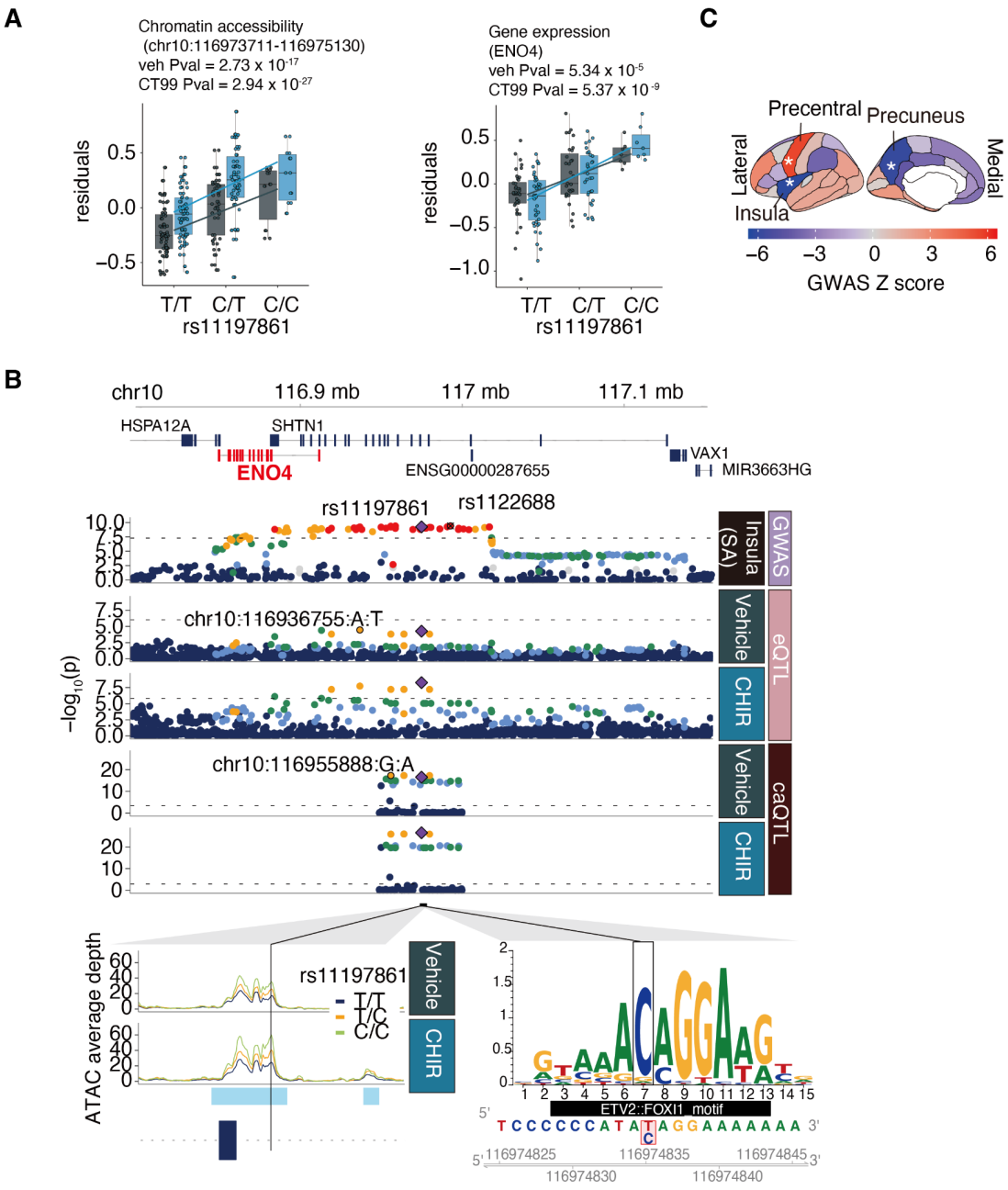

Supplementary Figure 2.23: Stimulus-specific *ENO4* eQTL colocalizing with regional cortical surface area GWAS

(A) Chromatin accessibility (chr10:116973711-116975130; left) and *ENO4* gene expression regulated by rs11197861. eQTL of *ENO4* was detected only in the stimulated condition (A, B). The eQTL is colocalized with several brain-related traits including surface area of Insula (B, C). (B) *P* values from Insula surface area GWAS, eQTL, caQTL for vehicle, CHIR condition are shown respectively. ETV2:FOXl1 motif is disrupted by the rs11197861-T located in the peak, which may

result in decreased chromatin accessibility and *ENO4* gene expression. (C) Z scores from regional cortical surface area(Grasby et al. 2020). In addition to Insula, surface area of precentral and precuneus are also associated with this SNP (indicated by asterisks; $p < 5 \times 10^{-8}$).

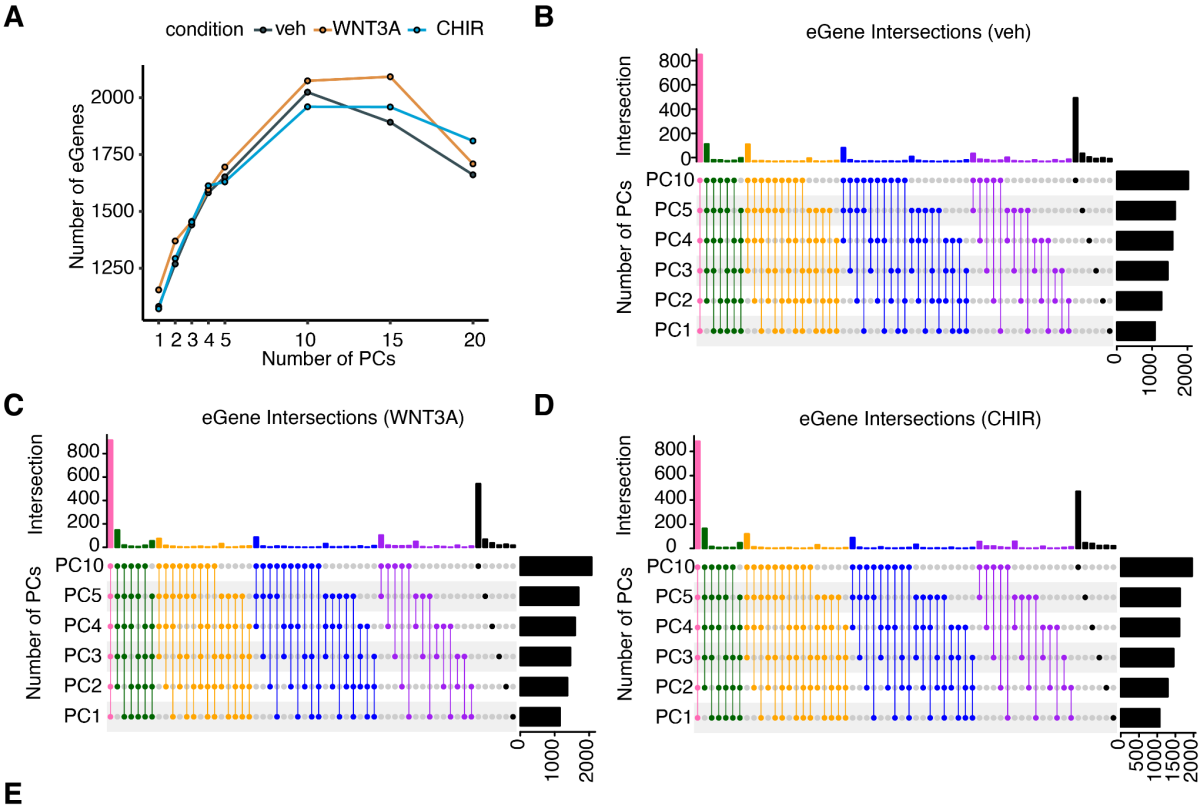

E

# of eSNPs per Gene

Round	# eGenes	condition
1	2024	Vehicle
2	65	Vehicle
1	2074	Wnt3A
2	72	Wnt3A
3	1	Wnt3A
1	1960	CHIR
2	65	CHIR
3	1	CHIR

Supplementary Figure 2.24: Optimizing control for known and unknown technical confounding in eQTL

We tested different numbers of PC variables to determine the number of PCs to include for correcting expression values prior to running limix_qtl. (A) The plot shows the number of discovered eGenes with respect to the number of PCs at FDR-adjusted P < 0.1. and the number of overlapping found eGenes across models (B-D). To identify independent eQTLs, we repeated eQTL mapping by including the index eSNP in the association model until no SNP passed the

genome-wide threshold (FDR-adjusted $P < 0.1$). In table (**E**), we show the number of SNPs discovered in each round of conditional associations.

CHAPTER 3: CELLULAR GENOME-WIDE ASSOCIATION STUDY IDENTIFIES COMMON VARIATION INFLUENCING LITHIUM-INDUCED NEURAL PROGENITOR PROLIFERATION

3.1 Introduction

Bipolar disorder (BD) is a highly heritable neuropsychiatric illness commonly treated with lithium salts (Geddes et al. 2004; Malhi, Gessler, and Outhred 2017; Geddes and Miklowitz 2013; Johansson et al. 2019). Lithium treatment is effective at preventing relapse of bipolar disorder episodes in 40-60% of individuals, indicating a high degree of variability in clinical response (Tohen et al. 2005; BALANCE investigators and collaborators et al. 2010; Viguera, Tondo, and Baldessarini 2000). Genetic background influences risk for BD (Mullins et al. 2021), as well as lithium response in individuals with BD (Grof et al. 2002; Hou et al. 2016; Song et al. 2016). These genetic effects are underscored by studies recapitulating lithium responsiveness in induced pluripotent stem cell (iPSC) lines generated from individuals with BD (Mertens et al. 2015; S. Stern et al. 2018; Shani Stern et al. 2020; Santos et al. 2021). Despite recent advances in identifying the genetic loci that underlie BD risk (Mullins et al. 2021), much less is known of the genetic underpinnings of lithium responsiveness (Senner et al. 2021). This is at least in part due to the difficulty of performing sufficiently powered pharmacogenomic studies in human populations, and lithium's diverse context- and cell-type-dependent effects (Wolter, Jimenez, et al. 2022). The mechanism underlying lithium's therapeutic effects is unclear, but an attractive hypothesis is that lithium increases adult neurogenesis by stimulating NPC proliferation, as observed for some antidepressant drugs (Santarelli et al. 2003; Sahay and Hen 2007; Boldrini et al. 2012, 2009; Perera et al. 2007; G. Chen et al. 2000). While the presence and timing of adult neurogenesis in the human brain has been questioned (Eriksson et al. 1998; Franjic et al. 2022), recent scRNA-seq in macaque and human hippocampus detected adult neural progenitors or

immature neurons (Hao et al. 2022; Wang et al. 2022; Zhou et al. 2022). Furthermore, lithium accumulates in neurogenic brain regions such as the hippocampus (Zanni et al. 2017; Schoepfer et al. 2021), increases the volume of the hippocampus in individuals with BD (Yucel et al. 2007, 2008; Bearden et al. 2008; Hajek et al. 2012), and stimulates adult hippocampal NPC proliferation in rodents (G. Chen et al. 2000). Based on this evidence, we designed an experiment to identify common genetic variants which influence lithium-induced NPC proliferation. To do this, we employed a library of genetically diverse primary human NPCs previously characterized by genotyping, RNA-seq, and ATAC-seq (Aygün et al. 2021; Liang et al. 2021; Stein et al. 2014).

3.2 Results

To identify genetic variants which modulate lithium induced proliferation, we utilized a library of fetally derived genetically diverse primary human NPC lines. Genetic effects on adult NPC proliferation may be observable in fetally derived NPCs because embryonic and adult neural stem cells exhibit similar gene expression profiles, signaling pathways, morphology, and cellular differentiation behaviors (Toda and Gage 2018; Kriegstein and Alvarez-Buylla 2009; Yuzwa et al. 2017; Hochgerner et al. 2018). We measured proliferation in these cells in the presence or absence of lithium using an EdU-incorporation assay, which fluorescently labels cells in S-phase of the cell cycle. Following a two-hour EdU pulse, cells were fixed, dual labeled with a fluorescent DNA content dye and EdU, and the number of cells within each phase of the cell cycle was quantified using flow cytometry (Fig. 1A). We found that lithium increased NPC proliferation at relatively low concentrations (≤2.5 mM), and decreased proliferation at higher concentrations (≥5 mM) (Supplemental Fig. 1A,B). Lithium has been shown to induce proliferation by activating Wnt signaling through competitive inhibition of GSK3B (Valvezan and Klein 2012). However, we did not observe activated Wnt signaling at proliferation-inducing concentrations using either a beta catenin activated luciferase reporter assay or qPCR measuring endogenous Wnt target gene expression (Supplemental Fig. 1C-E). GSK3B also directly

phosphorylates many transcription factors which in turn activate signaling pathways such as CREB and NFAT (Hur and Zhou 2010). We found that lithium activated expression of target genes of the NFAT signaling pathway at proliferation-inducing concentrations in NPCs (Qu, Sun, and Young 2011), but did not detectably affect gene expression of Wnt or CREB pathway associated genes (Supplemental Fig. 1G-J).

As the target serum concentration for long term lithium treatment is 0.6-1.2 mM, we focused on concentrations that approximate therapeutically relevant levels (0.75 and 1.5mM), as well as a higher concentration (3mM) that we hypothesized may be associated with negative side effects (Nolen et al. 2019). We measured lithium-induced proliferation using the previously described EdU incorporation and flow cytometry assay in a population of 80 genetically diverse NPC donors (Fig. 1A, see Supplemental Fig. 2, 3A-C and Methods). NPCs from all donor lines increased proliferation in a concentration dependent manner at 0.75 and 1.5 mM LiCl, while some NPC donor lines decreased proliferation at 3mM (Fig. 1B). Phenotypic values were normally distributed, and technical replicates (the same donor thawed at different times) were reasonably correlated (Supplemental Fig. 3D-H). Proliferation rates in vehicle and lithium conditions were strongly correlated (Supplemental Fig. 3I), which could mask the effect of genetic variation on lithium-induced proliferation. Therefore, our primary phenotype, termed ΔS-phase, subtracted the vehicle proliferation rate from the lithium exposure proliferation rate.

To identify genetic variants associated with lithium-induced NPC proliferation, we performed genome-wide association tests using a linear mixed effects model (Kang et al. 2010). While proliferation rates were not correlated with any measured biological or technical variables (Supplemental Figs. 3J-N), we included gestation week, sex, and multi-dimensional scaling components as covariates in the association model to control for ancestry. We identified 80 nominally significant ($p < 1x10-5$) loci across all conditions (vehicle, ΔS-phase 0.75, 1.5, and 3 mM LiCl), and one study-wide significant association ($p < 1.67x10-8$, corrected for the number of independent tests (Nyholt 2004)) (Fig. 1C, Supplemental Fig. 4, Supplemental Table 1). The

study-wide significant locus was associated with lithium induced proliferation (ΔS-phase) at 1.5 mM LiCl, but the association was attenuated in response to other lithium concentrations, and not detectably associated with vehicle proliferation rate (Fig. 1D-G). In all, these results demonstrate that GWAS performed in cultured cells can identify novel context-dependent pharmacogenomic effects (Jerber et al. 2021).

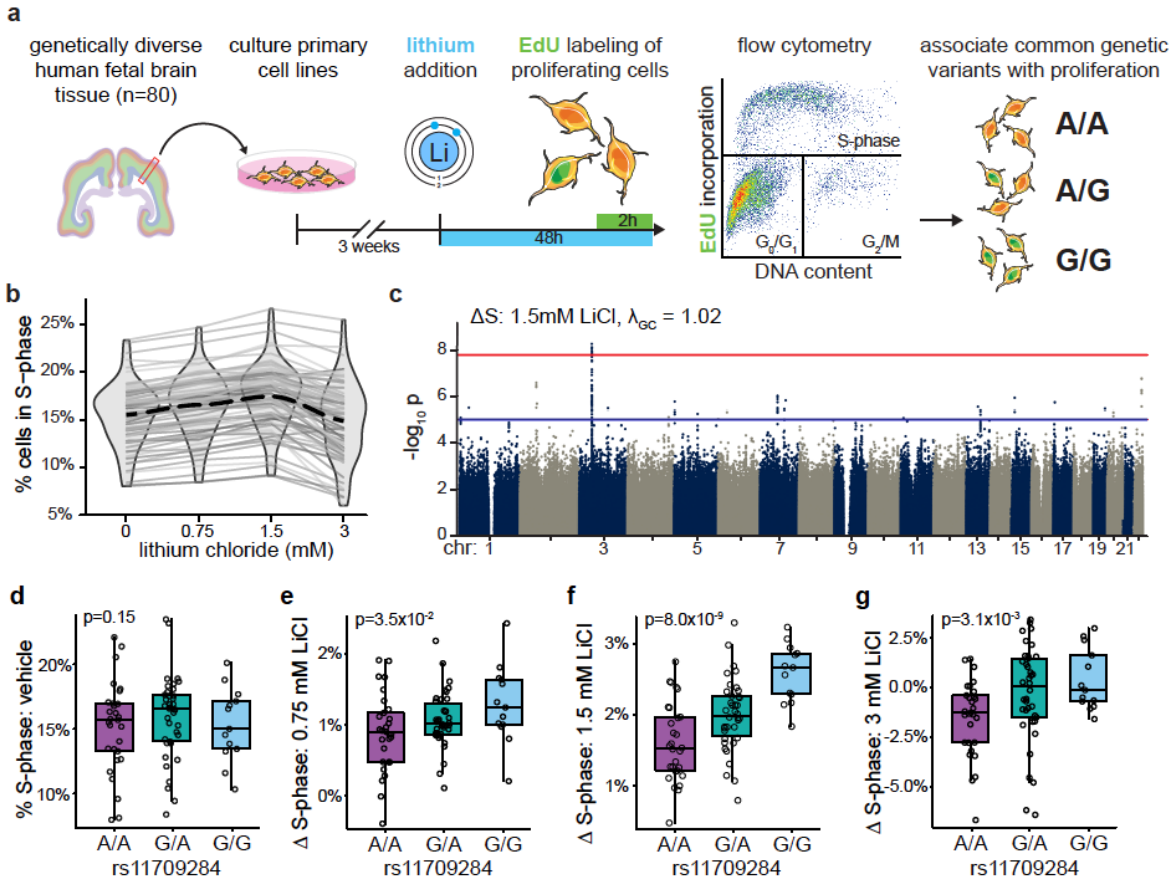

Figure 3.1: Cellular GWAS identifies genomic loci associated with lithium induced proliferation in NPCs

A) Experimental strategy to identify common genetic variants associated with lithium-induced NPC proliferation.

B) Percentage of cells in S-phase measured by EdU incorporation across indicated concentrations of LiCl in n=80 distinct NPC donors, each represented by a gray line. The

mean across donors is represented by the black dotted line. The distribution of cells in S-phase for each concentration is shown as a violin plot.

C) Manhattan plot showing GWAS of ΔS-phase in response to 1.5 mM LiCl. The red line denotes study-wide significance threshold ($p = 1.67 \times 10^{-8}$). The blue line denotes nominal significance threshold ($p = 1 \times 10^{-5}$).

D-G) Boxplots showing proliferation across genotypes at SNP rs11709284 in response to vehicle (D), ΔS-phase at 0.75mM (E), 1.5mM (F), and 3mM LiCl (G). Each point is a single NPC donor line with the indicated genotype. For all boxplots, the center line represents the median value, the bounds of the box are 25th and 75th percentiles, and the whiskers equal 1.5 times the interquartile range.

The study-wide significant locus at chr3p21.1 spans a >500kb gene dense region (Fig. 2A). This locus contains two SNPs with the lowest study-wide p-values (rs352140, p = 5.71x10-9; rs11709284, p = 8.00x10-9), which are weakly correlated by linkage disequilibrium (LD, r2 = 0.22). To evaluate whether rs352140 and rs11709284 tag independent loci, we conditioned the associations on either SNP, both of which reduced the significance of the association of the other, indicating that the association signal identifies a single but complex locus (Supplemental Fig. 5A-C).

To explore the association of this locus to other complex brain traits we tested for colocalization with existing brain-related GWAS summary statistics using conditional analysis (Ying Wu et al. 2019). We identified colocalizations with risk for BD (Mullins et al. 2021), schizophrenia (Trubetskoy et al. 2022), and inter-individual differences in intelligence (Savage et al. 2018) (Fig. 2B-D). Conditioning on each index SNP from these brain-related GWAS markedly reduced proliferation associations, especially for rs11709284 (Supplemental Fig. 5D-F), suggesting that causal variant(s) affecting lithium-induced proliferation and these complex brain traits are shared. We expect that the colocalization between lithium responsive

proliferation, inter-individual differences in intelligence, BD risk, and schizophrenia risk is driven by the strong genetic correlation and polygenic overlap among these traits (Smeland et al. 2020; Frei et al. 2019; Mullins et al. 2021), and suggests that the GNL3 locus is broadly relevant to brain function. Moving forward, we focus on rs11709284 as marking the lithium-induced proliferation associated locus given its stronger association with these other traits. The lithium-induced proliferation-increasing allele is a risk allele for BD and schizophrenia, and an intelligence-decreasing allele. The lithium induced proliferation locus was not associated with lithium response in individuals with BD (Hou et al. 2016) (Supplemental Fig. 5G). The lone genome-wide significant locus associated with lithium response in individuals with BD was also not associated with lithium induced proliferation or risk for BD (Supplemental Fig. 6). To explore patterns of polygenic overlap between lithium-sensitive proliferation and other traits, we selected variants associated with 1.5mM lithium-induced proliferation at increasing significance thresholds, and plotted other trait GWAS p-values at these selected variants using quantile-quantile (QQ) plots (Supplemental Fig 7, Supplemental Table 2). SNPs most significantly associated with lithium-induced NPC proliferation phenotype showed highest enrichment in neuropsychiatric disorder GWAS (bipolar disorder, schizophrenia, major depressive disorder, autism spectrum disorder), relatively moderate enrichment in non-disorder brain traits (intelligence, global cortical thickness), and little enrichment in non-brain traits (HDL being the only exception) (Supplemental Fig. 7A-D). This pattern of enrichment suggests that the genetic variants associated with lithium-sensitive NPC proliferation are also associated with risk for neuropsychiatric disorders.

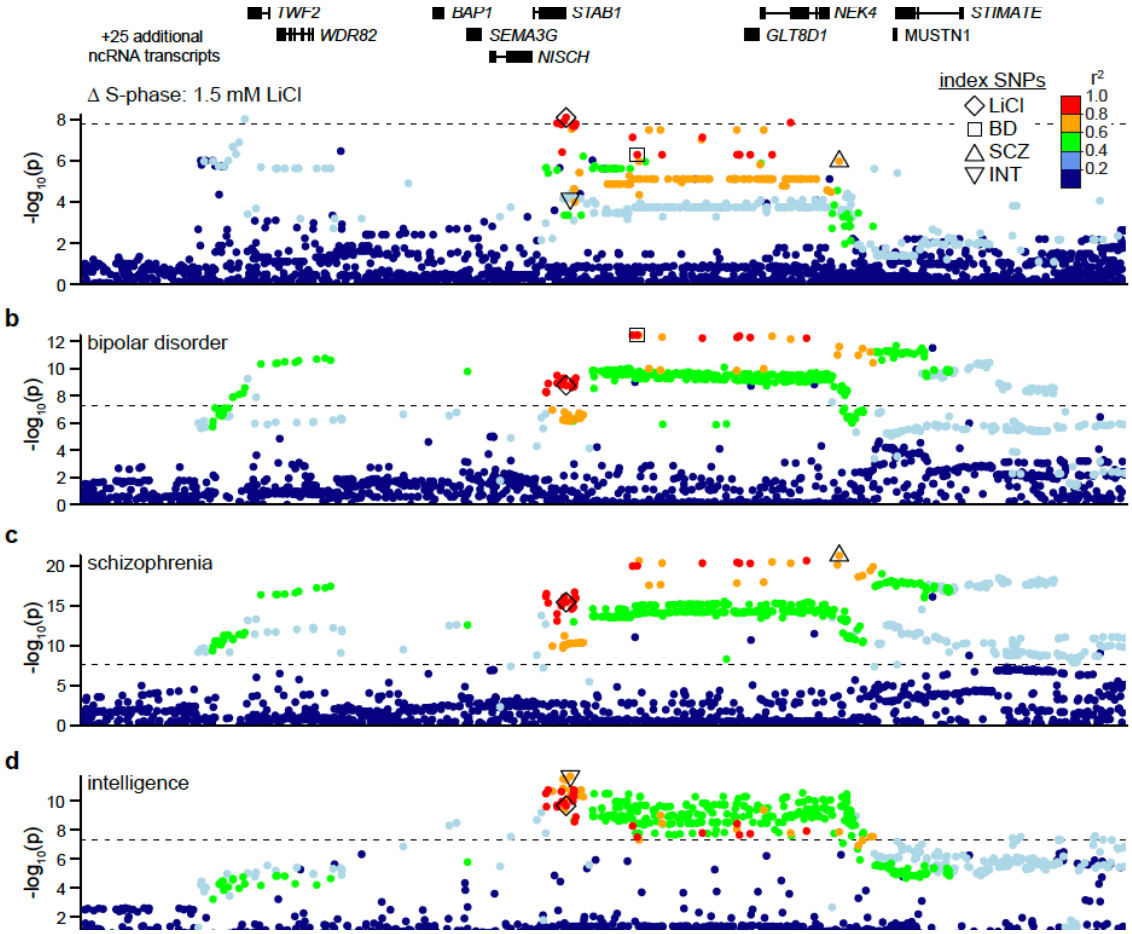

Figure 3.2: Lithium-induced proliferation at chr3p21.1 colocalizes with neuropsychiatric disorders and intelligence GWAS

A) Locus zoom of the 1.5 mM LiCl ΔS-phase phenotype. Dashed line denotes study-wide significance level. ◇: SNP of interest from this study (rs11709284). Each SNP is colored by LD (r^2) to rs11709284 in NPC donors.

B-D) GWAS results for BD (Mullins et al. 2021) (B), schizophrenia (The Schizophrenia Working Group of the Psychiatric Genomics Consortium et al. 2020) (C), and intelligence (Savage et al. 2018) (D) at the same locus as (a). SNP annotations: □: index SNP for BD (rs2336147). △: index SNP for schizophrenia (rs2710323). ▽: index SNP for intelligence (rs4687625). r^2 values relative to rs11709284 were calculated using the 1000 Genomes EUR reference panel (1000 Genomes Project Consortium et al. 2015). Dashed lines indicate standard genome wide significance threshold ($p = 5 \times 10^{-8}$).

To identify putative causal genes underlying the association with lithium induced proliferation, we considered a ~1.2 Mb window containing 29 protein coding genes surrounding rs11709284 (Supplemental Fig. 8A). Previous expression measurements via RNA-seq in these NPCs showed that 21 of these genes had detectable expression at baseline (Aygün et al. 2021; Liang et al. 2021) (Supplemental Fig. 8B). We quantified the expression of each of these genes over time in response to 1.5 mM LiCl in one NPC donor line using qPCR, and GNL3 was the only gene with significantly different expression at multiple timepoints (Supplemental Fig. 8C). Repeating this experiment in NPCs from three additional donors confirmed that 1.5 mM LiCl transiently induces GNL3 expression, peaking eight hours post exposure (Fig. 3A). Increasing lithium concentration also resulted in relatively higher GNL3 expression at 8 hours, without extending the duration of expression (Supplemental Fig. 8D).

GNL3, also known as nucleostemin, regulates cell cycle progression and genome stability, and is essential for maintenance of stem cell fate (L. Meng et al. 2013; Tsai and McKay 2002). GNL3 was also identified as a putative BD risk gene in the most recent BD GWAS (Mullins et al. 2021), and an integrated eQTL analysis of previous BD GWAS (Q. Meng et al. 2020). rs11709284 is an eQTL in GTEx for multiple nearby genes (PBRM1, NT5DC2, GLYCTK, NEK4), but most significantly for GNL3 in brain tissues, including frontal cortex and hippocampus (GTEx Consortium et al. 2017) (Fig. 3B,C), and these associations colocalize (Supplemental Fig. 9A-G). The allele associated with increased GNL3 is also associated with increased lithium-induced proliferation (Fig. 1F). We next assessed allele specific GNL3 expression in the population of NPCs using SNPs in LD with rs11709284 in the GNL3 open reading frame, and found that the allele associated with increased GNL3 expression at baseline was also associated with increased lithium-induced proliferation (Aygün et al. 2021) (Fig. 3D, Supplemental Fig. 9H). To assess how lithium affects the expression of each GNL3 allele, we used allele specific qPCR probes targeting a SNP in the 5'UTR of GNL3 ($r^2 = 0.68$)

(Supplemental Fig. 10A). Again, we observed that the allele associated with increased proliferation rates had increased GNL3 expression in a temporally controlled manner (Fig. 3E,F). Immunolabeling for GNL3 suggested that cells in S-phase have increased nuclear GNL3 puncta compared to cells which are not in S-phase (Fig. 3G,H). While lithium increased GNL3 RNA in bulk qPCR measurements (Fig. 3A), we were not able to detect that lithium further increased GNL3 protein levels in individual cells (Fig. 3H). This suggests that lithium is causing more cells to enter the cell cycle but is not directly affecting GNL3 expression on an individual cell basis. In all, this data suggests that GNL3 is a lithium and proliferation responsive gene, and that common genetic variants associated with increased GNL3 expression are also associated with increased lithium induced NPC proliferation.

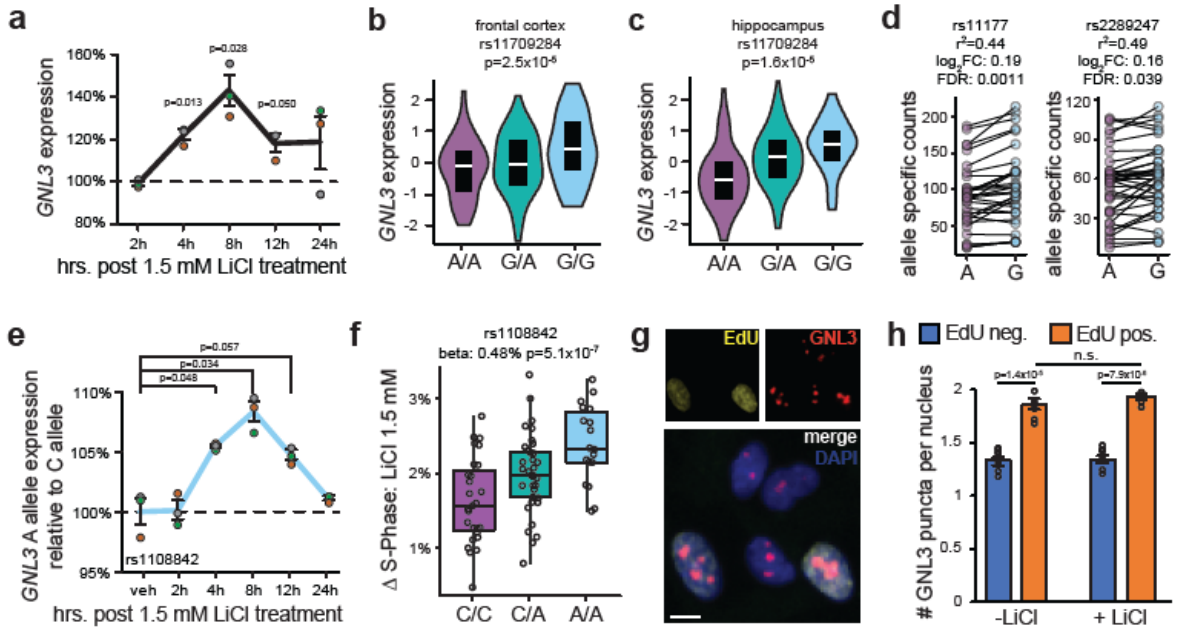

Figure 3.3: Lithium induced proliferation increasing alleles are also *GNL3* increasing alleles

A) *GNL3* expression in NPCs from three randomly selected donor lines following treatment with 1.5 mM LiCl, quantified by RT-qPCR. Each time-point was normalized to vehicle-

treated samples extracted at the same time (dashed line). Each colored dot is a distinct NPC donor line. All error bars throughout this study are standard error of the mean.

B,C) Allelic effects on *GNL3* expression at SNP rs11709284 in frontal cortex and hippocampus from GTEx (GTEx Consortium et al. 2017), FDR < 0.05. Alleles associated with increased *GNL3* expression are also associated with increased ΔS-phase (compare alleles with Fig. 1F). In all subsequent figures purple denotes the allele associated with less proliferation, whereas blue denotes the allele associated with increased proliferation from this study.

D) Allele specific expression of two SNPs in *GNL3* open reading frame in NPCs where donor lines are heterozygous for each SNP, assessed from baseline RNAseq data (Aygün et al. 2021). r^2 values relative to rs11709284. Alleles associated with increased *GNL3* expression at baseline are also associated with increased lithium ΔS-phase (compare alleles with Supplemental Fig. 9H).

E) Allele specific RT-qPCR for *GNL3* in response to 1.5 mM LiCl, quantified in NPCs from n=3 distinct donors which are heterozygous for a SNP in *GNL3* 5'-UTR (rs1108842). Relative expression of each allele was quantified by calculating the cycle difference between each allele at 0.5 Rn, as in (Wolter et al. 2020). Each colored dot represents NPCs from a distinct donor. Four technical qPCR replicates were acquired per donor and averaged, and the data was then normalized to vehicle, as in Fig. 3A. Significance was determined by paired t-test.

F) Proliferation phenotypes of SNP in *GNL3* 5'UTR (rs1108842). The A-allele is associated with higher lithium-induced proliferation, and increased *GNL3* expression in response to lithium.

G,H) NPCs treated with LiCl for 48 hrs with a 2 hr. EdU pulse, followed by labeling with anti-GNL3 antibody and DAPI. (G) Representative image demonstrates GNL3 is a nuclear protein. (H) Quantification of GNL3 puncta in cells in EdU- cells versus EdU+

cells in the presence and absence of LiCl. n=8 wells per condition, nine tiled images per well. Significance was determined by a paired t-test. Scale bar = 10 um.

Next, we sought to determine whether manipulating GNL3 expression is sufficient to affect lithium responsive NPC proliferation. We targeted the promoter of GNL3 with dCas9 fused to either a chromatin repressive (KRAB) or chromatin opening (VP64) domain (Thakore et al. 2015; Pickar-Oliver and Gersbach 2019), and identified guide RNAs (gRNAs) capable of decreasing or increasing GNL3 expression (Supplemental Fig. 10A, Fig. 4A). We found these constructs do not detectably affect expression of genes within a 250kb window surrounding the gRNA target sites, except for PBRM1, which shares a bidirectional promoter with GNL3 (Supplemental Fig. 10A-C). Because PBRM1 was not found to have lithium responsive gene expression, we focused on the effects of modulating GNL3 at this locus (Supplemental Figure 8C). Interestingly, changing baseline GNL3 levels did not affect the relative magnitude of lithium's activation of GNL3 expression (Supplemental Fig. 10B). Increasing GNL3 expression was sufficient to increase proliferation in the absence of lithium, while decreasing GNL3 expression had no detectable effect on baseline proliferation (Fig. 4B). In contrast, NPCs with decreased GNL3 expression had 52-54% less lithium-induced proliferation (Fig. 4C). Increasing GNL3 expression did not further affect lithium's induction of proliferation (Fig. 4C), which we speculate could be a ceiling effect as the dCas9 VP64 treated NPCs already had ~4% increased proliferation rate at baseline (Fig. 4B). In all, these experiments indicate that GNL3 is necessary for lithium's full proliferative effects in NPCs, and sufficient to induce NPC proliferation.

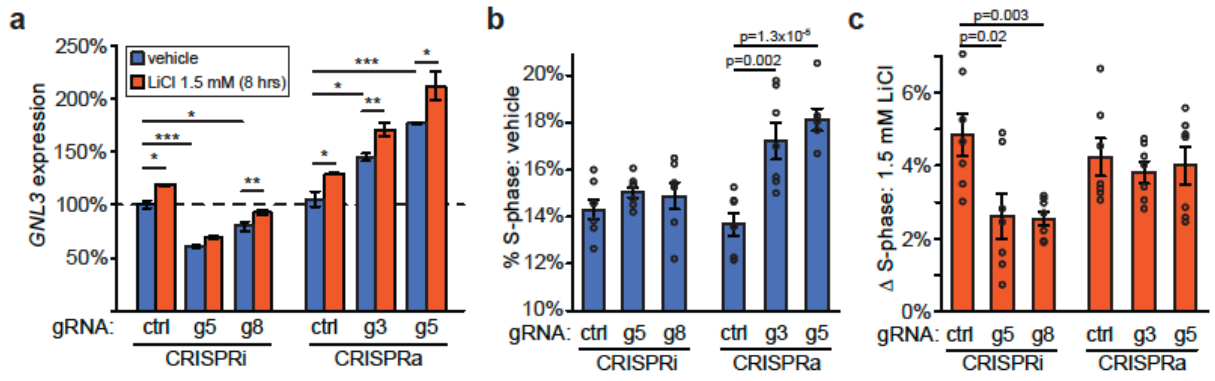

Figure 3.4: *GNL3* expression is necessary for the full effects of lithium-induced proliferation, and sufficient to induce NPC proliferation.

A) An NPC donor line heterozygous for index SNP (rs11709284) was transduced with lentivirus carrying the indicated gRNA, and dSpCas9:KRAB (CRISPRi) or dSpCas9:VP64 (CRISPRa). Cells were incubated for four days, followed by an eight hour treatment with 1.5 mM LiCl. *GNL3* expression was analyzed by RT-qPCR. Data normalized to neg. control gRNA (non-targeting, dashed line). n=4 qPCR replicates, significance determined by two sample t-test. * p<0.05, ** p<0.01, *** p<0.001.

B) Proportion of NPCs in S-phase expressing indicated dSpCas9 and gRNAs at baseline, analyzed by high content imaging, as in Fig. 3G. n=7 wells per condition, nine tiled images per well, significance determined by two sample t-test.

C) Change in the proportion of NPCs in S-phase in response to 1.5mM LiCl, while expressing indicated dSpCas9 and gRNAs. n=7 wells per condition, significance determined by two sample t-test.

3.3 Discussion

We performed a GWAS in cultured human NPCs and identified common genetic variants which impact lithium-induced proliferation. The chr3p21.1 locus was only detectable following lithium treatment (Fig. 1D,F), supporting the hypothesis that certain genetic variants influence traits only in specific contexts (Umans, Battle, and Gilad 2020). We also detected a colocalization between genetic effects on lithium induced proliferation and BD risk,

schizophrenia risk, and inter-individual differences in intelligence (Fig. 2 and Supplemental Fig. 5), demonstrating that genetic variation at this locus is also relevant for differences in brain-related traits and risk for neuropsychiatric disorders. We identified a single gene in this locus, GNL3, whose expression changed in response to lithium, has previously been implicated in BD risk (Mullins et al. 2021; Q. Meng et al. 2020), and has known roles in neural stem cell self-renewal by mitigating DNA damage induced by DNA replication (L. Meng et al. 2013; Tsai and McKay 2002) (Fig. 3 and Supplemental Fig. 8). We found that common genetic variation influences GNL3 expression, and using CRISPRi/a demonstrated that modulating GNL3 expression can influence proliferation in both the presence and absence of lithium (Fig. 4). In all, using a cell-culture GWAS system in a pharmacogenomics design and CRISPR-based experimental manipulations, we discover and validate a gene that contributes to differences in neural progenitor proliferation in response to lithium.

Colocalization analysis suggests that genetic variation at the chr3p21.1 locus modulates molecular, cellular, cognitive, and neuropsychiatric risk traits. Genetic predisposition for a disorder has previously been shown to be related to treatment response in that disorder (Kappel et al. 2022), which could explain the colocalization between risk for BD and cellular lithium response. Interestingly, combining schizophrenia and BD polygenic risk scores improves genetic prediction of lithium response in individuals with BD (Schubert et al. 2021), suggesting that shared genetic variation modulating risk for either disorder may also influence treatment responses. Previous studies describing strong genetic correlation and polygenic overlap between risk for BD, risk for schizophrenia, and inter-individual differences in intelligence also lead us to expect detection of some shared genetic effects for these traits (Smeland et al. 2020; Frei et al. 2019; Mullins et al. 2021). GNL3 may also function through additional cellular contexts other than lithium exposure in NPCs to alter risk for these disorders and inter-individual differences in cognitive ability.

Our results can be interpreted in environmental, developmental, and clinical contexts. Lithium's effects on NPC proliferation or other cellular processes via environmental or dietary sources could explain the correlation between lithium exposure and population-level measures of psychiatric health (Schrauzer and Shrestha 1990; Kessing et al. 2017; Memon et al. 2020). Lithium is also classified as a class D teratogen due to increased risk of fetal cardiac malformations (Newport et al. 2005; Poels, Bijma, et al. 2018), but effects on human brain tissues resulting from fetal exposure to lithium are unclear (Munk-Olsen et al. 2018; Forsberg et al. 2018). While fetal lithium exposure may lead to subtle neurodevelopmental alterations in animal models (Abu-Taweel 2012; Messiha 1986; Poels, Schrijver, et al. 2018; Giles and Bannigan 2006), whether fetal NPC proliferation contributes to these effects is unknown. Given the limited evidence for lithium's teratogenic effects on the human brain, we favor interpreting our results in the context of the clinical lithium response. If fetally derived NPCs can model the proliferative activity of adult hippocampal progenitor cells and NPC proliferation provides therapeutic benefit as has been shown for antidepressants (Santarelli et al. 2003; Sahay and Hen 2007; Perera et al. 2007; Boldrini et al. 2009, 2012), our results suggest genetic effects on GNL3 expression and lithium-induced NPC proliferation may contribute to variance in clinical outcomes of lithium treatment.

Our study must also be viewed in light of some limitations. The study-wide significant locus discovered here was not identified in GWAS for lithium response in BD individuals (Hou et al. 2016; Song et al. 2016). The disparity between these cellular and clinical phenotypes may be a result of limited sample sizes or differing population structure. Clinical lithium response GWAS were conducted using ~12,000 individuals in the Song et al. 2016 (Song et al. 2016) and ~1,500 individuals in the Hou et al. 2016 (Hou et al. 2016) studies, substantially smaller sample sizes than well-powered neuropsychiatric disorder GWAS (Mullins et al. 2021; Trubetskoy et al. 2022). Population structure differences may also obscure shared genetic effects (Martin et al. 2017). The Hou et al. and Song et al. lithium response GWAS were restricted to individuals with

European ancestries, while only 10% of cell lines used in our study were of European ancestry. Future lithium response GWAS with increased sample size and genetic diversity will improve our understanding of the genetic architecture of lithium response in BD and provide higher power for assessing colocalization. Another potential limitation is that lithium-induced proliferation in cultured NPCs may not accurately model the clinical lithium response. While lithium stimulates hippocampal NPC proliferation in adult rodents, and the fetal NPCs used here share many properties with adult hippocampal NPCs (G. Chen et al. 2000; Yuzwa et al. 2017; Hochgerner et al. 2018; Kriegstein and Alvarez-Buylla 2009), further experiments are necessary to evaluate a connection between NPC proliferation and clinical lithium response in humans. Experiments testing whether lithium induced NPC proliferation differs in iPSCs derived from lithium responders or non-responders may provide further insight into the clinical relevance of our findings (Mertens et al. 2015; S. Stern et al. 2018; Shani Stern et al. 2020; Santos et al. 2021). Finally, while our study focused on lithium's acute (48h) effects on proliferation following administration of a single therapeutically relevant concentration, lithium's beneficial effects typically occur through sustained maintenance treatment (Tondo et al. 1998). Further experiments will be necessary to evaluate how genetic variation alters proliferation or differentiation outcomes after prolonged exposure to lithium in a cell culture-based model.

Despite these limitations, our data lead us to hypothesize that manipulating GNL3 expression during lithium treatment may enhance clinical outcomes. Our findings also suggest that lithium's therapeutic effects will be reduced in individuals with genetic backgrounds producing lower GNL3 expression. These hypotheses can be tested by determining the effects on NPC proliferation, neurogenesis, and relevant behavioral paradigms after experimental manipulation of GNL3 expression in the brain during lithium exposure in rodents (O'Donnell and Gould 2007). In conclusion, our study sheds light on how common genetic variation can influence the cellular effects of a widely used mood stabilizing treatment. Our approach also

suggests that the genetic diversity inherent in libraries of human cell lines can be leveraged to identify novel therapeutically relevant genes and pathways.

3.4 Materials and Methods

Ethics statement for human tissue-derived cell-lines

Human NPC cell-lines in this study originated from prenatal tissue collected following voluntary termination of pregnancy at the UCLA Gene and Cell Therapy facility following IRB regulations.

NPC cultures

Primary human NPCs were obtained from fetal brain tissue, assumed to be derived from the dorsal telencephalon based on visual inspection, at approximately 14-21 gestation weeks, as previously described (Stein et al. 2014; Aygün et al. 2021; Liang et al. 2021). After single cell dissociation, cells were initially cultured as neurospheres before plating on fibronectin (Sigma, F1141) and Poly-L-Ornithine (Sigma, P3655) coated plates, passaged 2-3 times, cryopreserved, and transferred to UNC Chapel Hill. NPC media: Neurobasal A (Life Technologies, 10888-022) supplemented with 100 μg ml^{-1} primocin (Invivogen, ant-pm-2), 10% BIT 9500 (Stemcell Technologies, 09500), 1% glutamax (100x; Life Technologies, 35050061), 1 μg ml^{-1} heparin (Sigma-Aldrich, H3393-10KU), 20 ng ml^{-1} EGF/FGF (Life Technologies, PHG0313/PHG0023), 2 ng ml^{-1} LIF (Life Technologies, PHC9481) and 20 ng ml^{-1} PDGF (Life Technologies, PHG1034). We followed previously established protocols to maintain NPCs as proliferating neural progenitors and inhibit differentiation into neurons (Liang et al. 2021). No mycoplasma contamination was detected during regular pre-assay screens of cell culture media (ATCC, 30-1012K).

LiCl treatments

This describes the general approach for the lithium exposure performed in all experiments. LiCl (Sigma, 203637) was diluted in water to 3M and stored in single use aliquots

at -80˚C. NPCs were plated at densities dependent on culture plate size, as described below for each experiment. The following day LiCl was diluted in NPC media, without growth factors, to 10X concentration in 10% of the total volume media in each well. Control wells (vehicle) contained a volume of water equal to the amount of 3M LiCl required to obtain 10X concentration.

High-throughput proliferation assays

We thawed cryopreserved NPCs in batches of ~8-10 NPC donor lines, which were pseudorandomized for biological and technical variables (sex, gestation week, passage). We included at least one technical replicate (distinct cryovials of the same NPC donor line thawed and assayed multiple times) in each batch to assess technical reproducibility (29 unique NPC donor lines replicated in duplicate, Supplemental Fig. 3H). Each batch was cultured with weekly passaging for two weeks to allow recovery from thawing. On week three, cells were lifted using 0.05% Trypsin (Gibco, 25300062), and 12,500 cells per well were plated in each well of 96 well plates (Corning, 3610). 24 hours later, LiCl (0.75, 1.5, or 3 mM) or vehicle (water) was added as described above. After 46 hours, cells were treated with 10 uM EdU with a 10% media addition and incubated for 2 hours. Cells were then lifted off the plate using 0.05% trypsin (Gibco, 25300062) and transferred to a u-bottom 96-well plate. Cells were fixed with 4% PFA in PBS for 10 minutes. EdU labeling was performed using the Click-iT EdU Cell Proliferation Kit (ThermoFisher, C10337) per manufacturer's protocols. Total DNA content was labeled with the FxCycle Far Red dye (ThermoFisher, F10347). Cell suspensions were quantified using the Attune NxT 96-well Flow Cytometer. For each LiCl concentration, 4 wells per NPC donor line were quantified. For vehicle treatment (water), 8 wells per NPC donor line were acquired. Replicates were spatially distributed across each plate to avoid positional bias. All liquid handling steps, including the additions of LiCl, EdU, trypsin, fixation, and the Click-iT reaction, were performed using the Tecan Evo liquid handling robot to reduce handling variability.

Analysis of flow cytometry data

FCS output files from the Attune NxT were initially analyzed using FlowJo, using SSC to retain only singlets (Supplemental Fig. 2A,B). To perform automated gating of stages of the cell cycle, we combined technical replicates into a single FCS file, and bounds were drawn for G0/G1, S-phase, and G2/M using the automated gating software FlowDensity (Malek et al. 2015), with three non-elliptical gates (Supplemental Fig. 2C). These gates were then applied to each well independently. Technical replicates were averaged to obtain the percentage of cells in S-phase for each NPC donor line in each condition. Wells which failed for technical reasons (such as a bubble in the flow cytometer or no EdU labeling due to a failed Click-iT reaction), were identified by calculating the coefficient of variation (CV), followed by manual inspection of FCS files for all conditions where CV > 0.1. This filtering removed ~0.5% of wells. For donor lines which were assayed in multiple rounds, we averaged all replicates together for genetic associations.

Genome-wide association

The percentage of cells in S-phase for each experimental condition for each NPC donor line was calculated using the average across all wells. ΔS-phase was calculated by subtracting the percentage of cells in S-phase in vehicle condition from the percentage of cells in S-phase for each concentration of LiCl. We used a linear mixed effects model to conduct genetic association tests implemented with EMMAX software (Kang et al. 2010). In this model, we included an $m \times m$ Balding Nichols kinship matrix inferred from NPC genotypes (K) (Kang et al. 2008) as a random effect variable to control for effects of cryptic relatedness, and 10 multidimensional scaling (MDS) genotype components as covariates to mitigate confounding effects of population structure. While we did not find that sex or gestation week correlated with proliferation phenotypes (Supplemental Figs. 3J-L), we included sex and gestation week as standard technical covariates in the model.

CRISPR based modulation of gene expression

gRNAs were selected using the GPP sgRNA Designer (Broad Institute) and cloned into CRISPRi (pLV hU6-sgRNA hUbC-dCas9-KRAB-T2a-GFP; Addgene 71237) or CRISPRa (pLV hU6-gRNA (anti-sense) hUbC-VP64-dCas9-VP64-T2A-GFP; Addgene 66707) plasmids, which were kind gifts from the lab of Charles Gersbach. See supplemental information for Lentivirus production. For experiments in Fig. 4A an NPC donor line heterozygous for rs11709284 was plated at 200,000 cells per well in 12 well plates. 75 uL of each viral prep was delivered to each well. Cells were incubated for 96 hours. RNA extraction, cDNA synthesis, and qPCR were performed as described in Supplemental Information. Consistency of lentivirus infection and dCas9 expression was verified using qPCR for dCas9. The negative control gRNA is a random sequence that does not align to the human genome.

RNA extraction and RT-qPCR

200,000 NPCs were plated in each well of a 12 well plate (Fisher Scientific, 0720082). LiCl was added at different times, and RNA for all timepoints was collected simultaneously. Each timepoint had paired vehicle/LiCl exposed samples for normalization purposes. RNA was extracted using standard Trizol extraction method (Ambion, 15596026). cDNA was synthesized from 100-200 ng RNA using VILO SSIV Master Mix with ezDNAse (ThermoFisher, 11766051). qPCR was performed with SSO Advanced SYBR Green MasterMix (BioRad, 1725271). n=4 qPCR replicates were performed for all experiments. Relative gene expression was determined using the ΔΔCt method, normalized to *EIF4A2*. Each LiCl condition was normalized to its respective vehicle time point. Statistical tests for timepoint experiments use the paired Student's t-test (Fig. 3a,e, Supplemental Figs. 1b,d,e, 8c,d), all other qPCR experiments use the two-sample Student's t-test (Fig. 4a, Supplemental Figs.1f-j, 10c). qPCR primers are listed in Supplemental Table 3.

NPC line selection for GWAS and QC

Cell type heterogeneity in the NPC library could introduce phenotypic variation based on cell type, which could be a confounding factor in genetic associations. Proliferation assays were performed on 94 NPC donor lines, but we excluded NPC donors with outlier gene expression patterns likely resulting from cell-type heterogeneity due to errors in dissection. Principal component analysis was performed on previously acquired (Aygün et al. 2021) baseline expression of the 500 highest variance transcripts followed by k-means clustering (k=2) (Supplemental Fig. 3a-c). This analysis identified NPC donor lines with relatively low expression of the canonical NPC marker *PAX6*, and relatively high levels of *NKX2.1* and *VAX1*, markers of ventral inhibitory NPCs (Campbell 2003; Hallonet et al. 1998). To assess sample swaps or mixing between NPC lines we used verifyBamID (Jun et al. 2012), which flagged an additional 4 lines with FREEMIX or CHIPMIX scores greater than 0.04. This resulted in NPCs from 80 distinct donors that were carried forward into association analyses.

Quantifying proliferation via EdU incorporation and high content imaging

For experiments in Fig. 3g,h, a randomly selected NPC line was plated at 10,000 cells per well in black walled 96 well plates (Corning, 3603). 24 hours later LiCl was added to the plate as described above and incubated for 48 hours, with an EdU pulse during the last two hours of incubation. For experiments in Fig. 4b,c, a randomly selected NPC donor line was plated at 200,000 cells per well in 12 well plates. 75 uL of each CRISPRi/a viral prep was delivered to each well. Cells were incubated for 96 hours. Cells were then lifted off the plate using 0.05% trypsin, counted, and plated in black walled 96-well plates at 10,000 cells per well. 24 hours later cells were treated with LiCl at the indicated concentrations, and incubated for 48 hours with an EdU pulse during the last two hours of incubation. Cells were fixed on the plate with 4% PFA in PBS, and Click-iT EdU labeling was performed per the manufacturer's protocol (ThermoFisher, C10337). Cells were additionally labeled with anti-GNL3 antibody (ThermoFisher, AB_2532414, clone:3H20L2, 1:250 dilution), anti-GFP antibody to label Cas9+

cells (AbCam, ab5450, 1:1000 dilution) and DAPI (1:4000). Images were acquired at 20x using the GE IN CELL Analyzer 2200 high-content imager. Images were analyzed using a custom CellProfiler pipeline. We isolated Cas9+/DAPI+ positive cells, and quantified the number of GNL3 puncta per nucleus (puncta defined as nuclear object 3-10 pixels in diameter), and percentage of Cas9+/EdU+ cells using n=7-8 wells per condition, with 9 images captured per well. Cell counts of each image were averaged for each well, and wells were averaged across conditions. Significance was determined by a paired t-test, paired by well.

Lentivirus production

Lentivirus was produced in HEK293T cells using the third-generation packaging plasmids (Addgene, 12260, 12259). Multiple densities (200,000-600,000 cells) of HEK293T cells were plated in 12 well plates in 1 mL media. 24 hours later the cell density at ~90% confluency was transfected with 1200 ng psPAX2, 800 ng pMD2.G, and 1600 ng of each lentiviral plasmid, using 8 uL FuGene6 (Promega, E2691). Cells were incubated for 24 hours, followed by a 50% media change in the morning, and a 1 mL media addition in the afternoon. 24 hours later supernatant was collected, filtered using 0.45 μm filters, and stored in single use aliquots at -80˚C.

Wnt signaling luciferase assays

10,000 NPCs per well were plated in 96 well plates (Corning, 07-200-91), and 24 hours later were transduced with 10 uL lentivirus carrying BAR:luciferase lentivirus, and 2 uL Tk:*Renilla* lentivirus. Cells were incubated for two days, treated with LiCl as above, and incubated for 48 hours. Cell lysate was used in dual luciferase assays using the Dual-Glo luciferase system (Promega, E2920), measured on the GloMax Discover plate reader (Promega). BAR:Luciferase and Tk:*Renilla* plasmids were kind gifts from the lab of Ben Major (Major et al. 2007). Statistical significance was determined using paired Student's t-test.

GWAS Study Wide Significance Threshold

Study-wide significance threshold (as in Nyholt, *et al (Nyholt 2004)*) was used because we tested four phenotypes (S-phase: vehicle, ΔS-phase 0.75 mM, 1.5 mM, 3 mM LiCl). In brief, we first calculated the total number of independent tests across these GWAS using summary statistics (determined to be 2.996 independent tests), and then adjusted the standard genome-wide significance threshold (γ = 5x10^{-8}) by the effective number of independent tests (n), to derive a study-wide significance threshold using a Sidak correction of $\alpha = 1 - (1-\gamma)^{1/n}$ = 1.67x10^{-8}.

GWAS colocalization

We evaluated numerous GWAS summary statistics (Supplemental table 2) for colocalization with the study-wide significant locus on chromosome 3. We first filtered downloaded GWAS summary statistics for SNPs with genome-wide significant p-values (p < 5x10^{-8}) within 1Mb upstream or downstream from rs11709284. Next, we calculated LD between these SNPs and rs11709284 using either our population of NPC donors or 1000 Genomes Project Europeans (EUR) (Fairley et al. 2020). We required variants to exceed r^2 > 0.6 to be considered a colocalization candidate, and then used conditional analysis to provide evidence for colocalization (Civelek et al. 2017). We considered GWAS signals to be colocalized when the proliferation associated p-value no longer reached nominal significance (p > 1 x 10^{-5}) after conditioning on the GWAS index SNPs.

Cross-trait enrichment analysis

GWAS summary statistics (Supplemental Table 2) were filtered for variants also associated with proliferation phenotypes from this study under increasingly stringent p value thresholds (p < 1x10^{-3}, 1x10^{-4},1x10^{-5}, 1x10^{-6}, 1x10^{-7}). Observed distributions of filtered association p values from the various GWAS were compared to expectations under a null hypothesis where no genetic effect on the phenotype exists using quantile-quantile plots. Genomic inflation factor

(Devlin and Roeder 1999), λ_{GC}, was calculated from filtered p values to quantify enrichment of associations across traits.

Allele-specific gene expression via RNAseq and qPCR

ASE analysis was performed as described in Aygün et al. 2021(Aygün et al. 2021) with the following modification: we included variants supported by at least 10 allele-specific counts in total (at least 2 from either allele) from each of the heterozygous donors in the analysis. 3 NPC donor lines heterozygous for rs1108842 ($r^2_{rs11709284,rs1108842}$ = 0.68) were plated in 12 well plates and treated with LiCl as described above. cDNA was generated from 200 ng total RNA using VILO SSIV Mastermix (ThermoFisher). Allele specific expression levels were determined using TaqMan Universal Master Mix II (ThermoFisher), and TaqMan genotyping probes for rs1108842 (Applied Biosystems). Quantification of allele specific expression was calculated by assessing the difference between Ct values for each allele within each PCR well at ΔRn=0.5, as previously described (Wolter et al. 2020). Experiments were performed in three distinct NPC donors, n=4 technical replicates per NPC donor line. Each LiCl time point was normalized to its respective vehicle time point, and then further normalized to the 0-hour time point. Statistical significance was determined using paired Student's t-test.

3.5 Supplemental Information

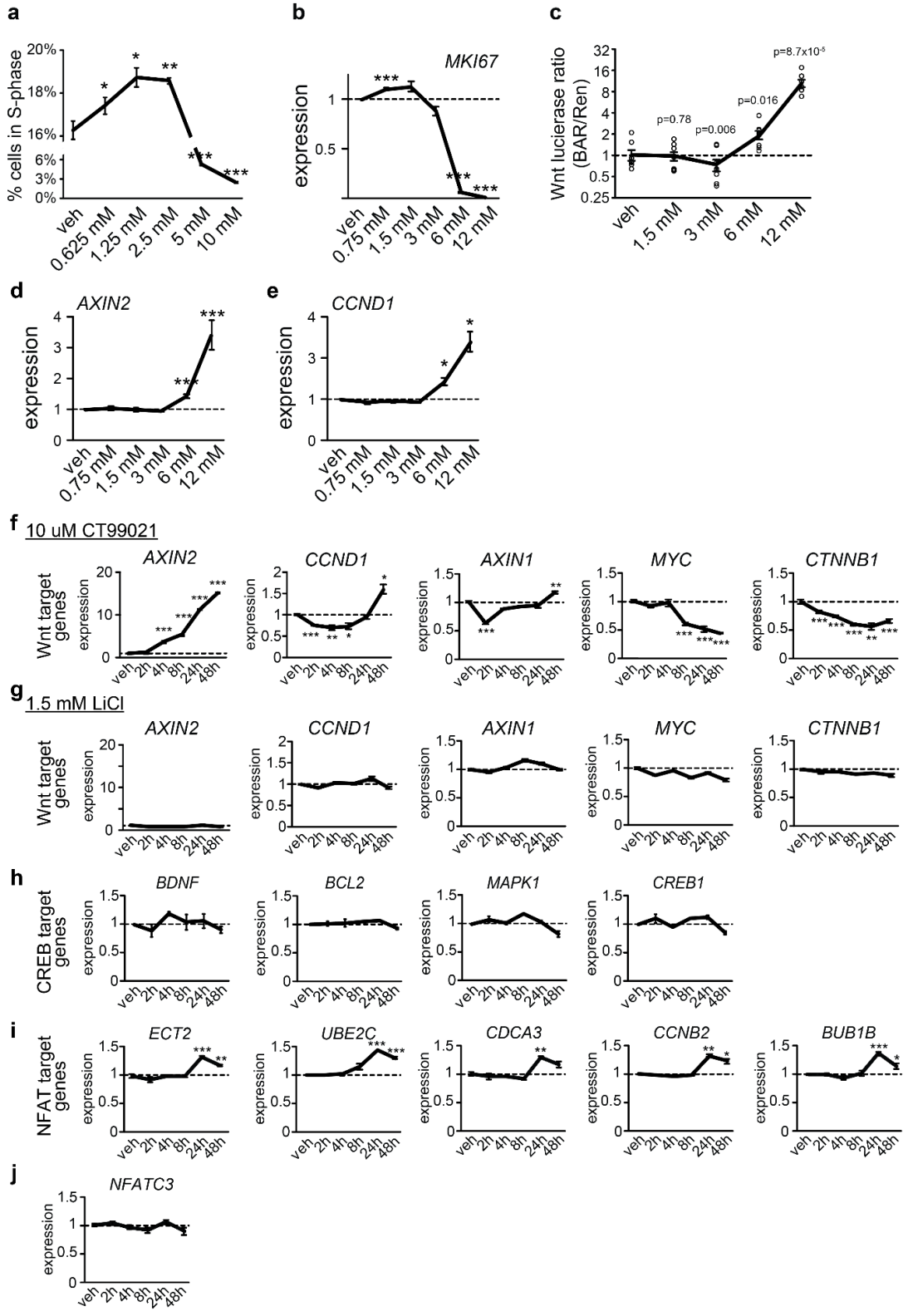

Supplemental Figure 3.1: Effects of lithium on NPCs

a) NPCs from one donor were exposed to LiCl for 48 hours, with an EdU pulse during the last two hours to label cells in S-phase. Cells were then lifted off the plate, fixed, labeled with a DNA content dye, and analyzed by flow cytometry. n=4 wells per concentration. Significance was determined by two sample t-test. All error bars are standard error of the mean. * $p<0.05$, ** $p<0.01$, *** $p<0.001$.

b) NPCs from three donors were exposed to LiCl for 48 hours at the indicated concentrations, followed by RNA extraction and RT-qPCR using primers for the proliferation marker gene *MKI67*. Data was normalized to the housekeeping gene *EIF4A2*. n=4 per wells per concentration. Significance was determined by paired t-test.

c) NPCs from 8 distinct donors were transduced with lentivirus carrying Firefly luciferase under control of the TCF/LEF sensitive promoter to measure Wnt signaling activity and a constitutively active Renilla luciferase to control for level of transduction. 48 hours later cells were treated with the indicated concentration of LiCl, followed by a 48 hour incubation. Cell lysate was then subjected to a dual luciferase assay. Firefly luciferase was normalized Renilla luciferase in each well. Data were normalized to vehicle. n=4 technical replicates per condition, significance at each concentration compared to vehicle was determined by paired t-test.

d-e) NPCs from three donors treated with LiCl for 48 hours at the indicated concentrations, followed by RNA extraction and RT-qPCR using primers for the indicated Wnt pathway associated genes. Data were normalized to the housekeeping gene *EIF4A2*. n=4 per condition, significance determined by paired t-test.

f-j) Gene expression in one NPC line across multiple timepoints following treatment with the highly selective Wnt activator CT99021 (f), or 1.5 mM LiCl (g-j). f,g: target genes of Wnt signaling pathway, h: target genes of the CREB signaling pathway, i: target genes of the NFAT signaling pathway (Qu, Sun, and Young 2011), **j**: *NFATC3* transcription factor.

Data normalized to the vehicle sample that was extracted at the same time (dashed line). n=4 wells per concentration. Significance was determined by two sample t-test.

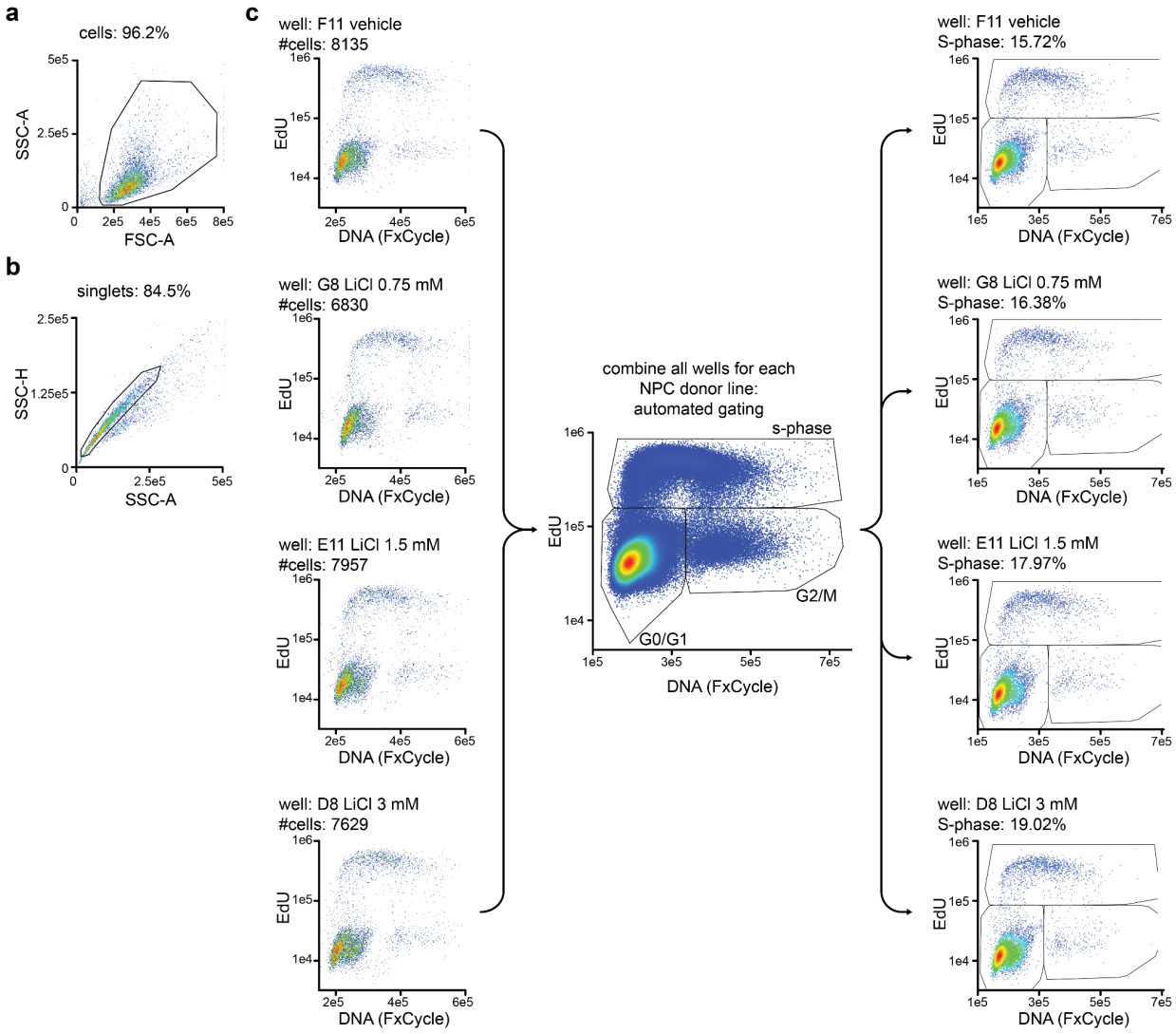

Supplemental Figure 3.2: Flow cytometry gating strategy

a) Density plots of a well from a representative NPC donor line. Forward scatter area (FSC-A) and side scatter area (SSC-A) were used to gate around cells and remove debris from analysis. This gate was manually drawn for a vehicle well, and applied to all wells corresponding to that NPC donor line. The percentage refers to the percent of events within the gate.

b) SSC height and SSC-A were used to isolate singlets.

c) Representative density plots from single cells isolated from b, for arbitrarily selected wells treated with each experimental condition. All wells from each NPC donor line were combined into a single FCS file, and FlowDensity (Malek et al. 2015) was used to automatically draw boundaries between cells in each phase of the cell cycle. These gates were then applied to each well individually to quantify the percentage of cells in S-phase.

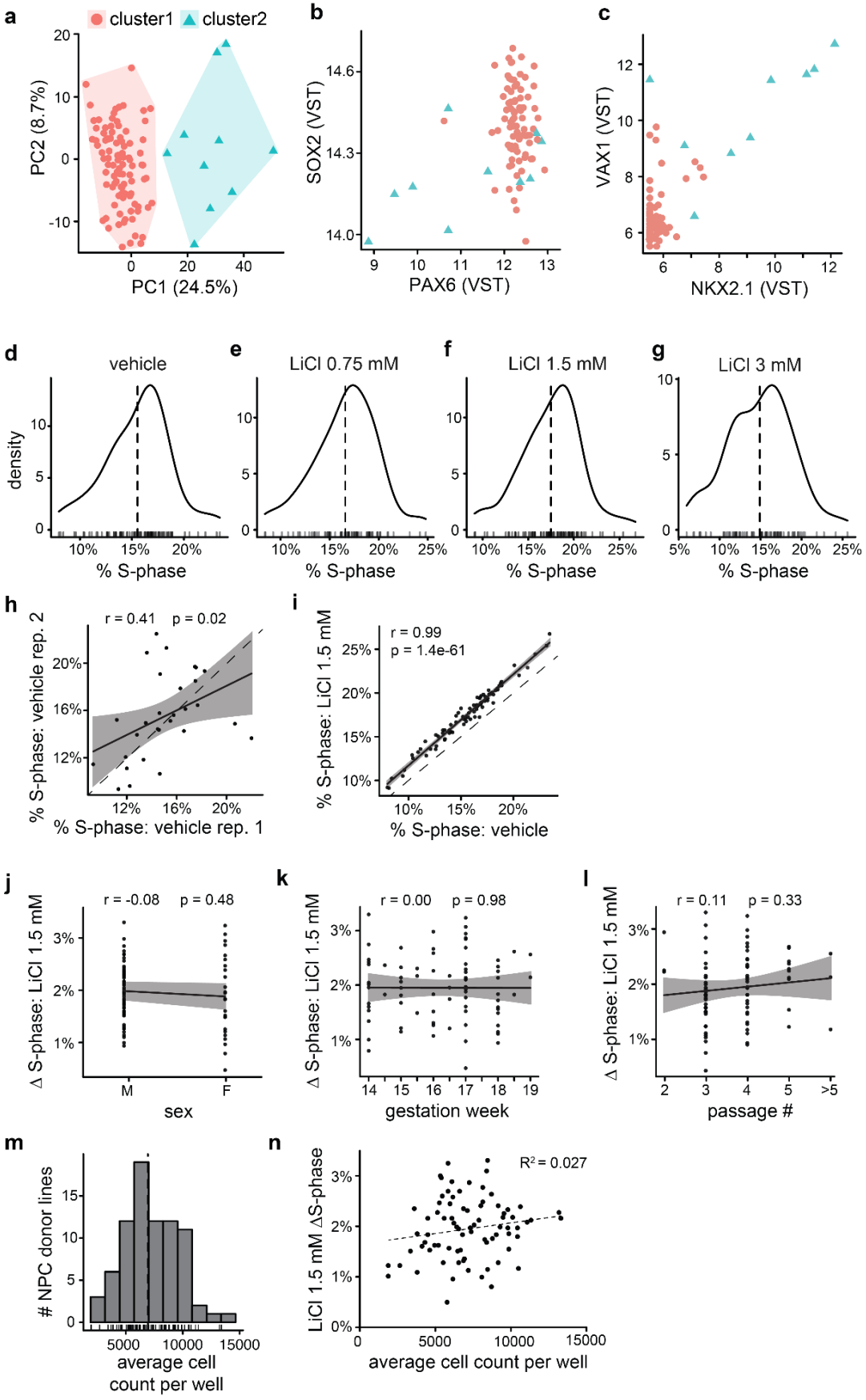
a
cluster1
cluster2
PC2 (8.7%)
PC1 (24.5%)
b
SOX2 (VST)
PAX6 (VST)
c
VAX1 (VST)
NKX2.1 (VST)
d
vehicle
e
LiCl 0.75 mM
f
LiCl 1.5 mM
g
LiCl 3 mM
density
% S-phase
h
r = 0.41 p = 0.02
% S-phase: vehicle rep. 2
% S-phase: vehicle rep. 1
i
r = 0.99
p = 1.4e-61
% S-phase: LiCl 1.5 mM
% S-phase: vehicle
j
r = -0.08 p = 0.48
Δ S-phase: LiCl 1.5 mM
sex
k
r = 0.00 p = 0.98
gestation week
l
r = 0.11 p = 0.33
passage #
m
NPC donor lines
average cell count per well
n
R² = 0.027
LiCl 1.5 mM ΔS-phase
average cell count per well

Supplemental Figure 3.3: Proliferation phenotype quality control

a) To identify transcriptional heterogeneity in the library of NPCs we performed principal component analysis (PCA) of baseline gene expression (Aygün et al. 2021) of the 500 highest variance genes in NPCs from 94 distinct NPC donor lines. Each donor line is a single point plotted in PC space. Clusters were identified by k-means clustering (k=2). Genetic association was performed in NPCs from cluster 1.

b) Scatterplot of VST-normalized *SOX2* and *PAX6* expression across NPCs in each cluster suggests that cluster 2 are outliers for expression of canonical NPC marker genes *PAX6* and *SOX2*.

c) Scatterplot of VST-normalized *VAX1* and *NKX2.1*, which are markers of cells derived from the medial ganglionic eminence (MGE) in the ventral telencephalon.

d-g) Distribution of proliferation rates across NPCs from 80 distinct donor lines at the indicated LiCl concentrations. Approximate normality suggests proliferation phenotypes are amenable to linear modeling in genetic association tests.

h) Correlation between technical replicates, defined as NPCs from the same donor line thawed and assayed in two different batches. Dashed line, y=x.

i) Correlation between proliferation in vehicle and 1.5 mM LiCl conditions. Dashed line, y=x.

j-n) Correlation between proliferation rate and technical variables: sex (j), gestation week (k), passage number (l), and average number of cells in each well (m,n).

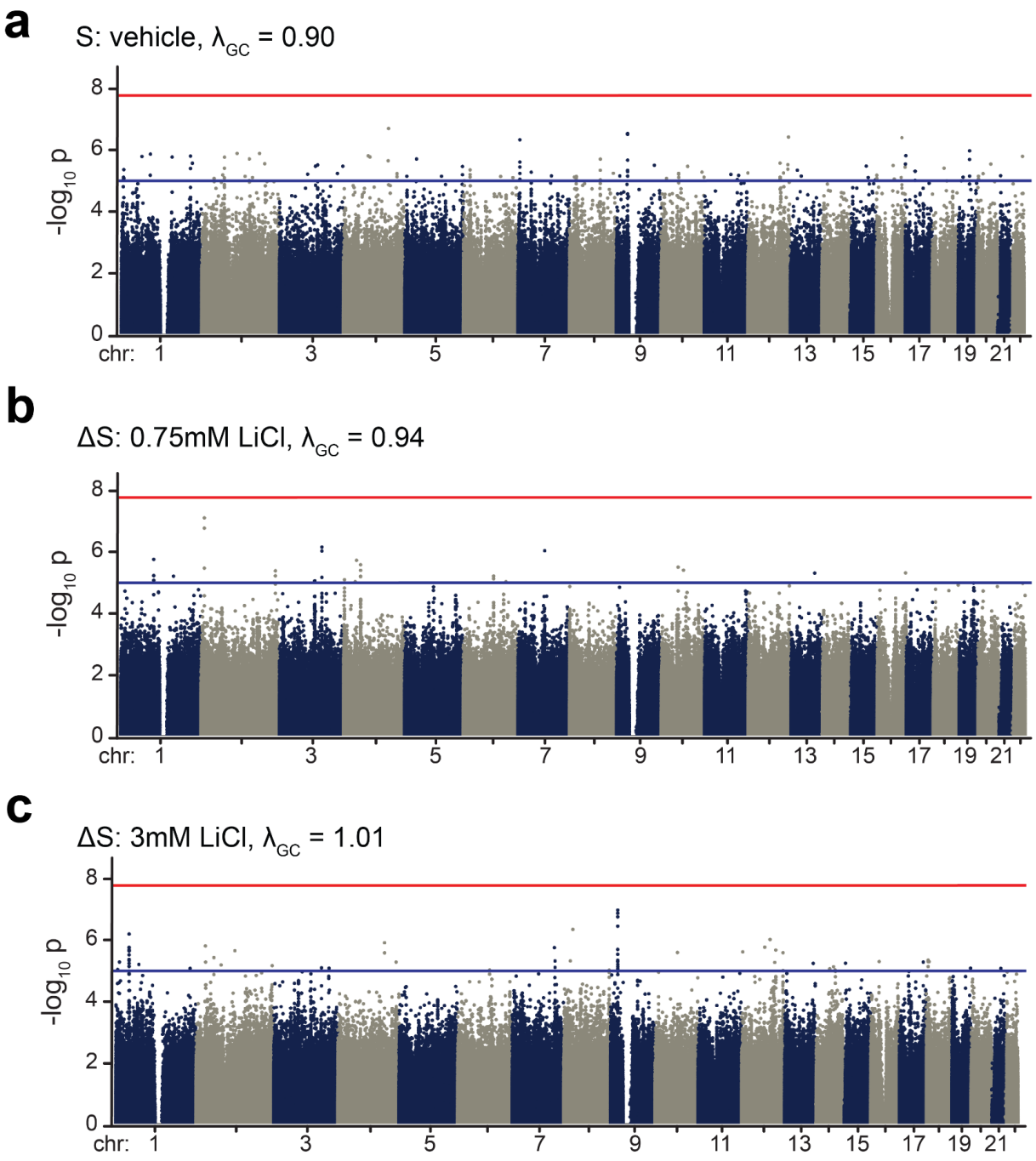

Supplemental Figure 3.4: Lithium induced proliferation GWAS results

Manhattan plots of GWAS results from vehicle S-phase (**a**), 0.75mM LiCl ΔS-phase (**b**), and 3mM LiCl ΔS-phase (**c**). Red line denotes study-wide significance level ($P < 1.67 \times 10^{-8}$); blue line denotes nominal significance level ($p < 1 \times 10^{-5}$)

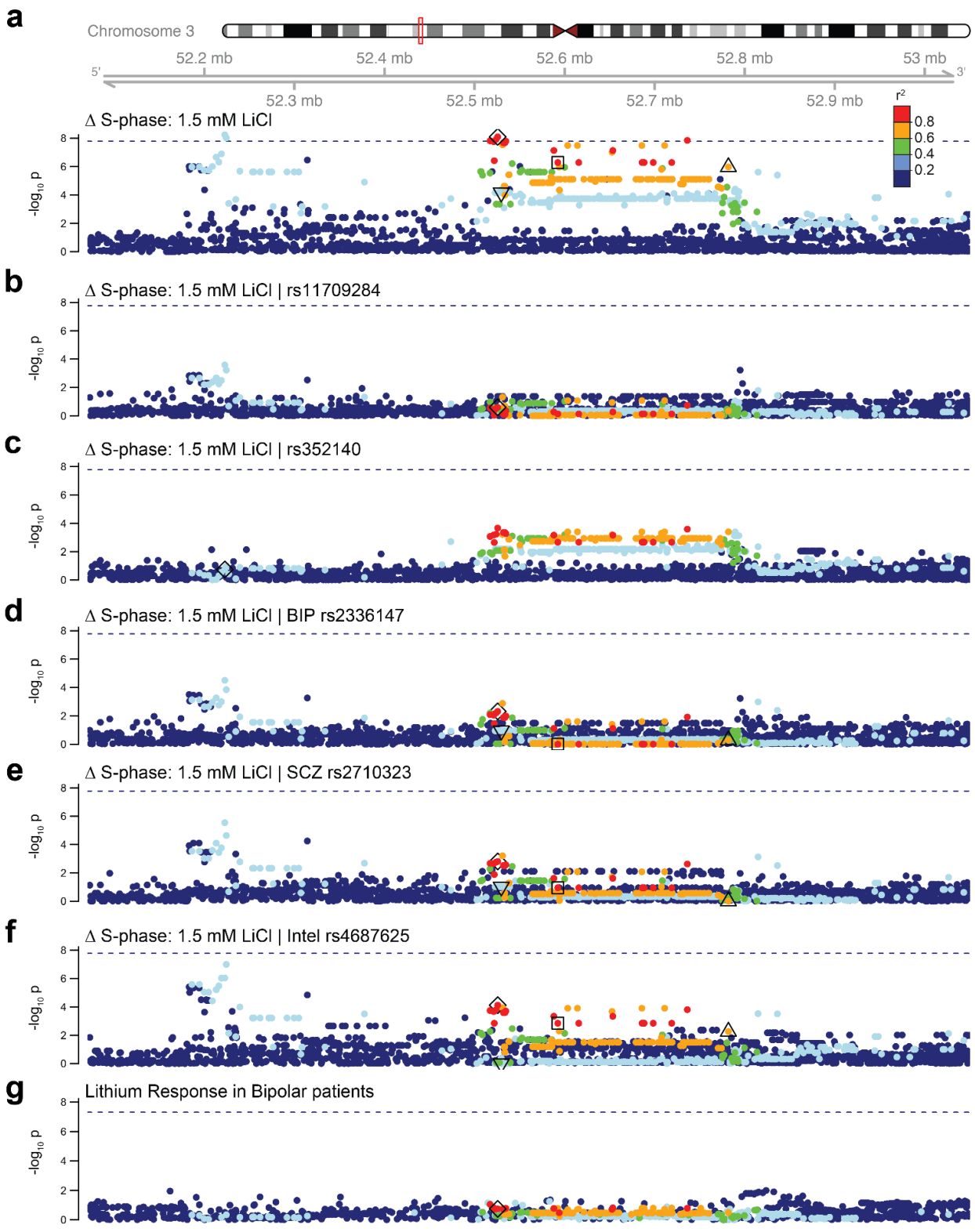
a
Chromosome 3
52.2 mb
52.4 mb
52.6 mb
52.8 mb
53 mb
5'
3'
52.3 mb
52.5 mb
52.7 mb
52.9 mb
r²
0.8
0.6
0.4
0.2
Δ S-phase: 1.5 mM LiCl
-log10 p
b
Δ S-phase: 1.5 mM LiCl | rs11709284
c
Δ S-phase: 1.5 mM LiCl | rs352140
d
Δ S-phase: 1.5 mM LiCl | BIP rs2336147
e
Δ S-phase: 1.5 mM LiCl | SCZ rs2710323
f
Δ S-phase: 1.5 mM LiCl | Intel rs4687625
g
Lithium Response in Bipolar patients

Supplemental Figure 3.5: GWAS results at chr3p21.1 - conditional tests and lithium response

a) Locus zoom of the study wide significant locus on chr3p21.1, associated with 1.5 mM LiCl ΔS-phase phenotype (Same data as Fig 2a). ◇: SNP from this study (rs11709284). Dashed line denotes the study-wide significance threshold ($p < 1.67x10^{-8}$) for all plots. For all plots, variants are colored by LD relative to rs11709284 in NPCs used for this study.

b) Locus zoom of 1.5 mM LiCl ΔS-phase phenotype while conditioning on rs11709284 (**b**) and rs352140 (**c**).

d-f) Locus zoom of 1.5 mM LiCl ΔS-phase phenotype while conditioning on indicated SNPs from colocalized traits: BD (Mullins et al. 2021) (**d**), schizophrenia (The Schizophrenia Working Group of the Psychiatric Genomics Consortium et al. 2020) (**e**), and intelligence (Savage et al. 2018) (**f**). SNP annotations: □: index SNP for BD (rs2336147). △: index SNP for schizophrenia (rs2710323). ▽: index SNP for intelligence (rs4687625).

g) Locus zoom for GWAS summary stats from the ConLiGen GWAS on lithium response in individuals with Bipolar disorder (Continuous variable, all populations) (Hou et al. 2016).

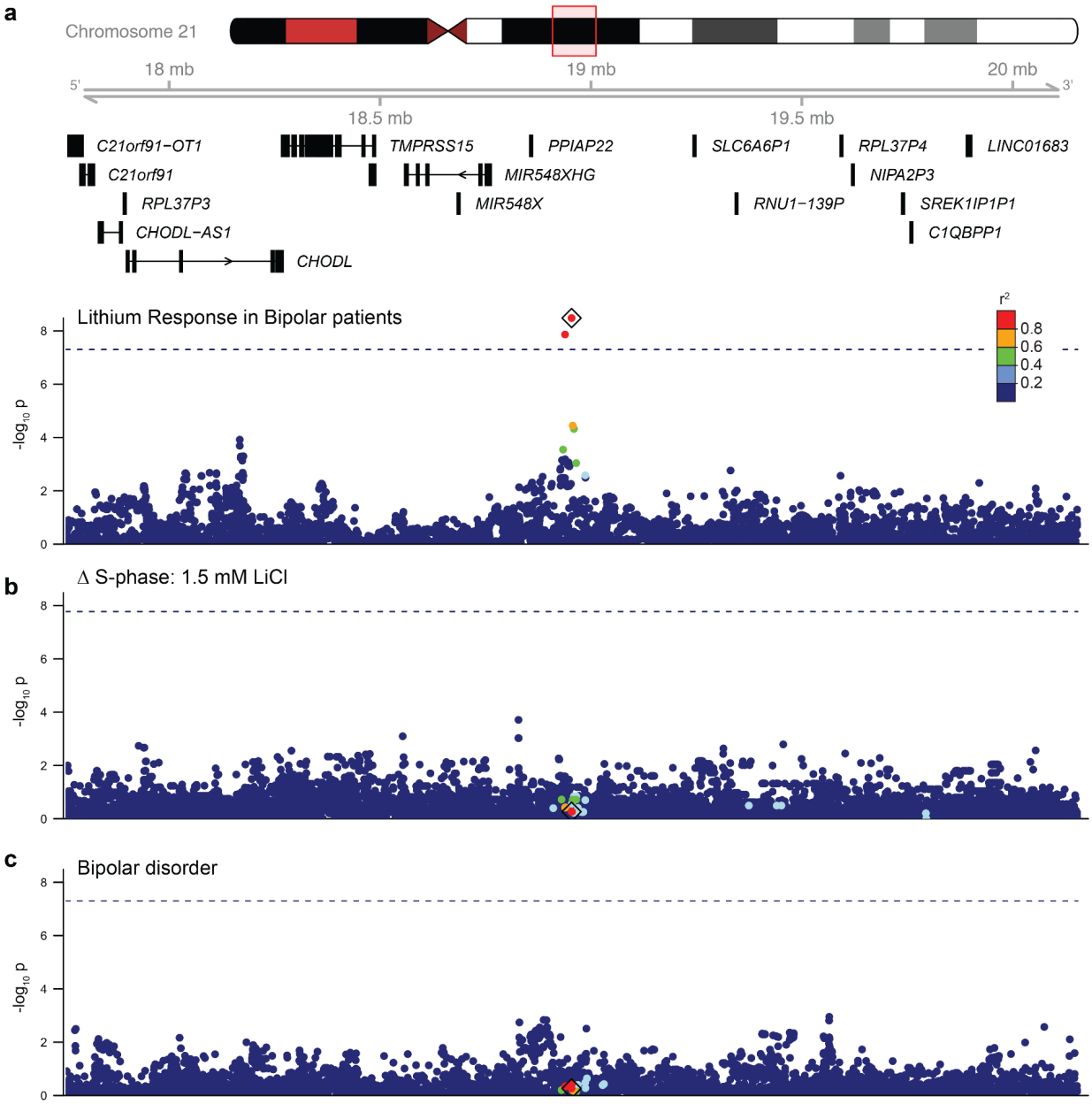

Supplemental Figure 3.6: A locus associated with lithium response in individuals with bipolar disorder does not colocalize with lithium-induced proliferation or Bipolar disorder risk

a) Locus zoom plot of Lithium response in bipolar patients phenotype at chr21q21.1 (Continuous variable, all populations) (Hou et al. 2016). ◇: index SNP (rs74795342). Each SNP is colored by LD (r^2) to rs74795342 in 1000 Genomes ALL reference panel. Dashed line denotes genome-wide significance threshold ($p < 5x10^{-8}$).

b) Locus zoom plot of 1.5 mM LiCl ΔS-phase phenotype. Dashed line denotes the study-wide significance threshold ($p < 1.67x10^{-8}$).

c) Locus zoom plot of Bipolar Disorder GWAS results (Mullins et al. 2021). Dashed line denotes genome-wide significance threshold ($p < 5x10^{-8}$).

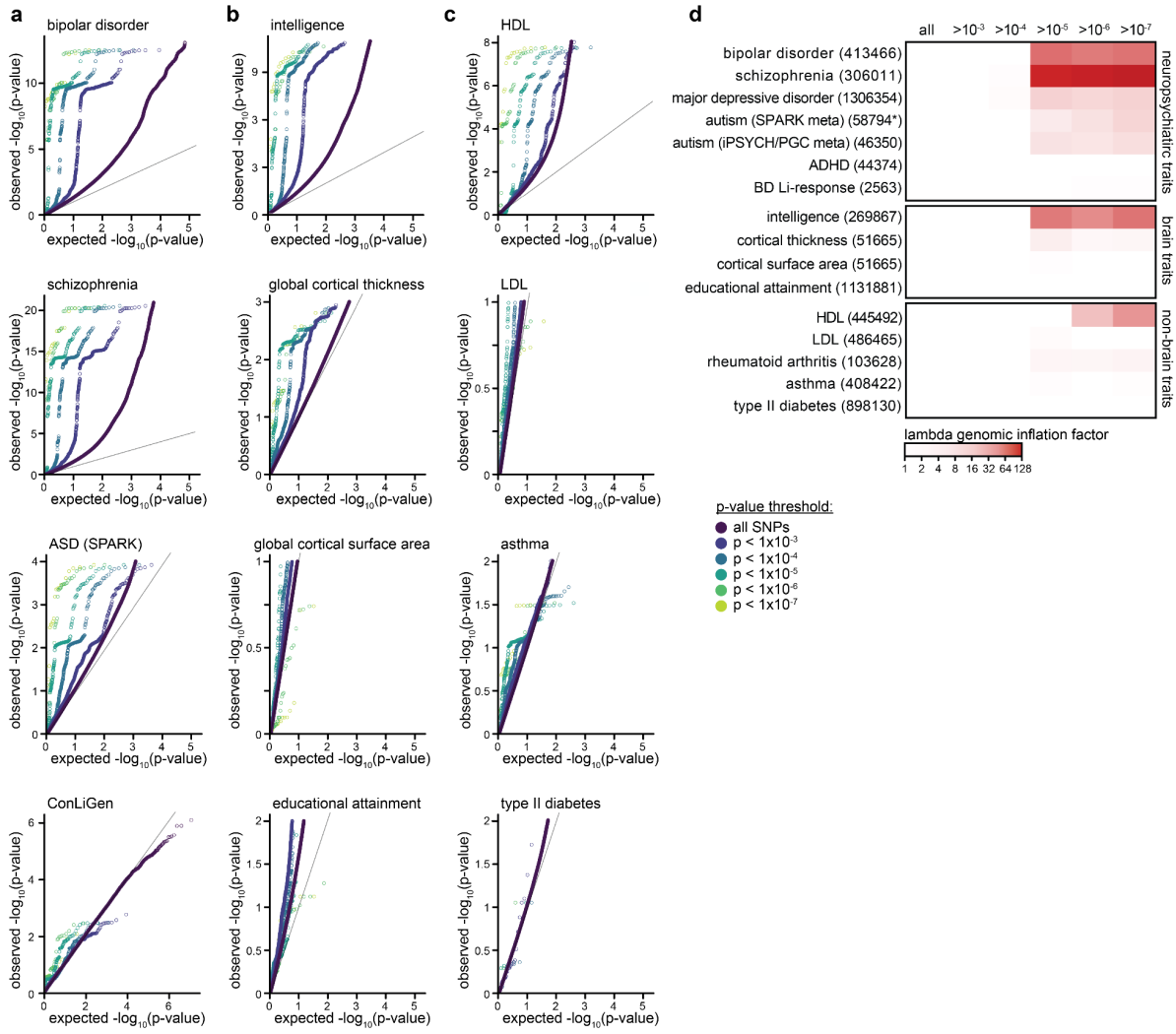

Supplemental Figure 3.7: Evaluation of shared genetic effects using quantile-quantile plots

(a-c) Quantile-quantile (QQ) plots of association p-values for neuropsychiatric disorder traits (a), brain traits (b), and non-brain traits (c) (references for GWAS used found in Supplemental Table 2). Point color denotes SNPs passing increasing filtering strength based

on p-value of association to 1.5 mM LiCl ΔS-phase. Each plot depicts the expected distribution of test-statistics on the x-axis vs. the observed test-statistics for the indicated trait on the y-axis. To visualize enrichment of significant GWAS results, y-axes were scaled to the maximum $-\log_{10}$(p value) for GWAS sumstats associated with 1.5mM LiCl ΔS-phase phenotype at a threshold of $p < 1 \times 10^{-7}$. (d) Lambda GC (Devlin and Roeder 1999) values for each GWAS filtered by ΔS-phase 1.5 mM LiCl GWAS results at increasing p value thresholds. Numbers in parentheses reflect total GWAS sample size for each trait. *sample size for ASD SPARK meta-analysis (Matoba et al. 2020) includes 6222 case-pseudocontrol pairs.

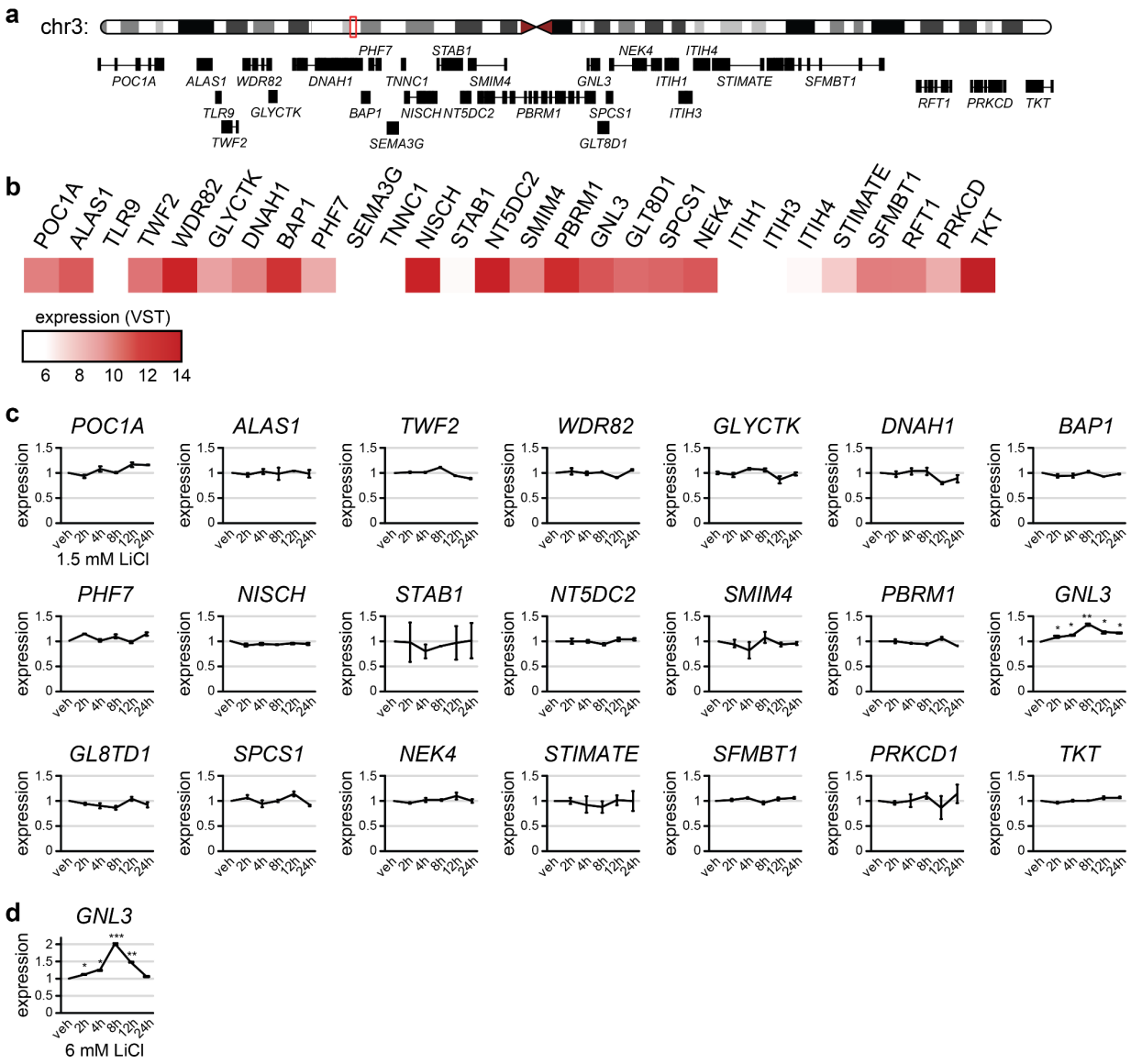

Supplemental Figure 3.8: Lithium induced gene expression of genes at the associated Chr3 locus

a) 1.2 Mb window surrounding the Chr3 locus, with gene models for all protein coding genes.

b) Expression levels (VST) of all genes in the window from (Aygün et al. 2021).

c) RT-qPCR from one NPC donor line of all genes with detectable expression at baseline, in response to 1.5 mM LiCl at various time points. *GNL3* is the only gene whose expression changes at multiple timepoints. Data analyzed as in Supplemental Fig. 1d-h. n=4

technical qPCR replicates. Statistical significance assessed by paired Student's t-test * $p<0.05$, ** $p<0.01$, *** $p<0.001$.

d) *GNL3* expression in response to 6 mM LiCl.

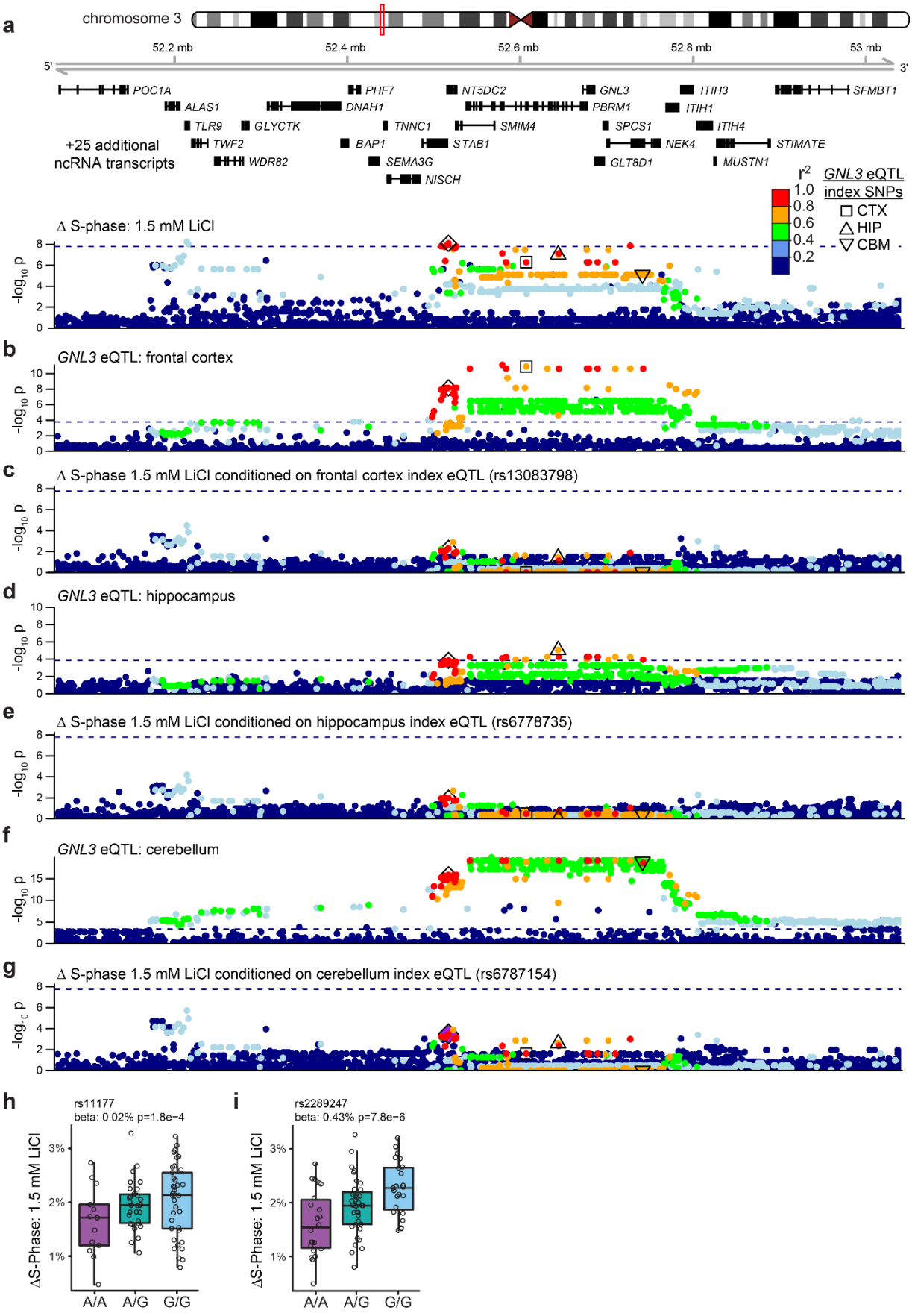
a
chromosome 3
52.2 mb
52.4 mb
52.6 mb
52.8 mb
53 mb
5'
3'
POC1A
PHF7
NT5DC2
GNL3
ITIH3
SFMBT1
ALAS1
DNAH1
PBRM1
ITIH1
TLR9
GLYCTK
TNNC1
SMIM4
SPCS1
ITIH4
+25 additional ncRNA transcripts
TWF2
BAP1
STAB1
NEK4
STIMATE
WDR82
SEMA3G
GLT8D1
MUSTN1
NISCH
r2
1.0
0.8
0.6
0.4
0.2
GNL3 eQTL index SNPs
CTX
HIP
CBM
Δ S-phase: 1.5 mM LiCl
-log10 p
b
GNL3 eQTL: frontal cortex
c
Δ S-phase 1.5 mM LiCl conditioned on frontal cortex index eQTL (rs13083798)
d
GNL3 eQTL: hippocampus
e
Δ S-phase 1.5 mM LiCl conditioned on hippocampus index eQTL (rs6778735)
f
GNL3 eQTL: cerebellum
g
Δ S-phase 1.5 mM LiCl conditioned on cerebellum index eQTL (rs6787154)
h
rs11177
beta: 0.02% p=1.8e−4
ΔS-Phase: 1.5 mM LiCl
A/A
A/G
G/G
i
rs2289247
beta: 0.43% p=7.8e−6

Supplemental Figure 3.9: Colocalizations with GNL3 eQTL

a) Locus zoom of the study wide significant locus associated with 1.5 mM LiCl ΔS-phase phenotype (Same data as Fig 2a/b). ◇: SNP of interest from this study (rs11709284). □: GTEx index eQTL SNP from Frontal Cortex (BA9) (rs13083798). △: GTEx index eQTL SNP from hippocampus (rs6778735). ▽: GTEx index eQTL SNP for cerebellum (rs6787154). Variants are colored by LD relative to rs11709284 in NPCs used for this study. Dashed line denotes the study-wide significance threshold ($p < 1.67x10^{-8}$).

b) GTEx eQTL for GNL3 (EUR) from Frontal Cortex (BA9) brain tissue. Dashed line denotes the eQTL significance threshold ($p < 0.000176$, FDR < 0.05). Variants are colored by LD relative to rs11709284 in the 1000 Genomes Project reference panel (EUR).

c) GWAS results as in (a), conditioned on GTEx eQTL index SNP from Frontal Cortex (BA9) brain tissue (rs13083798). Variants are colored by LD relative to rs11709284 in NPCs used for this study and annotated as in panel (a). Dashed line denotes the study-wide significance threshold ($p < 1.67x10^{-8}$).

d) GTEx eQTL for GNL3 (EUR) from hippocampus.

e) GWAS results as in (a), conditioned on GTEx eQTL (EUR) from hippocampus brain tissue (rs6778735).

f) GTEx eQTL for GNL3 (EUR) from cerebellum brain tissue.

g) GWAS results as in (a), conditioned on GTEx eQTL (EUR) from cerebellum brain tissue (rs6787154).

h,i) Boxplots showing proliferation across genotypes at SNP rs11177 (h) and rs2289247 (i). Related to Fig. 3d.

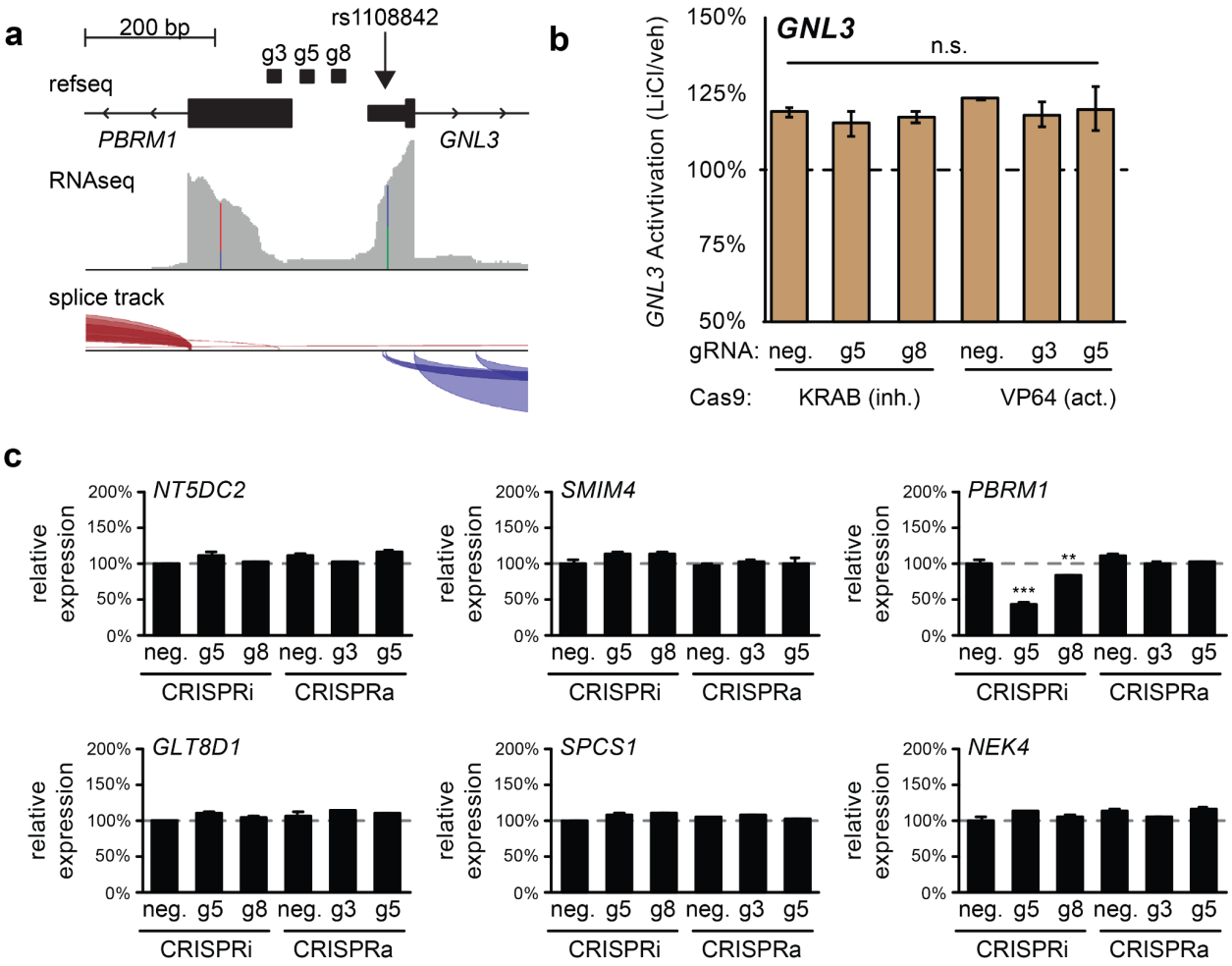

Supplemental Figure 3.10: CRISPRi/a targeting *GNL3* in NPCs

a) gRNA locations targeting the *GNL3* promoter. rs1108842 is the SNP in the *GNL3* 5'UTR used to assess allele specific expression in Fig. 3e.

b) *GNL3* expression in an NPC donor line transduced with the indicated lentivirus and treated with 1.5 mM LiCl. Data normalized to vehicle condition, related to Fig. 4a. Results suggest that regardless of baseline expression, lithium increases *GNL3* expression to uniform levels. n=4 technical qPCR replicates, significance determined by two sample Student's t-test.

c) RT-qPCR for the six nearest genes to gRNA target sites other than GNL3, to test for off target activity. Expression normalized to *EIF4A2*. n=4 technical qPCR replicates, significance determined by two sample Student's t-test. ** p<0.01, *** p<0.001.

Supplemental Table 3.1: Nominally significant clumped GWAS results

Nominally significant ($p < 1x10^{-5}$) GWAS loci from this study clumped using PLINK with 250kb windows and LD $r^2 > 0.2$. Each row reports the most significantly associated variant at each locus. Columns: Trait - associated proliferation phenotype, SNP - variant ID, rsid - variant rsID, CHR - chromosome, BP - chromosomal base-pair coordinates (hg38), P - association p-value, SEbeta - standard error adjusted effect size, TOTAL - number of SNPs in locus clumped with $r^2 > 0.2$, A1 - non-effect (typically minor) allele, A2 - effect allele, freqA1_WntI_n80 - reference allele (A1) frequency within donor-derived NPC lines in this study, freqA1_1kgALL - reference allele (A1) frequency in all subjects from the 1000 Genomes Project reference panel, freqA1_1kgEUR - reference (A1) allele frequency in European subjects from the 1000 Genomes Project reference panel.

Supplemental Table 3.2: GWAS summary statistics used for colocalization analysis and cross-trait enrichments

Columns: trait - description of GWAS trait, PMID/ref - PubMed ID or link to reference, Year - year of study, sample size - total number of subjects in study, nCase - number of cases in study, nControl - number of Control subjects in study, note - additional information about subjects and sample sizes

Supplemental Table 3.3: qPCR primers and gRNA sequences used in this study

Columns: Name - Forward, "F" and Reverse "R" qPCR primers labeled by target gene (rows 2-83), or guide RNAs targeting the GNL3 transcriptional start site (rows 84-86), Sequence - nucleotide sequence of primer or gRNA

CHAPTER 4: STIMULUS-SPECIFIC GENETIC EFFECTS ON GENE REGULATION DURING RESPONSE TO LITHIUM AND VALPROIC ACID TREATMENT IN PRIMARY NEURAL PROGENITOR CELLS

4.1 Introduction

Lithium (Li) and valproic Acid (VPA) are widely used first-line treatments for BD, but clinical responses are highly variable and mechanisms driving their effects are largely unknown. Fetal VPA exposure can impair neurodevelopment and increase risk for ASD. Genetic influences on clinical responses in patient populations are beginning to be characterized, but are limited by low power, difficulty in isolating specific effects due to the prevalence of polypharmacy, and uncontrolled compliance, duration, and dose across participants. Here, a "pharmacogenomics in a dish" approach aims to understand how genetic variation impacts response to these compounds. We describe the effects of Li and VPA on gene regulation, and how these changes are tuned by common genetic variation within primary human neural progenitor cells (hNPCs). Our experiment measured chromatin accessibility via ATAC-seq and gene expression via RNA-seq in 78 genotyped hNPC lines after 48 hour exposure to approximately clinically-relevant concentrations of either 1.5mM LiCl, 1mM VPA, or vehicle. This final data chapter compiles preliminary results from an ongoing study. Experimental and analytical methods are identical to those described in chapter 2: "Wnt activity reveals context-specific genetic effects on gene regulation in neural progenitors" (Matoba et al. 2023).

4.2 Effects of lithium or VPA stimulation on chromatin accessibility and gene expression

Over 10,000 and 45,000 regulatory elements showed significant changes in chromatin accessibility in response to Li or VPA, respectively (Figure 4.21, FDR < 0.1, |logFoldChange| < 0.25). Many transcription factor binding site (TFBS) motifs, such as RFX, were enriched within

regulatory regions opened by Li treatment. While Li is known to inhibit GSK3B, a critical component of the canonical Wnt pathway, TCF/Lef TFBS motifs were not enriched in peaks opening or closing due to Li stimulation. TFBS motifs such as LHX6, VENTX, and GSC were enriched within regulatory regions opened by VPA treatment. In contrast, some TFBS motifs mediating canonical Wnt pathway activation such as Lef1 and TCF7 were enriched within chromatin regions closed by VPA treatment (Figure 4.22).

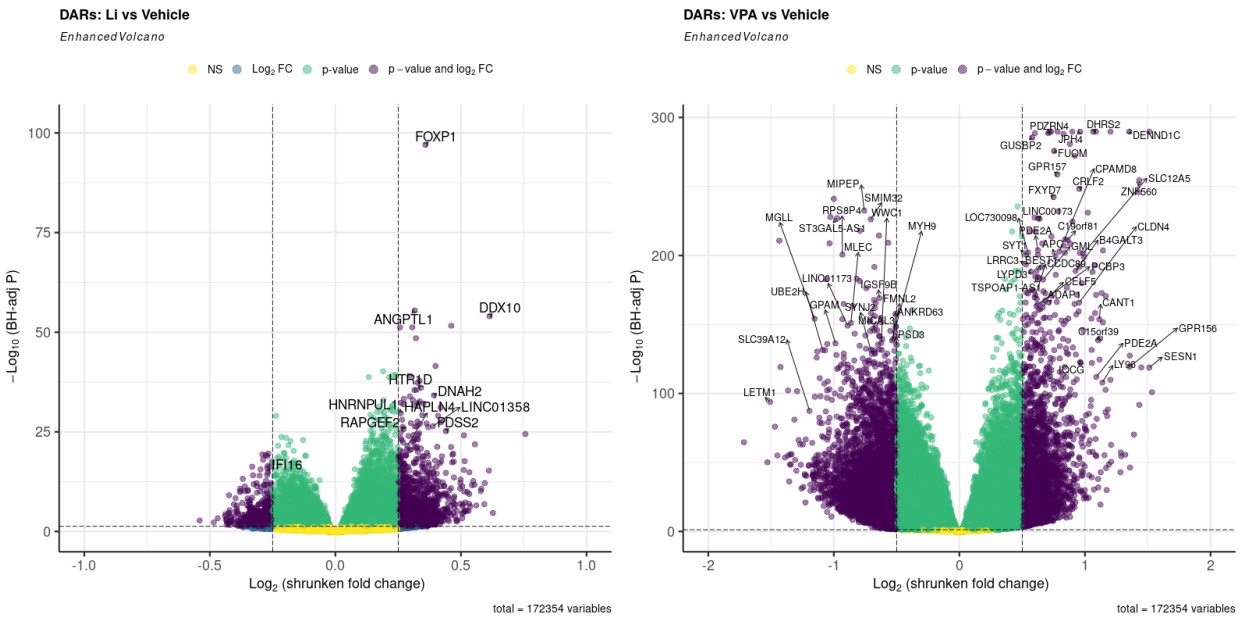

Figure 4.1: Differentially accessible chromatin regions (DARs) induced by Lithium and VPA

Differentially accessible chromatin regions (DARs) induced by 48h exposure to LiCl (left) or VPA (right). Each point is a chromatin region; labels denote nearest transcription start sites. DARs are defined by |LFC| > 0.25 and FDR < 0.05.

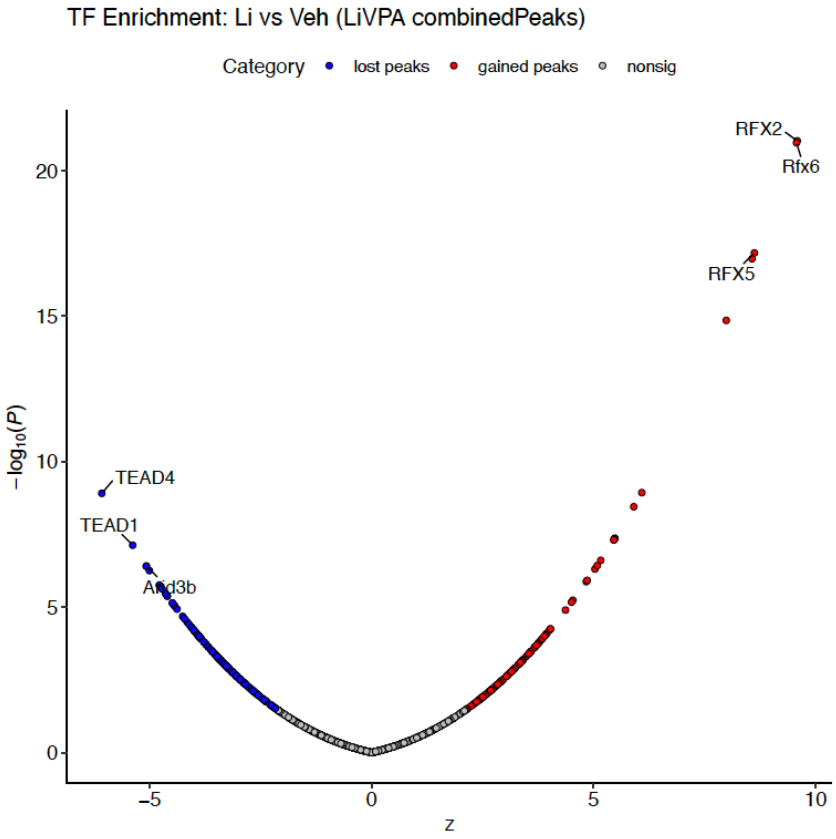
TF Enrichment: Li vs Veh (LiVPA combinedPeaks)
Category
lost peaks
gained peaks
nonsig
RFX2
Rfx6
RFX5
TEAD4
TEAD1
Add3b
20
15
10
5
0
−5
0
5
10
z
−log10(P)

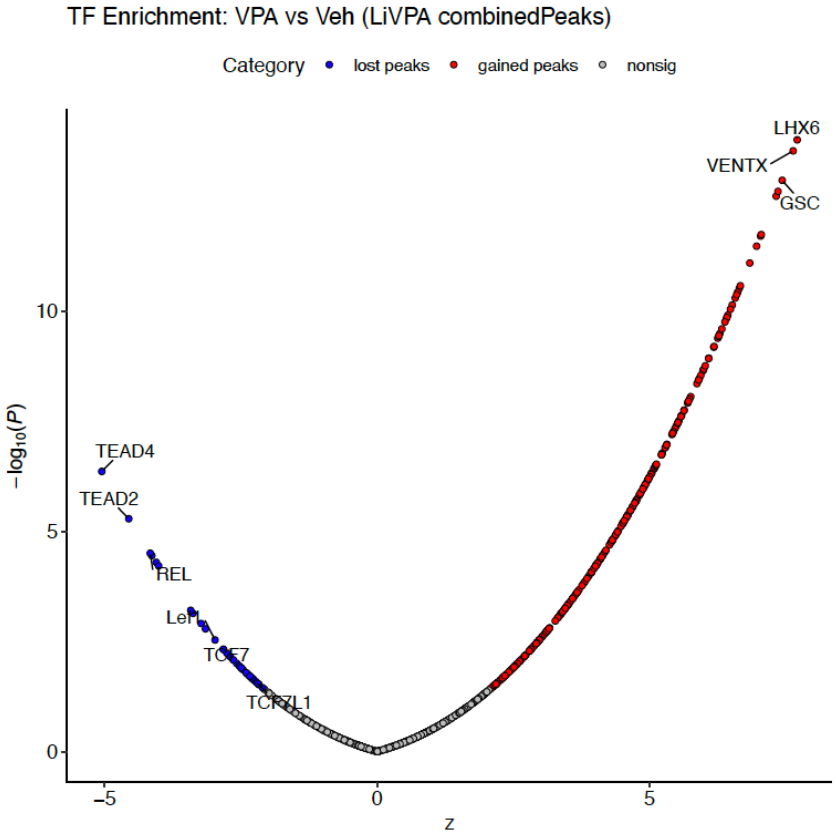
TF Enrichment: VPA vs Veh (LiVPA combinedPeaks)
Category
lost peaks
gained peaks
nonsig
LHX6
VENTX
GSC
TEAD4
TEAD2
REL
Lef1
TCF7
TCF7L1
10
5
0
−5
0
5
z
−log10(P)

Figure 4.2: TFBS motif enrichment within Lithium and VPA DARs

TFBS motif enrichment within Li (top) or VPA (bottom) DARs. Each point represents a TFBS motif from 841 predicted human TFs in the JASPAR 2022 database (Castro-Mondragon et al. 2022).

We detected 493 and 7,700 differentially expressed genes in response to Li or VPA treatments, respectively (Figure 4.23, FDR < 0.1, |logFoldChange| > 0.25). VPA mostly increased DEG expression, consistent with its activity as an HDAC inhibitor. Cellular proliferation genes were upregulated by Li and downregulated by VPA, consistent with proliferation assays conducted in the same samples (Figure 4.24).

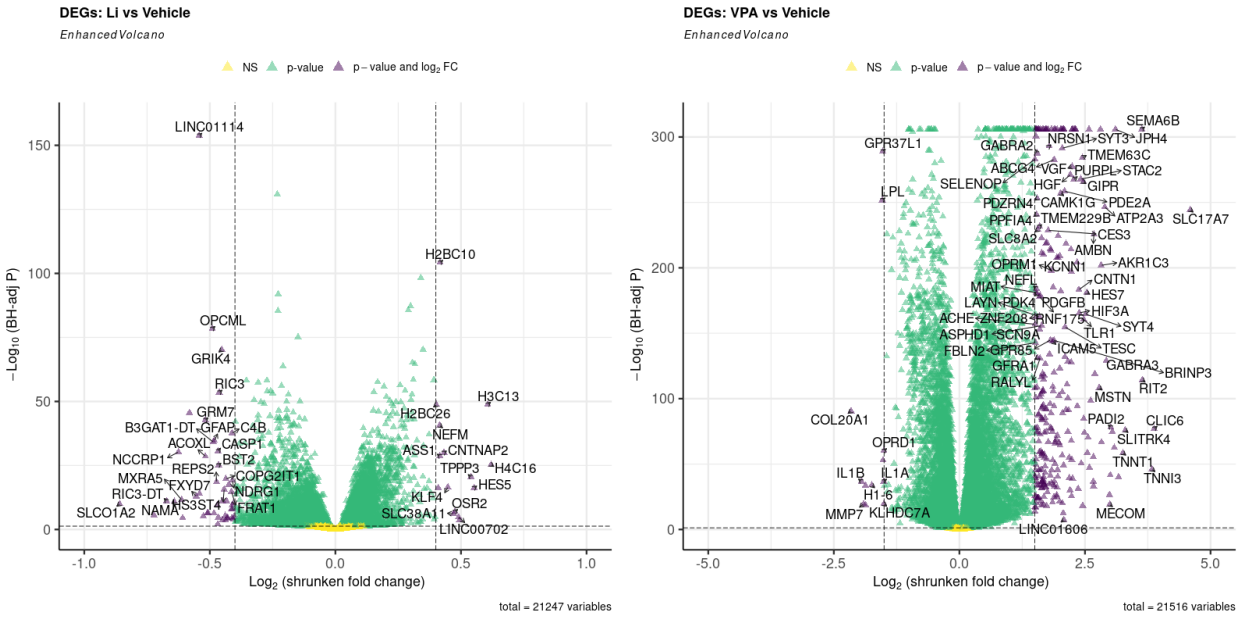

Figure 4.3: Differential gene expression in response to lithium or VPA

Differentially expressed genes (DEGs) induced by 48h exposure to Li (left) or VPA (right). Each point is a protein-coding gene. DEGs are defined by |LFC| > 0.25 and FDR < 0.05

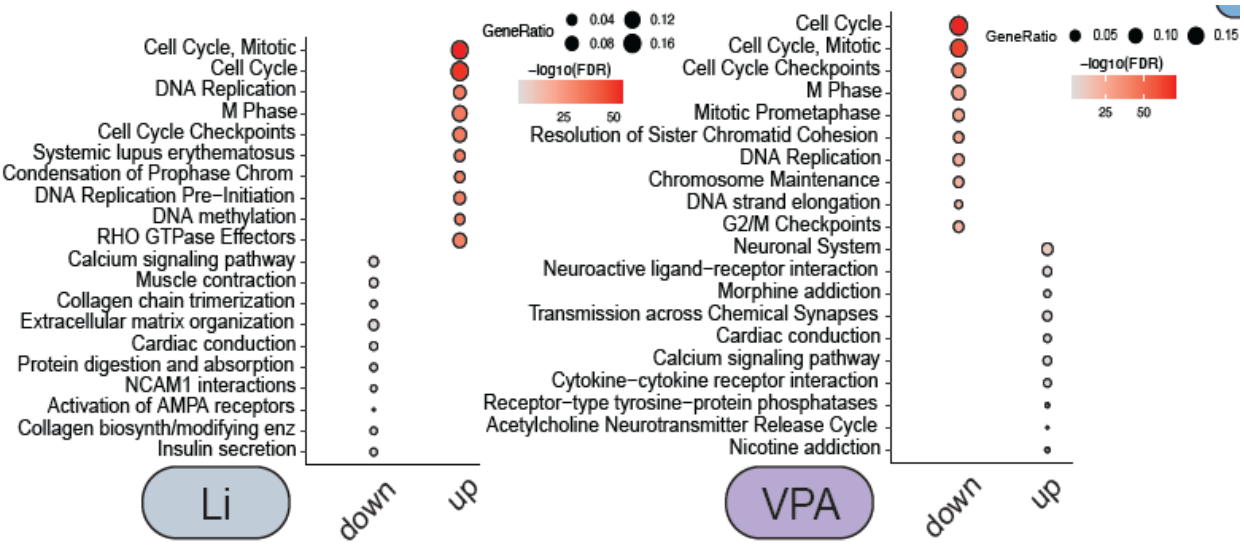

Figure 4.4: DEG gene ontology enrichment analysis

Gene ontology categories significantly (FDR < 0.1) downregulated (down) or upregulated (up) in response to lithium (left) or VPA treatment (right). Gene ratios reflect the fraction of total DEGs in each gene-ontology category.

4.3 Lithium and VPA stimulus-specific genetic effects on chromatin accessibility and gene expression

We mapped caQTLs and eQTLs in each of the vehicle, lithium, or VPA conditions. Estimated genetic effect sizes for the vehicle condition were correlated with those from previous experiments using a similar sample of hNPCs to assess the quality of these results and evaluate cross-experiment reproducibility. Vehicle condition caQTL and eQTL effect sizes were highly and significantly correlated, suggesting that hNPCs consistently model genetic effects on gene regulation (Figure 4.25). Stimulus-specific caQTLs regulated 20,762 and 4239 unique caPeaks following Li or VPA exposure, respectively, an up to 80% increase in discovery compared to 25,710 caPeaks detected under vehicle conditions. Stimulus-specific eQTLs regulated 439 and 462 unique eGenes following Li or VPA exposure, respectively, a ~50% increase in discovery compared to the 1899 eGenes detected under vehicle conditions (Figure 4.26).

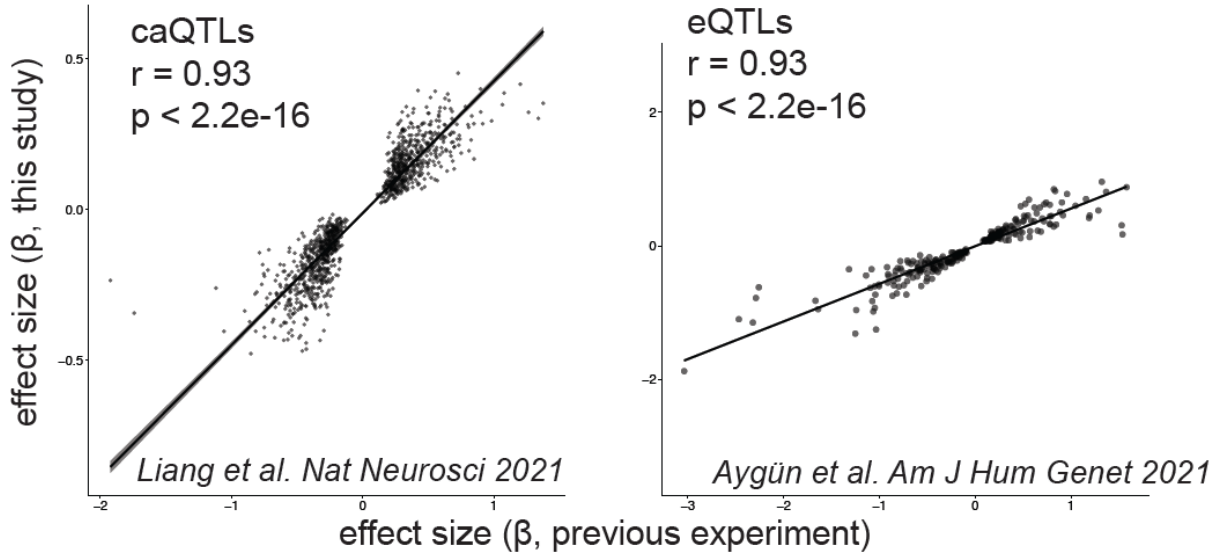

Figure 4.5: Correlation of vehicle caQTL and eQTL effect sizes across experiments

Effect size correlations between vehicle caQTLs (left) or eQTLs (right) captured in this study and those previous experiments (Liang et al. 2021; Aygün et al. 2021).

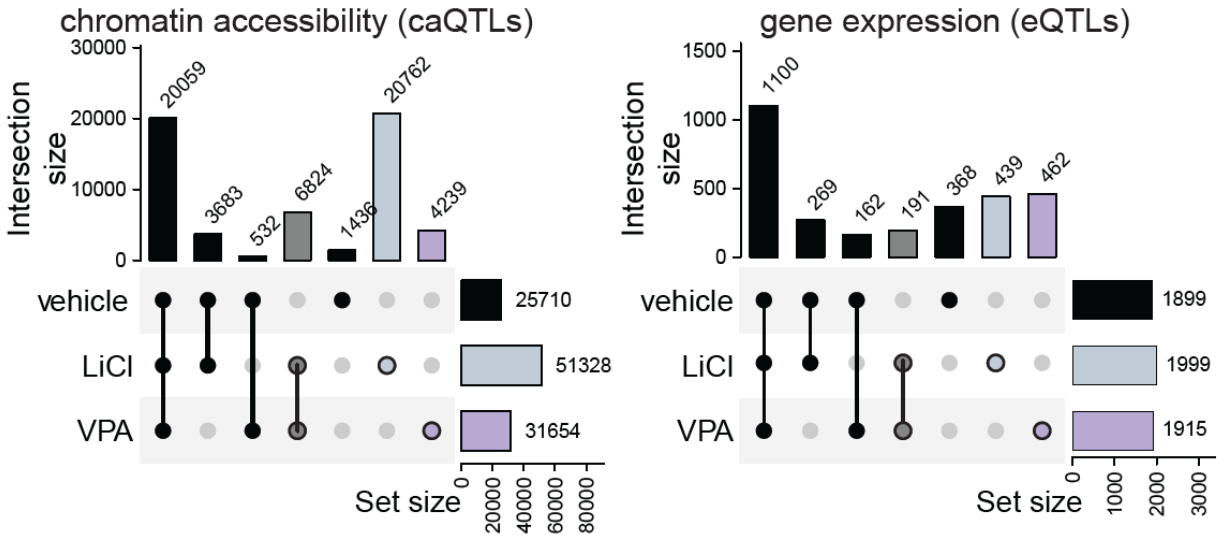

Figure 4.6: Stimulus-specific genetic effects on chromatin accessibility and gene expression following stimulation by lithium or VPA

Upset plot depicts sharing of unique caPeaks influenced by caQTLs (left) or eGenes influenced by eQTLs across stimulation conditions (FDR < 0.1). Colored bars show stimulus-specific genetic effects exclusive to lithium or VPA conditions.

4.4 Ongoing analyses and future directions

Epigenomic and transcriptomic profiles characterized the gene regulatory response to Li and VPA. Despite their shared roles as mood stabilizers, changes in chromatin accessibility and gene expression induced by each stimulus were notably distinct. A forthcoming more detailed appraisal of DARs and DEGs will elucidate molecular mechanisms underlying therapeutic effects. This will include linking li or VPA-responsive regulatory elements to the genes they regulate by calculating peak-gene correlations. Stimulus-specific QTLs showed novel genetic influences undetected in unstimulated cells. Future work will characterize genotype by stimulus interaction effects by mapping response-ca/eQTLs. I eagerly anticipate comparison of these molecular QTL signals with known genetic influences on clinical responses to lithium and VPA, as well as colocalization with neuropsychiatric disorder and brain structure GWAS. We anticipate upcoming analyses will shed light upon gene regulatory dynamics that may mediate responses to these treatments within neural progenitor cells, and facilitate pharmacogenomic interpretations that have the potential to improve clinical outcomes.

CHAPTER 5: DISCUSSION

This research characterized molecular and cellular phenotypes in hNPCs across a variety of stimulation conditions using ATAC-seq, RNA-seq, and cellular assays. Genetic effects on the molecular phenotypes of chromatin accessibility and gene expression were estimated using ca/eQTL mapping, while genetic effects on the cellular phenotypes of Wnt activation and proliferation were estimated using GWAS methods. A key strength of this work resides in its consideration of stimulated cell-states as important contexts that shape gene regulation and cellular processes. One branch of research considered stimulated the Wnt pathway, and is broadly applicable to understanding developmental gene regulatory dynamics in the fetal neocortex, and how these dynamics may modulate cellular processes and the expression of complex brain-traits. Another, and ongoing, branch of research explored molecular and cellular responses to mood stabilizing drugs and is relevant to understanding both the therapeutic mechanisms of these treatments, and the genetic determinants influencing individual treatment responses. I will now contextualize these context-specific results (heh), discuss their implications, recognize their limitations, and forecast their future trajectories.

Genetic effects aside, the extensive molecular and cellular phenotypic profiles we generated represent a rich and novel resource to understand context-specific effects on the epigenome, transcriptome, Wnt signaling, and proliferation. While other studies have captured omic data from fetal brain tissues, even at the single-cell level (M. Li et al. 2018; Zhong et al. 2018), they describe baseline cell-states. Our results extend modern approaches to study gene regulation using parallel multi-omics, here ATAC-seq and RNA-seq, into developmentally and clinically relevant cell-states. Use of up to 82 hNPC lines for each experimental condition, required for sufficiently powered QTL mapping discussed later, ensured robust molecular and

cellular profiling. Parallel chromatin accessibility and gene expression profiles allowed inference of gene regulatory mechanisms supported by correlations between chromatin accessibility and local gene expression. These peak-gene correlations identified genes under the influence of nearby regulatory elements, perhaps via chromatin contact, including cases where regulatory relationships were sensitive to developmental or clinical stimuli. The DARs characterized here describe dynamic regulatory elements that are enriched with genetic variants associated with the expression of complex brain traits. Enrichment of TFBSs within DARs nominate specific factors with regulatory function that can be modulated by genetic variation. DEGs, discovered in parallel with DARs, show the regulatory landscape's transcriptional output in response to stimuli and are enriched for genes with known links to brain diseases. A limitation of our approach is that we did not profile responses to multiple exposure durations or concentrations of stimuli. Exposure conditions were selected based on pilot experiments that attempted to balance stimulation of robust effects, approximation of clinically-relevant dosing, and avoidance of toxicity. As such, these results characterize responses to one exposure for each stimulation condition, and do not illuminate dose-dependent effects. Nevertheless, stimulus-specific DARs and DEGs represent a novel inventory of regulatory elements and genes that serve as an important resource for future studies. Specifically, Wnt-stimulated DARs and DEGs can inform mechanisms driving corticogenesis, while Li/VPA-stimulated DARs and DEGs will illuminate therapeutic mechanisms of these mood-stabilizing treatments.

A key advance of this research is its characterization of context-specific genetic effects on chromatin accessibility, gene expression, and proliferation in hNPCs. We detected myriad genetic effects that were undetected under vehicle conditions, building on the growing evidence that the function of some genetic variation depends on cell-state. Still, it should be stated that the majority of genetic effects were shared across vehicle and stimulated conditions, and these context-independent effects remain important footholds for understanding how genotype influences expression of phenotype. Advances in single-cell resolution QTL mapping, regardless

of stimulation state, will help to resolve whether these context-independent loci are specific to developing radial glia, or function across neural lineages and time. Thousands of significant genetic effects were detected across molecular phenotypes and stimulation conditions, suggesting that as few as 67 hNPC lines is sufficient for ca/eQTL mapping for variants with >=1% minor allele frequencies. Reduced, but still fruitful, ca/eQTL discovery is expected with slightly smaller sample sizes. Conversely, a larger sample size of hNPC genotypes may provide enhanced ca/eQTL discovery, enable the characterization of variants with smaller effect sizes, and improve detection of secondary signals within loci. Additional power to detect stimulus-specific molecular QTLs may be found by increasing the potency of the stimuli applied to maximize molecular effect sizes with respect to vehicle conditions, under the assumption that stimulus-specific molecular and genetic effects exhibit dose-dependency. While this study was well-powered to detect abundant stimulus-specific QTLs, sample size did restrict the discovery of response-ca/eQTLs, which depend on an alternative model capable of evaluating genotype by environment (or in this case, stimulus condition) interaction effects. Future studies seeking to characterize such interaction effects should consider larger sample sizes for this reason. Response-caQTLs regulated chromatin peaks enriched with specific TFBS relative to all other chromatin peaks, including binding sites for Wnt-response and neural specification TFs. This suggests that response-QTLs are especially capable of responding to developmental signals through interactions between genotype and environments where key regulatory factors are available. The combination of chromatin accessibility QTLs with gene expression QTLs enabled the inference of enhancer priming. These loci are marked by accessible chromatin under both vehicle and stimulated conditions alongside stimulation-dependent gene expression. Enhancer-primed loci may represent cases whereby gene expression is under the control of a regulatory element that is “waiting” for the presence of a transcription factor only present in a specific cell-state or context. I speculate whether some trans-eQTL loci identified in studies with larger sample sizes, may regulate the expression of transcription factors under such context-specific

control, such that the functional trans-eQTL variant directly modulates context-specific TF expression, and that TF in turn regulates the distal trans-eQTL target gene. Further characterization of the genomic signatures and biological functions of primed loci is warranted. Importantly, context-specificity provided new explanations for GWAS loci, with each additional stimulus revealing additional colocalizations. It stands to reason that similar cell-based molecular QTL approaches expanded to a variety of stimulation conditions in relevant cell types would further improve functional support for GWAS loci.

A cell-based approach allowed interrogation of Wnt-activation and proliferation phenotypes in a similar panel of hNPCs. These cellular phenotypes provided insights into hNPC responses to the Wnt agonist CHIR (CT99), Lithium, and VPA, but were flawed inputs for genetic association. GWAS detected many nominally significant associations to Wnt-activation and proliferation across vehicle and stimulated conditions, but only a single genome-wide significant association was identified at locus where common genetic variants influenced lithium-responsive proliferation. Our experimental design captured Wnt-activation and proliferation at the same 48h post-exposure time point. Retrospectively, simultaneous capture may not have been ideal, especially from the standpoint of the Wnt-activation luciferase assay. The majority of genetic effects on Wnt-signaling may occur quickly, during the first few hours following Wnt stimulation, and then dissipate over time. Proliferation differences in response to stimuli likely take longer to manifest because not all cells will be prepared to divide immediately upon stimulation, and cell-cycle completion may take up to 12h. Also, while the assays used here were effective at resolving differences in Wnt-activation and proliferation with respect to stimulation condition, measurement noise may obscure discovery of genetic effects across this panel of hNPC lines. Due to these limitations, increased sample sizes and improved phenotyping are recommended to ensure successful genetic association to these cellular traits. Even so, the sole genome-wide significant lithium-sensitive proliferation association signal colocalized with GWAS for bipolar disorder, schizophrenia, and inter-individual differences in intelligence.

Fortunately, the GWAS "hit" was amenable to functional experimentation, allowing us to determine that lithium-sensitive genetic effects on proliferation acted through GNL3, a gene with known roles in cell-cycle regulation. Unfortunately, although GNL3 showed Lithium-sensitive expression, this locus did not colocalize with Wnt- or lithium-specific caQTLs or eQTLs. Therefore, we were unable to trace a causal chain leading from genetic variation to the trio of colocalized brain-traits via shared genetic effects on chromatin, gene expression and cellular proliferation. In addition to improvements in sample sizes and assay methodology, simultaneous capture of both molecular and cellular phenotypes from the same hNPC cultures may facilitate detection of genetic effects that span multiple levels of biology. The possibility of supporting such mechanisms motivates building upon these studies.

In discussing the variety of genetic effects characterized in this research, it is worth reiterating that this particular cohort of hNPCs possess genetic backgrounds of diverse ancestries. This genotypic diversity is in contrast with most large sample-size genetic studies to date, including brain-trait GWAS, in which discovery is biased towards caucasian individuals of European descent. Whether novel genetic associations reported here are applicable across all populations is an open question. However, studies showing that the most GWAS-identified genetic effects, including for schizophrenia risk (de Candia et al. 2013), are shared across ancestries (Marigorta et al. 2018), and the ongoing development of methods to maximize cross-ancestry applicability of polygenic risk scores (Kachuri et al. 2023) are encouraging. Through this research, I note a need for standardized methodologies, including genetic effect model selection and false-discovery thresholding, and the development of new data integration tools that promote cross-comparisons between molecular, cellular, and complex traits. Additionally, the context-specific nature of genetic effects highlights the need for complementary context-specific functional genomic annotations of the genome, a context-specific offshoot of the ENCODE project, perhaps. Establishment of field-standard best practices, analysis pipelines for QTL approaches and improved platforms for integrating results from GWAS and functional

genomic annotations will go some way to gleaning biological insights from this growing field of study.

Molecular and cellular responses to the mood stabilizers lithium and VPA characterized these drugs' mechanisms of effect in neural progenitor cells. Interestingly, from the standpoint of Wnt-activation and proliferation, these treatments have opposite effects despite similar clinical indications. At low and medium concentrations, Lithium stimulated the canonical Wnt pathway and hNPC proliferation. In contrast, VPA potently suppressed Wnt-activation and proliferation at all concentrations tested. Contrasting cellular responses between these drugs are reflected in distinct molecular responses. Compared to lithium, VPA had more robust effects on both chromatin accessibility and gene expression. VPA mostly increased the expression of thousands of genes, which is consistent with its known activity as a histone deacetylase inhibitor. Gene ontology enrichments for lithium or VPA DEGs showed contrasting results consistent with their opposite effects on Wnt-activation and proliferation. For example, lithium upregulated cell-cycle genes while VPA downregulated cell-cycle genes and upregulated gene categories related to neuronal function such as synaptic transmission and neurotransmitter release. This suggests that lithium promotes the maintenance of a pluripotent neural progenitor cell-state, and VPA promotes the differentiation of hNPCs at the expense of self-renewal. How contrasting molecular and cellular effects are exerted by two drugs both prescribed to mitigate mania is puzzling and highlights the need for further elucidation therapeutic mechanisms underlying lithium and VPA responses.

Genetic association to molecular and cellular responses across hNPC lines can provide pharmacogenomic interpretations for lithium and VPA treatments. I will first consider the GNL3 locus where a genome-significant association to lithium-induced proliferation and colocalization with multiple brain trait GWAS signals was detected. Follow-up experiments at the locus suggested that genetic effects on GNL3 expression mediated effects on lithium-induced proliferation. As discussed in chapter 3, lithium's ability to stimulate the proliferation of adult

neural stem cells has been proposed as a possible mechanism of therapeutic effect. CRISPRi/a experiments showed that modulation of lithium-sensitive GNL3 expression affected hNPC proliferation, fueling speculation that genetic effects on this gene regulatory mechanism and downstream neural progenitor proliferation may contribute to differences in patient responses to treatment. Future studies in non-human model systems should evaluate whether modulation of GNL3 expression can influence neural progenitor proliferation in vivo, and whether this activity mediates therapeutic effects. It is important to note that we did not find evidence that genetic variation at the GNL3 locus was also associated with clinical outcomes in the available lithium-response GWAS' from individuals with BD, perhaps due to power limitations in those studies. Therefore, while these results support a role for neural progenitor cell proliferation in the response to lithium and demonstrate the feasibility of experimental manipulations to functionally characterize GWAS-identified loci, whether genetic influences on GNL3 also modulate clinical responses to lithium, and whether GNL3 function is a viable target for enhancing treatment outcomes remain open questions.

Pharmacogenomics of these and other treatments are facilitated by cell-based systems that can faithfully recapitulate in vivo properties and processes. The hNPCs utilized here are beneficial for modeling neural progenitor proliferation, but are derived from developing fetal tissue. Since lithium and VPA are prescribed to treat mania in adults, it is not clear whether effects detected in developing fetal hNPCs will translate to clinical applications in adults. While fetal neural progenitors share many molecular and cellular properties with adult neural progenitors (Yuzwa et al. 2017; Hochgerner et al. 2018; Kriegstein and Alvarez-Buylla 2009), hNPCs may be inherently linked to developmental, and not adult, time-points. For this reason, hNPCs may be best suited to studying molecular, cellular, and genetic effects that act during fetal corticogenesis to influence the expression of complex brain traits later on in life. This developmental influence on adult phenotypes is supported by partitioned heritability analysis within dynamic chromatin regions in hNPCs (Chapter 2, Figure 2.2) and the many

colocalizations we identified between hNPC molecular or cellular QTLs with neuropsychiatric, brain structure, and cognitive traits (Chapter 2, 3). Still, as highlighted above for the GNL3 locus, genetic effects on lithium- and VPA-responsive molecular and cellular phenotypes have so far failed to colocalize with existing clinical-response GWAS for these treatments. This may be due to a combination of power limitations hindering clinical-response studies and the possibility that fetal hNPCs do not adequately model important features of the clinical response. Ideal cell-based systems for pharmacogenomics studies should strive to recreate the cell types, cell states, and genetic backgrounds underlying variance in clinical responses. Consequently, iPSC-based approaches are appealing since they use cells derived from living adults who can be stratified by their clinical responses, diagnostic profiles, and demographic information (Lagomarsino et al. 2021), can be differentiated into a variety of cell-types, and are amenable to experimental manipulation. In contrast, the primary human cell-lines dissociated directly from fetal cortical tissue used here cannot be directly linked to clinical outcomes, although they do avoid potential molecular and cellular artifacts introduced by the genome remodeling required to reprogram iPSCs. Differentiated iPSC can generate the cell-types most relevant for pharmacogenomic interpretation, such as neurons. iPSC-derived cells can also be cultured as brain organoids which may recapitulate cell-types and functional phenotypes better than two-dimensional culture methods (Lago, Tomasik, and Bahn 2021). Currently, iPSC approaches are being applied to describe neuropsychiatric disease etiology (Evgrafov et al. 2020; Topol et al. 2015; Marchetto et al. 2017; Readhead et al. 2018), and clinical responses to lithium and other neuropsychiatric drugs (Mertens et al. 2015; S. Stern et al. 2018; Shani Stern et al. 2020; Santos et al. 2021). Work is ongoing to integrate lithium and VPA response profiles with results from iPSC and clinical studies in order to better understand patient variation in treatment responses. Ongoing and future analyses aim to describe mechanistic hypotheses involving lithium- or VPA-responsive genetic variation, chromatin, genes, and cellular processes that can be evaluated to facilitate pharmacogenomic interpretations.

In closing, this research generated several rich and complementary data sets spanning multiple levels of biology and cellular contexts. Together, these data emphasize the dynamic nature of the genome and its power to control cellular processes in response to specific cell-states. Ample opportunities for further investigation remain, for instance functional characterization of individual genomic loci that support causal hypotheses explaining brain trait GWAS or predicting clinical responses to lithium and VPA. The depth and complexity of this work is such that I hope it will serve as a lasting resource for exploring genetic regulation, cortical development, pharmacogenomics of mood stabilizers, and the impact of genetic variation upon phenotypic expression.

ENDNOTES

Overall, it Wnt pretty well. I did a lot. I learned a lot. There is much to do and learn yet, so I don't plan on stopping. Certainly, whichever way the Wnt blows, the growth, skills, knowledge, and friendships I gained along the way will light the winding path forward.

REFERENCES

1000 Genomes Project Consortium, Adam Auton, Lisa D. Brooks, Richard M. Durbin, Erik P. Garrison, Hyun Min Kang, Jan O. Korbel, et al. 2015. “A Global Reference for Human Genetic Variation.” Nature 526 (7571): 68–74.

Abu-Taweel, Gasem M. 2012. “Effects of Perinatal Exposure of Lithium on Neuro-Behaviour of Developing Mice Offspring.” Indian Journal of Experimental Biology 50 (10): 696–701.

Adams, Hieab H. H., Derrek P. Hibar, Vincent Chouraki, Jason L. Stein, Paul A. Nyquist, Miguel E. Rentería, Stella Trompet, et al. 2016. “Novel Genetic Loci Underlying Human Intracranial Volume Identified through Genome-Wide Association.” Nature Neuroscience 19 (12): 1569–82.

Aguet, François, Kaur Alasoo, Yang I. Li, Alexis Battle, Hae Kyung Im, Stephen B. Montgomery, and Tuuli Lappalainen. 2023. “Molecular Quantitative Trait Loci.” Nature Reviews Methods Primers 3 (1): 1–22.

Alasoo, Kaur, Julia Rodrigues, Subhankar Mukhopadhyay, Andrew J. Knights, Alice L. Mann, Kousik Kundu, HIPSCI Consortium, Christine Hale, Gordon Dougan, and Daniel J. Gaffney. 2018. “Shared Genetic Effects on Chromatin and Gene Expression Indicate a Role for Enhancer Priming in Immune Response.” Nature Genetics 50 (3): 424–31.

Albert, Frank W., and Leonid Kruglyak. 2015. “The Role of Regulatory Variation in Complex Traits and Disease.” Nature Reviews. Genetics 16 (4): 197–212.

Almasy, L., and J. Blangero. 2001. “Endophenotypes as Quantitative Risk Factors for Psychiatric Disease: Rationale and Study Design.” American Journal of Medical Genetics 105 (1): 42–44.

Aoyagi, Yuka, Ryosuke Kawakami, Hisayuki Osanai, Terumasa Hibi, and Tomomi Nemoto. 2015. “A Rapid Optical Clearing Protocol Using 2,2’-Thiodiethanol for Microscopic Observation of Fixed Mouse Brain.” PloS One 10 (1): e0116280.

Arendt, Detlev, Jacob M. Musser, Clare V. H. Baker, Aviv Bergman, Connie Cepko, Douglas H. Erwin, Mihaela Pavlicev, et al. 2016. “The Origin and Evolution of Cell Types.” Nature Reviews. Genetics 17 (12): 744–57.

Astori, Audrey, Johanna Tingvall-Gustafsson, Jacob Kuruvilla, Etienne Coyaud, Estelle M. N. Laurent, Maria Sunnerhagen, Josefine Åhsberg, et al. 2020. “ARID1a Associates with Lymphoid-Restricted Transcription Factors and Has an Essential Role in T Cell Development.” Journal of Immunology 205 (5): 1419–32.

Aygün, Nil, Angela L. Elwell, Dan Liang, Michael J. Lafferty, Kerry E. Cheek, Kenan P. Courtney, Jessica Mory, et al. 2021. “Brain-Trait-Associated Variants Impact Cell-Type-Specific Gene Regulation during Neurogenesis.” American Journal of Human Genetics 108 (9): 1647–68.

“Babraham Bioinformatics - FastQC A Quality Control Tool for High Throughput Sequence Data.” n.d. Accessed January 9, 2023. https://www.bioinformatics.babraham.ac.uk/projects/fastqc/.

Bain, Jenny, Lorna Plater, Matt Elliott, Natalia Shpiro, C. James Hastie, Hilary McLauchlan, Iva

Klevernic, J. Simon C. Arthur, Dario R. Alessi, and Philip Cohen. 2007. “The Selectivity of Protein Kinase Inhibitors: A Further Update.” Biochemical Journal 408 (3): 297–315.

BALANCE investigators and collaborators, John R. Geddes, Guy M. Goodwin, Jennifer Rendell, Jean-Michel Azorin, Andrea Cipriani, Michael J. Ostacher, Richard Morriss, Nicola Alder, and Ed Juszczak. 2010. “Lithium plus Valproate Combination Therapy versus Monotherapy for Relapse Prevention in Bipolar I Disorder (BALANCE): A Randomised Open-Label Trial.” The Lancet 375 (9712): 385–95.

Bastians, H., and H. Ponstingl. 1996. “The Novel Human Protein Serine/threonine Phosphatase 6 Is a Functional Homologue of Budding Yeast Sit4p and Fission Yeast ppe1, Which Are Involved in Cell Cycle Regulation.” Journal of Cell Science 109 (Pt 12) (December): 2865–74.

“BBMap.” 2022. SourceForge. July 15, 2022. https://sourceforge.net/projects/bbmap/.

Bearden, Carrie E., Paul M. Thompson, Rebecca A. Dutton, Benício N. Frey, Marco A. M. Peluso, Mark Nicoletti, Nicole Dierschke, et al. 2008. “Three-Dimensional Mapping of Hippocampal Anatomy in Unmedicated and Lithium-Treated Patients with Bipolar Disorder.” Neuropsychopharmacology: Official Publication of the American College of Neuropsychopharmacology 33 (6): 1229–38.

Bem, Joanna, Nikola Brożko, Chaitali Chakraborty, Marcin A. Lipiec, Kamil Koziński, Andrzej Nagalski, Łukasz M. Szewczyk, and Marta B. Wiśniewska. 2019. “Wnt/β-Catenin Signaling in Brain Development and Mental Disorders: Keeping TCF7L2 in Mind.” FEBS Letters 593 (13): 1654–74.

Bengoa-Vergniory, Nora, and Robert M. Kypta. 2015. “Canonical and Noncanonical Wnt Signaling in Neural Stem/progenitor Cells.” Cellular and Molecular Life Sciences: CMLS 72 (21): 4157–72.

Bennett, Craig M., and Michael B. Miller. 2010. “How Reliable Are the Results from Functional Magnetic Resonance Imaging?” Annals of the New York Academy of Sciences 1191 (March): 133–55.

Biechele, Travis L., Allison M. Adams, and Randall T. Moon. 2009. “Transcription-Based Reporters of Wnt/beta-Catenin Signaling.” Cold Spring Harbor Protocols 2009 (6): db.prot5223.

Bielen, Holger, and Corinne Houart. 2014. “The Wnt Cries Many: Wnt Regulation of Neurogenesis through Tissue Patterning, Proliferation, and Asymmetric Cell Division.” Developmental Neurobiology 74 (8): 772–80.

Bigos, Kristin L., and Daniel R. Weinberger. 2010. “Imaging Genetics--Days of Future Past.” NeuroImage 53 (3): 804–9.

Bis, Joshua C., Charles DeCarli, Albert Vernon Smith, Fedde van der Lijn, Fabrice Crivello, Myriam Fornage, Stephanie Debette, et al. 2012. “Common Variants at 12q14 and 12q24 Are Associated with Hippocampal Volume.” Nature Genetics 44 (5): 545–51.

Black, James R. M., and Simon J. Clark. 2016. “Age-Related Macular Degeneration: Genome-Wide Association Studies to Translation.” Genetics in Medicine: Official Journal of the American College of Medical Genetics 18 (4): 283–89.

Blitzer, Jeremy T., and Roel Nusse. 2006. “A Critical Role for Endocytosis in Wnt Signaling.” BMC Cell Biology 7 (July): 28.

Bogdan, Ryan, Betty Jo Salmeron, Caitlin E. Carey, Arpana Agrawal, Vince D. Calhoun, Hugh Garavan, Ahmad R. Hariri, et al. 2017. “Imaging Genetics and Genomics in Psychiatry: A Critical Review of Progress and Potential.” Biological Psychiatry 82 (3): 165–75.

Boldrini, Maura, René Hen, Mark D. Underwood, Gorazd B. Rosoklija, Andrew J. Dwork, J. John Mann, and Victoria Arango. 2012. “Hippocampal Angiogenesis and Progenitor Cell Proliferation Are Increased with Antidepressant Use in Major Depression.” Biological Psychiatry 72 (7): 562–71.

Boldrini, Maura, Mark D. Underwood, René Hen, Gorazd B. Rosoklija, Andrew J. Dwork, J. John Mann, and Victoria Arango. 2009. “Antidepressants Increase Neural Progenitor Cells in the Human Hippocampus.” Neuropsychopharmacology: Official Publication of the American College of Neuropsychopharmacology 34 (11): 2376–89.

Boulting, Gabriella L., Ershela Durresi, Bulent Ataman, Maxwell A. Sherman, Kevin Mei, David A. Harmin, Ava C. Carter, et al. 2021. “Activity-Dependent Regulome of Human GABAergic Neurons Reveals New Patterns of Gene Regulation and Neurological Disease Heritability.” Nature Neuroscience 24 (3): 437–48.

Bourgon, Richard, Robert Gentleman, and Wolfgang Huber. 2010. “Independent Filtering Increases Detection Power for High-Throughput Experiments.” Proceedings of the National Academy of Sciences of the United States of America 107 (21): 9546–51.

Boyd, J. Lomax, Stephanie L. Skove, Jeremy P. Rouanet, Louis-Jan Pilaz, Tristan Bepler, Raluca Gordân, Gregory A. Wray, and Debra L. Silver. 2015. “Human-Chimpanzee Differences in a FZD8 Enhancer Alter Cell-Cycle Dynamics in the Developing Neocortex.” Current Biology: CB 25 (6): 772–79.

Brainstorm Consortium, Verneri Anttila, Brendan Bulik-Sullivan, Hilary K. Finucane, Raymond K. Walters, Jose Bras, Laramie Duncan, et al. 2018. “Analysis of Shared Heritability in Common Disorders of the Brain.” Science 360 (6395). https://doi.org/10.1126/science.aap8757.

Breen, Gerome, Qingqin Li, Bryan L. Roth, Patricio O’Donnell, Michael Didriksen, Ricardo Dolmetsch, Paul F. O’Reilly, et al. 2016. “Translating Genome-Wide Association Findings into New Therapeutics for Psychiatry.” Nature Neuroscience 19 (11): 1392–96.

Brennand, K. J., A. Simone, N. Tran, and F. H. Gage. 2012. “Modeling Psychiatric Disorders at the Cellular and Network Levels.” Molecular Psychiatry 17 (12): 1239–53.

Brunt, Lucy, and Steffen Scholpp. 2018. “The Function of Endocytosis in Wnt Signaling.” Cellular and Molecular Life Sciences: CMLS 75 (5): 785–95.

Bryois, Julien, Daniela Calini, Will Macnair, Lynette Foo, Eduard Urich, Ward Ortmann, Victor Alejandro Iglesias, et al. 2022. “Cell-Type-Specific Cis-eQTLs in Eight Human Brain Cell Types Identify Novel Risk Genes for Psychiatric and Neurological Disorders.” Nature Neuroscience 25 (8): 1104–12.

Buenrostro, Jason D., Paul G. Giresi, Lisa C. Zaba, Howard Y. Chang, and William J. Greenleaf. 2013. “Transposition of Native Chromatin for Fast and Sensitive Epigenomic Profiling of

Open Chromatin, DNA-Binding Proteins and Nucleosome Position." Nature Methods 10 (12): 1213–18.

Bulik-Sullivan, Brendan K., Po-Ru Loh, Hilary K. Finucane, Stephan Ripke, Jian Yang, Schizophrenia Working Group of the Psychiatric Genomics Consortium, Nick Patterson, Mark J. Daly, Alkes L. Price, and Benjamin M. Neale. 2015. "LD Score Regression Distinguishes Confounding from Polygenicity in Genome-Wide Association Studies." Nature Genetics 47 (3): 291–95.

Bullmore, Ed, and Olaf Sporns. 2009. "Complex Brain Networks: Graph Theoretical Analysis of Structural and Functional Systems." Nature Reviews. Neuroscience 10 (3): 186–98.

Bystron, Irina, Colin Blakemore, and Pasko Rakic. 2008. "Development of the Human Cerebral Cortex: Boulder Committee Revisited." Nature Reviews. Neuroscience 9 (2): 110–22.

Campbell, Kenneth. 2003. "Dorsal-Ventral Patterning in the Mammalian Telencephalon." Current Opinion in Neurobiology 13 (1): 50–56.

Candia, Teresa R. de, S. Hong Lee, Jian Yang, Brian L. Browning, Pablo V. Gejman, Douglas F. Levinson, Bryan J. Mowry, et al. 2013. "Additive Genetic Variation in Schizophrenia Risk Is Shared by Populations of African and European Descent." American Journal of Human Genetics 93 (3): 463–70.

Cannon, Maren E., and Karen L. Mohlke. 2018. "Deciphering the Emerging Complexities of Molecular Mechanisms at GWAS Loci." American Journal of Human Genetics 103 (5): 637–53.

Cannon, Tyrone D., Yoonho Chung, George He, Daqiang Sun, Aron Jacobson, Theo G. M. van Erp, Sarah McEwen, et al. 2015. "Progressive Reduction in Cortical Thickness as Psychosis Develops: A Multisite Longitudinal Neuroimaging Study of Youth at Elevated Clinical Risk." Biological Psychiatry 77 (2): 147–57.

Cano-Gamez, Eddie, and Gosia Trynka. 2020. "From GWAS to Function: Using Functional Genomics to Identify the Mechanisms Underlying Complex Diseases." Frontiers in Genetics 11 (May): 424.

Capra, John A., Genevieve D. Erwin, Gabriel McKinsey, John L. R. Rubenstein, and Katherine S. Pollard. 2013. "Many Human Accelerated Regions Are Developmental Enhancers." Philosophical Transactions of the Royal Society of London. Series B, Biological Sciences 368 (1632): 20130025.

Caracci, Mario O., Miguel E. Avila, Francisca A. Espinoza-Cavieres, Héctor R. López, Giorgia D. Ugarte, and Giancarlo V. De Ferrari. 2021. "Wnt/β-Catenin-Dependent Transcription in Autism Spectrum Disorders." Frontiers in Molecular Neuroscience 14 (November): 764756.

Carithers, Latarsha J., Kristin Ardlie, Mary Barcus, Philip A. Branton, Angela Britton, Stephen A. Buia, Carolyn C. Compton, et al. 2015. "A Novel Approach to High-Quality Postmortem Tissue Procurement: The GTEx Project." Biopreservation and Biobanking 13 (5): 311–19.

Carlson, Christopher S., Tara C. Matise, Kari E. North, Christopher A. Haiman, Megan D. Fesinmeyer, Steven Buyske, Fredrick R. Schumacher, et al. 2013. "Generalization and Dilution of Association Results from European GWAS in Populations of Non-European Ancestry: The PAGE Study." PLoS Biology 11 (9): e1001661.

Casale, Francesco Paolo, Barbara Rakitsch, Christoph Lippert, and Oliver Stegle. 2015. “Efficient Set Tests for the Genetic Analysis of Correlated Traits.” Nature Methods 12 (8): 755–58.

Castro-Mondragon, Jaime A., Rafael Riudavets-Puig, Ieva Rauluseviciute, Roza Berhanu Lemma, Laura Turchi, Romain Blanc-Mathieu, Jeremy Lucas, et al. 2022. “JASPAR 2022: The 9th Release of the Open-Access Database of Transcription Factor Binding Profiles.” Nucleic Acids Research 50 (D1): D165–73.

Chang, Christopher C., Carson C. Chow, Laurent Cam Tellier, Shashaank Vattikuti, Shaun M. Purcell, and James J. Lee. 2015. “Second-Generation PLINK: Rising to the Challenge of Larger and Richer Datasets.” GigaScience 4 (February): 7.

Chen, Chien-Hsiun, Chau-Shoun Lee, Ming-Ta Michael Lee, Wen-Chen Ouyang, Chiao-Chicy Chen, Mian-Yoon Chong, Jer-Yuarn Wu, et al. 2014. “Variant GADL1 and Response to Lithium Therapy in Bipolar I Disorder.” The New England Journal of Medicine 370 (2): 119–28.

Chen, G., G. Rajkowska, F. Du, N. Seraji-Bozorgzad, and H. K. Manji. 2000. “Enhancement of Hippocampal Neurogenesis by Lithium.” Journal of Neurochemistry 75 (4): 1729–34.

Chenn, Anjen, and Christopher A. Walsh. 2002. “Regulation of Cerebral Cortical Size by Control of Cell Cycle Exit in Neural Precursors.” Science 297 (5580): 365–69.

Civelek, Mete, Ying Wu, Calvin Pan, Chelsea K. Raulerson, Arthur Ko, Aiqing He, Charles Tilford, et al. 2017. “Genetic Regulation of Adipose Gene Expression and Cardio-Metabolic Traits.” American Journal of Human Genetics 100 (3): 428–43.

Claussnitzer, Melina, Simon N. Dankel, Kyoung-Han Kim, Gerald Quon, Wouter Meuleman, Christine Haugen, Viktoria Glunk, et al. 2015. “FTO Obesity Variant Circuitry and Adipocyte Browning in Humans.” The New England Journal of Medicine 373 (10): 895–907.

Coetzee, Simon G., Gerhard A. Coetzee, and Dennis J. Hazelett. 2015. “motifbreakR: An R/Bioconductor Package for Predicting Variant Effects at Transcription Factor Binding Sites.” Bioinformatics 31 (23): 3847–49.

Connally, Noah James, Sumaiya Nazeen, Daniel Lee, Huwenbo Shi, John Stamatoyannopoulos, Sung Chun, Chris Cotsapas, Christopher A. Cassa, and Shamil R. Sunyaev. 2022. “The Missing Link between Genetic Association and Regulatory Function.” eLife 11 (December). https://doi.org/10.7554/eLife.74970.

Conomos, Gogarten, Brown, Chen, and Rice. n.d. “GENESIS: GENetic EStimation and Inference in Structured Samples (GENESIS): Statistical Methods for Analyzing Genetic Data from Samples with ….” Genesis .

Corces, M. Ryan, Alexandro E. Trevino, Emily G. Hamilton, Peyton G. Greenside, Nicholas A. Sinnott-Armstrong, Sam Vesuna, Ansuman T. Satpathy, et al. 2017. “An Improved ATAC-Seq Protocol Reduces Background and Enables Interrogation of Frozen Tissues.” Nature Methods 14 (10): 959–62.

Crapanzano, Calogero, Ilaria Casolaro, Chiara Amendola, and Stefano Damiani. 2022. “Lithium and Valproate in Bipolar Disorder: From International Evidence-Based Guidelines to Clinical Predictors.” Clinical Psychopharmacology and Neuroscience: The Official Scientific

Journal of the Korean College of Neuropsychopharmacology 20 (3): 403–14.

Croft, D., G. O'Kelly, G. Wu, R. Haw, M. Gillespie, L. Matthews, M. Caudy, et al. 2011. "Reactome: A Database of Reactions, Pathways and Biological Processes." Nucleic Acids Research 39 (Database): D691–97.

Cuomo, Anna S. E., Giordano Alvari, Christina B. Azodi, single-cell eQTLGen consortium, Davis J. McCarthy, and Marc Jan Bonder. 2021. "Optimizing Expression Quantitative Trait Locus Mapping Workflows for Single-Cell Studies." Genome Biology 22 (1): 188.

Danecek, Petr, James K. Bonfield, Jennifer Liddle, John Marshall, Valeriu Ohan, Martin O. Pollard, Andrew Whitwham, et al. 2021. "Twelve Years of SAMtools and BCFtools." GigaScience 10 (2). https://doi.org/10.1093/gigascience/giab008.

Das, Sayantan, Lukas Forer, Sebastian Schönherr, Carlo Sidore, Adam E. Locke, Alan Kwong, Scott I. Vrieze, et al. 2016. "Next-Generation Genotype Imputation Service and Methods." Nature Genetics 48 (10): 1284–87.

Davis, Joe R., Laure Fresard, David A. Knowles, Mauro Pala, Carlos D. Bustamante, Alexis Battle, and Stephen B. Montgomery. 2016. "An Efficient Multiple-Testing Adjustment for eQTL Studies That Accounts for Linkage Disequilibrium between Variants." American Journal of Human Genetics 98 (1): 216–24.

Denk, Winfried, and Heinz Horstmann. 2004. "Serial Block-Face Scanning Electron Microscopy to Reconstruct Three-Dimensional Tissue Nanostructure." PLoS Biology 2 (11): e329.

Devlin, B., and K. Roeder. 1999. "Genomic Control for Association Studies." Biometrics 55 (4): 997–1004.

Dhindsa, Ryan S., and David B. Goldstein. 2016. "Schizophrenia: From Genetics to Physiology at Last." Nature.

Di Lullo, Elizabeth, and Arnold R. Kriegstein. 2017. "The Use of Brain Organoids to Investigate Neural Development and Disease." Nature Reviews. Neuroscience 18 (10): 573–84.

Dimas, Antigone S., Samuel Deutsch, Barbara E. Stranger, Stephen B. Montgomery, Christelle Borel, Homa Attar-Cohen, Catherine Ingle, et al. 2009. "Common Regulatory Variation Impacts Gene Expression in a Cell Type-Dependent Manner." Science 325 (5945): 1246–50.

Doan, Ryan N., Byoung-Il Bae, Beatriz Cubelos, Cindy Chang, Amer A. Hossain, Samira Al-Saad, Nahit M. Mukaddes, et al. 2016. "Mutations in Human Accelerated Regions Disrupt Cognition and Social Behavior." Cell 167 (2): 341–54.e12.

Dobbyn, Amanda, Laura M. Huckins, James Boocock, Laura G. Sloofman, Benjamin S. Glicksberg, Claudia Giambartolomei, Gabriel E. Hoffman, et al. 2018. "Landscape of Conditional eQTL in Dorsolateral Prefrontal Cortex and Co-Localization with Schizophrenia GWAS." American Journal of Human Genetics 102 (6): 1169–84.

Dobin, Alexander, Carrie A. Davis, Felix Schlesinger, Jorg Drenkow, Chris Zaleski, Sonali Jha, Philippe Batut, Mark Chaisson, and Thomas R. Gingeras. 2013. "STAR: Ultrafast Universal RNA-Seq Aligner." Bioinformatics 29 (1): 15–21.

Dong, Pengfei, Gabriel E. Hoffman, Pasha Apontes, Jaroslav Bendl, Samir Rahman, Michael B.

Fernando, Biao Zeng, et al. 2022. “Population-Level Variation in Enhancer Expression Identifies Disease Mechanisms in the Human Brain.” Nature Genetics 54 (10): 1493–1503.

Donovan, Margaret K. R., Agnieszka D’Antonio-Chronowska, Matteo D’Antonio, and Kelly A. Frazer. 2020. “Cellular Deconvolution of GTEx Tissues Powers Discovery of Disease and Cell-Type Associated Regulatory Variants.” Nature Communications 11 (1): 955.

Doumpas, Nikolaos, Franziska Lampart, Mark D. Robinson, Antonio Lentini, Colm E. Nestor, Claudio Cantù, and Konrad Basler. 2019. “TCF/LEF Dependent and Independent Transcriptional Regulation of Wnt/β-Catenin Target Genes.” The EMBO Journal 38 (2). https://doi.org/10.15252/embj.201798873.

Du, Qiang, and David A. Geller. 2010. “Cross-Regulation Between Wnt and NF-κB Signaling Pathways.” Forum on Immunopathological Diseases and Therapeutics 1 (3): 155–81.

Elkon, Ran, and Reuven Agami. 2017. “Characterization of Noncoding Regulatory DNA in the Human Genome.” Nature Biotechnology 35 (8): 732–46.

Elliott, Lloyd T., Kevin Sharp, Fidel Alfaro-Almagro, Sinan Shi, Karla L. Miller, Gwenaëlle Douaud, Jonathan Marchini, and Stephen M. Smith. 2018. “Genome-Wide Association Studies of Brain Imaging Phenotypes in UK Biobank.” Nature 562 (7726): 210–16.

ENCODE Project Consortium, Jill E. Moore, Michael J. Purcaro, Henry E. Pratt, Charles B. Epstein, Noam Shoresh, Jessika Adrian, et al. 2020. “Expanded Encyclopaedias of DNA Elements in the Human and Mouse Genomes.” Nature 583 (7818): 699–710.

Eriksson, P. S., E. Perfilieva, T. Björk-Eriksson, A. M. Alborn, C. Nordborg, D. A. Peterson, and F. H. Gage. 1998. “Neurogenesis in the Adult Human Hippocampus.” Nature Medicine 4 (11): 1313–17.

Ernst, Jason, and Manolis Kellis. 2012. “ChromHMM: Automating Chromatin-State Discovery and Characterization.” Nature Methods 9 (3): 215–16.

Erp, T. G. M. van, D. P. Hibar, J. M. Rasmussen, D. C. Glahn, G. D. Pearlson, O. A. Andreassen, I. Agartz, et al. 2016. “Subcortical Brain Volume Abnormalities in 2028 Individuals with Schizophrenia and 2540 Healthy Controls via the ENIGMA Consortium.” Molecular Psychiatry 21 (4): 585.

Erp, Theo G. M. van, Esther Walton, Derrek P. Hibar, Lianne Schmaal, Wenhao Jiang, David C. Glahn, Godfrey D. Pearlson, et al. 2018. “Cortical Brain Abnormalities in 4474 Individuals With Schizophrenia and 5098 Control Subjects via the Enhancing Neuro Imaging Genetics Through Meta Analysis (ENIGMA) Consortium.” Biological Psychiatry, May. https://doi.org/10.1016/j.biopsych.2018.04.023.

Ertürk, Ali, Klaus Becker, Nina Jährling, Christoph P. Mauch, Caroline D. Hojer, Jackson G. Egen, Farida Hellal, Frank Bradke, Morgan Sheng, and Hans-Ulrich Dodt. 2012. “Three-Dimensional Imaging of Solvent-Cleared Organs Using 3DISCO.” Nature Protocols 7 (11): 1983–95.

Ertürk, Ali, Christoph P. Mauch, Farida Hellal, Friedrich Förstner, Tara Keck, Klaus Becker, Nina Jährling, et al. 2011. “Three-Dimensional Imaging of the Unsectioned Adult Spinal Cord to Assess Axon Regeneration and Glial Responses after Injury.” Nature Medicine 18 (1): 166–71.

Evgrafov, Oleg V., Chris Armoskus, Bozena B. Wrobel, Valeria N. Spitsyna, Tade Souaiaia, Jennifer S. Herstein, Christopher P. Walker, et al. 2020. “Gene Expression in Patient-Derived Neural Progenitors Implicates WNT5A Signaling in the Etiology of Schizophrenia.” Biological Psychiatry 88 (3): 236–47.

Ewels, Philip, Måns Magnusson, Sverker Lundin, and Max Käller. 2016. “MultiQC: Summarize Analysis Results for Multiple Tools and Samples in a Single Report.” Bioinformatics 32 (19): 3047–48.

Fairley, Susan, Ernesto Lowy-Gallego, Emily Perry, and Paul Flicek. 2020. “The International Genome Sample Resource (IGSR) Collection of Open Human Genomic Variation Resources.” Nucleic Acids Research 48 (D1): D941–47.

Farrell, M. S., T. Werge, P. Sklar, M. J. Owen, R. A. Ophoff, M. C. O’Donovan, A. Corvin, S. Cichon, and P. F. Sullivan. 2015. “Evaluating Historical Candidate Genes for Schizophrenia.” Molecular Psychiatry 20 (5): 555–62.

Findley, Anthony S., Alan Monziani, Allison L. Richards, Katherine Rhodes, Michelle C. Ward, Cynthia A. Kalita, Adnan Alazizi, et al. 2021. “Functional Dynamic Genetic Effects on Gene Regulation Are Specific to Particular Cell Types and Environmental Conditions.” eLife 10 (May). https://doi.org/10.7554/eLife.67077.

Finucane, Hilary K., Brendan Bulik-Sullivan, Alexander Gusev, Gosia Trynka, Yakir Reshef, Po-Ru Loh, Verneri Anttila, et al. 2015. “Partitioning Heritability by Functional Annotation Using Genome-Wide Association Summary Statistics.” Nature Genetics 47 (11): 1228–35.

Fischl, B., and A. M. Dale. 2000. “Measuring the Thickness of the Human Cerebral Cortex from Magnetic Resonance Images.” Proceedings of the National Academy of Sciences of the United States of America 97 (20): 11050–55.

Flint, Jonathan, and Marcus R. Munafò. 2007. “The Endophenotype Concept in Psychiatric Genetics.” Psychological Medicine 37 (2): 163–80.

Flint, Jonathan, and Marcus R. Munafò. 2013. “Candidate and Non-Candidate Genes in Behavior Genetics.” Current Opinion in Neurobiology 23 (1): 57–61.

Flint, Jonathan, Nicholas Timpson, and Marcus Munafò. 2014. “Assessing the Utility of Intermediate Phenotypes for Genetic Mapping of Psychiatric Disease.” Trends in Neurosciences 37 (12): 733–41.

Forsberg, L., M. Adler, I. Römer Ek, M. Ljungdahl, L. Navér, L. L. Gustafsson, G. Berglund, et al. 2018. “Maternal Mood Disorders and Lithium Exposure in Utero Were Not Associated with Poor Cognitive Development during Childhood.” Acta Paediatrica 107 (8): 1379–88.

Franjic, Daniel, Mario Skarica, Shaojie Ma, Jon I. Arellano, Andrew T. N. Tebbenkamp, Jinmyung Choi, Chuan Xu, et al. 2022. “Transcriptomic Taxonomy and Neurogenic Trajectories of Adult Human, Macaque, and Pig Hippocampal and Entorhinal Cells.” Neuron 110 (3): 452–69.e14.

Franke, Barbara, Jason L. Stein, Stephan Ripke, Verneri Anttila, Derrek P. Hibar, Kimm J. E. van Hulzen, Alejandro Arias-Vasquez, et al. 2016. “Genetic Influences on Schizophrenia and Subcortical Brain Volumes: Large-Scale Proof of Concept.” Nature Neuroscience 19 (3): 420–31.

Frayling, Timothy M., Nicholas J. Timpson, Michael N. Weedon, Eleftheria Zeggini, Rachel M. Freathy, Cecilia M. Lindgren, John R. B. Perry, et al. 2007. “A Common Variant in the FTO Gene Is Associated with Body Mass Index and Predisposes to Childhood and Adult Obesity.” Science 316 (5826): 889–94.

Freese, Jennifer L., Darya Pino, and Samuel J. Pleasure. 2010. “Wnt Signaling in Development and Disease.” Neurobiology of Disease 38 (2): 148–53.

Frei, Oleksandr, Dominic Holland, Olav B. Smeland, Alexey A. Shadrin, Chun Chieh Fan, Steffen Maeland, Kevin S. O’Connell, et al. 2019. “Bivariate Causal Mixture Model Quantifies Polygenic Overlap between Complex Traits beyond Genetic Correlation.” Nature Communications 10 (1): 2417.

Fromer, Menachem, Panos Roussos, Solveig K. Sieberts, Jessica S. Johnson, David H. Kavanagh, Thanneer M. Perumal, Douglas M. Ruderfer, et al. 2016. “Gene Expression Elucidates Functional Impact of Polygenic Risk for Schizophrenia.” Nature Neuroscience 19 (11): 1442–53.

Fürth, Daniel, Thomas Vaissière, Ourania Tzortzi, Yang Xuan, Antje Märtin, Iakovos Lazaridis, Giada Spigolon, et al. 2018. “An Interactive Framework for Whole-Brain Maps at Cellular Resolution.” Nature Neuroscience 21 (1): 139–49.

Gaulton, Kyle J., Sebastian Preissl, and Bing Ren. 2023. “Interpreting Non-Coding Disease-Associated Human Variants Using Single-Cell Epigenomics.” Nature Reviews. Genetics 24 (8): 516–34.

Gazal, Steven, Hilary K. Finucane, Nicholas A. Furlotte, Po-Ru Loh, Pier Francesco Palamara, Xuanyao Liu, Armin Schoech, et al. 2017. “Linkage Disequilibrium--Dependent Architecture of Human Complex Traits Shows Action of Negative Selection.” Nature Genetics 49 (10): 1421.

Geddes, John R., Sally Burgess, Keith Hawton, Kay Jamison, and Guy M. Goodwin. 2004. “Long-Term Lithium Therapy for Bipolar Disorder: Systematic Review and Meta-Analysis of Randomized Controlled Trials.” The American Journal of Psychiatry 161 (2): 217–22.

Geddes, John R., and David J. Miklowitz. 2013. “Treatment of Bipolar Disorder.” The Lancet 381 (9878): 1672–82.

Geijn, Bryce van de, Graham McVicker, Yoav Gilad, and Jonathan K. Pritchard. 2015. “WASP: Allele-Specific Software for Robust Molecular Quantitative Trait Locus Discovery.” Nature Methods 12 (11): 1061–63.

Geschwind, Daniel H., and Jonathan Flint. 2015. “Genetics and Genomics of Psychiatric Disease.” Science 349 (6255): 1489–94.

Giambartolomei, Claudia, Damjan Vukcevic, Eric E. Schadt, Lude Franke, Aroon D. Hingorani, Chris Wallace, and Vincent Plagnol. 2014. “Bayesian Test for Colocalisation between Pairs of Genetic Association Studies Using Summary Statistics.” PLoS Genetics 10 (5): e1004383.

Giles, James J., and John G. Bannigan. 2006. “Teratogenic and Developmental Effects of Lithium.” Current Pharmaceutical Design 12 (12): 1531–41.

Gilmore, Edward C., and Christopher A. Walsh. 2013. “Genetic Causes of Microcephaly and

Lessons for Neuronal Development." Wiley Interdisciplinary Reviews. Developmental Biology 2 (4): 461–78.

Girskis, Kelly M., Andrew B. Stergachis, Ellen M. DeGennaro, Ryan N. Doan, Xuyu Qian, Matthew B. Johnson, Peter P. Wang, et al. 2021. "Rewiring of Human Neurodevelopmental Gene Regulatory Programs by Human Accelerated Regions." Neuron 109 (20): 3239–51.e7.

Glahn, David C., Paul M. Thompson, and John Blangero. 2007. "Neuroimaging Endophenotypes: Strategies for Finding Genes Influencing Brain Structure and Function." Human Brain Mapping 28 (6): 488–501.

Glausier, J. R., and D. A. Lewis. 2013. "Dendritic Spine Pathology in Schizophrenia." Neuroscience 251 (October): 90–107.

Goey, Andrew Kl, Tristan M. Sissung, Cody J. Peer, and William D. Figg. 2016. "Pharmacogenomics and Histone Deacetylase Inhibitors." Pharmacogenomics 17 (16): 1807–15.

Gogarten, Stephanie M., Tamar Sofer, Han Chen, Chaoyu Yu, Jennifer A. Brody, Timothy A. Thornton, Kenneth M. Rice, and Matthew P. Conomos. 2019. "Genetic Association Testing Using the GENESIS R/Bioconductor Package." Bioinformatics 35 (24): 5346–48.

Gottesman, I. I., and J. Shields. 1973. "Genetic Theorizing and Schizophrenia." The British Journal of Psychiatry: The Journal of Mental Science 122 (566): 15–30.

Gottesman, Irving I., and Todd D. Gould. 2003. "The Endophenotype Concept in Psychiatry: Etymology and Strategic Intentions." The American Journal of Psychiatry 160 (4): 636–45.

Gottesman, Irving I., and James Shields. 1972. "Schizophrenia and Genetics. A Twin Study Vantage Point." In ACAD. PRESS, NEW YORK, NY.

Grandi, Fiorella C., Hailey Modi, Lucas Kampman, and M. Ryan Corces. 2022. "Chromatin Accessibility Profiling by ATAC-Seq." Nature Protocols 17 (6): 1518–52.

Grasby, Katrina L., Neda Jahanshad, Jodie N. Painter, Lucía Colodro-Conde, Janita Bralten, Derrek P. Hibar, Penelope A. Lind, et al. 2020. "The Genetic Architecture of the Human Cerebral Cortex." Science 367 (6484).

Gratten, Jacob, Naomi R. Wray, Matthew C. Keller, and Peter M. Visscher. 2014. "Large-Scale Genomics Unveils the Genetic Architecture of Psychiatric Disorders." Nature Neuroscience 17 (6): 782–90.

Grof, Paul, Anne Duffy, Patrizia Cavazzoni, Eva Grof, Julie Garnham, Marsha MacDougall, Claire O'Donovan, and Martin Alda. 2002. "Is Response to Prophylactic Lithium a Familial Trait?" The Journal of Clinical Psychiatry 63 (10): 942–47.

Grove, Jakob, Stephan Ripke, Thomas Damm Als, Manuel Mattheisen, Raymond Walters, Hyejung Won, Jonatan Pallesen, et al. 2017. "Common Risk Variants Identified in Autism Spectrum Disorder." bioRxiv. https://doi.org/10.1101/224774.

GTEx Consortium. 2020. "The GTEx Consortium Atlas of Genetic Regulatory Effects across Human Tissues." Science 369 (6509): 1318–30.

GTEx Consortium, Laboratory, Data Analysis &Coordinating Center (LDACC)—Analysis Working Group, Statistical Methods groups—Analysis Working Group, Enhancing GTEx (eGTEx) groups, NIH Common Fund, NIH/NCI, NIH/NHGRI, et al. 2017. “Genetic Effects on Gene Expression across Human Tissues.” Nature 550 (7675): 204–13.

Hajek, Tomas, Jeffrey Cullis, Tomas Novak, Miloslav Kopecek, Cyril Höschl, Ryan Blagdon, Claire O’Donovan, et al. 2012. “Hippocampal Volumes in Bipolar Disorders: Opposing Effects of Illness Burden and Lithium Treatment.” Bipolar Disorders 14 (3): 261–70.

Hallonet, M., T. Hollemann, R. Wehr, N. A. Jenkins, N. G. Copeland, T. Pieler, and P. Gruss. 1998. “Vax1 Is a Novel Homeobox-Containing Gene Expressed in the Developing Anterior Ventral Forebrain.” Development 125 (14): 2599–2610.

Hansen, David V., John L. R. Rubenstein, and Arnold R. Kriegstein. 2011. “Deriving Excitatory Neurons of the Neocortex from Pluripotent Stem Cells.” Neuron 70 (4): 645–60.

Hansen, Kasper D., Rafael A. Irizarry, and Zhijin Wu. 2012. “Removing Technical Variability in RNA-Seq Data Using Conditional Quantile Normalization.” Biostatistics 13 (2): 204–16.

Hao, Zhao-Zhe, Jia-Ru Wei, Dongchang Xiao, Ruifeng Liu, Nana Xu, Lei Tang, Mengyao Huang, et al. 2022. “Single-Cell Transcriptomics of Adult Macaque Hippocampus Reveals Neural Precursor Cell Populations.” Nature Neuroscience 25 (6): 805–17.

Harrison, Paul J. 2011. “Using Our Brains: The Findings, Flaws, and Future of Postmortem Studies of Psychiatric Disorders.” Biological Psychiatry 69 (2): 102–3.

Harrison-Uy, Susan J., and Samuel J. Pleasure. 2012. “Wnt Signaling and Forebrain Development.” Cold Spring Harbor Perspectives in Biology 4 (7): a008094.

Hatzis, Pantelis, Laurens G. van der Flier, Marc A. van Driel, Victor Guryev, Fiona Nielsen, Sergei Denissov, Isaäc J. Nijman, et al. 2008. “Genome-Wide Pattern of TCF7L2/TCF4 Chromatin Occupancy in Colorectal Cancer Cells.” Molecular and Cellular Biology 28 (8): 2732–44.

Hayden, Erika Check. 2014. “Technology: The $1,000 Genome.” Nature 507 (7492): 294–95.

Hazlett, Heather Cody, Hongbin Gu, Brent C. Munsell, Sun Hyung Kim, Martin Styner, Jason J. Wolff, Jed T. Elison, et al. 2017. “Early Brain Development in Infants at High Risk for Autism Spectrum Disorder.” Nature 542 (7641): 348–51.

Hébert, Jean M., and Gord Fishell. 2008. “The Genetics of Early Telencephalon Patterning: Some Assembly Required.” Nature Reviews. Neuroscience 9 (9): 678–85.

Hekselman, Idan, and Esti Yeger-Lotem. 2020. “Mechanisms of Tissue and Cell-Type Specificity in Heritable Traits and Diseases.” Nature Reviews. Genetics 21 (3): 137–50.

He, Xin, Chris K. Fuller, Yi Song, Qingying Meng, Bin Zhang, Xia Yang, and Hao Li. 2013. “Sherlock: Detecting Gene-Disease Associations by Matching Patterns of Expression QTL and GWAS.” American Journal of Human Genetics 92 (5): 667–80.

Hibar, Derrek P., Hieab H. H. Adams, Neda Jahanshad, Ganesh Chauhan, Jason L. Stein, Edith Hofer, Miguel E. Renteria, et al. 2017. “Novel Genetic Loci Associated with Hippocampal Volume.” Nature Communications 8 (January): 13624.

Hibar, Derrek P., Jason L. Stein, Miguel E. Renteria, Alejandro Arias-Vasquez, Sylvane Desrivières, Neda Jahanshad, Roberto Toro, et al. 2015. “Common Genetic Variants Influence Human Subcortical Brain Structures.” Nature 520 (7546): 224–29.

Hindorff, Lucia A., Praveen Sethupathy, Heather A. Junkins, Erin M. Ramos, Jayashri P. Mehta, Francis S. Collins, and Teri A. Manolio. 2009. “Potential Etiologic and Functional Implications of Genome-Wide Association Loci for Human Diseases and Traits.” Proceedings of the National Academy of Sciences of the United States of America 106 (23): 9362–67.

Hochgerner, Hannah, Amit Zeisel, Peter Lönnerberg, and Sten Linnarsson. 2018. “Conserved Properties of Dentate Gyrus Neurogenesis across Postnatal Development Revealed by Single-Cell RNA Sequencing.” Nature Neuroscience 21 (2): 290–99.

Hoen, Peter A. C. ’t, Marc R. Friedländer, Jonas Almlöf, Michael Sammeth, Irina Pulyakhina, Seyed Yahya Anvar, Jeroen F. J. Laros, et al. 2013. “Reproducibility of High-Throughput mRNA and Small RNA Sequencing across Laboratories.” Nature Biotechnology 31 (11): 1015–22.

Hofer, Edith, Gennady V. Roshchupkin, Hieab Adams, Maria Knol, Honghuang Lin, Shuo Li, Habil Zare, et al. 2018. “Genetic Determinants of Cortical Structure (Thickness, Surface Area and Volumes) among Disease Free Adults in the CHARGE Consortium.” bioRxiv. https://doi.org/10.1101/409649.

Hoffman, Gabriel E., and Kristen J. Brennand. 2018. “Mapping Regulatory Variants in hiPSC Models.” Nature Genetics 50 (1): 1–2.

Holland, Dominic, Chun-Chieh Fan, Oleksandr Frei, Alexey A. Shadrin, Olav B. Smeland, V. S. Sundar, -. Enigma, Ole A. Andreassen, and Anders M. Dale. 2017. “Estimating Phenotypic Polygenicity and Causal Effect Size Variance from GWAS Summary Statistics While Accounting for Inflation due to Cryptic Relatedness.” bioRxiv. https://doi.org/10.1101/133132.

Holland, Dominic, Yunpeng Wang, Wesley K. Thompson, Andrew Schork, Chi-Hua Chen, Min-Tzu Lo, Aree Witoelar, et al. 2016. “Estimating Effect Sizes and Expected Replication Probabilities from GWAS Summary Statistics.” Frontiers in Genetics 7 (February): 15.

Holstein, Thomas W. 2012. “The Evolution of the Wnt Pathway.” Cold Spring Harbor Perspectives in Biology 4 (7): a007922.

Holtmaat, Anthony, and Karel Svoboda. 2009. “Experience-Dependent Structural Synaptic Plasticity in the Mammalian Brain.” Nature Reviews. Neuroscience 10 (9): 647–58.

Honey, Christopher J., Jean-Philippe Thivierge, and Olaf Sporns. 2010. “Can Structure Predict Function in the Human Brain?” NeuroImage 52 (3): 766–76.

Hormozdiari, Farhad, Martijn van de Bunt, Ayellet V. Segrè, Xiao Li, Jong Wha J. Joo, Michael Bilow, Jae Hoon Sul, Sriram Sankararaman, Bogdan Pasaniuc, and Eleazar Eskin. 2016. “Colocalization of GWAS and eQTL Signals Detects Target Genes.” American Journal of Human Genetics 99 (6): 1245–60.

Horstmann, Heinz, Christoph Körber, Kurt Sätzler, Daniel Aydin, and Thomas Kuner. 2012. “Serial Section Scanning Electron Microscopy (S3EM) on Silicon Wafers for Ultra-

Structural Volume Imaging of Cells and Tissues." PloS One 7 (4): e35172.

Hoseth, Eva Z., Florian Krull, Ingrid Dieset, Ragni H. Mørch, Sigrun Hope, Erlend S. Gardsjord, Nils Eiel Steen, et al. 2018. "Exploring the Wnt Signaling Pathway in Schizophrenia and Bipolar Disorder." Translational Psychiatry 8 (1): 55.

Hou, Liping, Urs Heilbronner, Franziska Degenhardt, Mazda Adli, Kazufumi Akiyama, Nirmala Akula, Raffaella Ardau, et al. 2016. "Genetic Variants Associated with Response to Lithium Treatment in Bipolar Disorder: A Genome-Wide Association Study." The Lancet 387 (10023): 1085–93.

Huang, Qin Qin, Scott C. Ritchie, Marta Brozynska, and Michael Inouye. 2018. "Power, False Discovery Rate and Winner's Curse in eQTL Studies." Nucleic Acids Research 46 (22): e133.

Huang, Shih-Min A., Yuji M. Mishina, Shanming Liu, Atwood Cheung, Frank Stegmeier, Gregory A. Michaud, Olga Charlat, et al. 2009. "Tankyrase Inhibition Stabilizes Axin and Antagonizes Wnt Signalling." Nature 461 (7264): 614–20.

Hur, Eun-Mi, and Feng-Quan Zhou. 2010. "GSK3 Signalling in Neural Development." Nature Reviews. Neuroscience 11 (8): 539–51.

Ikram, M. Arfan, Myriam Fornage, Albert V. Smith, Sudha Seshadri, Reinhold Schmidt, Stéphanie Debette, Henri A. Vrooman, et al. 2012. "Common Variants at 6q22 and 17q21 Are Associated with Intracranial Volume." Nature Genetics 44 (5): 539–44.

Im, Kiho, and P. Ellen Grant. 2018. "Sulcal Pits and Patterns in Developing Human Brains." NeuroImage, March. https://doi.org/10.1016/j.neuroimage.2018.03.057.

Jerber, Julie, Daniel D. Seaton, Anna S. E. Cuomo, Natsuhiko Kumasaka, James Haldane, Juliette Steer, Minal Patel, et al. 2021. "Population-Scale Single-Cell RNA-Seq Profiling across Dopaminergic Neuron Differentiation." Nature Genetics 53 (3): 304–12.

Jha, Shaili C., Kai Xia, Mihye Ahn, Jessica B. Girault, Gang Li, Li Wang, Dinggang Shen, et al. 2019. "Environmental Influences on Infant Cortical Thickness and Surface Area." Cerebral Cortex 29 (3): 1139–49.

Jho, Eek-Hoon, Tong Zhang, Claire Domon, Choun-Ki Joo, Jean-Noel Freund, and Frank Costantini. 2002. "Wnt/beta-catenin/Tcf Signaling Induces the Transcription of Axin2, a Negative Regulator of the Signaling Pathway." Molecular and Cellular Biology 22 (4): 1172–83.

Johansson, Viktoria, Ralf Kuja-Halkola, Tyrone D. Cannon, Christina M. Hultman, and Anna M. Hedman. 2019. "A Population-Based Heritability Estimate of Bipolar Disorder - In a Swedish Twin Sample." Psychiatry Research 278 (August): 180–87.

Johnson, Emma C., Richard Border, Whitney E. Melroy-Greif, Christiaan A. de Leeuw, Marissa A. Ehringer, and Matthew C. Keller. 2017. "No Evidence That Schizophrenia Candidate Genes Are More Associated With Schizophrenia Than Noncandidate Genes." Biological Psychiatry 82 (10): 702–8.

Johnson, Matthew B., and Beth Stevens. 2018. "Pruning Hypothesis Comes of Age." Nature 554 (7693): 438–39.

Ju, Dan, Daniel Hui, Dorothy A. Hammond, Ambroise Wonkam, and Sarah A. Tishkoff. 2022. "Importance of Including Non-European Populations in Large Human Genetic Studies to Enhance Precision Medicine." Annual Review of Biomedical Data Science 5 (August): 321–39.

Jun, Goo, Matthew Flickinger, Kurt N. Hetrick, Jane M. Romm, Kimberly F. Doheny, Gonçalo R. Abecasis, Michael Boehnke, and Hyun Min Kang. 2012. "Detecting and Estimating Contamination of Human DNA Samples in Sequencing and Array-Based Genotype Data." American Journal of Human Genetics 91 (5): 839–48.

Kachuri, Linda, Nilanjan Chatterjee, Jibril Hirbo, Daniel J. Schaid, Iman Martin, Iftikhar J. Kullo, Eimear E. Kenny, et al. 2023. "Principles and Methods for Transferring Polygenic Risk Scores across Global Populations." Nature Reviews. Genetics, August. https://doi.org/10.1038/s41576-023-00637-2.

Kageyama, Ryoichiro, Toshiyuki Ohtsuka, Hiromi Shimojo, and Itaru Imayoshi. 2009. "Dynamic Regulation of Notch Signaling in Neural Progenitor Cells." Current Opinion in Cell Biology 21 (6): 733–40.

Kahn, René S., Iris E. Sommer, Robin M. Murray, Andreas Meyer-Lindenberg, Daniel R. Weinberger, Tyrone D. Cannon, Michael O'Donovan, et al. 2015. "Schizophrenia." Nature Reviews. Disease Primers 1 (November): 15067.

Kang, Hyun Min, Jae Hoon Sul, Susan K. Service, Noah A. Zaitlen, Sit-Yee Kong, Nelson B. Freimer, Chiara Sabatti, and Eleazar Eskin. 2010. "Variance Component Model to Account for Sample Structure in Genome-Wide Association Studies." Nature Genetics 42 (4): 348–54.

Kang, Hyun Min, Noah A. Zaitlen, Claire M. Wade, Andrew Kirby, David Heckerman, Mark J. Daly, and Eleazar Eskin. 2008. "Efficient Control of Population Structure in Model Organism Association Mapping." Genetics 178 (3): 1709–23.

Kappel, Djenifer B., Sophie E. Legge, Leon Hubbard, Isabella R. Willcocks, Adrian King, John Jansen, Marinka Helthuis, et al. 2022. "Genomic Stratification of Clozapine Prescription Patterns Using Schizophrenia Polygenic Scores." medRxiv, February, 2022.02.18.22271204.

Kasela, Silva, François Aguet, Sarah Kim-Hellmuth, Brielin C. Brown, Daniel C. Nachun, Russell P. Tracy, Peter Durda, et al. 2023. "Interaction Molecular QTL Mapping Discovers Cellular and Environmental Modifiers of Genetic Regulatory Effects." bioRxiv. https://doi.org/10.1101/2023.06.26.546528.

Kasthuri, Narayanan, Kenneth Jeffrey Hayworth, Daniel Raimund Berger, Richard Lee Schalek, José Angel Conchello, Seymour Knowles-Barley, Dongil Lee, et al. 2015. "Saturated Reconstruction of a Volume of Neocortex." Cell 162 (3): 648–61.

Kato, Tadafumi. 2007. "Molecular Genetics of Bipolar Disorder and Depression." Psychiatry and Clinical Neurosciences 61 (1): 3–19.

Kendler, K. S., and M. C. Neale. 8/2010. "Endophenotype: A Conceptual Analysis." Molecular Psychiatry 15 (8): 789–97.

Kessing, Lars Vedel, Thomas Alexander Gerds, Nikoline Nygård Knudsen, Lisbeth Flindt Jørgensen, Søren Munch Kristiansen, Denitza Voutchkova, Vibeke Ernstsen, et al. 2017.

"Association of Lithium in Drinking Water With the Incidence of Dementia." JAMA Psychiatry 74 (10): 1005–10.

Klein, Marieke, Raymond K. Walters, Ditte Demontis, Jason L. Stein, Derrek P. Hibar, Hieab H. Adams, Janita Bralten, et al. 2017. "Genetic Markers of ADHD-Related Variations in Intracranial Volume." bioRxiv. https://doi.org/10.1101/184192.

Klein, Niek de, Ellen A. Tsai, Martijn Vochteloo, Denis Baird, Yunfeng Huang, Chia-Yen Chen, Sipko van Dam, et al. 2023. "Brain Expression Quantitative Trait Locus and Network Analyses Reveal Downstream Effects and Putative Drivers for Brain-Related Diseases." Nature Genetics, February, 1–12.

Kleissas, Dean, Robert Hider, Derek Pryor, Timothy Gion, Priya Manavalan, Jordan Matelsky, Alex Baden, et al. 2017. "The Block Object Storage Service (bossDB): A Cloud-Native Approach for Petascale Neuroscience Discovery." bioRxiv. https://doi.org/10.1101/217745.

Klemm, Sandy L., Zohar Shipony, and William J. Greenleaf. 2019. "Chromatin Accessibility and the Regulatory Epigenome." Nature Reviews. Genetics 20 (4): 207–20.

Knowles, David A., Courtney K. Burrows, John D. Blischak, Kristen M. Patterson, Daniel J. Serie, Nadine Norton, Carole Ober, Jonathan K. Pritchard, and Yoav Gilad. 2018. "Determining the Genetic Basis of Anthracycline-Cardiotoxicity by Molecular Response QTL Mapping in Induced Cardiomyocytes." eLife 7 (May). https://doi.org/10.7554/eLife.33480.

Kosoy, Roman, John F. Fullard, Biao Zeng, Jaroslav Bendl, Pengfei Dong, Samir Rahman, Steven P. Kleopoulos, et al. 2022. "Genetics of the Human Microglia Regulome Refines Alzheimer's Disease Risk Loci." Nature Genetics 54 (8): 1145–54.

Krebs, Kristi, and Lili Milani. 2019. "Translating Pharmacogenomics into Clinical Decisions: Do Not Let the Perfect Be the Enemy of the Good." Human Genomics 13 (1): 39.

Kretzschmar, Hans. 2009. "Brain Banking: Opportunities, Challenges and Meaning for the Future." Nature Reviews. Neuroscience 10 (1): 70–78.

Kriegstein, Arnold, and Arturo Alvarez-Buylla. 2009. "The Glial Nature of Embryonic and Adult Neural Stem Cells." Annual Review of Neuroscience 32: 149–84.

Krumm, Niklas, Brian J. O'Roak, Jay Shendure, and Evan E. Eichler. 2014. "A de Novo Convergence of Autism Genetics and Molecular Neuroscience." Trends in Neurosciences 37 (2): 95–105.

Kumar, Dhirendra, Senthilkumar Cinghu, Andrew J. Oldfield, Pengyi Yang, and Raja Jothi. 2021. "Decoding the Function of Bivalent Chromatin in Development and Cancer." Genome Research 31 (12): 2170–84.

Kumasaka, Natsuhiko, Andrew J. Knights, and Daniel J. Gaffney. 2016. "Fine-Mapping Cellular QTLs with RASQUAL and ATAC-Seq." Nature Genetics 48 (2): 206–13.

Kumasaka, Natsuhiko, Andrew J. Knights, and Daniel J. Gaffney. 2019. "High-Resolution Genetic Mapping of Putative Causal Interactions between Regions of Open Chromatin." Nature Genetics 51 (1): 128–37.

Kunz, Martin, Michael Herrmann, Doris Wedlich, and Dietmar Gradl. 2004. “Autoregulation of Canonical Wnt Signaling Controls Midbrain Development.” Developmental Biology 273 (2): 390–401.

Kuwajima, Takaaki, Austen A. Sitko, Punita Bhansali, Chris Jurgens, William Guido, and Carol Mason. 2013. “ClearT: A Detergent- and Solvent-Free Clearing Method for Neuronal and Non-Neuronal Tissue.” Development 140 (6): 1364–68.

Lagomarsino, Valentina N., Richard V. Pearse 2nd, Lei Liu, Yi-Chen Hsieh, Marty A. Fernandez, Elizabeth A. Vinton, Daniel Paull, et al. 2021. “Stem Cell-Derived Neurons Reflect Features of Protein Networks, Neuropathology, and Cognitive Outcome of Their Aged Human Donors.” Neuron 109 (21): 3402–20.e9.

Lago, Santiago G., Jakub Tomasik, and Sabine Bahn. 2021. “Functional Patient-Derived Cellular Models for Neuropsychiatric Drug Discovery.” Translational Psychiatry 11 (1): 128.

Lai, Hei Ming, Alan King Lun Liu, Harry Ho Man Ng, Marc Goldfinger, Tsz Wing Chau, John DeFelice, Bension Tilley, Wai Man Wong, Wutian Wu, and Steve Gentleman. 2018. “Methods for next Generation Three-Dimensional Histology for Human Neural Tissues,” August. https://doi.org/10.1038/protex.2018.087.

Lappalainen, Tuuli, and Daniel G. MacArthur. 2021. “From Variant to Function in Human Disease Genetics.” Science 373 (6562): 1464–68.

Lappalainen, Tuuli, Michael Sammeth, Marc R. Friedländer, Peter A. C. ’t Hoen, Jean Monlong, Manuel A. Rivas, Mar Gonzàlez-Porta, et al. 2013. “Transcriptome and Genome Sequencing Uncovers Functional Variation in Humans.” Nature 501 (7468): 506–11.

Le, Brandon D., and Jason L. Stein. 2019. “Mapping Causal Pathways from Genetics to Neuropsychiatric Disorders Using Genome-Wide Imaging Genetics: Current Status and Future Directions.” Psychiatry and Clinical Neurosciences, March. https://doi.org/10.1111/pcn.12839.

Lederbogen, Florian, Peter Kirsch, Leila Haddad, Fabian Streit, Heike Tost, Philipp Schuch, Stefan Wüst, et al. 2011. “City Living and Urban Upbringing Affect Neural Social Stress Processing in Humans.” Nature 474 (7352): 498–501.

Lenzenweger, Mark F. 2013. “Thinking Clearly about the Endophenotype-Intermediate Phenotype-Biomarker Distinctions in Developmental Psychopathology Research.” Development and Psychopathology 25 (4 Pt 2): 1347–57.

Liang, Dan, Angela L. Elwell, Nil Aygün, Oleh Krupa, Justin M. Wolter, Felix A. Kyere, Michael J. Lafferty, et al. 2021. “Cell-Type-Specific Effects of Genetic Variation on Chromatin Accessibility during Human Neuronal Differentiation.” Nature Neuroscience, May. https://doi.org/10.1038/s41593-021-00858-w.

Liao, Yang, Gordon K. Smyth, and Wei Shi. 2019. “The R Package Rsubread Is Easier, Faster, Cheaper and Better for Alignment and Quantification of RNA Sequencing Reads.” Nucleic Acids Research 47 (8): e47.

Liebmann, Thomas, Nicolas Renier, Karima Bettayeb, Paul Greengard, Marc Tessier-Lavigne, and Marc Flajolet. 2016. “Three-Dimensional Study of Alzheimer’s Disease Hallmarks Using the iDISCO Clearing Method.” Cell Reports 16 (4): 1138–52.

Li, Heng, and Richard Durbin. 2009. “Fast and Accurate Short Read Alignment with Burrows-Wheeler Transform.” Bioinformatics 25 (14): 1754–60.

Li, Mingfeng, Gabriel Santpere, Yuka Imamura Kawasawa, Oleg V. Evgrafov, Forrest O. Gulden, Sirisha Pochareddy, Susan M. Sunkin, et al. 2018. “Integrative Functional Genomic Analysis of Human Brain Development and Neuropsychiatric Risks.” Science 362 (6420). https://doi.org/10.1126/science.aat7615.

Liu, A. K. L., M. E. D. Hurry, O. T. W. Ng, J. DeFelice, H. M. Lai, R. K. B. Pearce, G. T-C Wong, R. C-C Chang, and S. M. Gentleman. 2016. “Bringing CLARITY to the Human Brain: Visualization of Lewy Pathology in Three Dimensions.” Neuropathology and Applied Neurobiology 42 (6): 573–87.

Li, Yang I., Bryce van de Geijn, Anil Raj, David A. Knowles, Allegra A. Petti, David Golan, Yoav Gilad, and Jonathan K. Pritchard. 2016. “RNA Splicing Is a Primary Link between Genetic Variation and Disease.” Science 352 (6285): 600–604.

Li, Zhiqiang, Jianhua Chen, Hao Yu, Lin He, Yifeng Xu, Dai Zhang, Qizhong Yi, et al. 2017. “Genome-Wide Association Analysis Identifies 30 New Susceptibility Loci for Schizophrenia.” Nature Genetics 49 (11): 1576–83.

Lodato, Michael A., Mollie B. Woodworth, Semin Lee, Gilad D. Evrony, Bhaven K. Mehta, Amir Karger, Soohyun Lee, et al. 2015. “Somatic Mutation in Single Human Neurons Tracks Developmental and Transcriptional History.” Science 350 (6256): 94–98.

Love, Michael I., Wolfgang Huber, and Simon Anders. 2014. “Moderated Estimation of Fold Change and Dispersion for RNA-Seq Data with DESeq2.” Genome Biology 15 (12): 550.

Lun, Aaron T. L., and Gordon K. Smyth. 2016. “Csaw: A Bioconductor Package for Differential Binding Analysis of ChIP-Seq Data Using Sliding Windows.” Nucleic Acids Research 44 (5): e45.

Luo, Yunhai, Benjamin C. Hitz, Idan Gabdank, Jason A. Hilton, Meenakshi S. Kagda, Bonita Lam, Zachary Myers, et al. 2020. “New Developments on the Encyclopedia of DNA Elements (ENCODE) Data Portal.” Nucleic Acids Research 48 (D1): D882–89.

Macrae, Trisha A., Julie Fothergill-Robinson, and Miguel Ramalho-Santos. 2023. “Regulation, Functions and Transmission of Bivalent Chromatin during Mammalian Development.” Nature Reviews. Molecular Cell Biology 24 (1): 6–26.

Major, Michael B., Nathan D. Camp, Jason D. Berndt, Xianhua Yi, Seth J. Goldenberg, Charlotte Hubbert, Travis L. Biechele, et al. 2007. “Wilms Tumor Suppressor WTX Negatively Regulates WNT/beta-Catenin Signaling.” Science 316 (5827): 1043–46.

Malek, Mehrnoush, Mohammad Jafar Taghiyar, Lauren Chong, Greg Finak, Raphael Gottardo, and Ryan R. Brinkman. 2015. “flowDensity: Reproducing Manual Gating of Flow Cytometry Data by Automated Density-Based Cell Population Identification.” Bioinformatics 31 (4): 606–7.

Malhi, Gin S., Danielle Gessler, and Tim Outhred. 2017. “The Use of Lithium for the Treatment of Bipolar Disorder: Recommendations from Clinical Practice Guidelines.” Journal of Affective Disorders 217 (August): 266–80.

Mangan, Riley J., Fernando C. Alsina, Federica Mosti, Jesús Emiliano Sotelo-Fonseca, Daniel A. Snellings, Eric H. Au, Juliana Carvalho, et al. 2022. “Adaptive Sequence Divergence Forged New Neurodevelopmental Enhancers in Humans.” Cell 185 (24): 4587–4603.e23.

Marchetto, Maria C., Haim Belinson, Yuan Tian, Beatriz C. Freitas, Chen Fu, Krishna Vadodaria, Patricia Beltrao-Braga, et al. 2017. “Altered Proliferation and Networks in Neural Cells Derived from Idiopathic Autistic Individuals.” Molecular Psychiatry 22 (6): 820–35.

Marigorta, Urko M., Juan Antonio Rodríguez, Greg Gibson, and Arcadi Navarro. 2018. “Replicability and Prediction: Lessons and Challenges from GWAS.” Trends in Genetics: TIG 34 (7): 504–17.

Martin, Alicia R., Christopher R. Gignoux, Raymond K. Walters, Genevieve L. Wojcik, Benjamin M. Neale, Simon Gravel, Mark J. Daly, Carlos D. Bustamante, and Eimear E. Kenny. 2017. “Human Demographic History Impacts Genetic Risk Prediction across Diverse Populations.” American Journal of Human Genetics 100 (4): 635–49.

Martin, Alicia R., Masahiro Kanai, Yoichiro Kamatani, Yukinori Okada, Benjamin M. Neale, and Mark J. Daly. 2019. “Clinical Use of Current Polygenic Risk Scores May Exacerbate Health Disparities.” Nature Genetics 51 (4): 584–91.

Martin-Brevet, Sandra, Borja Rodríguez-Herreros, Jared A. Nielsen, Clara Moreau, Claudia Modenato, Anne M. Maillard, Aurélie Pain, et al. 2018. “Quantifying the Effects of 16p11.2 Copy Number Variants on Brain Structure: A Multisite Genetic-First Study.” Biological Psychiatry 84 (4): 253–64.

Matoba, Nana, Brandon D. Le, Jordan M. Valone, Justin M. Wolter, Jessica Mory, Dan Liang, Nil Aygun, et al. 2023. “WNT Activity Reveals Context-Specific Genetic Effects on Gene Regulation in Neural Progenitors.” bioRxiv. https://doi.org/10.1101/2023.02.07.527357.

Matoba, Nana, Dan Liang, Huaigu Sun, Nil Aygün, Jessica C. McAfee, Jessica E. Davis, Laura M. Raffield, et al. 2020. “Common Genetic Risk Variants Identified in the SPARK Cohort Support DDHD2 as a Candidate Risk Gene for Autism.” Translational Psychiatry 10 (1): 265.

McInnes, Gregory, Sook Wah Yee, Yash Pershad, and Russ B. Altman. 2021. “Genomewide Association Studies in Pharmacogenomics.” Clinical Pharmacology and Therapeutics 110 (3): 637–48.

McLean, Cory Y., Dave Bristor, Michael Hiller, Shoa L. Clarke, Bruce T. Schaar, Craig B. Lowe, Aaron M. Wenger, and Gill Bejerano. 2010. “GREAT Improves Functional Interpretation of Cis-Regulatory Regions.” Nature Biotechnology 28 (5): 495–501.

Meer, Dennis van der, Jaroslav Rokicki, Tobias Kaufmann, Aldo Córdova-Palomera, Torgeir Moberget, Dag Alnæs, Francesco Bettella, et al. 2018. “Brain Scans from 21,297 Individuals Reveal the Genetic Architecture of Hippocampal Subfield Volumes.” Molecular Psychiatry, October. https://doi.org/10.1038/s41380-018-0262-7.

Memon, Anjum, Imogen Rogers, Sophie M. D. D. Fitzsimmons, Ben Carter, Rebecca Strawbridge, Diego Hidalgo-Mazzei, and Allan H. Young. 2020. “Association between Naturally Occurring Lithium in Drinking Water and Suicide Rates: Systematic Review and Meta-Analysis of Ecological Studies.” The British Journal of Psychiatry: The Journal of Mental Science 217 (6): 667–78.

Meng, Lingjun, Tao Lin, Guang Peng, Joseph K. Hsu, Sun Lee, Shiaw-Yih Lin, and Robert Y. L. Tsai. 2013. “Nucleostemin Deletion Reveals an Essential Mechanism That Maintains the Genomic Stability of Stem and Progenitor Cells.” Proceedings of the National Academy of Sciences of the United States of America 110 (28): 11415–20.

Meng, Qingtuan, Le Wang, Rujia Dai, Jiawen Wang, Zongyao Ren, Sihan Liu, Yan Xia, et al. 2020. “Integrative Analyses Prioritize GNL3 as a Risk Gene for Bipolar Disorder.” Molecular Psychiatry, August. https://doi.org/10.1038/s41380-020-00866-5.

Mertens, Jerome, Qiu-Wen Wang, Yongsung Kim, Diana X. Yu, Son Pham, Bo Yang, Yi Zheng, et al. 2015. “Differential Responses to Lithium in Hyperexcitable Neurons from Patients with Bipolar Disorder.” Nature 527 (7576): 95–99.

Messiha, F. S. 1986. “Lithium and the Neonate: Developmental and Metabolic Aspects.” Alcohol 3 (2): 107–12.

Meyer-Lindenberg, Andreas, and Daniel R. Weinberger. 2006. “Intermediate Phenotypes and Genetic Mechanisms of Psychiatric Disorders.” Nature Reviews. Neuroscience 7 (10): 818–27.

Minnoye, Liesbeth, Georgi K. Marinov, Thomas Krausgruber, Lixia Pan, Alexandre P. Marand, Stefano Secchia, William J. Greenleaf, et al. 2021. “Chromatin Accessibility Profiling Methods.” Nature Reviews Methods Primers 1 (1): 10.

Miranda, Kildare, Wendell Girard-Dias, Marcia Attias, Wanderley de Souza, and Isabela Ramos. 2015. “Three Dimensional Reconstruction by Electron Microscopy in the Life Sciences: An Introduction for Cell and Tissue Biologists.” Molecular Reproduction and Development 82 (7-8): 530–47.

Mitchell, Kevin J. 2018. “Neurogenomics--towards a More Rigorous Science.” The European Journal of Neuroscience 47 (2): 109–14.

Mochida, Ganeshwaran H., and Christopher A. Walsh. 2004. “Genetic Basis of Developmental Malformations of the Cerebral Cortex.” Archives of Neurology 61 (5): 637–40.

Mosimann, Christian, George Hausmann, and Konrad Basler. 2009. “Beta-Catenin Hits Chromatin: Regulation of Wnt Target Gene Activation.” Nature Reviews. Molecular Cell Biology 10 (4): 276–86.

Mulligan, Kimberly A., and Benjamin N. R. Cheyette. 2017. “Neurodevelopmental Perspectives on Wnt Signaling in Psychiatry.” Molecular Neuropsychiatry 2 (4): 219–46.

Mullins, Niamh, Andreas J. Forstner, Kevin S. O’Connell, Brandon Coombes, Jonathan R. I. Coleman, Zhen Qiao, Thomas D. Als, et al. 2021. “Genome-Wide Association Study of More than 40,000 Bipolar Disorder Cases Provides New Insights into the Underlying Biology.” Nature Genetics, May. https://doi.org/10.1038/s41588-021-00857-4.

Munji, Roeben N., Youngshik Choe, Guangnan Li, Julie A. Siegenthaler, and Samuel J. Pleasure. 2011. “Wnt Signaling Regulates Neuronal Differentiation of Cortical Intermediate Progenitors.” The Journal of Neuroscience: The Official Journal of the Society for Neuroscience 31 (5): 1676–87.

Munk-Olsen, Trine, Xiaoqin Liu, Alexander Viktorin, Hilary K. Brown, Arianna Di Florio, Brian

M. D'Onofrio, Tara Gomes, et al. 2018. "Maternal and Infant Outcomes Associated with Lithium Use in Pregnancy: An International Collaborative Meta-Analysis of Six Cohort Studies." The Lancet. Psychiatry 5 (8): 644–52.

Musunuru, Kiran, Alanna Strong, Maria Frank-Kamenetsky, Noemi E. Lee, Tim Ahfeldt, Katherine V. Sachs, Xiaoyu Li, et al. 2010. "From Noncoding Variant to Phenotype via SORT1 at the 1p13 Cholesterol Locus." Nature 466 (7307): 714–19.

Nelson, Matthew R., Hannah Tipney, Jeffery L. Painter, Judong Shen, Paola Nicoletti, Yufeng Shen, Aris Floratos, et al. 2015. "The Support of Human Genetic Evidence for Approved Drug Indications." Nature Genetics 47 (8): 856–60.

Nelson, W. James, and Roel Nusse. 2004. "Convergence of Wnt, Beta-Catenin, and Cadherin Pathways." Science 303 (5663): 1483–87.

Newport, D. Jeffrey, Adele C. Viguera, Aquila J. Beach, James C. Ritchie, Lee S. Cohen, and Zachary N. Stowe. 2005. "Lithium Placental Passage and Obstetrical Outcome: Implications for Clinical Management during Late Pregnancy." The American Journal of Psychiatry 162 (11): 2162–70.

Ng, Bernard, Charles C. White, Hans-Ulrich Klein, Solveig K. Sieberts, Cristin McCabe, Ellis Patrick, Jishu Xu, et al. 2017. "An xQTL Map Integrates the Genetic Architecture of the Human Brain's Transcriptome and Epigenome." Nature Neuroscience 20 (10): 1418–26.

Nica, Alexandra C., Stephen B. Montgomery, Antigone S. Dimas, Barbara E. Stranger, Claude Beazley, Inês Barroso, and Emmanouil T. Dermitzakis. 2010. "Candidate Causal Regulatory Effects by Integration of Expression QTLs with Complex Trait Genetic Associations." PLoS Genetics 6 (4): e1000895.

Niehrs, Christof, and Sergio P. Acebron. 2012. "Mitotic and Mitogenic Wnt Signalling." The EMBO Journal 31 (12): 2705–13.

Niemsiri, Vipavee, Sarah Brin Rosenthal, Caroline M. Nievergelt, Adam X. Maihofer, Maria C. Marchetto, Renata Santos, Tatyana Shekhtman, et al. 2022. "Network-Based Integrative Analysis of Lithium Response in Bipolar Disorder Using Transcriptomic and GWAS Data." bioRxiv. https://doi.org/10.1101/2022.01.10.21268493.

Nolen, W. A., R. W. Licht, A. H. Young, G. S. Malhi, M. Tohen, E. Vieta, R. W. Kupka, et al. 2019. "ISBD/IGSLI Task Force on the Treatment with Lithium What Is the Optimal Serum Level for Lithium in the Maintenance Treatment of Bipolar Disorder? A Systematic Review and Recommendations from the ISBD/IGSLI Task Force on Treatment with Lithium Version 2." Bipolar Disorders 21 (5): 394–409.

Nusse, Roel, and Hans Clevers. 2017. "Wnt/β-Catenin Signaling, Disease, and Emerging Therapeutic Modalities." Cell 169 (6): 985–99.

Nyholt, Dale R. 2004. "A Simple Correction for Multiple Testing for Single-Nucleotide Polymorphisms in Linkage Disequilibrium with Each Other." American Journal of Human Genetics 74 (4): 765–69.

O'Donnell, Kelley C., and Todd D. Gould. 2007. "The Behavioral Actions of Lithium in Rodent Models: Leads to Develop Novel Therapeutics." Neuroscience and Biobehavioral Reviews 31 (6): 932–62.

Oelen, Roy, Dylan H. de Vries, Harm Brugge, M. Grace Gordon, Martijn Vochteloo, single-cell eQTLGen consortium, BIOS Consortium, et al. 2022. “Single-Cell RNA-Sequencing of Peripheral Blood Mononuclear Cells Reveals Widespread, Context-Specific Gene Expression Regulation upon Pathogenic Exposure.” Nature Communications 13 (1): 3267.

Ogata, H., S. Goto, K. Sato, W. Fujibuchi, H. Bono, and M. Kanehisa. 1999. “KEGG: Kyoto Encyclopedia of Genes and Genomes.” Nucleic Acids Research 27 (1): 29–34.

Ohtaka-Maruyama, Chiaki, and Haruo Okado. 2015. “Molecular Pathways Underlying Projection Neuron Production and Migration during Cerebral Cortical Development.” Frontiers in Neuroscience 9 (December): 447.

Orchard, Peter, Yasuhiro Kyono, John Hensley, Jacob O. Kitzman, and Stephen C. J. Parker. 2020. “Quantification, Dynamic Visualization, and Validation of Bias in ATAC-Seq Data with Ataqv.” Cell Systems 10 (3): 298–306.e4.

Os, Jim van, Gunter Kenis, and Bart P. F. Rutten. 2010. “The Environment and Schizophrenia.” Nature 468 (7321): 203–12.

Ozsolak, Fatih, and Patrice M. Milos. 2011. “RNA Sequencing: Advances, Challenges and Opportunities.” Nature Reviews. Genetics 12 (2): 87–98.

Packer, Alan. 2016. “Neocortical Neurogenesis and the Etiology of Autism Spectrum Disorder.” Neuroscience and Biobehavioral Reviews 64 (May): 185–95.

Pakkenberg, Bente, Dorte Pelvig, Lisbeth Marner, Mads J. Bundgaard, Hans Jørgen G. Gundersen, Jens R. Nyengaard, and Lisbeth Regeur. 2003. “Aging and the Human Neocortex.” Experimental Gerontology 38 (1-2): 95–99.

Pakkenberg, B., and H. J. Gundersen. 1997. “Neocortical Neuron Number in Humans: Effect of Sex and Age.” The Journal of Comparative Neurology 384 (2): 312–20.

Panagiotou, Orestis A., John P. A. Ioannidis, and Genome-Wide Significance Project. 2012. “What Should the Genome-Wide Significance Threshold Be? Empirical Replication of Borderline Genetic Associations.” International Journal of Epidemiology 41 (1): 273–86.

Panousis, Nikolaos I., Omar El Garwany, Andrew Knights, Jesse Cheruiyot Rop, Natsuhiko Kumasaka, Maria Imaz, Lorena Boquete Vilarino, et al. 2023. “Gene Expression QTL Mapping in Stimulated iPSC-Derived Macrophages Provides Insights into Common Complex Diseases.” bioRxiv. https://doi.org/10.1101/2023.05.29.542425.

Pardiñas, Antonio F., Peter Holmans, Andrew J. Pocklington, Valentina Escott-Price, Stephan Ripke, Noa Carrera, Sophie E. Legge, et al. 2018. “Common Schizophrenia Alleles Are Enriched in Mutation-Intolerant Genes and in Regions under Strong Background Selection.” Nature Genetics 50 (3): 381–89.

Pardiñas, Antonio F., Michael J. Owen, and James T. R. Walters. 2021. “Pharmacogenomics: A Road Ahead for Precision Medicine in Psychiatry.” Neuron 109 (24): 3914–29.

Parikshak, Neelroop N., Vivek Swarup, T. Grant Belgard, Manuel Irimia, Gokul Ramaswami, Michael J. Gandal, Christopher Hartl, et al. 2018. “Author Correction: Genome-Wide Changes in lncRNA, Splicing, and Regional Gene Expression Patterns in Autism.” Nature 560 (7718): E30.

Park, Hyun Woo, Young Chul Kim, Bo Yu, Toshiro Moroishi, Jung-Soon Mo, Steven W. Plouffe, Zhipeng Meng, et al. 2015. “Alternative Wnt Signaling Activates YAP/TAZ.” Cell 162 (4): 780–94.

Pasaniuc, Bogdan, and Alkes L. Price. 2017. “Dissecting the Genetics of Complex Traits Using Summary Association Statistics.” Nature Reviews. Genetics 18 (2): 117–27.

Pavlaki, Ioanna, Michael Shapiro, Giuseppina Pisignano, Stephanie M. E. Jones, Jelena Telenius, Silvia Muñoz-Descalzo, Robert J. Williams, Jim R. Hughes, and Keith W. Vance. 2022. “Chromatin Interaction Maps Identify Wnt Responsive Cis-Regulatory Elements Coordinating Paupar-Pax6 Expression in Neuronal Cells.” PLoS Genetics 18 (6): e1010230.

Peddie, Christopher J., and Lucy M. Collinson. 2014. “Exploring the Third Dimension: Volume Electron Microscopy Comes of Age.” Micron 61 (June): 9–19.

Perera, Tarique D., Jeremy D. Coplan, Sarah H. Lisanby, Cecilia M. Lipira, Mohamed Arif, Cristina Carpio, Gila Spitzer, et al. 2007. “Antidepressant-Induced Neurogenesis in the Hippocampus of Adult Nonhuman Primates.” The Journal of Neuroscience: The Official Journal of the Society for Neuroscience 27 (18): 4894–4901.

Peterson, Roseann E., Karoline Kuchenbaecker, Raymond K. Walters, Chia-Yen Chen, Alice B. Popejoy, Sathish Periyasamy, Max Lam, et al. 2019. “Genome-Wide Association Studies in Ancestrally Diverse Populations: Opportunities, Methods, Pitfalls, and Recommendations.” Cell 179 (3): 589–603.

“Picard.” n.d. Accessed January 9, 2023. http://broadinstitute.github.io/picard/.

Pickar-Oliver, Adrian, and Charles A. Gersbach. 2019. “The next Generation of CRISPR-Cas Technologies and Applications.” Nature Reviews. Molecular Cell Biology 20 (8): 490–507.

Pickrell, Joseph K., Tomaz Berisa, Jimmy Z. Liu, Laure Ségurel, Joyce Y. Tung, and David A. Hinds. 2016. “Detection and Interpretation of Shared Genetic Influences on 42 Human Traits.” Nature Genetics 48 (7): 709–17.

Piñero, Janet, Juan Manuel Ramírez-Anguita, Josep Saüch-Pitarch, Francesco Ronzano, Emilio Centeno, Ferran Sanz, and Laura I. Furlong. 2020. “The DisGeNET Knowledge Platform for Disease Genomics: 2019 Update.” Nucleic Acids Research 48 (D1): D845–55.

Pingault, Jean-Baptiste, Paul F. O’Reilly, Tabea Schoeler, George B. Ploubidis, Frühling Rijsdijk, and Frank Dudbridge. 2018. “Using Genetic Data to Strengthen Causal Inference in Observational Research.” Nature Reviews. Genetics, June. https://doi.org/10.1038/s41576-018-0020-3.

Poels, Eline M. P., Hilmar H. Bijma, Megan Galbally, and Veerle Bergink. 2018. “Lithium during Pregnancy and after Delivery: A Review.” International Journal of Bipolar Disorders 6 (1): 26.

Poels, Eline M. P., Lisanne Schrijver, Astrid M. Kamperman, Manon H. J. Hillegers, Witte J. G. Hoogendijk, Steven A. Kushner, and Sabine J. Roza. 2018. “Long-Term Neurodevelopmental Consequences of Intrauterine Exposure to Lithium and Antipsychotics: A Systematic Review and Meta-Analysis.” European Child & Adolescent Psychiatry 27 (9): 1209–30.

Polderman, Tinca J. C., Beben Benyamin, Christiaan A. de Leeuw, Patrick F. Sullivan, Arjen van Bochoven, Peter M. Visscher, and Danielle Posthuma. 2015. “Meta-Analysis of the Heritability of Human Traits Based on Fifty Years of Twin Studies.” Nature Genetics 47 (7): 702–9.

Pollard, Katherine S., Melissa J. Hubisz, Kate R. Rosenbloom, and Adam Siepel. 2010. “Detection of Nonneutral Substitution Rates on Mammalian Phylogenies.” Genome Research 20 (1): 110–21.

Preissl, Sebastian, Kyle J. Gaulton, and Bing Ren. 2023. “Characterizing Cis-Regulatory Elements Using Single-Cell Epigenomics.” Nature Reviews. Genetics 24 (1): 21–43.

Purcell, Shaun M., Jennifer L. Moran, Menachem Fromer, Douglas Ruderfer, Nadia Solovieff, Panos Roussos, Colm O’Dushlaine, et al. 2014. “A Polygenic Burden of Rare Disruptive Mutations in Schizophrenia.” Nature 506 (7487): 185–90.

Quinlan, Aaron R., and Ira M. Hall. 2010. “BEDTools: A Flexible Suite of Utilities for Comparing Genomic Features.” Bioinformatics 26 (6): 841–42.

Qu, Zhaoxia, Dongming Sun, and Wise Young. 2011. “Lithium Promotes Neural Precursor Cell Proliferation: Evidence for the Involvement of the Non-Canonical GSK-3β-NF-AT Signaling.” Cell & Bioscience 1 (1): 18.

Rakic, P. 1988. “Specification of Cerebral Cortical Areas.” Science 241 (4862): 170–76.

Rakic, Pasko. 2009. “Evolution of the Neocortex: A Perspective from Developmental Biology.” Nature Reviews. Neuroscience 10 (10): 724–35.

Readhead, Benjamin, Brigham J. Hartley, Brian J. Eastwood, David A. Collier, David Evans, Richard Farias, Ching He, et al. 2018. “Expression-Based Drug Screening of Neural Progenitor Cells from Individuals with Schizophrenia.” Nature Communications 9 (1): 4412.

Reimand, Jüri, Meelis Kull, Hedi Peterson, Jaanus Hansen, and Jaak Vilo. 2007. “g:Profiler—a Web-Based Toolset for Functional Profiling of Gene Lists from Large-Scale Experiments.” Nucleic Acids Research 35 (suppl_2): W193–200.

Renier, Nicolas, Eliza L. Adams, Christoph Kirst, Zhuhao Wu, Ricardo Azevedo, Johannes Kohl, Anita E. Autry, et al. 2016. “Mapping of Brain Activity by Automated Volume Analysis of Immediate Early Genes.” Cell 165 (7): 1789–1802.

Richardson, Douglas S., and Jeff W. Lichtman. 2015. “Clarifying Tissue Clearing.” Cell 162 (2): 246–57.

Rietveld, Cornelius A., Sarah E. Medland, Jaime Derringer, Jian Yang, Tõnu Esko, Nicolas W. Martin, Harm-Jan Westra, et al. 2013. “GWAS of 126,559 Individuals Identifies Genetic Variants Associated with Educational Attainment.” Science 340 (6139): 1467–71.

Roadmap Epigenomics Consortium, Anshul Kundaje, Wouter Meuleman, Jason Ernst, Misha Bilenky, Angela Yen, Alireza Heravi-Moussavi, et al. 2015. “Integrative Analysis of 111 Reference Human Epigenomes.” Nature 518 (7539): 317–30.

Roden, Dan M., Howard L. McLeod, Mary V. Relling, Marc S. Williams, George A. Mensah, Josh F. Peterson, and Sara L. Van Driest. 2019. “Pharmacogenomics.” The Lancet 394 (10197):

521–32.

Roeske, Maxwell J., Christine Konradi, Stephan Heckers, and Alan S. Lewis. 2021. "Hippocampal Volume and Hippocampal Neuron Density, Number and Size in Schizophrenia: A Systematic Review and Meta-Analysis of Postmortem Studies." Molecular Psychiatry 26 (7): 3524–35.

Rooij, Daan van, Evdokia Anagnostou, Celso Arango, Guillaume Auzias, Marlene Behrmann, Geraldo F. Busatto, Sara Calderoni, et al. 2018. "Cortical and Subcortical Brain Morphometry Differences Between Patients With Autism Spectrum Disorder and Healthy Individuals Across the Lifespan: Results From the ENIGMA ASD Working Group." The American Journal of Psychiatry 175 (4): 359–69.

Roussos, Panos, Amanda C. Mitchell, Georgios Voloudakis, John F. Fullard, Venu M. Pothula, Jonathan Tsang, Eli A. Stahl, et al. 2014. "A Role for Noncoding Variation in Schizophrenia." Cell Reports 9 (4): 1417–29.

Sahay, Amar, and Rene Hen. 2007. "Adult Hippocampal Neurogenesis in Depression." Nature Neuroscience 10 (9): 1110–15.

Santarelli, Luca, Michael Saxe, Cornelius Gross, Alexandre Surget, Fortunato Battaglia, Stephanie Dulawa, Noelia Weisstaub, et al. 2003. "Requirement of Hippocampal Neurogenesis for the Behavioral Effects of Antidepressants." Science 301 (5634): 805–9.

Santos, Renata, Sara B. Linker, Shani Stern, Ana P. D. Mendes, Maxim N. Shokhirev, Galina Erikson, Lynne Randolph-Moore, et al. 2021. "Deficient LEF1 Expression Is Associated with Lithium Resistance and Hyperexcitability in Neurons Derived from Bipolar Disorder Patients." Molecular Psychiatry, January. https://doi.org/10.1038/s41380-020-00981-3.

Sasabayashi, Daiki, Ryo Yoshimura, Tsutomu Takahashi, Yoichiro Takayanagi, Shimako Nishiyama, Yuko Higuchi, Yuko Mizukami, et al. 2021. "Reduced Hippocampal Subfield Volume in Schizophrenia and Clinical High-Risk State for Psychosis." Frontiers in Psychiatry / Frontiers Research Foundation 12 (March): 642048.

Satizabal, Claudia L., Hieab H. H. Adams, Derrek P. Hibar, Charles C. White, Jason L. Stein, Markus Scholz, Murali Sargurupremraj, et al. 2017. "Genetic Architecture of Subcortical Brain Structures in Over 40,000 Individuals Worldwide." bioRxiv. https://doi.org/10.1101/173831.

Savage, Jeanne E., Philip R. Jansen, Sven Stringer, Kyoko Watanabe, Julien Bryois, Christiaan A. de Leeuw, Mats Nagel, et al. 2018. "Genome-Wide Association Meta-Analysis in 269,867 Individuals Identifies New Genetic and Functional Links to Intelligence." Nature Genetics 50 (7): 912–19.

Schadt, Eric E., John Lamb, Xia Yang, Jun Zhu, Steve Edwards, Debraj Guhathakurta, Solveig K. Sieberts, et al. 2005. "An Integrative Genomics Approach to Infer Causal Associations between Gene Expression and Disease." Nature Genetics 37 (7): 710–17.

Schaid, Daniel J., Wenan Chen, and Nicholas B. Larson. 2018. "From Genome-Wide Associations to Candidate Causal Variants by Statistical Fine-Mapping." Nature Reviews. Genetics 19 (8): 491–504.

Schizophrenia Working Group of the Psychiatric Genomics Consortium. 2014. "Biological

Insights from 108 Schizophrenia-Associated Genetic Loci." Nature 511 (7510): 421–27.

Schoepfer, J., R. Gernhäuser, S. Lichtinger, A. Stöver, M. Bendel, C. Delbridge, T. Widmann, S. Winkler, and M. Graw. 2021. "Position Sensitive Measurement of Trace Lithium in the Brain with NIK (neutron-Induced Coincidence Method) in Suicide." Scientific Reports 11 (1): 6823.

Schrauzer, G. N., and K. P. Shrestha. 1990. "Lithium in Drinking Water and the Incidences of Crimes, Suicides, and Arrests Related to Drug Addictions." Biological Trace Element Research 25 (2): 105–13.

Schubert, Klaus Oliver, Anbupalam Thalamuthu, Azmeraw T. Amare, Joseph Frank, Fabian Streit, Mazda Adl, Nirmala Akula, et al. 2021. "Combining Schizophrenia and Depression Polygenic Risk Scores Improves the Genetic Prediction of Lithium Response in Bipolar Disorder Patients." Translational Psychiatry 11 (1): 606.

Schwartzentruber, Jeremy, Stefanie Foskolou, Helena Kilpinen, Julia Rodrigues, Kaur Alasoo, Andrew J. Knights, Minal Patel, et al. 2018. "Molecular and Functional Variation in iPSC-Derived Sensory Neurons." Nature Genetics 50 (1): 54–61.

Sekar, Aswin, Allison R. Bialas, Heather de Rivera, Avery Davis, Timothy R. Hammond, Nolan Kamitaki, Katherine Tooley, et al. 2016. "Schizophrenia Risk from Complex Variation of Complement Component 4." Nature 530 (7589): 177–83.

Sellgren, Carl M., Jessica Gracias, Bradley Watmuff, Jonathan D. Biag, Jessica M. Thanos, Paul B. Whittredge, Ting Fu, et al. 2019. "Increased Synapse Elimination by Microglia in Schizophrenia Patient-Derived Models of Synaptic Pruning." Nature Neuroscience, February. https://doi.org/10.1038/s41593-018-0334-7.

Seltzer, Laurie E., and Alex R. Paciorkowski. 2014. "Genetic Disorders Associated with Postnatal Microcephaly." American Journal of Medical Genetics. Part C, Seminars in Medical Genetics 166C (2): 140–55.

Senner, Fanny, Mojtaba Oraki Kohshour, Safa Abdalla, Sergi Papiol, and Thomas G. Schulze. 2021. "The Genetics of Response to and Side Effects of Lithium Treatment in Bipolar Disorder: Future Research Perspectives." Frontiers in Pharmacology 12 (March): 638882.

Shalem, Ophir, Neville E. Sanjana, and Feng Zhang. 2015. "High-Throughput Functional Genomics Using CRISPR-Cas9." Nature Reviews. Genetics 16 (5): 299–311.

Shannon, Paul, and Matt Richards. 2022. "MotifDb: An Annotated Collection of Protein-DNA Binding Sequence Motifs, . R Package Version 1.37.1." https://doi.org/10.18129/B9.bioc.MotifDb.

Shtutman, Michael, Jacob Zhurinsky, Inbal Simcha, Chris Albanese, Mark D'Amico, Richard Pestell, and Avri Ben-Ze'ev. 1999. "The Cyclin D1 Gene Is a Target of the β-catenin/LEF-1 Pathway." Proceedings of the National Academy of Sciences 96 (10): 5522–27.

Small, Kerrin S., Marijana Todorčević, Mete Civelek, Julia S. El-Sayed Moustafa, Xiao Wang, Michelle M. Simon, Juan Fernandez-Tajes, et al. 2018. "Regulatory Variants at KLF14 Influence Type 2 Diabetes Risk via a Female-Specific Effect on Adipocyte Size and Body Composition." Nature Genetics 50 (4): 572–80.

Smeland, Olav B., Shahram Bahrami, Oleksandr Frei, Alexey Shadrin, Kevin O'Connell, Jeanne Savage, Kyoko Watanabe, et al. 2020. "Genome-Wide Analysis Reveals Extensive Genetic Overlap between Schizophrenia, Bipolar Disorder, and Intelligence." Molecular Psychiatry 25 (4): 844–53.

Smit, Dirk J. A., Margaret J. Wright, Jacquelyn L. Meyers, Nicholas G. Martin, Yvonne Y. W. Ho, Stephen M. Malone, Jian Zhang, et al. 2018. "Genome-Wide Association Analysis Links Multiple Psychiatric Liability Genes to Oscillatory Brain Activity." Human Brain Mapping 39 (11): 4183–95.

Smith, Stephen M., Gwenaëlle Douaud, Winfield Chen, Taylor Hanayik, Fidel Alfaro-Almagro, Kevin Sharp, and Lloyd T. Elliott. 2021. "An Expanded Set of Genome-Wide Association Studies of Brain Imaging Phenotypes in UK Biobank." Nature Neuroscience 24 (5): 737–45.

Soneson, Charlotte, Michael I. Love, and Mark D. Robinson. 2015. "Differential Analyses for RNA-Seq: Transcript-Level Estimates Improve Gene-Level Inferences." F1000Research 4 (December): 1521.

Song, J., S. E. Bergen, A. Di Florio, R. Karlsson, A. Charney, D. M. Ruderfer, E. A. Stahl, et al. 2016. "Genome-Wide Association Study Identifies SESTD1 as a Novel Risk Gene for Lithium-Responsive Bipolar Disorder." Molecular Psychiatry 21 (9): 1290–97.

Sousa, André M. M., Kyle A. Meyer, Gabriel Santpere, Forrest O. Gulden, and Nenad Sestan. 2017. "Evolution of the Human Nervous System Function, Structure, and Development." Cell 170 (2): 226–47.

SPARK Consortium. Electronic address: pfeliciano@simonsfoundation.org, and SPARK Consortium. 2018. "SPARK: A US Cohort of 50,000 Families to Accelerate Autism Research." Neuron 97 (3): 488–93.

Speed, Doug, Na Cai, UCLEB Consortium, Michael R. Johnson, Sergey Nejentsev, and David J. Balding. 2017. "Reevaluation of SNP Heritability in Complex Human Traits." Nature Genetics 49 (7): 986–92.

Stefansson, Bjarki, Takashi Ohama, Abbi E. Daugherty, and David L. Brautigan. 2008. "Protein Phosphatase 6 Regulatory Subunits Composed of Ankyrin Repeat Domains." Biochemistry 47 (5): 1442–51.

Stefansson, Hreinn, Andreas Meyer-Lindenberg, Stacy Steinberg, Brynja Magnusdottir, Katrin Morgen, Sunna Arnarsdottir, Gyda Bjornsdottir, et al. 2014. "CNVs Conferring Risk of Autism or Schizophrenia Affect Cognition in Controls." Nature 505 (7483): 361–66.

Stein, Jason L., Sarah E. Medland, Alejandro Arias Vasquez, Derrek P. Hibar, Rudy E. Senstad, Anderson M. Winkler, Roberto Toro, et al. 2012. "Identification of Common Variants Associated with Human Hippocampal and Intracranial Volumes." Nature Genetics 44 (5): 552–61.

Stein, Jason L., Luis de la Torre-Ubieta, Yuan Tian, Neelroop N. Parikshak, Israel A. Hernández, Maria C. Marchetto, Dylan K. Baker, et al. 2014. "A Quantitative Framework to Evaluate Modeling of Cortical Development by Neural Stem Cells." Neuron 83 (1): 69–86.

Stern, Shani, Sara Linker, Krishna C. Vadodaria, Maria C. Marchetto, and Fred H. Gage. 2018. "Prediction of Response to Drug Therapy in Psychiatric Disorders." Open Biology 8 (5).

https://doi.org/10.1098/rsob.180031.

Stern, Shani, Anindita Sarkar, Dekel Galor, Tchelet Stern, Arianna Mei, Yam Stern, Ana P. D. Mendes, et al. 2020. “A Physiological Instability Displayed in Hippocampal Neurons Derived From Lithium-Nonresponsive Bipolar Disorder Patients.” Biological Psychiatry 88 (2): 150–58.

Stern, S., Renata Santos, M. C. Marchetto, A. P. D. Mendes, G. A. Rouleau, S. Biesmans, Q. W. Wang, et al. 2018. “Neurons Derived from Patients with Bipolar Disorder Divide into Intrinsically Different Sub-Populations of Neurons, Predicting the Patients’ Responsiveness to Lithium.” Molecular Psychiatry 23 (6): 1453–65.

Stoner, Rich, Maggie L. Chow, Maureen P. Boyle, Susan M. Sunkin, Peter R. Mouton, Subhojit Roy, Anthony Wynshaw-Boris, Sophia A. Colamarino, Ed S. Lein, and Eric Courchesne. 2014. “Patches of Disorganization in the Neocortex of Children with Autism.” The New England Journal of Medicine 370 (13): 1209–19.

Stranger, Barbara E., Alexandra C. Nica, Matthew S. Forrest, Antigone Dimas, Christine P. Bird, Claude Beazley, Catherine E. Ingle, et al. 2007. “Population Genomics of Human Gene Expression.” Nature Genetics 39 (10): 1217–24.

Sullivan, Patrick F. 2017. “How Good Were Candidate Gene Guesses in Schizophrenia Genetics?” Biological Psychiatry 82 (10): 696–97.

Sullivan, Patrick F., Arpana Agrawal, Cynthia M. Bulik, Ole A. Andreassen, Anders D. Børglum, Gerome Breen, Sven Cichon, et al. 2018. “Psychiatric Genomics: An Update and an Agenda.” The American Journal of Psychiatry 175 (1): 15–27.

Sullivan, Patrick F., and Daniel H. Geschwind. 2019. “Defining the Genetic, Genomic, Cellular, and Diagnostic Architectures of Psychiatric Disorders.” Cell 177 (1): 162–83.

Sun, Daqiang, Christopher R. K. Ching, Amy Lin, Jennifer K. Forsyth, Leila Kushan, Ariana Vajdi, Maria Jalbrzikowski, et al. 2018. “Large-Scale Mapping of Cortical Alterations in 22q11.2 Deletion Syndrome: Convergence with Idiopathic Psychosis and Effects of Deletion Size.” Molecular Psychiatry, June. https://doi.org/10.1038/s41380-018-0078-5.

Sun, Tao, and Robert F. Hevner. 2014. “Growth and Folding of the Mammalian Cerebral Cortex: From Molecules to Malformations.” Nature Reviews. Neuroscience 15 (4): 217–32.

Sutterland, A. L., G. Fond, A. Kuin, M. W. J. Koeter, R. Lutter, T. van Gool, R. Yolken, A. Szoke, M. Leboyer, and L. de Haan. 2015. “Beyond the Association. Toxoplasma Gondii in Schizophrenia, Bipolar Disorder, and Addiction: Systematic Review and Meta-Analysis.” Acta Psychiatrica Scandinavica 132 (3): 161–79.

Swanson, L. W. 1995. “Mapping the Human Brain: Past, Present, and Future.” Trends in Neurosciences 18 (11): 471–74.

Taal, H. Rob, Beate St Pourcain, Elisabeth Thiering, Shikta Das, Dennis O. Mook-Kanamori, Nicole M. Warrington, Marika Kaakinen, et al. 2012. “Common Variants at 12q15 and 12q24 Are Associated with Infant Head Circumference.” Nature Genetics 44 (5): 532–38.

Taliun, Daniel, Daniel N. Harris, Michael D. Kessler, Jedidiah Carlson, Zachary A. Szpiech, Raul Torres, Sarah A. Gagliano Taliun, et al. 2021. “Sequencing of 53,831 Diverse Genomes from

the NHLBI TOPMed Program." Nature 590 (7845): 290–99.

Tansey, K. E., E. Rees, D. E. Linden, S. Ripke, K. D. Chambert, J. L. Moran, S. A. McCarroll, et al. 2016. "Common Alleles Contribute to Schizophrenia in CNV Carriers." Molecular Psychiatry 21 (8): 1085–89.

Thakore, Pratiksha I., Anthony M. D'Ippolito, Lingyun Song, Alexias Safi, Nishkala K. Shivakumar, Ami M. Kabadi, Timothy E. Reddy, Gregory E. Crawford, and Charles A. Gersbach. 2015. "Highly Specific Epigenome Editing by CRISPR-Cas9 Repressors for Silencing of Distal Regulatory Elements." Nature Methods 12 (12): 1143–49.

The International HapMap 3 Consortium. 2010. "Integrating Common and Rare Genetic Variation in Diverse Human Populations." Nature 467 (7311): 52–58.

The Schizophrenia Working Group of the Psychiatric Genomics Consortium, Stephan Ripke, James T. R. Walters, and Michael C. O'Donovan. 2020. "Mapping Genomic Loci Prioritises Genes and Implicates Synaptic Biology in Schizophrenia." bioRxiv. medRxiv. https://doi.org/10.1101/2020.09.12.20192922.

Thompson, Paul M., Kiralee M. Hayashi, Greig I. De Zubicaray, Andrew L. Janke, Stephen E. Rose, James Semple, Michael S. Hong, et al. 2004. "Mapping Hippocampal and Ventricular Change in Alzheimer Disease." NeuroImage 22 (4): 1754–66.

Thompson, Paul M., Jason L. Stein, Sarah E. Medland, Derrek P. Hibar, Alejandro Arias Vasquez, Miguel E. Renteria, Roberto Toro, et al. 2014. "The ENIGMA Consortium: Large-Scale Collaborative Analyses of Neuroimaging and Genetic Data." Brain Imaging and Behavior 8 (2): 153–82.

Thomsen, Soren K., Anne Raimondo, Benoit Hastoy, Shahana Sengupta, Xiao-Qing Dai, Austin Bautista, Jenny Censin, et al. 2018. "Type 2 Diabetes Risk Alleles in PAM Impact Insulin Release from Human Pancreatic β-Cells." Nature Genetics 50 (8): 1122–31.

Toda, Tomohisa, and Fred H. Gage. 2018. "Review: Adult Neurogenesis Contributes to Hippocampal Plasticity." Cell and Tissue Research 373 (3): 693–709.

Tohen, Mauricio, Waldemar Greil, Joseph R. Calabrese, Gary S. Sachs, Lakshmi N. Yatham, Bruno Müller Oerlinghausen, Athanasios Koukopoulos, et al. 2005. "Olanzapine versus Lithium in the Maintenance Treatment of Bipolar Disorder: A 12-Month, Randomized, Double-Blind, Controlled Clinical Trial." The American Journal of Psychiatry 162 (7): 1281–90.

Tomer, Raju, Matthew Lovett-Barron, Isaac Kauvar, Aaron Andalman, Vanessa M. Burns, Sethuraman Sankaran, Logan Grosenick, Michael Broxton, Samuel Yang, and Karl Deisseroth. 2015. "SPED Light Sheet Microscopy: Fast Mapping of Biological System Structure and Function." Cell 163 (7): 1796–1806.

Tondo, L., R. J. Baldessarini, J. Hennen, and G. Floris. 1998. "Lithium Maintenance Treatment of Depression and Mania in Bipolar I and Bipolar II Disorders." The American Journal of Psychiatry 155 (5): 638–45.

Topol, Aaron, Shijia Zhu, Ngoc Tran, Anthony Simone, Gang Fang, and Kristen J. Brennand. 2015. "Altered WNT Signaling in Human Induced Pluripotent Stem Cell Neural Progenitor Cells Derived from Four Schizophrenia Patients." Biological Psychiatry 78 (6): e29–34.

Toro, Roberto, Michel Perron, Bruce Pike, Louis Richer, Suzanne Veillette, Zdenka Pausova, and Tomás Paus. 2008. “Brain Size and Folding of the Human Cerebral Cortex.” Cerebral Cortex 18 (10): 2352–57.

Torre-Ubieta, Luis de la, Jason L. Stein, Hyejung Won, Carli K. Opland, Dan Liang, Daning Lu, and Daniel H. Geschwind. 2018. “The Dynamic Landscape of Open Chromatin during Human Cortical Neurogenesis.” Cell 172 (1-2): 289–304.e18.

Tost, Heike, Dieter F. Braus, Shabnam Hakimi, Matthias Ruf, Christian Vollmert, Fabian Hohn, and Andreas Meyer-Lindenberg. 2010. “Acute D2 Receptor Blockade Induces Rapid, Reversible Remodeling in Human Cortical-Striatal Circuits.” Nature Neuroscience 13 (8): 920–22.

Touzet, Hélène, and Jean-Stéphane Varré. 2007. “Efficient and Accurate P-Value Computation for Position Weight Matrices.” Algorithms for Molecular Biology: AMB 2 (December): 15.

Trevino, Alexandro E., Fabian Müller, Jimena Andersen, Laksshman Sundaram, Arwa Kathiria, Anna Shcherbina, Kyle Farh, et al. 2021. “Chromatin and Gene-Regulatory Dynamics of the Developing Human Cerebral Cortex at Single-Cell Resolution.” Cell, August. https://doi.org/10.1016/j.cell.2021.07.039.

Trubetskoy, Vassily, Antonio F. Pardiñas, Ting Qi, Georgia Panagiotaropoulou, Swapnil Awasthi, Tim B. Bigdeli, Julien Bryois, et al. 2022. “Mapping Genomic Loci Implicates Genes and Synaptic Biology in Schizophrenia.” Nature 604 (7906): 502–8.

Tsai, Robert Y. L., and Ronald D. G. McKay. 2002. “A Nucleolar Mechanism Controlling Cell Proliferation in Stem Cells and Cancer Cells.” Genes & Development 16 (23): 2991–3003.

Umans, Benjamin D., Alexis Battle, and Yoav Gilad. 2020. “Where Are the Disease-Associated eQTLs?” Trends in Genetics: TIG, September. https://doi.org/10.1016/j.tig.2020.08.009.

Valvezan, Alexander J., and Peter S. Klein. 2012. “GSK-3 and Wnt Signaling in Neurogenesis and Bipolar Disorder.” Frontiers in Molecular Neuroscience 5 (January): 1.

Veyrac, Alexandra, Sophie Reibel, Joëlle Sacquet, Mireille Mutin, Jean-Philippe Camdessanche, Pappachan Kolattukudy, Jérôme Honnorat, and François Jourdan. 2011. “CRMP5 Regulates Generation and Survival of Newborn Neurons in Olfactory and Hippocampal Neurogenic Areas of the Adult Mouse Brain.” PloS One 6 (10): e23721.

Vigo, Daniel, Graham Thornicroft, and Rifat Atun. 2016. “Estimating the True Global Burden of Mental Illness.” The Lancet. Psychiatry 3 (2): 171–78.

Viguera, A. C., L. Tondo, and R. J. Baldessarini. 2000. “Sex Differences in Response to Lithium Treatment.” The American Journal of Psychiatry 157 (9): 1509–11.

Visscher, Peter M., Naomi R. Wray, Qian Zhang, Pamela Sklar, Mark I. McCarthy, Matthew A. Brown, and Jian Yang. 2017. “10 Years of GWAS Discovery: Biology, Function, and Translation.” American Journal of Human Genetics 101 (1): 5–22.

Voight, Benjamin F., Laura J. Scott, Valgerdur Steinthorsdottir, Andrew P. Morris, Christian Dina, Ryan P. Welch, Eleftheria Zeggini, et al. 2010. “Twelve Type 2 Diabetes Susceptibility Loci Identified through Large-Scale Association Analysis.” Nature Genetics 42 (7): 579–89.

Vojinovic, Dina, Hieab H. Adams, Xueqiu Jian, Qiong Yang, Albert Vernon Smith, Joshua C. Bis, Alexander Teumer, et al. 2018. “Genome-Wide Association Study of 23,500 Individuals Identifies 7 Loci Associated with Brain Ventricular Volume.” Nature Communications 9 (1): 3945.

Volpato, Viola, James Smith, Cynthia Sandor, Janina S. Ried, Anna Baud, Adam Handel, Sarah E. Newey, et al. 2018. “Reproducibility of Molecular Phenotypes after Long-Term Differentiation to Human iPSC-Derived Neurons: A Multi-Site Omics Study.” Stem Cell Reports 11 (4): 897–911.

Wang, Wei, Mengdi Wang, Meng Yang, Bo Zeng, Wenying Qiu, Qiang Ma, Xiaoxi Jing, et al. 2022. “Transcriptome Dynamics of Hippocampal Neurogenesis in Macaques across the Lifespan and Aged Humans.” Cell Research, June. https://doi.org/10.1038/s41422-022-00678-y.

Wanner, A. A., M. A. Kirschmann, and C. Genoud. 2015. “Challenges of Microtome-Based Serial Block-Face Scanning Electron Microscopy in Neuroscience.” Journal of Microscopy 259 (2): 137–42.

Warrier, Varun, Eva-Maria Stauffer, Qin Qin Huang, Emilie M. Wigdor, Eric A. W. Slob, Jakob Seidlitz, Lisa Ronan, et al. 2023. “Genetic Insights into Human Cortical Organization and Development through Genome-Wide Analyses of 2,347 Neuroimaging Phenotypes.” Nature Genetics, August. https://doi.org/10.1038/s41588-023-01475-y.

Wexler, Eric M., Andres Paucer, Harley I. Kornblum, Theodore D. Palmer, and Daniel H. Geschwind. 2009. “Endogenous Wnt Signaling Maintains Neural Progenitor Cell Potency.” Stem Cells 27 (5): 1130–41.

Wojcik, Genevieve L., Mariaelisa Graff, Katherine K. Nishimura, Ran Tao, Jeffrey Haessler, Christopher R. Gignoux, Heather M. Highland, et al. 2019. “Genetic Analyses of Diverse Populations Improves Discovery for Complex Traits.” Nature, June. https://doi.org/10.1038/s41586-019-1310-4.

Wolking, Stefan, Ciarán Campbell, Caragh Stapleton, Mark McCormack, Norman Delanty, Chantal Depondt, Michael R. Johnson, et al. 2021. “Role of Common Genetic Variants for Drug-Resistance to Specific Anti-Seizure Medications.” Frontiers in Pharmacology 12 (June): 688386.

Wolking, Stefan, Herbert Schulz, Anne T. Nies, Mark McCormack, Elke Schaeffeler, Pauls Auce, Andreja Avbersek, et al. 2020. “Pharmacoresponse in Genetic Generalized Epilepsy: A Genome-Wide Association Study.” Pharmacogenomics 21 (5): 325–35.

Wolter, Justin M., Jessica A. Jimenez, Jason L. Stein, and Mark J. Zylka. 2022. “ToxCast Chemical Library Wnt Screen Identifies Diethanolamine as an Activator of Neural Progenitor Proliferation.” FASEB BioAdvances, March. https://doi.org/10.1096/fba.2021-00163.

Wolter, Justin M., Brandon D. Le, Nana Matoba, Michael J. Lafferty, Nil Aygün, Dan Liang, Kenan Courtney, et al. 2022. “Cellular Genome-Wide Association Study Identifies Common Genetic Variation Influencing Lithium Induced Neural Progenitor Proliferation.” Biological Psychiatry, August. https://doi.org/10.1016/j.biopsych.2022.08.014.

Wolter, Justin M., Hanqian Mao, Giulia Fragola, Jeremy M. Simon, James L. Krantz, Hannah O.

Bazick, Baris Oztemiz, Jason L. Stein, and Mark J. Zylka. 2020. “Cas9 Gene Therapy for Angelman Syndrome Traps Ube3a-ATS Long Non-Coding RNA.” Nature, October. https://doi.org/10.1038/s41586-020-2835-2.

Won, Hyejung, Jerry Huang, Carli K. Opland, Chris L. Hartl, and Daniel H. Geschwind. 2019. “Human Evolved Regulatory Elements Modulate Genes Involved in Cortical Expansion and Neurodevelopmental Disease Susceptibility.” Nature Communications 10 (1): 2396.

Won, Hyejung, Luis de la Torre-Ubieta, Jason L. Stein, Neelroop N. Parikshak, Jerry Huang, Carli K. Opland, Michael J. Gandal, et al. 2016. “Chromosome Conformation Elucidates Regulatory Relationships in Developing Human Brain.” Nature 538 (7626): 523–27.

Wood, Andrew R., Tonu Esko, Jian Yang, Sailaja Vedantam, Tune H. Pers, Stefan Gustafsson, Audrey Y. Chu, et al. 2014. “Defining the Role of Common Variation in the Genomic and Biological Architecture of Adult Human Height.” Nature Genetics 46 (11): 1173–86.

Wray, Naomi R., Stephan Ripke, Manuel Mattheisen, Maciej Trzaskowski, Enda M. Byrne, Abdel Abdellaoui, Mark J. Adams, et al. 2018. “Genome-Wide Association Analyses Identify 44 Risk Variants and Refine the Genetic Architecture of Major Depression.” Nature Genetics 50 (5): 668–81.

Wu, Yang, Ting Qi, Naomi R. Wray, Peter M. Visscher, Jian Zeng, and Jian Yang. 2023. “Joint Analysis of GWAS and Multi-Omics QTL Summary Statistics Reveals a Large Fraction of GWAS Signals Shared with Molecular Phenotypes.” Cell Genomics 0 (0). https://doi.org/10.1016/j.xgen.2023.100344.

Wu, Ying, K. Alaine Broadaway, Chelsea K. Raulerson, Laura J. Scott, Calvin Pan, Arthur Ko, Aiqing He, et al. 2019. “Colocalization of GWAS and eQTL Signals at Loci with Multiple Signals Identifies Additional Candidate Genes for Body Fat Distribution.” Human Molecular Genetics 28 (24): 4161–72.

Xiao, Rui, and Michael Boehnke. 2011. “Quantifying and Correcting for the Winner’s Curse in Quantitative-Trait Association Studies.” Genetic Epidemiology 35 (3): 133–38.

Xiao, X., H. Chang, and M. Li. 2017. “Molecular Mechanisms Underlying Noncoding Risk Variations in Psychiatric Genetic Studies.” Molecular Psychiatry 22 (4): 497–511.

Yang, Jian, Teresa Ferreira, Andrew P. Morris, Sarah E. Medland, Genetic Investigation of ANthropometric Traits (GIANT) Consortium, DIAbetes Genetics Replication And Meta-analysis (DIAGRAM) Consortium, Pamela A. F. Madden, et al. 2012. “Conditional and Joint Multiple-SNP Analysis of GWAS Summary Statistics Identifies Additional Variants Influencing Complex Traits.” Nature Genetics 44 (4): 369–75, S1–3.

Yang, Jian, S. Hong Lee, Michael E. Goddard, and Peter M. Visscher. 2011. “GCTA: A Tool for Genome-Wide Complex Trait Analysis.” American Journal of Human Genetics 88 (1): 76–82.

Yan, Jian, Yunjiang Qiu, André M. Ribeiro Dos Santos, Yimeng Yin, Yang E. Li, Nick Vinckier, Naoki Nariai, et al. 2021. “Systematic Analysis of Binding of Transcription Factors to Noncoding Variants.” Nature 591 (7848): 147–51.

Yao, Zizhen, John K. Mich, Sherman Ku, Vilas Menon, Anne-Rachel Krostag, Refugio A. Martinez, Leon Furchtgott, et al. 2017. “A Single-Cell Roadmap of Lineage Bifurcation in

Human ESC Models of Embryonic Brain Development." Cell Stem Cell 20 (1): 120–34.

Ye, Li, William E. Allen, Kimberly R. Thompson, Qiyuan Tian, Brian Hsueh, Charu Ramakrishnan, Ai-Chi Wang, et al. 2016. "Wiring and Molecular Features of Prefrontal Ensembles Representing Distinct Experiences." Cell 165 (7): 1776–88.

Yucel, Kaan, Margaret C. McKinnon, Valerie H. Taylor, Kathryn Macdonald, Martin Alda, L. Trevor Young, and Glenda M. MacQueen. 2007. "Bilateral Hippocampal Volume Increases after Long-Term Lithium Treatment in Patients with Bipolar Disorder: A Longitudinal MRI Study." Psychopharmacology 195 (3): 357–67.

Yucel, Kaan, Valerie H. Taylor, Margaret C. McKinnon, Kathryn Macdonald, Martin Alda, L. Trevor Young, and Glenda M. MacQueen. 2008. "Bilateral Hippocampal Volume Increase in Patients with Bipolar Disorder and Short-Term Lithium Treatment." Neuropsychopharmacology: Official Publication of the American College of Neuropsychopharmacology 33 (2): 361–67.

Yuzwa, Scott A., Michael J. Borrett, Brendan T. Innes, Anastassia Voronova, Troy Ketela, David R. Kaplan, Gary D. Bader, and Freda D. Miller. 2017. "Developmental Emergence of Adult Neural Stem Cells as Revealed by Single-Cell Transcriptional Profiling." Cell Reports 21 (13): 3970–86.

Zanni, Giulia, Wojciech Michno, Elena Di Martino, Anna Tjärnlund-Wolf, Jean Pettersson, Charlotte Elizabeth Mason, Gustaf Hellspong, Klas Blomgren, and Jörg Hanrieder. 2017. "Lithium Accumulates in Neurogenic Brain Regions as Revealed by High Resolution Ion Imaging." Scientific Reports 7 (January): 40726.

Zeggini, Eleftheria, Anna L. Gloyn, Anne C. Barton, and Louise V. Wain. 2019. "Translational Genomics and Precision Medicine: Moving from the Lab to the Clinic." Science 365 (6460): 1409–13.

Zeng, Biao, Jaroslav Bendl, Roman Kosoy, John F. Fullard, Gabriel E. Hoffman, and Panos Roussos. 2022. "Multi-Ancestry eQTL Meta-Analysis of Human Brain Identifies Candidate Causal Variants for Brain-Related Traits." Nature Genetics, January. https://doi.org/10.1038/s41588-021-00987-9.

Zhang, Chen, Xiao Xiao, Tao Li, and Ming Li. 2021. "Translational Genomics and beyond in Bipolar Disorder." Molecular Psychiatry 26 (1): 186–202.

Zhang, Yan, Guanghao Qi, Ju-Hyun Park, and Nilanjan Chatterjee. 2018. "Estimation of Complex Effect-Size Distributions Using Summary-Level Statistics from Genome-Wide Association Studies across 32 Complex Traits." Nature Genetics 50 (9): 1318–26.

Zhong, Suijuan, Shu Zhang, Xiaoying Fan, Qian Wu, Liying Yan, Ji Dong, Haofeng Zhang, et al. 2018. "A Single-Cell RNA-Seq Survey of the Developmental Landscape of the Human Prefrontal Cortex." Nature 555 (7697): 524–28.

Zhou, Yi, Yijing Su, Shiying Li, Benjamin C. Kennedy, Daniel Y. Zhang, Allison M. Bond, Yusha Sun, et al. 2022. "Molecular Landscapes of Human Hippocampal Immature Neurons across Lifespan." Nature, July, 1–7.

Zhu, Miao-Miao, Hui-Lan Li, Li-Hong Shi, Xiao-Ping Chen, Jia Luo, and Zan-Ling Zhang. 2017. "The Pharmacogenomics of Valproic Acid." Journal of Human Genetics 62 (12): 1009–14.

Zhu, Zhihong, Futao Zhang, Han Hu, Andrew Bakshi, Matthew R. Robinson, Joseph E. Powell, Grant W. Montgomery, et al. 2016. “Integration of Summary Data from GWAS and eQTL Studies Predicts Complex Trait Gene Targets.” Nature Genetics 48 (5): 481–87.

Ziembik, Magdalena A., Timothy P. Bender, James M. Larner, and David L. Brautigan. 2017. “Functions of Protein Phosphatase-6 in NF-κB Signaling and in Lymphocytes.” Biochemical Society Transactions 45 (3): 693–701.